

# **Characterisation of Chromatin Extracellular Traps in Rainbow Trout (*Oncorhynchus mykiss*)**

---

Thesis submitted for the degree of

Doctor of Philosophy

**UNIVERSITY of  
STIRLING**



By

**Andre Paul Van (MSci)**

Institute of Aquaculture, University of Stirling

Stirling, Scotland

February 2018



## **Declaration**

I hereby declare that the work and results presented in this thesis was conducted by me at the Institute of Aquaculture, University of Stirling, Scotland. The work presented in this thesis has not been previously submitted for any other degree or qualification.

The literature consulted has been cited and where appropriated, collaborative assistance has been acknowledged.

Word count: Approximately 58,000 words

Stirling, February 2018

Andre Paul Van

## Acknowledgements

To begin, I would like to express my sincere gratitude to my kind parents and extended family for their continuous support and encouragement.

Secondly, I would like to thank my supervisors who have given me valuable guidance, support, and patience throughout the course of this project. Initially, Professor James Bron, for advice and sharing their expertise within the field of microscopy; Professor Valerie Smith, for further direction throughout the project and facilitating the enriching and colourful experience of my first international conference; finally, and most importantly, Dr Andrew Desbois, for giving me the opportunity to begin this project, and inculcating me to write good-ly and curtail my use of jargon.

I would like to particularly thank Neila Alvarez de Haro, for guiding me throughout my lab work, along with the numerous experiments during the early to late hours. I deeply appreciate and cherish our time working together.

I would like to thank everybody at Frandy Fishery – Dawn Fresh, for supplying some of their rainbow trout to allow my research to continue and giving me insight towards the day-to-day processes within the hatchery.

Special thanks go towards the technical staff at the Institute of Aquaculture: Hilary McEwan, Karen Snedden, Jacquie Ireland, Kerry Bartie, Rona Werner, Brian Craig, and all others who gave me technical support and keeping the labs running smoothly.

Finally, I would like to thank all my friends – you know who you are. Especially Matthijs Metselaar, Marie Smedley, Sanne Dolieslager, Sean Monaghan, Sam Houston, Stuart McMillian, and the people in the University of Stirling Cycle and Triathlon Club for keeping me on my toes/wheels. Thank you, Carolina Fernandez, for giving me all the support I could ask for.

## Abstract

One of the greatest challenges in finfish aquaculture is combating losses caused by infectious bacterial diseases, and a better understanding of the interactions between the host immune system and pathogens is essential for developing new methods to manage infections and outbreaks. Extracellular traps (ETs) are decondensed nuclear chromatin released by neutrophils into the extracellular matrix that can ensnare and kill microbes. Since the discovery of ETs in humans, these innate immune effectors have been characterised across the animal kingdom, including in some fish species, though their existence in salmonids has yet to be confirmed. Therefore, the aim of this thesis was to confirm and characterise the release of ETs in the rainbow trout (*Oncorhynchus mykiss*) and investigate the interaction of these structures with fish pathogenic bacteria. To do this, a triple-layer Percoll gradient technique was employed to give highly enriched cell suspensions of polymorphonuclear cells (PMNs) derived from head-kidney tissue preparations. Treatment of PMN-enriched cell suspensions with the nucleic-acid-specific stain, SYTOX Green, revealed the presence of ET-like structures that had been released without stimulation. These ET-like structures were confirmed by immunostaining techniques to contain the diagnostic proteinaceous markers of ETs: neutrophil elastase, myeloperoxidase and the H2A histone. Previously characterised inhibitors and inducers of ET release from phagocytic immune cells in other animals confirmed that calcium ionophore (Cal), flagellin, and cytochalasin D shared similar activities for ET-release by rainbow trout PMNs. However, interestingly, as the common ET-inducer phorbol-myristate acetate (PMA) and ET-inhibitor diphenyleneiodonium (DPI) did not exert their expected potency in ET release assays with the PMNs, perhaps indicating that these fish cells are less dependent on NADPH oxidase signalling for ET release compared to mammals and most invertebrate species. The PMN-derived ETs were demonstrated to bind to and trap the extracellular nuclease-deficient bacterial fish pathogen, *Vibrio anguillarum* (Vib 87) when co-cultured. Finally, extracellular nuclease activity produced by a *V. anguillarum* isolate (Vib 6) during culture was able to degrade ETs released by rainbow trout PMNs in a dose-dependent manner. Moreover, viable colony counts, fluorescent and phase contrast microscopy demonstrated that *V. anguillarum* Vib 6 eluded trapping by ETs, while an extracellular nuclease-deficient isolate did not. These observations are consistent with the suggestion that nucleases are a microbial virulence factor during host infection. Confirming the existence and antimicrobial potential of extracellular traps released by rainbow trout PMNs may provide a platform towards the development of novel therapeutics to reduce mortalities in finfish aquaculture caused by infectious microbial pathogens.

# Table of contents

Acknowledgements.....	ii
Abstract.....	iii
Table of contents .....	iv
List of Figures .....	ix
List of Tables .....	xviii
Abbreviations and definitions .....	xx
1. Chapter 1: General Introduction .....	1
1.1. Aquaculture and disease management.....	1
1.2. Fish Immune systems .....	2
1.2.1. Innate immune system.....	4
1.2.2. Teleost hematopoiesis .....	6
1.2.3. Polymorphonuclear cells.....	7
1.2.4. Enrichment and culture of leukocytes from fish tissues .....	13
1.3. Extracellular traps .....	13
1.3.1. Extracellular traps in fish.....	20
1.3.2. Visualising and quantifying extracellular trap release <i>in vitro</i> .....	22
1.3.3. Antimicrobial activity of extracellular traps.....	24
1.3.4. Inducers and inhibitors of extracellular trap release .....	30
1.3.5. Extracellular trap-associated pathogenesis.....	36
1.4. Microbial evasion strategies against extracellular traps.....	37
1.4.1. Extracellular nuclease.....	38
1.5. Aims and Objectives .....	39
2. Chapter 2: Isolation of polymorphonuclear cells and quantification of extracellular traps	40
2.1. Introduction.....	40
2.2. Materials and Methods.....	42
2.2.1. Reagents .....	42

2.2.2.	Source of fish and husbandry .....	43
2.2.3.	Separation of PMNs rainbow trout head kidney cell suspensions .....	43
2.2.4.	Cytospin preparation and RapiDiff staining .....	45
2.2.5.	Comparing cell proportions from cytospin slide preparations .....	45
2.2.6.	Relationship between PMN proportions, fish weight, and water temperature .....	46
2.2.7.	Assessing cell viability with trypan blue exclusion in different culture conditions over time.....	46
2.2.8.	Evaluation of a fluorescence microtiter plate assay for high-throughput quantification of ETs .....	47
2.2.9.	Statistical analyses .....	49
2.3.	Results .....	50
2.3.1.	Comparing cell proportions after discontinuous Percoll gradient isolation .....	50
2.3.2.	Relationship between PMN proportions, fish mass and tank temperature.....	53
2.3.3.	Comparing trout PMN viability in low FCS doses and media supplementation.....	53
2.3.4.	Confirming DNA concentration is proportional to SYTOX-DNA fluorescence read in a plate reader.....	58
2.3.5.	Use of fluorescence to quantify ETs .....	58
2.4.	Discussion .....	62
3.	Chapter 3: Confirming release of extracellular traps by polymorphonuclear cells isolated from head kidney of rainbow trout.....	66
3.1.	Introduction.....	66
3.2.	Materials and Methods .....	69
3.2.1.	Confirming spontaneous release of ET-like structures are specific to PMN-enriched cell suspensions.....	69
3.2.2.	Confirming the DNA composition of presumed ETs by digestion with DNase-I	70
3.2.3.	Determining the presence of myeloperoxidase, neutrophil elastase, and histone H2A in ET-like structures by immunocytochemistry .....	71
3.2.4.	Investigating the three-dimensional structure of the ETs.....	72
3.2.5.	Investigating the effect of known ET release inhibitors on ET release from trout PMN-enriched cell suspensions.....	73
3.2.6.	Culture and heat-inactivation of <i>Vibrio anguillarum</i> .....	73

3.2.7.	Investigating the effect of known ET release inducers on ET release from trout PMN-enriched cell suspensions .....	76
3.2.8.	Examining individual ET release variation between fish .....	76
3.2.9.	Statistical analyses .....	77
3.3.	Results.....	77
3.3.1.	Confirming spontaneous release of ET-like structures are specific to PMN-enriched cell suspensions .....	77
3.3.2.	Confirming the DNA composition of presumed ETs by digestion with DNase-I 78	
3.3.3.	Determining the presence of myeloperoxidase, neutrophil elastase, and histone H2A in ET-like structures by immunocytochemistry .....	82
3.3.4.	Investigating the three-dimensional structure of the ETs.....	82
3.3.5.	Investigating the effect of known ET release inhibitors on ET release from trout PMN-enriched cell suspensions .....	86
3.3.6.	Investigating the effect of known ET release inducers on ET release from trout PMN-enriched cell suspensions .....	91
3.3.7.	Investigating individual variation in spontaneous ET release.....	99
3.4.	Discussion .....	104
4.	Chapter 4: Extracellular nuclease activity of <i>Vibrio anguillarum</i> .....	109
4.1.	Introduction.....	109
4.2.	Materials and Methods.....	113
4.2.1.	Bacterial culture and confirmation of nuclease activity of <i>Vibrio anguillarum</i> isolates	113
4.2.2.	Quantification of nuclease activity by DNase agar .....	115
4.2.3.	Detection of nuclease activity in cell-free <i>Vibrio anguillarum</i> supernatant.....	117
4.2.4.	Standardisation of culture filtrate by concentration .....	117
4.2.5.	Inhibition of <i>Vibrio anguillarum</i> Vib 6 culture filtrate nuclease activity .....	118
4.2.6.	Freeze-thaw stability of <i>Vibrio anguillarum</i> Vib 6 culture filtrate nuclease activity	119
4.2.7.	Assaying stability of <i>Vibrio anguillarum</i> Vib 6 culture filtrate nuclease activity in different temperature, pH and NaCl concentration .....	119



4.2.8.	Investigating the production of extracellular nuclease during <i>Vibrio anguillarum</i> Vib 6 growth.....	120
4.2.9.	Investigating if <i>Vibrio anguillarum</i> Vib 6 culture filtrate can degrade ETs released by rainbow trout PMNs .....	121
4.2.10.	Investigating if nucleic acids within Atlantic salmon skin mucus are susceptible to degradation by <i>Vibrio anguillarum</i> Vib 6 culture filtrate.....	122
4.2.11.	Assaying growth of <i>Vibrio anguillarum</i> in mucus .....	123
4.2.12.	Statistical analyses .....	123
4.3.	Results .....	124
4.3.1.	Quantification of nuclease activity by DNase agar .....	124
4.3.2.	Confirmation of nuclease activity of <i>Vibrio anguillarum</i> isolates .....	124
4.3.3.	Detection of nuclease activity in cell-free <i>Vibrio anguillarum</i> supernatant ....	127
4.3.4.	Inhibition of <i>Vibrio anguillarum</i> Vib 6 culture filtrate nuclease activity .....	127
4.3.5.	Freeze-thaw stability of <i>Vibrio anguillarum</i> Vib 6 culture filtrate .....	131
4.3.6.	Stability of <i>Vibrio anguillarum</i> Vib 6 culture filtrate nuclease activity in different temperature, pH, and NaCl concentration .....	131
4.3.7.	Investigating the production of extracellular nuclease during <i>Vibrio anguillarum</i> Vib 6 growth.....	136
4.3.8.	Investigating if <i>Vibrio anguillarum</i> Vib 6 culture filtrate can degrade ETs released by rainbow trout PMNs .....	136
4.3.9.	Investigating if nucleic acids within Atlantic salmon skin mucus are susceptible to degradation by <i>Vibrio anguillarum</i> Vib 6 culture filtrate.....	139
4.3.10.	Growth of <i>Vibrio anguillarum</i> in Atlantic salmon skin mucus .....	139
4.4.	Discussion .....	142
5.	Chapter 5: Investigating the antimicrobial properties of rainbow trout extracellular traps	146
5.1.	Introduction.....	146
5.2.	Materials and Methods .....	148
5.2.1.	Effect of calcium ionophore and DNase-I on viability of <i>Vibrio anguillarum</i> ..	148
5.2.2.	Effect of centrifugation on sedimentation of <i>Vibrio anguillarum</i> in 96-well culture plates .....	149

5.2.3.	Investigating the effect of ETs on abundance of <i>Vibrio anguillarum</i> CFU after co-incubation with bacteria.....	150
5.2.4.	Staining and observation of <i>Vibrio anguillarum</i> under fluorescence microscopy 151	
5.2.5.	Statistical analyses .....	152
5.3.	Results.....	152
5.3.1.	Effect of calcium ionophore and DNase-I on viability of <i>Vibrio anguillarum</i> ..	152
5.3.2.	Investigating the effect of centrifugation on <i>Vibrio anguillarum</i> sedimentation in 96-well culture plates .....	153
5.3.3.	Investigating the effect of ETs on abundance of CFU after co-incubation with bacteria	157
5.3.4.	Confirming <i>Vibrio anguillarum</i> interaction with ETs by microscopy.....	160
5.4.	Discussion .....	164
6.	Chapter 6: General Discussion .....	168
	Appendix.....	175
1.1.	Trout commercial feed .....	175
1.2.	RPMI media supplementation .....	176
1.3.	Trypan blue exclusion protocol .....	177
1.4.	Rapid Romanowsky staining protocol .....	178
1.5.	Atlantic salmon .....	179
1.5.1.	Methods.....	179
1.5.2.	Results.....	180
1.6.	Background fluorescence of compounds used as ET inducers .....	184
1.7.	Degrading ETs with DNase-I.....	187
1.8.	Examining cell morphology within PMN-enriched cell suspension following exposure to PMA at 100 nM .....	188
1.9.	Examining individual fish response to flagellin or PMA.....	189
1.10.	Spontaneous ET release variation of ten diploid and ten triploid Atlantic salmon 190	
1.11.	Bacterial culture and standard curve .....	191
1.12.	Nuclease activity screen of <i>Vibrio anguillarum</i> isolate.....	192

1.13. Nuclease activity of <i>Vibrio anguillarum</i> Vib 6 during culture.....	193
References .....	194

## List of Figures

Figure 1.1. Figure showing the anatomy of a rainbow trout, highlighting the location of the anterior/head kidney in red, responsible for haematopoiesis. Photo used with permission from the artist ©Dave Carlson.....	9
Figure 1.2. Figure representing human PMN, lymphocyte, thrombocyte, and erythrocyte differentiation from haematopoietic stem cells showing specific cell surface cluster of differentiation (CD) markers. Long-term haematopoietic stem cell (LT-HSC), short-term haematopoietic stem cell (ST-HSC), multipotent progenitor cell (MPP), common lymphoid progenitor cell (CLP), common myeloid progenitor cell (CMP), granulocyte-macrophage progenitor (GMP), promyelocyte (PM), myelocyte (MC), metamyelocyte (MM), human polymorphonuclear cell (PMN), megakaryocyte-erythroid progenitor cell (MEP). The terminally differentiated cells are also found in trout.....	12
Figure 1.3. Figure representing the distinct cell signalling events induced by PMA or Cal which lead to ET release. PMA is one of the most characterised inducers of ET release, which mimics diacylglycerol to activate protein kinase C (PKC). Activated PKC can phosphorylate the p47phox subunit of NADPH oxidase, promoting the formation of a functional NADPH oxidase complex on cell membranes. This enzyme is responsible for the generation of ROS, leading to release of ETs. Alternatively, Cal is understood to bind and form stable divalent cations with extracellular Ca <sup>2+</sup> , allowing cell membrane permeability. Ca <sup>2+</sup> can open SK3 channels on the mitochondrial membranes causing a rapid influx of mitochondrial Ca <sup>2+</sup> , leading to the generation of ROS and ultimately, ET release (Figure 1.4). .....	18
Figure 1.4. Figure representing fundamental events in neutrophils/PMNs that lead to ET release though NADPH oxidase-dependent and independent pathways. Exposure of neutrophils/PMNs to ET-inducing chemical and biological compounds induces extracellular calcium entry or activation of PKC, and this leads to initiation of ET release cascade (Figure 1.3). The increase of intracellular ROS is followed by nuclear and granule membrane rupture and processing of chromatin by granule proteins, leading to the chromatin decondensation and ultimately ET release.....	19
Figure 2.1. Representative images showing cytopsin preparations from rainbow trout leukocyte cell solutions after rapid Romanowsky staining to show specific cell types based on morphology and staining characteristics. (a,b) Polymorphonuclear cells (PMN) with a dark-purple lobed nucleus; (c,d) Monocyte/macrophages (Mo/M) with a kidney-shaped	

nucleus, indicated by black arrows, approximately the same size as a PMN; (e.f) Lymphocytes (L) are labelled with black arrows; (g,h) Erythrocytes (E). Scale bar = 10  $\mu\text{m}$ .<sup>51</sup>

Figure 2.2. Scatter plot showing the relationship between rainbow trout mass against the proportion of PMNs attained after isolation with triple-layer Percoll gradients. Each point consists of the mean number of PMNs calculated from three fields of view from cytopsin preparations after enriching trout head kidney tissue for PMNs. There was significant correlation between fish mass and PMN proportion ( $F_{1,4} = 29.73$ ;  $p < 0.05$ ). Error bars represent the s.e.m.  $n = 6$  trout. .... 54

Figure 2.3. Scatter plot showing the relationship between tank temperature ( $^{\circ}\text{C}$ ) at time of sampling and PMN proportions obtained from triple-layer Percoll preparations from rainbow trout. ( $F_{1,4} = 22.13$ ;  $p < 0.05$ ). Error bars represent s.e.m.  $n = 6$  trout. .... 55

Figure 2.4. Viability of cells in PMN-enriched suspensions ( $1 \times 10^6$  cells  $\text{mL}^{-1}$ ) in the absence or presence of 0.5 – 10% FCS supplementation in RPMI cell medium over 72 h at  $13^{\circ}\text{C}$ , as measured by trypan blue exclusion. Error bars represent s.e.m.  $n = 4$ . .... 56

Figure 2.5. Viability of cells in PMN-enriched suspensions ( $1 \times 10^6$  cells  $\text{mL}^{-1}$ ) during 72 h in the presence of (a) RPMI3 with and without HEPES buffer (25 mM), which shows no significant difference in cell viability at 0 and 24 h ( $p < 0.05$ ); (b) The use of L-15 or RPMI3 did not show significant differences in cell viability at 0 and 24 h ( $p < 0.05$ ). For both graphs, a significant difference in cell viability was detected between each treatment at 48 and 72 h ( $p > 0.05$ ). Error bars represent s.e.m. (are not visible in all cases).  $n = 4$ . .... 57

Figure 2.6. Scatterplot showing the relationship between salmon sperm DNA (SS-DNA in  $\text{ng mL}^{-1}$ ) with SYTOX-stained arbitrary fluorescence (AFU). SYTOX-DNA fluorescence is linearly proportional to SS-DNA concentration in a 96-well plate. Error bars represent s.e.m. but not all are visible. ( $F_{1,16} = 348.7$ ;  $p < 0.05$ );  $n = 5$ . .... 59

Figure 2.7. Representative fluorescence microscopy images of selected presumed trout ETs (white arrows) released by PMN-enriched cell suspensions by triple-layer Percoll gradients ( $4 \times 10^5$  cells  $\text{mL}^{-1}$  in a 96-well plate;  $20\times$  magnification). (a) Unstimulated controls treated with RPMI1 for 6 h (b) Incubated with Cal ( $5 \mu\text{g mL}^{-1}$ ) for 6 h. Cells were stained with SYTOX Green ( $5 \mu\text{M}$ ) before observing with fluorescence microscopy. The mean count of presumed ETs out of total cells from an image as above was well was compared to the mean fluorescence of triplicate wells containing PMNs enriched cell suspensions. Error bars =  $100 \mu\text{m}$ . .... 60

Figure 2.8. Scatterplot showing the relationship between mean arbitrary fluorescence units from SYTOX-stained extracellular DNA from enriched PMN cell suspensions *in vitro* (both unstimulated controls and Cal-stimulated), and the mean presumed-ET counts by percentage of total cells in fields of view of matched samples. ( $F_{1,52} = 409.8$ ;  $p < 0.001$ )  $n = 54$ . .... 61

Figure 3.1. Representative phase contrast and fluorescence microscopy images showing trout erythrocyte suspensions ( $1 \times 10^5$  cells  $\text{mL}^{-1}$ ) incubated for 24 h at  $15^\circ\text{C}$  exposed to RPMI1, and stained with SYTOX green (5  $\mu\text{M}$ , 5 min, room temperature) and DAPI (1  $\mu\text{M}$ , 5 min, room temperature). (a) Phase contrast image showing the morphology of cells within the suspension; (b) DAPI-filter channel showing both intracellular and extracellular nucleic acids stained with DAPI (blue), as DAPI is a membrane-permeable dye; (c) FITC filter channel shows SYTOX Green-stained nucleic acid which only stains extracellular nucleic acids, or membrane compromised cells; (d) Overlay of all three filters. These images show that trout erythrocyte suspensions do not spontaneously release the ET-like structures observed in PMN-enriched cell suspensions. Scale bar = 50  $\mu\text{m}$ ..... 79

Figure 3.2. Bar chart showing the mean fold-change in fluorescence of wells containing trout PMN-enriched cell suspensions ( $4 \times 10^5$  cells  $\text{mL}^{-1}$ ) after initial exposure to Cal (5  $\mu\text{g mL}^{-1}$ , 3 h,  $15^\circ\text{C}$ ) to stimulate release of ET-like structures, and then to DNase-I (0.01 – 100 U  $\text{mL}^{-1}$ ) for 3 h at  $15^\circ\text{C}$ . Exposure of ET-like structures to 10 and 100 U  $\text{mL}^{-1}$  DNase-I significantly reduced fluorescence attributed to ET-like structures compared to controls not treated with DNase, indicating ET-like structures are digested by DNA.  $*p < 0.05$  compared to a control not exposed to DNase-I at each time point. Error bars represent s.e.m.  $n = 5$  wells..... 80

Figure 3.3. Representative fluorescence microscopy images of stained ET-like structures released from trout PMN-enriched cell suspensions ( $4 \times 10^5$  cells  $\text{mL}^{-1}$ ) exposed to Cal (5  $\mu\text{g mL}^{-1}$ , 3h,  $15^\circ\text{C}$ ), treated with (a)  $\text{dH}_2\text{O}$  in DNase buffer, as a negative control for DNase treatment; (b) treated with DNase-I (100 U  $\text{mL}^{-1}$ , 3 h,  $15^\circ\text{C}$ ), stained with SYTOX Green (5  $\mu\text{M}$ , 5 min, room temperature). This figure confirms that the ET-like structures in the PMN-enriched cell suspensions were composed of nucleic acids, as they were susceptible to degradation by DNase-I. Scale bars = 100  $\mu\text{m}$ ..... 81

Figure 3.4. Representative fluorescence microscopy images of immunocytochemically stained ET-like structures released from trout PMN-enriched cell suspensions ( $4 \times 10^5$  cells  $\text{mL}^{-1}$ ) exposed to Cal (5  $\mu\text{g mL}^{-1}$ , 3h,  $15^\circ\text{C}$ ), confirming the presence of proteins characteristic for extracellular traps (ETs) in association with extracellular DNA. (a-c) DAPI filter showing the staining of ET-like structures (white arrows) with membrane-permeable nucleic acid-specific DAPI. (d-f) FITC-conjugated anti-myeloperoxidase (MPO, 1:20), neutrophil elastase (NE, 1:20), and histone H2A antibodies (1:2000) demonstrate positive staining which co-localises with the ET-like structures. (g-i) Merged DAPI and FITC channels confirming the co-localisation of ET-like fibres with MPO, NE, and H2A with DAPI-stained DNA fibres, respectively (white arrows)..... 84

Figure 3.5. Confocal microscopy re-constructed 3-dimensional image of SYTOX Green-stained cell suspension (5  $\mu\text{M}$ , 5 min, room temperature). Cells within the PMN-enriched cell suspension (incubated for 24 h at  $15^\circ\text{C}$ ) are shown at the top of the image with DNA, most probably an ET, as indicated by white arrows. A large ET fibre can be observed extending

below from the cluster of cells observed above. The full video is found at <https://goo.gl/4RQg2Z>. ..... 85

Figure 3.6. Bar chart showing the mean fold-change in fluorescence from wells containing trout PMN-enriched cell suspensions ( $4 \times 10^5$  cells mL<sup>-1</sup>) after initial exposure to Cyto D (0 – 20  $\mu$ M, 30 min, 15°C), and then induced to form ETs with Cal (5  $\mu$ g mL<sup>-1</sup>) for up to 6 h at 15°C. Exposure of PMN-enriched cell suspensions to 5, 10, or 20  $\mu$ M Cyto D resulted significantly less fluorescence (attributable to ETs) compared to controls not exposed to Cyto D at 6 h, indicating that Cyto D is causing the reduction in ET release. \* $p < 0.05$  compared to a control not exposed to Cal at each time point. Error bars represent s.e.m.  $n = 4$  fish. .... 87

Figure 3.7. Representative fluorescence microscopy images of trout PMN-enriched cell suspensions ( $4 \times 10^5$  cells mL<sup>-1</sup>) stained with SYTOX Green (5  $\mu$ M, 5 min, room temperature) after initial 30 min exposure to: (a) RPMI1 negative control (b) Cyto D (10  $\mu$ M, 30 min, 15°C), followed by exposure to Cal (5  $\mu$ g mL<sup>-1</sup>, 3h, 15°C). Exposure to Cyto D before Cal resulted in less ETs released from the PMN-enriched cell suspension compared to cells that were not exposed to Cyto D. Within the cells treated with Cyto D, some membrane-compromised cells with fragmented nuclei resembling apoptotic bodies were observed (white arrows), indicating Cyto D may be inducing apoptosis. Scale bar = 100  $\mu$ m. .... 88

Figure 3.8. Bar chart showing the mean fold-change in fluorescence from wells containing trout PMN-enriched cell suspensions ( $4 \times 10^5$  cells mL<sup>-1</sup>) after exposure to DPI (0.1 – 25  $\mu$ M) for up to 12 h at 15°C. Exposure of PMN-enriched cell suspensions to 5, 10, and 25  $\mu$ M DPI alone resulted significantly greater fluorescence (attributable to ETs) at 12 h compared to controls not exposed to DPI, indicating that DPI can induce ET release. \* $p < 0.05$  compared to a control not exposed to DPI at each time point. Error bars represent s.e.m.  $n = 4$  fish... 89

Figure 3.9. Representative fluorescence microscopy images of trout PMN-enriched cell suspensions ( $4 \times 10^5$  cells mL<sup>-1</sup>) stained with 5  $\mu$ M SYTOX Green (5  $\mu$ M, 5 min, room temperature) after exposure to (a) RPMI1 negative control (b) DPI 10  $\mu$ M, both for 3 h, 15°C. Exposure to DPI resulted in more visible ETs compared to non-exposed controls. Exposure of cells to DPI resulted in visibly more ET release compared to negative controls. Scale bar = 100  $\mu$ m. .... 90

Figure 3.10. Bar chart showing the mean fold-change in fluorescence from wells containing trout PMN-enriched cell suspensions ( $4 \times 10^5$  cells mL<sup>-1</sup>) after exposure to: (a) Cal, (b) flagellin, (c) pLPS, (d) PMA for up to 12 h at 15°C, and stained with SYTOX Green (5  $\mu$ M, 5 min, room temperature). Exposure of PMN-enriched cell suspensions to 1  $\mu$ g mL<sup>-1</sup> Cal or greater at 1 h; 100 ng mL<sup>-1</sup> flagellin at 1 h, or 40 nM of PMA or greater at 9 h resulted in significantly greater fluorescence (attributable to ETs) compared to negative controls, indicating that Cal, flagellin, and PMA can induce ET release. \* $p < 0.05$  compared to a control

not exposed to Cal, flagellin, pLPS, or PMA at each time point. Error bars represent s.e.m.  $n = 4$  fish..... 95

Figure 3.11. (a-e) Representative phase contrast images of representative trout PMN-enriched cell suspensions ( $4 \times 10^5$  cells mL<sup>-1</sup>) exposed to: (a) unexposed control; (b) Cal 5  $\mu\text{g mL}^{-1}$ ; (c) flagellin 100 ng mL<sup>-1</sup>; (d) pLPS 50  $\mu\text{g mL}^{-1}$ ; (e) PMA 40 nM; (f-j) for 6 h at 15°C. Paired SYTOX Green-stained cells (5  $\mu\text{M}$ , 5 min, room temperature) under a FITC filter, showing extracellular DNA and membrane-compromised, non-viable cells. ETs are indicated by white arrows which are absent in unstimulated controls and pLPS-treated PMNs (k-o) Merged overlay of phase contrast images and fluorescence images. Scale bar = 100  $\mu\text{m}$ .. 97

Figure 3.12. Bar chart showing the mean fold-change in fluorescence from wells containing trout PMN-enriched cell suspensions ( $4 \times 10^5$  cells mL<sup>-1</sup>) to heat-inactivated *V. anguillarum* (Vib 6 and Vib 87) for up to 12 h at 15°C, then staining with SYTOX Green (5  $\mu\text{M}$ , 5 min, room temperature). Exposure of PMN-enriched cell suspensions to heat-inactivated *V. anguillarum* (both Vib 6 and Vib 87) did not result in a significant difference in fluorescence (attributable to ETs) at any time point compared to negative controls, indicating that heat-inactivated *V. anguillarum* does not induce ET release.  $*p < 0.05$  compared to a control not exposed to *V. anguillarum* at each time point. Error bars represent s.e.m.  $n = 4$  fish. .... 98

Figure 3.13. Bar chart showing the mean fold-change in fluorescence from wells containing trout PMN-enriched cell suspensions ( $4 \times 10^5$  cells mL<sup>-1</sup>) to Cal (5  $\mu\text{g mL}^{-1}$ ) at 10 min intervals over 60 min at 15°C, then staining with SYTOX Green (5  $\mu\text{M}$ , 5 min, room temperature). Exposure of PMN-enriched cell suspensions to Cal resulted in a significant difference in fluorescence (attributable to ETs) compared to negative controls at every time point, indicating that Cal induces ET release immediately upon exposure to cells within the PMN-enriched cell suspension.  $*p < 0.05$  compared to a control not exposed to Cal at each time point. Error bars represent s.e.m.  $n = 4$  fish..... 100

Figure 3.14. Scatterplot showing the mean fold-change in fluorescence from wells containing trout PMN-enriched cell suspensions ( $4 \times 10^5$  cells mL<sup>-1</sup>) from individual fish (labelled 1 to 6) to DPI (25  $\mu\text{M}$ ) or PMA (40 nM) for up to 12 h at 15°C, then staining with SYTOX Green (5  $\mu\text{M}$ , 5 min, room temperature). Each line represents the fluorescence compared to negative controls (being 1-fold) associated with cells from an individual fish. Data from experiment (Figure 3.10) represent labelled fish 1 to 4, and the two additional fish is labelled 5 and 6, (a) DPI (25  $\mu\text{M}$ ) resulted in four out of the six fish (1, 2, 3, and 4) releasing ETs upon stimulation throughout 12 h. (b) Out of six fish tested per treatment, two fish (1 and 2) resulted in a significant response when stimulated with PMA (40 nM) throughout 12 h. Error bars represent s.e.m.  $n = 6$  fish, 3 wells..... 101

Figure 3.15. Representative fluorescence microscopy images of trout PMN-enriched cell suspensions ( $4 \times 10^5$  cells mL<sup>-1</sup>) isolated from trout numbered in Figure 3.14b, stained with 5  $\mu\text{M}$  SYTOX Green (5  $\mu\text{M}$ , 5 min, room temperature) after exposure to PMA at 40 or 60 nM

for 9 h at 15°C. These images demonstrate that different fish have a different ET release response when exposed to the same concentration of PMA. (a) Trout number 4 exposed to 40 nM PMA or (b) 60 nM PMA resulting in ET release; (c) Trout number 1 (in relation to Figure 3.14b) exposed to 40 nM PMA (d) 60 nM PMA. Scale bar = 100 µm ..... 102

Figure 3.16. Scatterplot showing the relationship between trout mass against spontaneous ET release from trout PMN-enriched cell suspensions ( $4 \times 10^5$  cells mL<sup>-1</sup>) incubated for 1 h at 15°C, then stained with SYTOX Green (5 µM, 5 min, room temperature). These data show a significant negative correlation of fluorescence (attributable to ETs), with fish of greater wet mass having lower spontaneous ET release ( $R^2 = 0.4388$ ;  $F_{1,17} = 13.29$ ;  $p < 0.01$ ).  $n = 19$  trout, weighing 43.8 – 373.0 g. .... 103

Figure 4.1. The total clear zone area after incubation (with the agent being examined for nuclease activity) was calculated from the mean of perpendicular diameters ( $d^1$  and  $d^2$ ) measured after 24 h incubation with at 22°C. The area (3.14 mm<sup>2</sup>) from the 2-mm diameter holes punched in the DNase agar was subtracted from the total clear zone area..... 116

Figure 4.2. Scatterplot showing the relationship between DNase-I concentration (U mL<sup>-1</sup>) against mean clear zone area (mm<sup>2</sup>) of the DNase agar, indicating relative nuclease activity. This graph shows there is a strong relationship ( $R^2 = 0.9443$ ) between DNase-I concentration in 2-mm diameter wells in DNase agar and nuclease activity.  $y = 1.7522x + 169.86$ . All concentrations of DNase-I except 5 U mL<sup>-1</sup> gave a visibly detectable digestion of DNase agar. Error bars represent s.e.m.  $n = 3$ ..... 125

Figure 4.3. Representative images of DNase agar digestion by (a) *V. anguillarum* Vib 87, (b) *V. anguillarum* Vib 6, and (c) *Y. ruckeri* YR 1 bacterial solutions after growth on DNase agar for 24 h at 22°C. Clear zone area indicates digestion of DNase agar caused by nuclease activity present in the solution containing the bacteria. All bacteria were cultured in a shaking incubator (150 RPM, 16 h, 22°C) adjusted to  $A_{600}$ : 0.7 before inoculating into 2-mm diameter wells on DNase agar. Scale bar = 6 mm. .... 126

Figure 4.4. (a) Representative images of clear zones in the DNase agar *V. anguillarum* Vib 6 culture filtrate after 24 h at 22°C, with the clear zone relative nuclease activity. Bacteria was cultured in a shaking incubator (150 RPM, 16 h, 22°C), bacteria were removed with a 0.22-µm syringe filter. The culture filtrate was condensed with rotating vacuum evaporation (35°C) up to 60 min (removing some for assay every 10 min), and the culture filtrate was assayed by inoculating into 2-mm<sup>2</sup> diameter wells on DNase agar. (b) Bar chart showing *V. anguillarum* Vib 6 culture filtrate nuclease activity measured by mean clear zone area (mm<sup>2</sup>) on DNase agar after 24 h at 22°C incubation. Culture filtrate was concentrated with rotating vacuum evaporation (medium temperature setting) over 60 min, showing as the culture filtrate becomes more concentrated, nuclease activity increases. The nuclease activity of the filtrate was assayed at 10 min condensing intervals, by inoculating into 2-mm diameter wells on DNase agar. Error bars represent s.e.m.  $n = 3$ ..... 128



Figure 4.5. Bar chart showing *V. anguillarum* Vib 6 culture filtrate (Cf: 0.2) nuclease activity after exposed to EDTA (0 – 25 mM, 24 h at 22°C), measured by mean clear zone area (mm<sup>2</sup>) on DNase agar. Incubation with 10, and 25 mM EDTA, but not 1 mM, was sufficient to limit free cations required for nuclease activity within the *V. anguillarum* Vib 6 culture filtrate compared to non-exposed controls. \**p*<0.05. Error bars represent s.e.m. *n* = 3..... 129

Figure 4.6. Bar chart showing *V. anguillarum* Vib 6 culture filtrate (Cf: 0.2) nuclease activity (light grey bars) in the presence of EDTA (25 mM, black bars), against DNase-I (5 – 600 U mL<sup>-1</sup>; grey bars), measured by mean clear zone area (mm<sup>2</sup>) on DNase agar after 24 h at 22°C incubation. The *V. anguillarum* Vib6 filtrate nuclease activity was calculated to be equivalent to 131.58 U mL<sup>-1</sup> at Cf: 0.2, and ~26.32 U mL<sup>-1</sup> when uncondensed. Error bars represent s.e.m. *n* = 3..... 130

Figure 4.7. Bar chart showing *V. anguillarum* Vib 6 culture filtrate (Cf: 0.2) nuclease activity after three freeze-thaw cycles from -20°C to thawing at room temperature, measured by mean clear zone area (mm<sup>2</sup>) on DNase agar after 24 h at 22°C incubation. No statistically significant differences were observed between mean nuclease activity between the three cycles compared to the control indication robustness of the nuclease in the filtrate. Error bars represent s.e.m. *n* = 3..... 132

Figure 4.8. Bar chart showing *V. anguillarum* Vib 6 culture filtrate (Cf: 0.2) nuclease activity after exposure to heat blocks with temperatures ranging from 4°C to 60°C, for up to 60 min, measured by mean clear zone area (mm<sup>2</sup>) on DNase agar after 24 h at 22°C incubation. Nuclease activity was abolished between 0 – 10 min of incubation at 50°C and 60°C, while the activity of the nuclease remains constant at other temperatures and time points. There was no statistical difference between nuclease activity at every time point or temperature. Not all bars visible as no clear zones were detected in some instances. Error bars represent s.e.m. *n* = 3..... 133

Figure 4.9. Scatterplot showing the relative nuclease activity by mean DNase agar digestion area (mm<sup>2</sup>) after 24 h, 22°C incubation with Vib 6 nuclease filtrate (◆) and whole bacteria (■) over different pH (6.5 – 11). Bacteria was prepared to A<sub>600</sub>: 1.6. The optimum pH for nuclease activity was observed at 8.5. For filtrate:  $y = 14.754x^3 - 469.33x^2 + 4777x - 14462$ , R<sup>2</sup> = 0.9374; for bacteria  $y = 16.409x^3 - 531.85x^2 + 5584.7x - 18199$ , R<sup>2</sup> = 0.9412. Error bars represent s.e.m. *n* = 3..... 134

Figure 4.10. Scatterplot showing the relative nuclease activity by mean DNase agar digestion area (mm<sup>2</sup>) after 24 h, 22°C incubation with Vib 6 nuclease filtrate (◆) and whole bacteria (■) over different salinities (0.5 – 4%). Whole bacteria was prepared to A<sub>600</sub>: 1.6. For filtrate:  $y = 34.115x^2 - 368.36x + 928.39$ , R<sup>2</sup> = 0.9665; bacteria:  $y = 31.838x^2 - 392.21x + 1443$ , R<sup>2</sup> = 0.9778. Error bars represent s.e.m. *n* = 6..... 135

Figure 4.11. Scatterplot showing liquid culture of *V. anguillarum* Vib 6 in TSB 2% NaCl (150 RPM, 22°C) over 29 h (x-axis), against nuclease activity per bacteria, expressed by mean

clear zone area (mm<sup>2</sup>) over absorbance (A<sub>600</sub>) (y-axis). This shows that at 5 h, *V. anguillarum* Vib 6 produces enough nuclease to be detected by the DNase agar assay. During *V. anguillarum* Vib 6 culture, the bacteria expresses a consistent amount of extracellular nuclease activity. Error bars represent s.e.m. (present with A<sub>600</sub>, but too small to be observed). *n* = 4 biological replicates. .... 137

Figure 4.12. Bar chart showing the amount fluorescence emitted from wells containing PMN-enriched cell suspensions (4 × 10<sup>5</sup> CFU mL<sup>-1</sup>) induced to form ETs with Cal (5 µg mL<sup>-1</sup>, 3 h, 15°C), stained with SYTOX Green (5 µM, 5 min, room temperature). The fluorescence is indicative of the amount of extracellular nucleic acid polymers (including ETs) are present. The ETs within each well was exposed to different treatments: 'Control + ETs' contained PMN-enriched cell suspensions induced to form ETs with Cal and incubated with dH<sub>2</sub>O and DNase buffer (1x). 'Control - ETs' contained PMN-enriched cell suspensions induced with Cal and incubated with DNase 10 U mL<sup>-1</sup> diluted with dH<sub>2</sub>O, and DNase buffer (1x). 'Vib 6 filtrate (Cf: 0.2, 0.4, unconcentrated)' contained the contained PMN-enriched cell suspensions induced with Cal and incubated with difference concentrates of *V. anguillarum* Vib 6 culture filtrates. 'Vib 87 filtrate (Cf: 0.2)' is the same treatment as above, using a nuclease-deficient isolate. Letters indicate statistical differences (*p*<0.05). Error bars represent s.e.m. *n* = 5 wells. .... 138

Figure 4.13. Bar chart showing the amount fluorescence emitted from wells containing 0.22-µm-filtered fish skin mucus stained with SYTOX Green (5 µM, 5 min, room temperature). The fluorescence is indicative of the nucleic acid polymers present within the mucus. The mucus in the wells were treated with DNase-I (10 U mL<sup>-1</sup>), *V. anguillarum* Vib 6, or Vib 87 culture filtrate (both condensed to 20% of original mass/ Cf: 0.2), compared to negative controls treated with dH<sub>2</sub>O. Letters indicate statistical differences (*p*<0.05). Error bars represent s.e.m. *n* = 3 wells. .... 140

Figure 4.14. Scatterplot showing culture of *V. anguillarum* strains in TSB 2% NaCl supplemented with 10, 20, 30, and 40% Atlantic salmon skin mucus, 150 RPM, 22°C. (a) Vib 6, (b), Vib 87, (c) NB 10 Error bars not shown to improve graph clarity. *n* = 6. .... 141

Figure 5.1. Scatterplot showing the relationship between *V. anguillarum* Vib 87 viability over time (as measured by mean CFU recovered from the well) in the presence or absence of Cal (5 µg mL<sup>-1</sup>, 4 h, 22°C). Suspensions of *V. anguillarum* Vib 87 in PBS were tested at (a) 10<sup>5</sup> CFU mL<sup>-1</sup>; (b) 10<sup>4</sup> CFU mL<sup>-1</sup>; and (c) 10<sup>3</sup> CFU mL<sup>-1</sup>. No significant differences were detected between mean CFU recovered from wells with and without Cal at each bacterial concentration and time point (*p*<0.05). Error bars represent s.e.m. *n* = 3..... 154

Figure 5.2. Scatterplot showing the relationship between *V. anguillarum* Vib 87 and Vib 6 (10<sup>3</sup> CFU mL<sup>-1</sup>) viability over time (as measured by mean CFU recovered from the well) in the presence or absence of DNase-I (100 Ut mL<sup>-1</sup>, 4 h, 22°C). No significant differences

were detected between mean CFU recovered from wells with DNase-I or control treatments (dH<sub>2</sub>O with DNase buffer) at each time point ( $p > 0.05$ ). Error bars represent s.e.m.  $n = 3$ . 155

Figure 5.3. Bar graph showing (a) *V. anguillarum* Vib 87, (b) *V. anguillarum* Vib 6 ( $10^4$  CFU mL<sup>-1</sup>) bacterial CFU recovered from different positions within a well of a 96-well plate after centrifugation (510 × g, 10 min, 22°C). Wells subjected to centrifugation had significantly fewer CFU recovered at the top of the well compared to the top of non-centrifuged control wells; while significantly greater CFU was recovered from the bottom of centrifuged wells compared to the bottom of non-centrifuged control wells. \* $p < 0.05$ . Error bars represent s.e.m.  $n = 3$ . 156

Figure 5.4. Bar graph showing the amount of *V. anguillarum* (Vib 87) CFUs recovered after incubation with trout extracellular traps (released from PMN-enriched cell suspensions after incubation with Cal 5 µg mL<sup>-1</sup>) at 15°C. CFUs was sampled before centrifugation (pre-spin), immediately after centrifugation (0 h), and 1 h at 15°C. *V. anguillarum* Vib 87 was incubated with cell media as a control (Vib 87 only), with Cal and DNase (Vib 87 + Cal + DNase), in the presence of ETs (Vib 87 + ETs), and with DNase-degraded ETs (Vib 87 - ETs). No significant differences of CFUs were found between all treatments before centrifugation (pre-spin). Immediately after centrifugation (0 h), the Vib 87 + ETs treatment resulted in significantly less CFUs recovered than *V. anguillarum* Vib 87 – ETs; which was also observed after 1 h incubation. \* $p < 0.05$ . Error bars represent s.e.m.  $n = 6$ . 158

Figure 5.5. Bar graph showing the amount of *V. anguillarum* CFUs recovered (comparing Vib 87 and Vib 6) after incubation with trout extracellular traps (released from PMN-enriched cell suspensions after incubation with Cal 5 µg mL<sup>-1</sup>) at 15°C. (a) *V. anguillarum* Vib 87 CFUs recovered after incubation with ETs (Vib + ETs) resulted in significantly less CFUs at 0, 1 and 4 h at 15°C when compared to incubation with DNase-digested ETs (Vib - ETs) and controls without cells (Vib 87 only). (b) Vib 6 CFUs recovered after incubation with ETs (Vib 6 + ETs) was not significantly different from the DNase-digested ETs (Vib 6 - ETs) and Vib 6 only controls at 0, 1, and 4 h at 15°C. \* $p < 0.05$ . Error bars represent s.e.m.  $n = 3$ . 159

Figure 5.6. Representative phase contrast and fluorescent images showing co-localisation of *V. anguillarum* Vib 87 stained by DAPI (1 µM) incubated with trout ETs ( $4 \times 10^7$  CFU mL<sup>-1</sup>, 1 h, 15°C) generated from Cal-induced PMN-enriched cell suspensions ( $4 \times 10^5$  CFU mL<sup>-1</sup>, 30 min, 15°C). ETs were stained with SYTOX Green (5 µM, 5 min). (a) Trout PMNs and *V. anguillarum* Vib 87 under phase contrast; (b) DAPI channel showing DAPI-stained *V. anguillarum* Vib 87 in blue; (c) FITC channel showing a mesh of trout ETs stained with SYTOX Green; (d) Merged DAPI and FITC images which show *V. anguillarum* Vib 87 in blue co-localising with ETs in green. The magnified section shows a distinction between staining of the bacteria and extracellular traps, confirming no counterstaining was occurring between the DAPI and SYTOX Green. Scale bar = 100 µm, all images were taken at the same magnification. 161

Figure 5.7. Representative fluorescent microscopy images with both DAPI and FITC channels merged together showing wells containing *V. anguillarum* Vib 87 or Vib 6 co-incubated with trout ETs ( $4 \times 10^7$  CFU mL<sup>-1</sup>, 1 h, 15°C) released from Cal-induced PMN-enriched cell suspensions ( $4 \times 10^5$  cells mL<sup>-1</sup>, 30 min, 15°C). *V. anguillarum* was stained blue by DAPI (1 µM) while ETs were stained green by SYTOX Green (5 µM). (a-b) Shows nuclease-deficient *V. anguillarum* Vib 87 co-incubated with ET fibres which were still intact after incubation for 1 h; while (c-d) shows nuclease-producing *V. anguillarum* Vib 6 co-incubated with ET fibres which appeared fragmented without cohesive structure, indicating the action of the nuclease is responsible for degrading the ETs. White arrows (c) indicate the remaining fragments of DNA which do not hold a fibrous structure, indicating nuclease from *V. anguillarum* Vib 6 degrades the ETs. Scale bars = 100 µm..... 162

Figure 5.8. Representative screen-captures from phase contrast videos showing wells containing *V. anguillarum* Vib 87 co-incubated with trout ETs ( $4 \times 10^7$  CFU mL<sup>-1</sup>, 1 h, 15°C) released from Cal-induced PMN-enriched cell suspensions ( $4 \times 10^5$  cells mL<sup>-1</sup>, 30 min, 15°C). Videos (a) and (b) were taken from different wells, both showing the highly motile *V. anguillarum* Vib 87 appearing stuck to, and entirely covered the ET fibres. Free-swimming bacteria can also be observed in the video. The magnified section shows a close-up of an ET appeared to be covered in the grainy-looking bacteria. Magnification x20; scale bar = 100 µm. Videos can be found online using links of Video (a): <https://goo.gl/GQGpHo> ; Video (b) <https://goo.gl/qXYDSb> ..... 163

## List of Tables

Table 1.1. Table showing the components of ETs from neutrophil / PMNs, macrophages, mast cells, and eosinophils, and basophils. #Indicates components which collectively satisfy the definition of ETs. ....	17
Table 1.2. Table of confirmed diagnostic ET markers in fish species. ....	21
Table 1.3. Examples of the different methods used to visualise and quantify ETs. ....	25
Table 1.4. Current evidence for bacterial trapping in ETs released by fish species, showing the inducer used to stimulate ET release, species of bacteria studied, and how the bacterial interaction was detected and measured. Interaction of bacteria with ETs were not investigated in studies involving <i>Pimephales promelas</i> , <i>Danio rerio</i> , and <i>Lates calcarifer</i> . ..	29
Table 1.5. Known chemical and biological inducers of ET release in different animal species. ....	32
Table 1.6. Known chemical and biological inhibitors of ET release in different animal species.....	34

Table 1.7. Current list of chemical and biological inducers and inhibitors of ET release used in different fish species showing effect of compound, minimum concentration which elicited a response, and earliest time point where a response was reportedly statistically significant.	35
Table 2.1. Volumes of Percoll, HBSS (10x) and dH <sub>2</sub> O required to make up 10 or 15 mL Percoll solutions as discontinuous double or triple layer gradients in a universal tube. ....	44
Table 2.2 Comparison of proportions of polymorphonuclear cell (PMN) and monocyte/macrophage (Mo/M) cells obtained from double and triple-layer Percoll gradient separation methods in rainbow trout. Cytospin preparations of enriched cell populations were stained with rapid Romanowsky stains to allow classification by microscopic observation of cell morphologies. A minimum count from 5 fields of view (FOV) per fish was made to enumerate cell proportions.....	52
Table 3.1. Bacterial isolates used in this Chapter. All isolates were stored at -70°C before isolating for experiments as described in Section 3.2.6.....	75
Table 4.1. Table showing the bacterial isolates/strains used in this Chapter. All isolates/strains were stored at -70°C before isolating for experiments as described in Section 4.2.1. ....	114

## Abbreviations and definitions

x g	Relative centrifugal force
°C	Degree celcius
µg	Microgram
µL	Microliter
µM	Micromolar
2-APB	2-aminoethoxydiphenyl borate
A <sub>600</sub>	Absorbance at 600 nm wavelength
ABAH	4-aminobenzoic acid hydrazide
AFU	Arbitrary fluorescence units
AMP	Antimicrobial peptide
BF	Bright field (microscopy)
CaI	Calcium ionophore
CFU	Colony forming unit
CGD	Chronic granulomatous disease
CHSE-214	Chinhook salmon embryo cells
CMK	Suc-Ala-Ala-Pro-Val chloromethyl ketone
Cyto D	Cytochalasin D
DAPI	4',6-diamidino-2-phenylindole
dH <sub>2</sub> O	Distilled water
DMSO	Dimethyl sulfoxide
DNA	Deoxyribonucleic acid
DNase	Deoxyribonuclease
DPI	Diphenyleneiodonium chloride
ECP	Eosinophil cationic protein
EDTA	Ethylenediaminetetraacetic acid
ET	Extracellular trap
FAO	Food and Agriculture Organization of the United Nations
Fc	Fragment crystallizable region
FCS	Foetal calf/bovine serum
GALT	Gut-associated lymphoid tissue
GCSF	Granulocyte colony stimulating factor
GI	Gastrointestinal
h	Hour
H2A	Histone H2A
H <sub>2</sub> O <sub>2</sub>	Hydrogen peroxide
HBSS	Hank's balanced salt solution
HCl	Hydrochloric acid
HSC	Haematopoietic stem cell
IgG	Immunoglobulin G
IL	Interleukin
IoA	Institute of Aquaculture
LL-37	Cathelicidin
LPS	Lipopolysaccharide
mAb	Monoclonal antibody
MALT	Mucosa-associated lymphoid tissue
MeOH	Methanol
MEP	Megakaryocyte-erythroid progenitor
MET	Macrophage extracellular trap
min	Minute
mL	Millilitre
MM	Metamyelocyte
Mo/M	Monocyte/ Macrophage
MPO	Myeloperoxidase
MPP	Multipotent progenitor cell
ms	Milliseconds
mya	Million years ago
NAC	N-acetylcysteine
NaCl	Sodium chloride

NADPH	nicotinamide adenine dinucleotide phosphate
NADPH oxidase	Nicotinamide adenine dinucleotide phosphate-oxidase
NE	Neutrophil elastase
NET	Neutrophil extracellular trap
ng	Nanogram
nm	nanometre
nM	Nanomolar
PAD4	Protein arginine deiminase 4
PBS	Phosphate buffered saline
PFA	Paraformaldehyde
Poly IC	Polyinosinic:polycytidylic acid
PS	Phosphatidylserine
PKC	Protein kinase C
PM	Promyelocyte
PR3	Proteinase 3
pLPS	Pure lipopolysaccharide
PMA	Phorbol myristate acetate
PMN	Polymorphonuclear cell (granulocyte)
RA	Rheumatoid Arthritis
RapiDiff	Rapid Romanowski differentiation stain
RNA	Ribonucleic acid
ROS	Reactive oxygen species
RPM	Revolutions per minute
RPMI	Roswell Park Memorial Institute medium
s.e.m.	Standard error of the mean
SEM	Scanning electron microscopy
SK	Potassium channel of small conductance
SLE	Systemic Lupus Erythematosus
TLR	Toll-like receptor
TNF	Tumour necrosis factor
TSA	Tryptone soya agar
TSA	Tryptone soy agar
TSB	Tryptone soya broth
TSB	Tryptone soy broth
TX-100	Triton X-100
U	Units
Vib	<i>Vibrio anguillarum</i> isolate/ strain
YR	<i>Yersinia ruckeri</i> isolate/ strain





# Chapter 1: General Introduction

## 1.1. Aquaculture and disease management

The growing demand of seafood products has extended beyond what is sustainable from wild fisheries. In 2014, global aquaculture products including finfish, mollusks and crustaceans were estimated to be 17% of global total animal protein supply, and more than 50% of total fish production (FAO, 2017). The same year, finfish harvested from aquaculture amounted to 51.9 million tons, with an estimated first-sale value of US\$160.2 billion (Ababouch *et al.*, 2016). Within the finfish, salmonids are one of the most valued fish for consumption and holds 17% of the total value of internationally traded fish, and farmed salmon exceeds 2 million tonnes compared to 700 thousand tonnes supplied from wild-fisheries (FAO, 2017). The global human population is estimated to reach 9 billion by 2050, which places a critical demand for aquaculture products due to the unsustainable exploitation of wild fisheries. In response, the aquaculture industry has taken a more prominent role in providing fish and shellfish for the global demand, while reducing the pressure from wild fisheries (Forti, 2017).

Transmissible diseases in aquaculture have an enormous detrimental impact on wild and farmed fish, resulting serious ecological and economic problems (Stentiford *et al.*, 2017). Industry-wide losses due to diseases exceed US\$6 billion per year, with certain sectors such as the shrimp industry resulting in losses greater than 40% of global production (The World Bank, 2014; Ababouch *et al.*, 2016; Stentiford *et al.*, 2017). Moreover, climate change has placed additional burden on the industry, as increasing global temperatures have resulted in the increased prevalence of diseases usually found in warmer conditions (de Silva *et al.*, 2009).

Globally, salmonids such as rainbow trout (*Oncorhynchus mykiss*) and Atlantic salmon (*Salmo salar*) are some of the most extensively farmed and highly valued fish, with the majority of production in Chile, Turkey, Canada, Norway, and the United Kingdom (Arnfinn Aunsmo *et al.*, 2015; FAO, 2017; Forti, 2017). While salmonids are susceptible to a range of bacterial, fungal, viral, and parasitological infections, research to date has led to the introduction of successful control measures in the form of antibiotics, vaccines, or husbandry and stock management practices for diseases that were once associated with severe losses (Cabello, 2006). However, poor biosecurity and overuse of antibiotics on salmonid farms allowed microbial pathogens to acquire resistance to multiple classes of antibiotics (Cabello, 2006; Smith, 2008; Buschmann *et al.*, 2012). Though some of these challenges were resolved through the introduction of efficacious vaccines, there are still several certain infectious diseases which do not have available effective vaccines. Some of these diseases include Red Mark Syndrome, Rainbow Trout Fry Syndrome, and Infectious Salmon Anemia (Somerset

*et al.*, 2005; Birkbeck *et al.*, 2007; Metselaar *et al.*, 2010; Hoare *et al.*, 2017). In addition, the development and high prevalence of antibiotic resistance by microbial pathogens in aquaculture such as *Vibrio spp.* and *Aeromonas spp.*, has rendered antibiotics like tetracycline an unsuitable long-term treatment (Kim *et al.*, 2004; Watts *et al.*, 2017). Thus, there remains the need to develop new treatments and strategies to combat infectious disease within aquaculture systems. A deeper insight into the immune mechanisms and immune cells that limit pathogen propagation is crucial for the development of new effective strategies to combat infectious disease. Yet, there is a lag of understanding and research within fish immunology compared to humans and mammals, due to the lack of resources and research tools available for fish research. The lack of research tools for fish is compounded by the biological diversity of fish species which have uniquely functioning immune systems, resulting in a greater challenge for the development of medical interventions to treat infectious fish diseases. Ultimately, a greater push towards understanding the immune strategies implemented by the host or pathogen infection strategies may lead to the development of novel therapeutics and treatments to reduce infectious, microbial disease-related mortalities in aquaculture.

## **1.2. Fish Immune systems**

Fish are a heterogeneous group of organisms that consist three major groups: agnathans (lampreys and hagfish), chondrichthyes (sharks and rays), and teleosts (bony fish); these groups contain in excess of 30,000 species and colonise vastly different environments, from deep oceans to freshwater streams. Fish have evolved immune systems able to combat bacterial, fungal, viral, or parasitic agents that cohabit the aquatic environment, and their immune systems are structurally similar to the higher vertebrates such as mammals (Uribe *et al.*, 2011). The immune system in fish is divided into innate and adaptive responses. More than 98% of multicellular organisms rely on an innate, non-specific immune system that is supported mainly phagocytic cells and secretion of antimicrobial molecules (Hoover *et al.*, 1998; Scocchi *et al.*, 2009). The innate immune response is the first response encountered by pathogens once they have invaded the host, whereby the cells of the innate immune system responds in a non-antigen-specific fashion unlike the adaptive immune response (Uribe *et al.*, 2011; Delves *et al.*, 2017). The structure of the innate immune system can be divided into three components, i) anatomical barriers such as skin, mucus, mucosal barriers, and the acidity of the gastrointestinal (GI); ii) humoral immunity which involves the complement system, pro-inflammatory cytokines, naturally occurring antibodies that are produced without any previous infection, proteases, pentraxins, and other antimicrobial peptides (AMPs); iii) cellular immunity which is mediated by cells that can phagocytose microbes or degranulate and release cytotoxic compounds (Table 1.1). These phagocytic cells mainly consist of neutrophils, monocyte/macrophages and dendritic cells, while cells which degranulate consist

mainly of mast cells, eosinophils and basophils. The structure of the adaptive immune system is divided into T-cell or B-cell mediated immunity, whereby these cells require presented antigens and costimulatory factors to prime a highly specific immune response.

Upon successful bypass of the first part of the innate system, the invading microbial pathogens encounters the innate immune system which acts as a first line of defence to manage the invasion, whereby white blood cells (leukocytes) of the innate system called phagocytes, engulf and kills the pathogens non-specifically through phagocytosis (Delves *et al.*, 2017). Phagocytosis is an active process, dependent on actin polymerisation, that allows the cytoskeletal to change and permit internalisation of the pathogen into the cell. The internalised pathogen is contained in a phagosome, whereby reactive oxygen species (ROS) produced by nicotinamide adenine dinucleotide phosphate (NADPH) oxidase, are fused with the phagosomes to directly kill the pathogen in a process called respiratory burst (Aldieri *et al.*, 2008). Upon recognition of pathogens by phagocytes, pro-inflammatory cytokines such as interleukin 1 beta (IL-1 $\beta$ ) and tumour necrosis factor alpha (TNF- $\alpha$ ), and chemotactic cytokines called chemokines such as interleukin-8 (IL-8) which control the migratory patterns of immune cells are produced by phagocytic cells such as neutrophils and macrophages, acting as signals to further promote recruitment of these phagocytes and primes a protective response within the host (Griffith *et al.*, 2014). These chemokines also control the homeostatic trafficking of a larger group of immune cells including B-cells, dendritic cell precursors, granulocytes and mast cells between the hematopoietic tissues, circulation, and peripheral tissues (Griffith *et al.*, 2014). The digested material is processed by the phagocyte and presented with co-stimulatory molecules to cells of the adaptive immune system, initiating the adaptive response (Delves *et al.*, 2017). Here, the host begins to develop an adaptive immune response that is coordinated by the crosstalk of cells and humoral mediators between innate and adaptive immune systems (Secombes *et al.*, 2011; Wangkahart *et al.*, 2016; Zou *et al.*, 2016; Thompson, 2017). The adaptive immune response is slowly developed to ensure high specificity to the pathogen. As a result, the adaptive response is slow-responding which take days to fully establish in comparison to the non-specific innate response that activates within minutes of infection (Delves *et al.*, 2017). The receptors responsible for recognising microbial pathogens are called pathogen recognition receptors (PRRs), and the proteins which are secreted and act in an endocrine and paracrine fashion between different immune components are called cytokines (Griffith *et al.*, 2014; Delves *et al.*, 2017). Different cells of the immune response can be characterised by their specific subset of cell surface markers called cluster of differentiation (CD), which usually act as receptors or ligands on leukocytes (Delves *et al.*, 2017). The PRRs, cytokines, and CD markers on of fish cells often share similar function and structure to that of higher vertebrates; however, mammalian immune systems

are better characterised than fish systems (Richards *et al.*, 2001; Fernández *et al.*, 2002; Tort *et al.*, 2003; Elson *et al.*, 2007; Zou *et al.*, 2007; Secombes *et al.*, 2011; Thompson, 2017).

### **1.2.1. Innate immune system**

The innate immune system in fish is first performed by the physical barriers on the exterior of the fish, serving to protect tissues that are directly exposed to the aquatic environment, and preventing pathogen entry into the host. These barriers include skin, scales, epithelial cells of the gills, the gut, and the mucus that covers the surface of the fish. Fish skin mucus acts as a natural, physical, semi-permeable barrier that allows the exchange of gases, nutrients, water, and biological compounds. Mucus contains an abundance of mucin, which is a group of highly glycosylated proteins with strongly adhesive properties that serve to immobilise pathogens (Fast *et al.*, 2002). Furthermore, mucus contains various enzymes that contribute microbial defence, such as lysozyme (possessing bacteriolytic activity), acid-alkaline phosphatases, lectins, various secreted immunoglobulins, proteases, and AMPs including the alpha-helical amphipathic peptides, defensins, cysteine-rich AMPs, and histone fragments (Fast *et al.*, 2002; Fernández *et al.*, 2002; Ángeles Esteban, 2012). Several phagocytic leukocytes including mast cells, eosinophils and neutrophils have been found on fish skin and in skin mucus which can contribute to immune defence through phagocytosis, release of antimicrobial compounds, and stimulating nearby adaptive immune cells (Murray *et al.*, 2003; Rakers *et al.*, 2013; Parra *et al.*, 2015).

#### **1.2.1.1. Cells of the innate immune system**

Phagocytic cells such as monocytes/macrophages (mononuclear cells), mast cells, and granulocytes that include neutrophils, basophils, and eosinophils (often referred to as polymorphonuclear cells, i.e. PMNs) are important at recognising and killing invasive microbial pathogens (Kaattari, 1992; Martin *et al.*, 2010). If a pathogen has succeeded in bypassing penetrating the physical barriers, phagocytic cells can help to clear the invasive microorganisms whereby phagocytosis is initiated by cell recognising foreign structures called pathogen-associated molecular patterns (PAMPs). These PAMPs are small molecular motifs which are conserved within classes of microbes, such as microbial polysaccharides, lipopolysaccharides (LPS), peptidoglycans, bacterial and viral DNA or RNA (Jyonouchi *et al.*, 1993; Elson *et al.*, 2007; Sepulcre *et al.*, 2009; Pietretti *et al.*, 2014). Toll-like receptors (TLRs), which are a type of PRR, are responsible for recognising specific types of PAMPs. So far, 21 TLRs have been reported in teleosts (TLR1-5, 5S, TLR7-9, TLR13, 14, TLR18-23 and TLR25-28), and many are mammalian TLR orthologs that share the same function; though there are also teleost-specific TLRs (Pietretti *et al.*, 2014; Nie *et al.*, 2018). Among these, the structure

and function of teleost TLR1-3, 5, and 7-9 are similar to their mammalian counterparts, though teleost TLR4 is structurally conserved but may not recognise LPS unlike in mammals (Sepulcre *et al.*, 2009; Nie *et al.*, 2018). The recognition of TLRs to PAMPs coated leads to the activation of pathogen-specific immune responses that are coordinated and dependent on which type of TLR is activated. Different immune cells respond by initiating distinct transcriptomic programmes which regulate the response of the cell or tissue, these normally include the production of several cytokines to elicit additional immune responses, such as further recruitment of phagocytic cells to the site of infection by chemokines (Pietretti *et al.*, 2014). The efficacy of the innate response functions in the absence of memory, i.e. does not rely on previous recognition of PAMPs and is inducible within minutes (Tort *et al.*, 2003).

Mast cells, granulocytes, and natural killer cells can also release toxic intracellular granules into the external milieu by a process called degranulation (Carlson *et al.*, 1993; Kato *et al.*, 1998; Alter *et al.*, 2004; Reite *et al.*, 2006; Havixbeck *et al.*, 2015). These granules are bioactive compounds and proteins which vary depending on cell type (Table 1.1). Granules from granulocytes and natural killer cells consist of proteins which form pores in microbial membranes, break up bacterial membrane structures through proteolytic activity, or promote generation of cytotoxic chemical such as hypochlorous acid; while granules of mast cells contain greater proportions of histamine. Natural killer cells are known to mediate antiviral clearance by lysing virus-infected cells (Delves *et al.*, 2017), though antiviral immunity is beyond the scope of this thesis.

The cells of the innate immune response are directly involved with a process called inflammation. Inflammation is a biological response to infection and injury which acts as to eliminate the initial cause of infection and damage (Reite *et al.*, 2006). Circulating phagocytes such as monocytes, macrophages, and neutrophils recognise pathogens and respond by phagocytosing the pathogens and secreting several cytokines and compounds classified as inflammatory mediators (Reite *et al.*, 2006; Collet, 2014). These cytokines promote leukocyte recruitment by increasing the local levels of leukocyte adhesion molecule on endothelial cells, or act as a chemotactic agent for phagocytes to assist in clearance of the infection. Other compounds secreted from the leukocytes include histamine, nitric oxide and prostaglandins which serve to induce vascular alterations which promote blood flow by vasodilation. Overall, this response is regarded as the first cell-mediated action against infection and injury, but usually requires constant stimulation by pathogens to be sustained.

#### **1.2.1.2. Humoral components of the innate response**

Humoral innate immunity relates to the antimicrobial action of secreted molecules, which include AMPs, naturally occurring antibodies, complement, proteases, and pentraxins. These proteins are constantly produced by a variety of leukocytes and serve to directly or indirectly

kill and/or inhibit the growth of pathogens (Delves *et al.*, 2017). AMPs act to kill pathogens through different modes of action such as inhibition of DNA synthesis, forming pores in the microbial membrane, interfering with protein folding or cell wall synthesis (Smith *et al.*, 2015). Some of these AMPs include proteases which can cleave membrane proteins on microbial membranes, which may interfere with the lifecycle of the organism (Firth *et al.*, 2000; Perera *et al.*, 2012). Circulating complement factors can bind to bacterial membranes and initiate the formation of membrane attack complexes which form pores in microbial membranes, or alternatively act as signals to promote phagocytosis in a process called opsonisation (Boshra *et al.*, 2006; Delves *et al.*, 2017). Pentraxins are also multifunctional antimicrobial proteins which can assist in promoting complement binding to microbial surfaces and opsonise microbes for phagocytosis (Noursadeghi *et al.*, 2000; Lee *et al.*, 2017).

### **1.2.2. Teleost hematopoiesis**

In mammals, the multipotent haematopoietic stem cells (HSC) of the bone marrow are responsible for the production of the majority of blood cells. HSCs differentiate into lymphoid or myeloid progenitor cells, whereby the lymphoid progenitors can further differentiate into natural killer cells, lymphoid dendritic cells, and lymphocytes; while myeloid progenitors develop into all other cell types including erythrocytes, megakaryocytes, granulocytes (monocyte/macrophage and neutrophils), and macrophages (Delves *et al.*, 2017). The combination of specific circulating transcription factors and cytokines recognised by the specific receptors on HSCs result in the development and differentiation of specific blood cell types (Doulatov *et al.*, 2012; Zou *et al.*, 2016). Different blood cell types express unique proportions of CD cell surface molecules which can be used for immunophenotyping the cells.

Despite the extensive evolutionary divergence between teleost fish and mammals, haematopoietic organisation and blood cell functions are largely conserved (Fänge *et al.*, 1985; Hamdani *et al.*, 1998; Zou *et al.*, 2007, 2016; Thompson, 2017). Although most of the primary and secondary lymphoid organs are present in both mammals and fish, the distribution of organ function is dissimilar (Press *et al.*, 1999). Unlike in mammals, the primary haematopoietic organ in fish is the head kidney (also called the anterior kidney or pronephros) which is located posterior to the cranium (Figure 1.1), and is responsible for the production of most erythrocytes, macrophages and granulocytes (Ainsworth, 1992; Press *et al.*, 1999; Willett *et al.*, 1999; Sasaki *et al.*, 2002; Tort *et al.*, 2003; Kobayashi *et al.*, 2006; Zapata *et al.*, 2006; Havixbeck *et al.*, 2015). Other organs such as the thymus, spleen, gut-associated lymphoid tissue (GALT), mucosa-associated lymphoid tissue (MALT), and intertubular tissue of trunk kidney (mesonephros) also possess haematopoietic activity. These tissues have a role in production of T and B lymphocytes, the storage and recycling of blood cells, and

activation of phagocytic cells (Fänge *et al.*, 1985; Tort *et al.*, 2003; Kobayashi *et al.*, 2006; Zapata *et al.*, 2006). Like most teleosts, salmonid fish also have the head kidney as their primary haematopoietic tissue (Sorensen *et al.*, 1997; Pettersen *et al.*, 2000; Sasaki *et al.*, 2002; Rombout *et al.*, 2005). Like mammals, fish also possess specialised professional phagocytic cells, including macrophages and monocytes, granulocytes and dendritic cells (Lieschke *et al.*, 2001; Katzenback *et al.*, 2009; Flerova *et al.*, 2013). Various fish cytokines are also homologous in function and structure with mammalian counterparts, such as IL-10, IL-1 $\beta$  and TNF- $\alpha$  (Zou *et al.*, 2016). The ancestor of all teleost fish and salmonids have undergone whole-genome duplication events around 320-350 mya, and 50-80 mya, respectively, compared to mammals which have implications on gene functions, as this generates new genes which can acquire novel function (Glasauer *et al.*, 2014). This has been theorised to result in the diverse characteristics of fishes observed today, which include teleost-specific TLRs and cytokine function (Glasauer *et al.*, 2014; Zou *et al.*, 2016).

The classical dichotomy of leukocyte lineages is conserved between fish and mammals, whereby maturing cells develop down a myeloid or lymphoid pathway (Rombout *et al.*, 2005). In comparison to mammals, the mechanisms governing haematopoiesis in fish have been less studied, though the tools developed and pioneered in human and mammalian immunology research have aided the characterisation of fish haematology, as many of the reagents and research techniques have been adapted to fish (Secombes *et al.*, 2011; Zou *et al.*, 2016). The classification of fish leukocytes is based on morphological, functional, cytometric, and staining characteristics compared with mammalian counterparts (Katzenback *et al.*, 2009).

### **1.2.3. Polymorphonuclear cells**

Polymorphonuclear cells (PMNs) consist of granulocytes with lobed nuclei which consist mainly of neutrophils, eosinophils and basophils in fish, and these cells possess many morphological and functional similarities to mammals (Lamas *et al.*, 1991; Ainsworth, 1992; Tort *et al.*, 2003; Palić *et al.*, 2011; Havixbeck *et al.*, 2015). PMNs in fish also develop through a myeloid cell differentiation pathway (myelopoiesis) similar to human neutrophils (Figure 1.2). In fish, common myeloid progenitor cells derived from HSC reservoirs in the head kidney differentiate into neutrophils when exposed to specific transcription factors and cytokines such as granulocyte-colony stimulating factor (GCSF) (Figure 1.2) (Ainsworth, 1992; Reite *et al.*, 2006). As PMNs mature in fish, the nucleus becomes more distinct and the PMN develops more granules similarly to human neutrophils (Ainsworth, 1992; Katzenback *et al.*, 2012). Once fully matured, the PMNs migrate out of the head kidney across the sinusoidal endothelium, and into the circulation, whereby they will be recruited to sites of infection by chemotaxis towards interleukins such as IL-8, IL-1 $\beta$ , and TNF- $\alpha$  (Havixbeck *et al.*, 2015;

Thompson, 2017). The presence of granule types depends on the stage in maturity, though mature PMNs possess high concentrations of neutrophil elastase (NE), myeloperoxidase (MPO), cathepsin G, proteinase 3, defensins, and lysozyme within the cytoplasm (Gullberg *et al.*, 1997).

Neutrophils are the most abundant granulocytes in fish and mammals and are responsible for mounting rapid and potent antimicrobial responses towards invading pathogens (Hamdani *et al.*, 1998; Katzenback *et al.*, 2009; Flerova *et al.*, 2013). The primary function of a neutrophil is to phagocytose microbial pathogens (Theilgaard-Mönch *et al.*, 2006) Like mammalian neutrophils, fish neutrophils also degranulate in response to pathogen recognition (Reite *et al.*, 2006; Uribe *et al.*, 2011; Havixbeck *et al.*, 2015). Neutrophils are also intimately linked with inflammation and are found in great abundance at inflammatory sites (Elson *et al.*, 2007). Pro-inflammatory cytokines released by phagocytic cells in response to pathogens stimulate the further recruitment of neutrophils by attracting them via the release of chemokines and cytokines, to bolster phagocytosis and degranulation responses (Baggiolini *et al.*, 1992; Xing *et al.*, 1998).

Importantly, not all neutrophils in fish have the same distinct polymorphic, lobed nucleus as in humans, leading to confusion in the nomenclature surrounding fish neutrophils (Ainsworth, 1992; Sorensen *et al.*, 1997; Hamdani *et al.*, 1998; Pettersen *et al.*, 2000; Rombout *et al.*, 2005); for example, cyprinids such as goldfish (*Carassius auratus*) and June suckers (*Chasmistes liorus*) have neutrophils with kidney-shaped nuclei, while salmonids such as Atlantic salmon (*Salmo salar*), Arctic grayling (*Thymallus arcticus*) and cutthroat and rainbow trout (*Oncorhynchus clarki lewisi*, or *Oncorhynchus mykiss*) have lobed nuclei like in mammals. These neutrophils in both the cyprinids and salmonids both share similar function with their human counterparts (Hamdani *et al.*, 1998; Modrá *et al.*, 1998; Pettersen *et al.*, 2000; Rombout *et al.*, 2005; Katzenback *et al.*, 2009; Palić *et al.*, 2011). Due to the dissimilarity between cells of different species, it is worth noting that the term 'neutrophil' is frequently used interchangeably with neutrophil-like cells, polymorphonuclear (PMN) cells, or heterophils (Ainsworth, 1992; Kemenade *et al.*, 1994; Dekker *et al.*, 2000; Chuammitri *et al.*, 2009; Behrendt *et al.*, 2010; Palić *et al.*, 2011; Pijanowski *et al.*, 2013). Further complication stems from the lack of monoclonal antibodies (mAb) available for fish CD markers, leaving cell identification very elusive compared to humans. To avoid confusion, from here on the term 'PMN' will be used when referring to non-human neutrophils or neutrophil-like cells which have neutrophil function and staining characteristics. In addition, Chapter 2 makes clear the cells considered to be PMNs in the material used throughout this thesis.



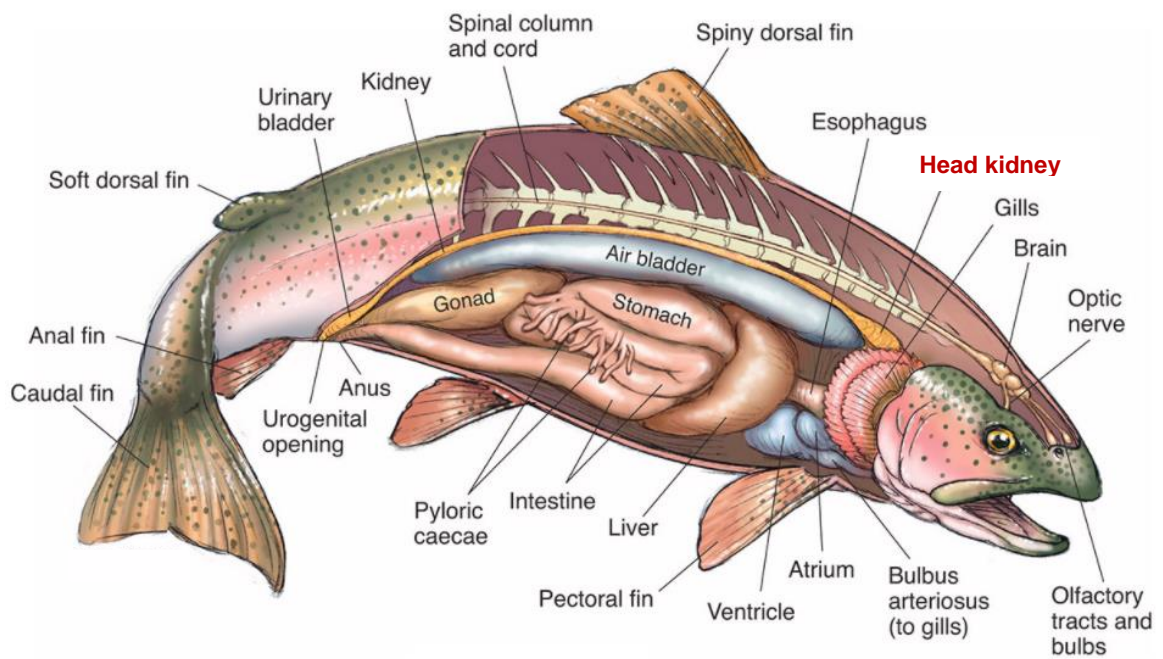


**Figure 1.1.** Figure showing the anatomy of a rainbow trout, highlighting the location of the anterior/head kidney in red, responsible for haematopoiesis. Photo used with permission from the artist ©Dave Carlson.

Rainbow trout is a member of the Pacific Salmonidae (Kendall, 1988) and species within this family share almost indistinguishable immune systems regarding structure and cell functions. PMNs in rainbow trout and Atlantic salmon are morphologically similar, with a lobed nucleus and these cells share similar functional roles to human neutrophils in non-specific phagocytosis and inflammation (Afonso *et al.*, 1998; Hamdani *et al.*, 1998; Pettersen *et al.*, 2000; Sasaki *et al.*, 2002; Øverland *et al.*, 2010; Chalmers *et al.*, 2017). In addition, the methods established to isolate and enrich for PMNs from Atlantic salmon can be applied successfully to rainbow trout (Hamdani *et al.*, 1998; Sasaki *et al.*, 2002; Øverland *et al.*, 2010). In contrast to salmon, rainbow trout are less affected by seasonal modification, as salmon undergo many physiological and immunological changes during smoltification, a process influenced by season (Johansson *et al.*, 2016); thus, rainbow trout are often a favoured candidate to study immune system and structure to represent the Salmonidae.

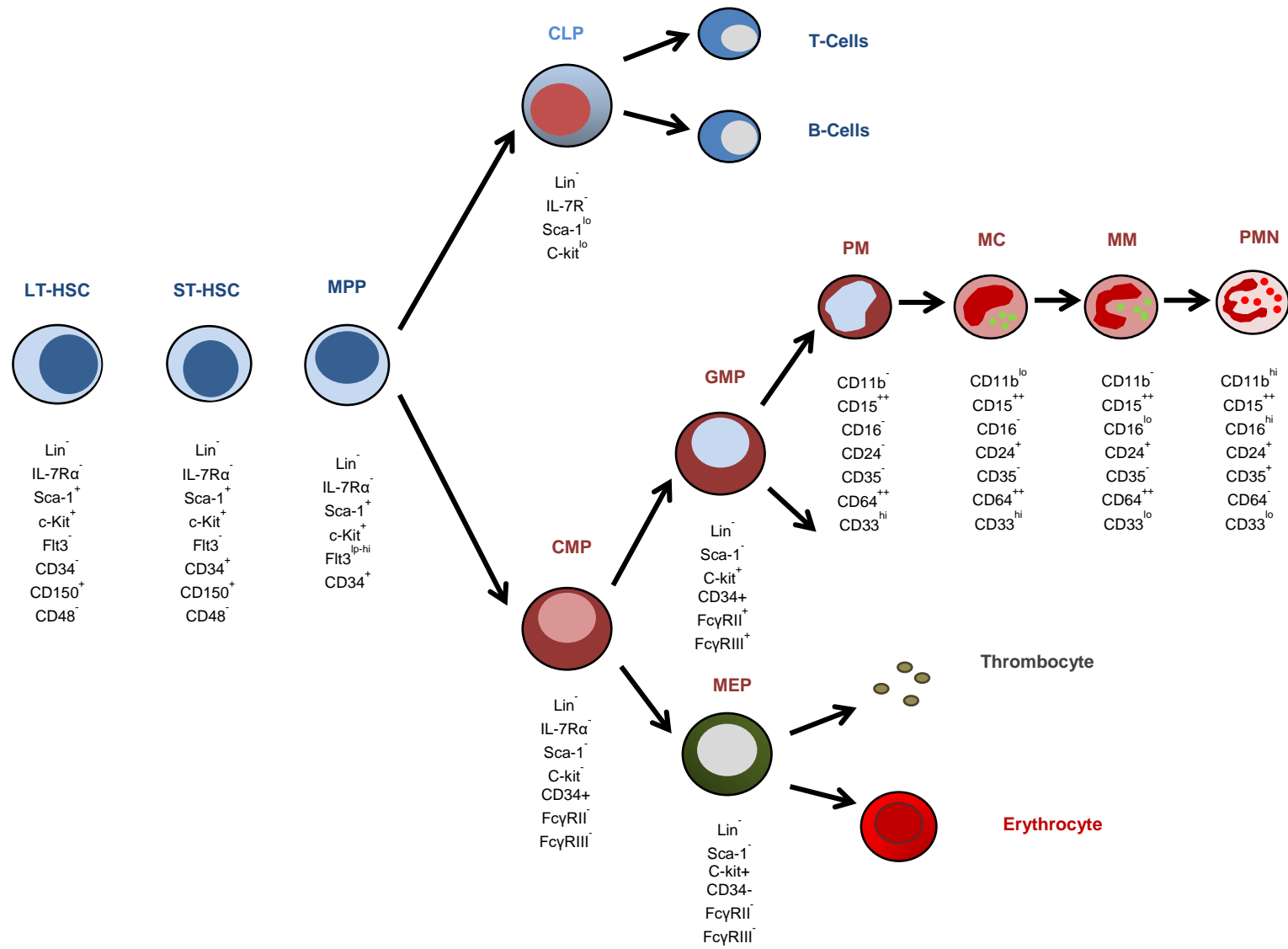


**Figure 1.2.** Figure representing human PMN, lymphocyte, thrombocyte, and erythrocyte differentiation from haematopoietic stem cells showing specific cell surface cluster of differentiation (CD) markers. Long-term haematopoietic stem cell (LT-HSC), short-term haematopoietic stem cell (ST-HSC), multipotent progenitor cell (MPP), common lymphoid progenitor cell (CLP), common myeloid progenitor cell (CMP), granulocyte-macrophage progenitor (GMP), promyelocyte (PM), myelocyte (MC), metamyelocyte (MM), polymorphonuclear cell (PMN), megakaryocyte-erythroid progenitor cell (MEP). The terminally differentiated cells are also found in trout (Quinn, 2013).

#### **1.2.4. Enrichment and culture of leukocytes from fish tissues**

In salmonids, PMNs are the most abundant granulocyte in the head kidney and these cells develop in this tissue before migrating to secondary lymphoid sites such as the spleen (Pettersen *et al.*, 2000; Sasaki *et al.*, 2002; Øverland *et al.*, 2010; Thompson, 2017). The abundance of PMNs, macrophages, and other granulocytes in fish head kidney tissue means that this tissue is often dissected to enrich for these cells for *in vitro* studies (Sasaki *et al.*, 2002; Thompson, 2017).

Rate-zonal centrifugation is a type of density gradient centrifugation that is used routinely to separate particles including cells by relative size and mass due to differential sedimentation rates. Different gradient media such as Histodenz, Histopaque, Percoll, sucrose, and glycerol allow separation of particles from viruses, cellular organelles, to whole cells (Frei, 2011). Percoll is a non-toxic colloidal silica medium used to separate cells, organelles and, occasionally, membrane vesicles by rate-zonal centrifugation. Percoll is used frequently to separate different blood cell types depending on the specific relative densities between cell types (Frei, 2011). In fish, the enrichment of PMNs often involves rate-zonal centrifugation of cell suspensions prepared from dissected head kidney tissue on Percoll or Histopaque gradients (Sorensen *et al.*, 1997; Pettersen *et al.*, 2000; Øverland *et al.*, 2010; Chi *et al.*, 2015; Pijanowski *et al.*, 2015; Masterman, 2016; Wangkahart *et al.*, 2016).

Different cell media types can significantly affect the viability, adhesion, density, and productivity of cultured cells, as they possess unique profiles of nutrients, vitamins, salts, serum proteins, carbohydrates or cofactors that are required to maintain cell viability (Moore *et al.*, 1967). Furthermore, selection of appropriate medium depends largely on the requirements of the specific cell type under investigation. With primary leukocyte suspensions, Roswell Park Memorial Institute medium (RPMI) is often used and this medium does not contain any proteins, lipids or growth factors and it is often supplemented with heat-inactivated 10% foetal calf serum (FCS) to provide cells with the growth factors, hormones, and nutrients required to maintain viability. However, the constituents within FCS are not well defined and can interfere with PMN chemotaxis and activation and so can hinder experimental observations (Macanovic *et al.*, 1997; Ottonello *et al.*, 2004; Zhiyun Wei *et al.*, 2016).

### **1.3. Extracellular traps**

The discovery of neutrophil extracellular traps (ETs) by Brinkmann *et al.* (2004) demonstrated that human neutrophils released nuclear DNA into the extracellular milieu in response to stimulation with chemical and natural compounds such as phorbol myristate acetate (PMA) or LPS (Brinkmann *et al.*, 2004). When stained with fluorescent nucleic acid intercalating dyes,

this released DNA was observed to be degraded by the nucleic-acid-degrading nuclease enzyme, deoxyribonuclease-I (DNase-I). Neutrophil ETs are defined as decondensed extracellular chromatin released by neutrophils and that is associated with the granule proteins, neutrophil elastase (NE) and myeloperoxidase (MPO) (Brinkmann *et al.*, 2004; Fuchs *et al.*, 2007).

Within three hours of exposure to PMA, human neutrophils display a morphological loss of the lobed nuclei, and the cytoplasm and contents within the nucleus mix before the chromatin is released into the extracellular milieu (Brinkmann *et al.*, 2004; Fuchs *et al.*, 2007). The neutrophils releasing their DNA die by this process (called ETosis) and undergo events that are distinct from apoptosis or necrosis. ETosis is characterised by the wide spreading of extracellular DNA from the cell and the lack of DNA-fragmentation or nuclear blebbing (Deschesnes *et al.*, 2001; Fuchs *et al.*, 2007). One distinct cellular event occurring during apoptosis is the flipping of phosphatidylserine (PS) from the inner cell membrane to the outer membrane cell membrane before cell lysis. During ETosis, the flipping of PS was not found to occur before cell lysis, further indicating that the cell death mechanisms are distinct (Fuchs *et al.*, 2007). In additional support of ETosis being distinct from other cell death mechanisms, inhibitors of apoptosis and necrosis do not prevent cells releasing ET DNA (Fuchs *et al.*, 2007). However, recent studies have demonstrated that mouse PMNs displaying chemotactic and phagocytic capacity after the release of nuclear DNA indicating their viability despite releasing ETs; thus, the term, ETosis may not always be appropriate as the cells do not always have a lysed fate (Yipp *et al.*, 2012).

The molecular mechanism underlying neutrophil ET release is still under debate, though studies in humans confirm that chemical and biological inducers, such as PMA and LPS, result in protein kinase C (PKC) activation which plays an early role in initiating neutrophil ET release. PMA is a potent activator of PKC by mimicking the activating ligand diacylglycerol (Brandes *et al.*, 2005). Activated PKC can phosphorylate subunits of NADPH oxidase (p47phox) such that they form a functional complex at the cell membrane that generates intracellular ROS that is required for respiratory burst and neutrophil ET release (Figure 1.3) (Brandes *et al.*, 2005; Kaplan *et al.*, 2012; Parker, Dragunow, *et al.*, 2012; Gray *et al.*, 2013). Biological compounds such as bacterial LPS, or fungal  $\beta$ -glucan are also dependent on inducing ET release through the activity of NADPH oxidase (Fuchs *et al.*, 2007; Papayannopoulos, 2017). Alternatively, intracellular calcium influx is known to have a prominent role in inducing mitochondrial-generated ROS through the activation of calcium-activated potassium channel of small conductance (SK channel) (Douda *et al.*, 2015). Calcium ionophore (Cal, or A23187) which binds extracellular  $\text{Ca}^{2+}$  to form stable divalent cations, allows the ions to cross cell membranes which opens the SK channels on the mitochondria (Guyot *et al.*, 1993). Rapid influx of  $\text{Ca}^{2+}$  into the mitochondrial matrix is well known to generate

ROS independently of NADPH oxidase (Brookes *et al.*, 2004), and ultimately, ET release (Figure 1.3) (Doua *et al.*, 2015). However, exactly how ROS induces ET release remains unclear, though it seems to act as a signalling molecule (Fuchs *et al.*, 2007; Van Der Linden *et al.*, 2017).

Following intracellular ROS generation, NE localises in the nucleus by an unknown mechanism to degrade linker histones (H1), and processing core histones, resulting in the characteristic decondensation (Papayannopoulos *et al.*, 2010). MPO subsequently migrates to the nucleus to seemingly enhance chromatin condensation with NE, though the exact contribution of MPO is not clear (Papayannopoulos *et al.*, 2010). After chromatin decondensing, the neutrophils release their DNA in the form of ETs (Figure 1.4). The importance of these granule proteins for ET release has been confirmed in experiments with mice knocked out for NE and human patients with neutrophil that lack MPO activity, as in neither case do the neutrophils release ETs (Papayannopoulos *et al.*, 2010; Metzler *et al.*, 2011). Various granule proteins present in granulocytes are also associated with neutrophil ETs (Table 1.1), though not all associated proteins are thought to contribute to the processing the chromatin like NE or MPO. In mammals, citrullination of H3 histones by arginine deiminase 4 (PAD4) is sometimes detected before neutrophil ET release and this protein has been hypothesised to contribute to the process of chromatin decondensation (Kaplan *et al.*, 2012). This is evident from mice knocked out for PAD4, as these animals fail to produce neutrophil ETs and are more susceptible to infections by *S. aureus* as the bacteria can disseminate more widely around the host (Li *et al.*, 2010).

Importantly, neutrophil ETs have been demonstrated by microscopic analysis and assays measuring bacterial abundance, i.e. colony forming units, to trap and possibly kill pathogens such as *Staphylococcus aureus* and *Shigella flexneri* (Brinkmann *et al.*, 2004). The immunological significance of neutrophil ETs is also indicated by the reoccurring and persistent bacterial and fungal infections in patients that suffer from chronic granulomatous disease (CGD) (Winkelstein *et al.*, 2000), as CGD is a hereditary condition characterised by a lack of functional NADPH oxidase that is required to produce ROS to kill ingested pathogens in phagosomes. Neutrophils isolated from these patients could not produce neutrophil ETs (Bianchi *et al.*, 2009). Importantly, gene therapy of patients to rescue NADPH oxidase function can result in restoration of neutrophil ET release and significantly reduce the number of patients acquiring a fungal infection (Bianchi *et al.*, 2009).

Since the discovery of ETs release by human neutrophils, other studies have shown that extracellular DNA release in a manner resembling ETosis is performed by other human cell types including eosinophils (Yousefi *et al.*, 2008; Ueki *et al.*, 2016), macrophages (Chow *et al.*, 2010; Liu *et al.*, 2014), and mast cells (Von Köckritz-Blickwede *et al.*, 2008) (Table 1.1).

The DNA released by these macrophages and mast cells stain positively with antibodies against histones and granule proteins, while eosinophils may also release mitochondrial DNA during the ET response (Yousefi *et al.*, 2008). Extracellular mitochondrial DNA has also been reported to be released by human neutrophils during ET release and this was distinguished from nuclear DNA by the lack of histone detection by immunocytochemical staining (Yousefi *et al.*, 2008). Even so, the consensus is that neutrophil ET release is *primarily* performed by neutrophils and the trap is formed from DNA of nuclear origin (Papayannopoulos, 2017).

ET release by immune cells has also been characterised in various non-human species, including mice (Yipp *et al.*, 2012), dogs (Jeffery *et al.*, 2015), cats (Wardini *et al.*, 2010), monkeys (Fuchs *et al.*, 2010), cattle (Lippolis *et al.*, 2006), seals (Reichel *et al.*, 2015), birds (Chuammitri *et al.*, 2009), crabs (Robb *et al.*, 2014), oysters (Poirier *et al.*, 2014), shrimp (Ng *et al.*, 2013). Plants may also release chromatin in a manner resembling ET release, as a way to reduce exposure of the root tip cells to soil pathogens (Tran *et al.*, 2016). The ETs of different species have been confirmed typically by their morphological similarity (fibres appearing to extrude out from cells which stain positively with fluorescent nucleic acid dyes) and positive immunocytochemical detection of NE, MPO, and/or histones (or homologues).

It is noteworthy that the cells responsible for releasing ET in vertebrates and invertebrates have phagocytic capacity, and these cell types include neutrophil PMNs (Brinkmann *et al.*, 2004), haemocytes (Ng *et al.*, 2013; Robb *et al.*, 2014), heterophils (Chuammitri *et al.*, 2009), macrophages (Boe *et al.*, 2015), mast cells (Von Köckritz-Blickwede *et al.*, 2008), and eosinophils (Yousefi *et al.*, 2008). Furthermore, the ETs released from these phagocytic cells from crabs and shrimp demonstrate function to trap microbes, in addition to sharing morphological and structural features with human neutrophil ETs (Patat *et al.*, 2004; Robb *et al.*, 2014; Zhang *et al.*, 2016). Taken together, the release of ETs and phagocytosis are primitive and evolutionarily conserved strategies to combat microbial infection.



**Table 1.1.** Table showing the components of ETs from neutrophil / PMNs, macrophages, mast cells, and eosinophils, and basophils. #Indicates components which collectively satisfy the definition of ETs.

ET constituents	Cell type	Function	Notes	Reference
Azurocidin	Neutrophils	Antimicrobial	Heparin binding protein	(Urban <i>et al.</i> , 2009)
Bacterial Permeability Increasing Protein (BPI)	Neutrophils	Antimicrobial	Pore-forming	(Urban <i>et al.</i> , 2009)
Basogranulin	Basophils	Unknown		(Morshed <i>et al.</i> , 2014)
Calprotectin	Neutrophils	Chelates divalent metal ions. Restricts intercellular ions	Binds and restricts free iron	(Urban <i>et al.</i> , 2009)
Calprotectin	Neutrophils	Antimicrobial	Binds and restricts free iron	(Urban <i>et al.</i> , 2009)
Catalase	Neutrophils	Antimicrobial	Catalysis of H <sub>2</sub> O <sub>2</sub> to H <sub>2</sub> O + O <sub>2</sub>	(Urban <i>et al.</i> , 2009)
Cathelicidin (LL-37)	Neutrophils, Macrophage, Mast cells	Antimicrobial, Nuclease resistance	Pore-forming	(Von Köckritz-Blickwede <i>et al.</i> , 2008; Neumann <i>et al.</i> , 2014)
Cathepsin	Neutrophils	Antimicrobial	Protease	(Urban, <i>et al.</i> 2009; Papayannopoulos, <i>et al.</i> 2010)
<b>Chromatin</b> #	All eukaryotes	Genetic information		(Brinkmann <i>et al.</i> , 2004)
Defensin	Neutrophils	Antimicrobial	Pore-forming	(Urban <i>et al.</i> , 2009; Saitoh <i>et al.</i> , 2012)
Eosinophil Cationic Protein (ECP)	Eosinophils	Antiparasitic	Toxin	(Yousefi <i>et al.</i> , 2008)
Gelatinase	Neutrophils	Antimicrobial	Protease	(Brinkmann, <i>et al.</i> 2004)
<b>Histones</b> *	Eukaryotes	Antimicrobial, DNA packaging	Destabilises bacterial membranes	(Brinkmann <i>et al.</i> , 2004)
Lactoferrin	Neutrophils	Antimicrobial	Binds and restricts free iron	(Brinkmann, <i>et al.</i> 2004)
Lysozyme	Neutrophils, Macrophages	Antimicrobial	Protease	(Urban <i>et al.</i> , 2009)
Major Basic Protein (MBP)	Eosinophils	Antiparasitic	Toxin	(Yousefi <i>et al.</i> , 2008)
<b>MPO</b> *	Neutrophils, Macrophages	Antimicrobial	Produces HOCl from H <sub>2</sub> O <sub>2</sub> and Cl-	(Papayannopoulos <i>et al.</i> , 2010; Liu <i>et al.</i> , 2014)
<b>Neutrophil elastase</b> #	Neutrophils	Antimicrobial	Protease	(Papayannopoulos, <i>et al.</i> 2010)
Proteinase3 (PR3)	Neutrophils	Antimicrobial	Proteinase	(Papayannopoulos <i>et al.</i> , 2010)
Tryptase/ MCP (Mast Cell Protease)	Mast cell	Antimicrobial	Protease	(Von Köckritz-Blickwede <i>et al.</i> , 2008)

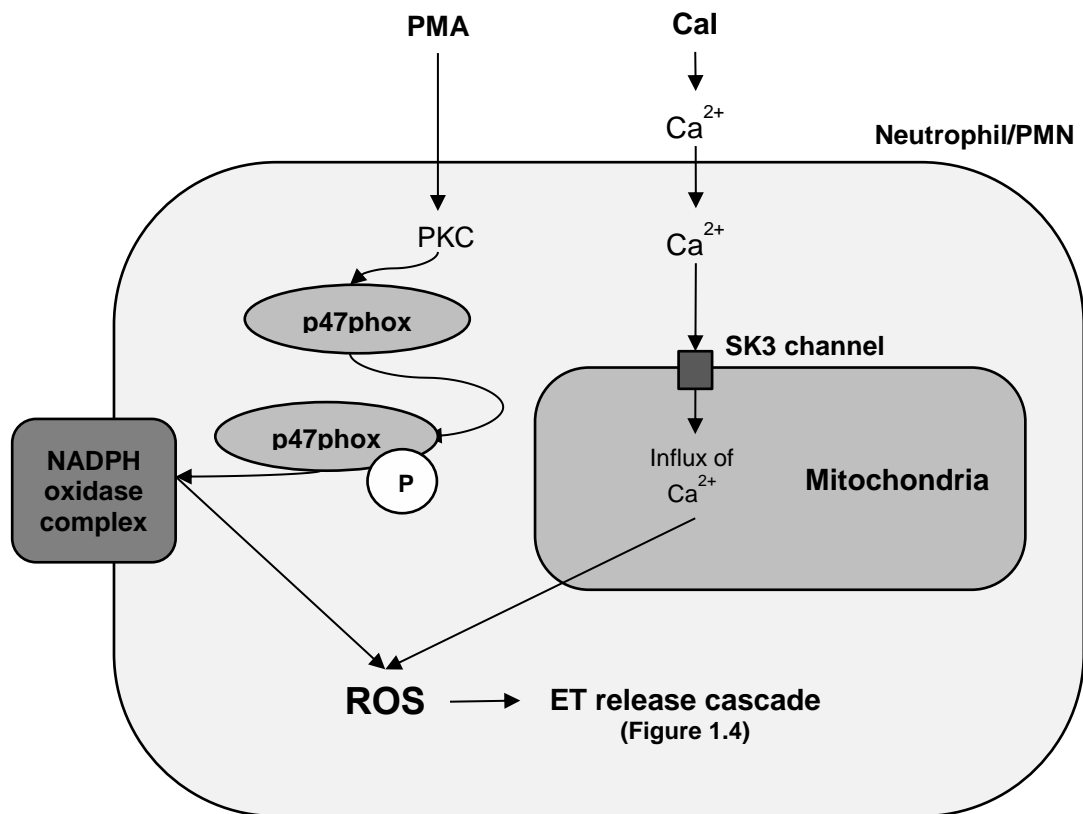


**Figure 1.3.** Figure representing the distinct cell signalling events induced by PMA or Cal which lead to ET release. PMA is one of the most characterised inducers of ET release, which mimics diacylglycerol to activate protein kinase C (PKC). Activated PKC can phosphorylate the p47phox subunit of NADPH oxidase, promoting the formation of a functional NADPH oxidase complex on cell membranes. This enzyme is responsible for the generation of ROS, leading to release of ETs. Alternatively, Cal is understood to bind and form stable divalent cations with extracellular  $Ca^{2+}$ , allowing cell membrane permeability.  $Ca^{2+}$  can open SK3 channels on the mitochondrial membranes causing a rapid influx of mitochondrial  $Ca^{2+}$ , leading to the generation of ROS and ultimately, ET release (Figure 1.4).

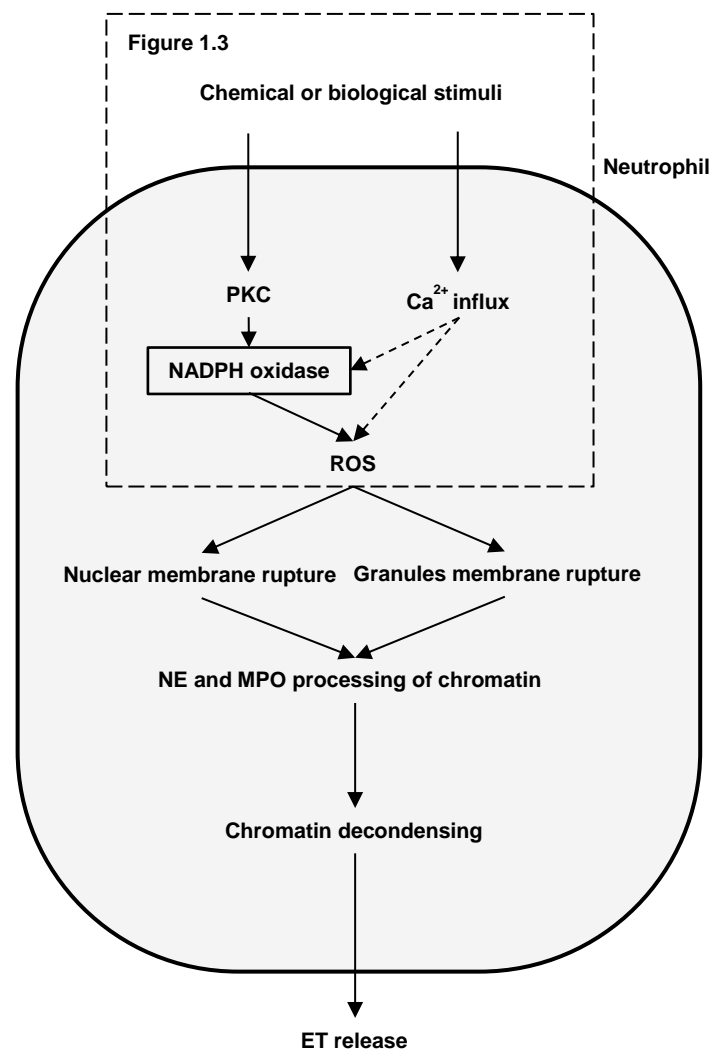


**Figure 1.4.** Figure representing fundamental events in neutrophils/PMNs that lead to ET release through NADPH oxidase-dependent and independent pathways. Exposure of neutrophils/PMNs to ET-inducing chemical and biological compounds induces extracellular calcium entry or activation of PKC, and this leads to initiation of ET release cascade (Figure 1.3). The increase of intracellular ROS is followed by nuclear and granule membrane rupture and processing of chromatin by granule proteins, leading to the chromatin decondensation and ultimately ET release.

### 1.3.1. Extracellular traps in fish

With respect to fish, ETs were first described in PMN-enriched cell suspensions isolated from the head kidney of fathead minnows (*Pimephales promelas*) and zebrafish (*Danio rerio*) with the use of fluorescence microscopy and immunocytochemical staining of ET markers (Palić, Andreasen, *et al.*, 2007; Palić, Ostojić, *et al.*, 2007). However, neither study identified a reliable inhibitor of ET release, or confirmed immunocytochemical co-localisation of histones fragments, or both MPO and NE that are characteristic of ETs (Table 1.2). These initial studies sparked a cascade of research in the European carp (*Cyprinus carpio*), whereby two groups separately confirmed the production of ETs from carp PMNs. One group focused primarily on the antimicrobial activity of the carp ETs (Brogden *et al.*, 2012, 2014), while the other group focused more on characterising the response and investigating the signalling mechanisms (Pijanowski *et al.*, 2013, 2015). Indeed, carp PMNs are dependent NADPH-oxidase for ET release, though the studies in minnows and zebrafish found Cal to be more potent than PMA at similar concentrations towards inducing ET release, indicating less dependency on NADPH oxidase.

In addition to PMNs, macrophages isolated from the carp head kidney have also been observed to release ETs after incubation with LPS (Pijanowski *et al.*, 2015). This was confirmed after observing ET-like DNA structures coming from cell-remnants that stained positively with an antibody against WCL15 – a monocyte and macrophage specific marker (Pijanowski *et al.*, 2015). More recent studies have demonstrated that flatfish such as turbot (*Scophthalmus maximus*) and sole (*Cynoglossus semilaevis*) and barramundi (*Lates calcarifer*) to also release ETs from PMN-enriched cell suspensions (Chi *et al.*, 2015; Masterman, 2016; Zhao *et al.*, 2017). However, the ETs released by flatfish and barramundi remain to be confirmed for ET-associated markers such as NE and MPO, thus, the ETs await diagnostic confirmation (Table 1.2). Immunostaining of ET specific markers is required to confirm that the extracellular DNA observed originates from PMNs, though the availability of specific antibodies for fish PMN granules presents an ongoing challenge for studying ETs in these species. To date, there has yet to be a study to confirm ETs in the salmonid family, which are an economically and commercially important species.

**Table 1.2.** Table of confirmed diagnostic ET markers in fish species.

<b>Antibody target</b>	<b>Fish species</b>	<b>Reference</b>
<b>Histone</b>	Carp ( <i>Cyprinus carpio</i> ), Turbot ( <i>Scophthalmus maximus</i> )	(Brogden <i>et al.</i> , 2012; Chi <i>et al.</i> , 2015)
<b>Neutrophil elastase</b>	Carp ( <i>Cyprinus carpio</i> ), Zebrafish ( <i>Danio rerio</i> )	(Palić, Andreasen, <i>et al.</i> , 2007; Pijanowski <i>et al.</i> , 2013)
<b>Myeloperoxidase</b>	Fathead minnow ( <i>Pimephales promelas</i> )	(Palić, Ostojić, <i>et al.</i> , 2007)

### 1.3.2. Visualising and quantifying extracellular trap release *in vitro*

Fluorescent nucleic acid dyes are fluorophores which have a high affinity for nucleic acids. This means they can absorb electromagnetic energy at specific wavelengths and subsequently re-emit the energy at a lower wavelength in the form of light, i.e. fluorescence (Thermo Fisher Scientific, 2010). Some of these dyes such as SYTOX Green cannot diffuse through cell membranes and show little selectivity for intercalating between base pairs; while others such as DAPI can permeate through cell membranes and specifically bind nucleic acid A-T base pairs (Thermo Fisher Scientific, 2010). These dyes are often used to visualise the presence of extracellular nucleic acids (like chromatin) and indicate the presence ETs. Scanning electron microscopy (SEM) may also be used to visualise the ETs *in vitro*, though this requires several steps involving dehydrating and coating the ETs that can disrupt the delicate ET fibres (von Köckritz-Blickwede *et al.*, 2010).

A significant challenge when studying ETs is selecting the method to quantify ET release in cell suspensions. These methods can be grouped into three main categories: i) fluorimetry of ETs dyed by nucleic acid dyes such as SYTOX Green, PicoGreen, or 4',6-diamidino-2-phenylindole (DAPI); ii) fluorimetry of immunocytochemically stained markers of ETs such as  $\alpha$ -NE and  $\alpha$ -MPO; iii) counting number of cells releasing ETs or area of ETs per field of view on a microscope. The various techniques have advantages and disadvantages, which can lead to challenges when comparing observations between laboratories.

Measuring the fluorescence emitted from fluorescent DNA-intercalating dyes is a popular approach to measure the abundance of ETs released in a suspension of PMNs *in vitro*, and this method allows for high-throughput processing of samples. Often, membrane-impermeable dyes such as SYTOX Green or PicoGreen are used to dye total ETs as this approach therefore excludes the DNA contributed by live cells that have intact membranes that prevent the dye from entering living cells and binding to intracellular nucleic acids. However, not all extracellular nucleic acids form the intrinsic structure of an ET, as cells undergoing apoptosis or necrosis may also release DNA and RNA during cell membrane rupture (de Buhr *et al.*, 2016; Maini *et al.*, 2016). Thus, immunocytochemical analysis is required to determine if extracellular DNA is found with the ET-associated proteins such as histones, NE, and MPO (Jorch *et al.*, 2017) that characterise and distinguish an ET.

SYTOX green assays are sometimes favoured over PicoGreen counterparts as the latter is not sensitive enough to detect relatively small amounts of chromatin that may be released in low density PMN suspensions when releasing ETs (de Buhr *et al.*, 2016). However, these methods do not distinguish between different modes of cell death, and so fluorescence emitted from membrane-compromised, non-viable cells contribute to the overall fluorescence. To allow comparison between plates, fold-change fluorescence can be used which also accounts

for the variation of ET release between individuals (Jeffery *et al.*, 2015, 2016). Some compounds such as LPS that is used to induce ET release may also contain nucleic acid contaminants that may skew results when using a fluorimetry-based assay (Tan *et al.*, 2009; Rezania *et al.*, 2011). PAMPs, such as zymosan,  $\beta$ -glucan and LPS, are commonly acquired through phenol-based extraction methods and this may lead to the final product containing contaminants, including those that dye positively with nucleic acid dyes and affect ET data readings (Tan *et al.*, 2009; Rezania *et al.*, 2011). Whole bacteria used to induce ETs may also skew the overall fluorescence of a sample in the same manner; thus, the subtraction of fluorescence from control wells containing these compounds from treatment wells with cells is vital to reduce the effect of DNA contamination on fluorescence readings aiming to quantify ETs. Due to these limitations, human observation by fluorescence microscopy is highly advised to confirm the presence of ETs and the absence of considerable fluorescence signals from contaminants and cells dying by necrosis and apoptosis (von Köckritz-Blickwede *et al.*, 2010).

Immunocytochemical analysis can be used to quantify ET release in cell suspensions, as co-localisation of antibodies against NE and histone fragments diagnostically confirm the detection of ETs. Measuring the fluorescence of fluorophore-conjugated antibodies against NE and histones (specific to extracellular proteins unless cell membranes were permeabilised) gives a more specific measurement than measuring solely fluorescence of nucleic acid-binding dyes. However, during the processing of samples, cells adhere to glass coverslips prior to ET release, and frequent wash steps must be performed to ensure the binding specificity of antibodies (de Buhr *et al.*, 2016). This processing can disrupt the ETs, which are relatively delicate structures that can be removed during these washes, and lead to underestimates of ET abundance (von Köckritz-Blickwede *et al.*, 2010). Furthermore, the availability of teleost species-specific mAbs may be problematic, as using polyclonal antibodies may reduce specificity and result in weaker detection.

Another way to quantify ETs is the enumeration of ETs in fields of view under the microscope (von Köckritz-Blickwede *et al.*, 2010; Robb *et al.*, 2014; Maini *et al.*, 2016). For this, photographs of the same field of view of cell suspensions labelled with fluorescent antibody or nucleic acid dyes are acquired in phase contrast and suitable fluorescence conditions, and these fluorescent images are overlaid and quantified by image analysis to allow enumeration of ETs (von Köckritz-Blickwede *et al.*, 2010; Robb *et al.*, 2014; Maini *et al.*, 2016). A similar quantification method is to perform ET counts from electron microscopy images (von Köckritz-Blickwede *et al.*, 2010; Manzenreiter *et al.*, 2012). However, due to the relatively low throughput and subjective nature of such counting methods due to the variability of ET shapes, the results are difficult to compare between laboratories. For example, released ETs *in vitro* appear as 'comet'-like structures, or instead produce a 'diffuse'-like structure, which can be

easily interpreted as more than one ET (Hakkim *et al.*, 2011). Furthermore, when large numbers of ETs are clumped together, it becomes even more difficult to distinguish between individual ETs (Hakkim *et al.*, 2011).

More recently, flow cytometry methods have been developed to quantify ETs (Zhao *et al.*, 2015). One method measures co-localisation of fluorescent DNA stains with ET-associated granule proteins such as MPO and NE in cell suspensions after inducing the cells to release ETs (Zhao *et al.*, 2015). Although this 'Multispectral Imaging Flow Cytometry' method can greatly increase objectivity, this technique can only detect cells undergoing ETosis, or having recently undergone ETosis, as lysed cells are not detected with the flow cytometer (Zhao *et al.*, 2015). Furthermore, there are pitfalls with the use of antibodies to quantify ET release *in vitro*, such as the loss of ETs through wash steps required to ensure antibody specificity. Regardless, improved methods are being developed to gradually improve the techniques used to quantify ET release, though a more standardised approach would be desirable moving forward to allow for more consistency and reproducibility in observations, allowing for more reliable comparisons between studies.

### **1.3.3. Antimicrobial activity of extracellular traps**

ETs have been shown to exert antimicrobial effects, including the ability to physically adhere to and 'trap' microbes (Brinkmann *et al.*, 2004). Observations of microbial trapping have been supported with fluorescent and electron microscopy *in vitro* and has demonstrated the binding of *E. coli* to ETs *in vivo* in the liver during murine sepsis, and trapping of *Klebsiella pneumoniae* in lungs of infected mice (Papayannopoulos *et al.*, 2010; Yipp *et al.*, 2013). The immobilisation of microbial pathogens by ETs likely prevents further dissemination within the host, thus allowing immune cells time to be recruited to the infected region to assist with the clearance of the entangled microbes (Stephan *et al.*, 2015). Some studies have exposed microbial pathogens to ETs *in vitro* and have shown a reduction in colony forming units (CFU) after co-incubation, therefore indicating that the microbes have been trapped (and therefore aggregated) or killed (Brinkmann *et al.*, 2004; Urban *et al.*, 2009). Typically, these observations are supported by visualising the microbe entangled within the ETs using fluorescence or SEM (Table 1.3) (Brinkmann *et al.*, 2004; de Buhr *et al.*, 2016). Another method to quantify microbial trapping involves measuring the co-localisation of fluorescently-labelled microbes with fluorescently stained ETs (von Köckritz-Blickwede *et al.*, 2010; Brogden, 2013).



**Table 1.3.** Examples of the different methods used to visualise and quantify ETs.

Dye	Method	Measurement parameter	Pros	Cons	References
<b>SYTOX Green/PicoGreen; Antibody against histone-DNA complex</b>	Fluorescence microscopy ET counts	ET counts	Able to distinguish between cell death modes	Can be affected by selection of fields of view	(Robb <i>et al.</i> , 2014; Maini <i>et al.</i> , 2016)
<b>Antibody against elastase and histone-DNA complexes + membrane permeable dye</b>	Fluorescence microscopy + image analysis	ET counts or degree of ET degradation	Objective and high-throughput quantification	Can be less objective by the images used for analysis. Clumps of ETs derived from multiple cells can affect the data	(Brinkmann, Goosmann, <i>et al.</i> , 2012; de Buhr <i>et al.</i> , 2015)
<b>SYTOX/PicoGreen</b>	Fluorimetry	Extracellular DNA	Objective and fast quantification	No differentiation between modes of cell death; requires images to confirm	(Palić, Ostojić, <i>et al.</i> , 2007; Gray <i>et al.</i> , 2013; Jeffery <i>et al.</i> , 2016)
<b>SYTOX/PicoGreen after nuclease digestion</b>	Fluorimetry	Extracellular DNA	Objective and fast quantification	Less sensitive compared to antibody-mediated ET quantification	(Pilszczek <i>et al.</i> , 2010; Menees <i>et al.</i> , 2015)
<b>Antibody against NE/MPO with cell-permeable dye</b>	Flow cytometry	Percentage of ET formation	Objective, automated, enables differentiation between suicidal vital ET release	Imaging of cells only currently undergoing ETosis and thus may miss cells that have already lysed	(de Buhr <i>et al.</i> , 2015; Zhao <i>et al.</i> , 2015)
<b>Antibody against H3cit with cell-permeable dye</b>	Flow cytometry	Percentage of ET formation	Objective, automated, can be combined with sorting	Does not detect H3cit-independent events; Imaging of cells only currently undergoing ETosis and thus may miss cells that have already lysed	(Gavillet <i>et al.</i> , 2015)

<b>Uranyl-acetate, osmium tetroxide, ruthenium red-osmium tetroxide, Cuproinic blue</b>	TEM	Morphology of NET-releasing cells	Visible differentiation between necrosis and ET release, can be used in combination with immunostaining of ET-associated granule proteins	May be subjective by selection of field of view	(Krautgartner <i>et al.</i> , 2008; von Köckritz-Blickwede <i>et al.</i> , 2010)
<b>Osmium tetroxide/gold</b>	SEM	Amount and structure of NETs-releasing cells	Visible differentiation between necrosis and ET release; can be used in combination with immunostaining of ET-associated granule proteins	May be subjective by selection of field of view, fibrin mimics ET structures	(Krautgartner <i>et al.</i> , 2008; von Köckritz-Blickwede <i>et al.</i> , 2010)

ET: extracellular trap; SYTOX: fluorescent DNA-binding cell-impermeable dye; TEM: transmission electron microscopy; SEM: scanning electron microscopy; H3cit: citrullinated histone H3

Trapping or killing by ETs is difficult to distinguish, though inhibiting the phagocytic capacity of PMNs with actin polymerisation inhibitors can reduce the number of bacteria that are killed by phagocytic action (Stephan *et al.*, 2015). If a reduction in CFU is still observed after inhibiting phagocytosis, the microbes are likely trapped within the ETs and not lost through phagocytic processes. Failure to recover fully the microbes after degrading the ETs with DNases indicates that the bacteria were likely killed by intact ETs (Fuchs *et al.*, 2007; Brinkmann and Zychlinsky, 2012). Whether or not ETs can trap or kill microbes will depend on the species and strain of the microorganism, as some bacterial strains display innate resistance towards ETs (Storisteanu *et al.*, 2017).

The interaction between microbes and ETs is likely promoted by the electrostatic charge of the DNA composing the core of the ET structure and the presence of pathogen-binding surfactant protein D, which promotes contact with negatively-charged bacterial membranes (Brinkmann *et al.*, 2007; Epanand *et al.*, 2009; Douda *et al.*, 2011). ETs are hypothesised to exert bactericidal activity due to the actions of numerous bactericidal proteins decorating the ETs (Table 1.1) because many of the granule proteins found in association with ETs are lethal to bacteria (Perera *et al.*, 2012; Stapels *et al.*, 2015). For example, histones are known to be antimicrobial, as their cationic properties means they can physically interact with and disrupt bacterial membranes (Fernández *et al.*, 2002; Patat *et al.*, 2004; Smith *et al.*, 2010, 2015; Halverson *et al.*, 2015). The bactericidal effect of histones can be reduced by incubating with exogenous phosphatases or excess Mg<sup>2+</sup> ions, as these effectively eliminate the cationic charge of histones (Halverson *et al.*, 2015). With respect to fish, histone H1 (Richards *et al.*, 2001) and H2A (Fernández *et al.*, 2002) proteins isolated from Atlantic salmon and rainbow trout, respectively, exert dose-dependent antimicrobial activity. H2A is effective at sub-micromolar concentrations against Gram-positive bacteria such as *Staphylococcus aureus* and *Renibacterium salmoninarum* and against the yeast *Saccharomyces cerevisiae*, though at these concentrations there was no bactericidal activity against Gram-negative bacteria including *Aeromonas salmonicida* (Fernández *et al.*, 2002).

Granule proteins decorating ETs, such as MPO, produce hyperchlorous acid (HOCl) from H<sub>2</sub>O<sub>2</sub> and Cl<sup>-</sup> which are themselves bactericidal (Palmer *et al.*, 2012; Muñoz Caro *et al.*, 2014), while NE can hydrolyse various virulence factors on the outer membrane of bacteria, rendering them ineffective (Weinrauch *et al.*, 2002; Hahn *et al.*, 2011; Perera *et al.*, 2012). Inhibitors of MPO (e.g., 4-aminobenzoic acid hydrazide [ABAH] and NE inhibitors, e.g., Suc-Ala-Ala-Pro-Val chloromethyl ketone [CMK]) result in significant reductions of ET release by bovine PMNs, thus demonstrating their importance for ET release (Metzler *et al.*, 2011; Munoz-Caro *et al.*, 2015). NE is bactericidal against Gram-negative bacteria such as *Klebsiella pneumoniae* and *E. coli*, and it can also act in a complex with other granule protein cofactors like proteinase 3 and cathelicidin-related protein LL-37 (Standish *et al.*, 2009; Gupta *et al.*, 2010). Other granule

proteins such as calprotectin can inhibit fungal growth by limiting the availability of essential free zinc ions that are required for *Aspergillus* infection (Bianchi *et al.*, 2009; Urban *et al.*, 2009).

Beyond directly killing microbes, the granule proteins that decorate the ETs can also serve to protect the structural integrity of ETs. For instance, LL-37, kills microbes directly by forming pores in the bacterial membrane (Mojsoska *et al.*, 2015), but a cationic moiety of LL-37 can also protect ET structures and calf thymus DNA against degradation by *S. aureus* nucleases, but the mechanism underlying this remains unknown (Neumann *et al.*, 2014).

Trapping of bacteria in ETs released from fish PMNs has been shown for carp, turbot and tongue sole (summarised in Table 1.4). The studies in the flatfish species demonstrated trapping by inducing ET release in a PMN-enriched cell suspension with a potent inducer and then adding the bacteria to the suspension. Then, the number of bacterial CFUs recovered after exposure to ETs were compared to controls with DNase-digested ETs, whereby differences in CFUs may be attributed to the antimicrobial effect of ETs (Chi *et al.*, 2015; Zhao *et al.*, 2017). With the tongue sole, the fish pathogens *Pseudomonas fluorescens* and *Vibrio harveyi*, but not *Edwardsiella tarda*, showed a reduction in CFU compared to the control, thus indicating trapping in ETs, while further confirmation was provided by SEM observations (Zhao *et al.*, 2017). In carp, *Aeromonas hydrophila* was also found to be entangled in ETs released by PMNs when observed by fluorescence microscopy and enumerating CFU after co-incubation (Brogden *et al.*, 2014).

**Table 1.4.** Current evidence for bacterial trapping in ETs released by fish species, showing the inducer used to stimulate ET release, species of bacteria studied, and how the bacterial interaction was detected and measured. Interaction of bacteria with ETs were not investigated in studies involving *Pimephales promelas*, *Danio rerio*, and *Lates calcarifer*.

<b>Fish species</b>	<b>Inducer of ET release</b>	<b>Bacterial species</b>	<b>Evidence for trapping</b>	<b>Method</b>	<b>Reference</b>
<b><i>Cyprinus carpio</i></b>	B-glucan <i>Aeromonas hydrophila</i>	<i>Aeromonas hydrophila</i>	+	CFU recovery Fluorescence microscopy	(Brogden <i>et al.</i> , 2014)
<b><i>Scophthalmus maximus</i></b>	LPS	<i>Edwardsiella tarda</i> <i>Pseudomonas fluorescens</i> <i>Vibrio harveyi</i>	- + +	CFU recovery	(Chi <i>et al.</i> , 2015)
<b><i>Cynoglossus semilaevis</i></b>	LPS	<i>Escherichia coli</i> <i>Pseudomonas fluorescens</i>	+ +	CFU recovery	(Zhao <i>et al.</i> , 2017)

#### 1.3.4. Inducers and inhibitors of extracellular trap release

ET release can be induced by various chemical and biological compounds (Table 1.5), and many potent inducers of ET release from human neutrophils have been characterised, and often elicit similar responses in PMNs from other organisms (Chuammitri *et al.*, 2009; Yipp *et al.*, 2012; Muñoz Caro *et al.*, 2014; Robb *et al.*, 2014; Jeffery *et al.*, 2015; Reichel *et al.*, 2015). Chemical inducers such as PMA potently induce ET release from PMNs in many organisms and is regularly used as a positive control when assessing the potency of unknown compounds (Hoppenbrouwers *et al.*, 2017). Biological inducers include whole microbial organisms, bacteria, fungi, protozoa and unicellular parasites (Urban *et al.*, 2006; Baker *et al.*, 2008; Guimaraes-Costa *et al.*, 2009; Pilsczek *et al.*, 2010; Juneau *et al.*, 2011; Abdallah *et al.*, 2012), and microbial-derived PAMPs such as LPS, flagellin,  $\beta$ -glucan, polyinosinic:polycytidylic acid (Poly IC) and hyphae (Brinkmann *et al.*, 2004; Urban *et al.*, 2006; Brogden *et al.*, 2012; Floyd *et al.*, 2016), and host-derived cytokines and inflammatory mediators such as IL- $\beta$ , IL-8, and TNF $\alpha$  (Clark *et al.*, 2007; Baker *et al.*, 2008; Keshari *et al.*, 2012).

The cell signalling pathways which these inducers act through to trigger ET release from PMNs remains to be completely deciphered, as PMA, or the majority of PAMP and bacterial-induced ET release tends to result in NADPH oxidase-dependent ET release, while Cal induces ET released through mechanisms independent of NADPH oxidase activity as mentioned above (Figure 1.4) (Pilsczek *et al.*, 2010; Parker, Dragunow, *et al.*, 2012; Arai *et al.*, 2014; Douda *et al.*, 2015; Papayannopoulos, 2017). Pre-exposing PMNs, macrophages and haemocytes isolated from humans, mice, cows, dogs, crabs or oysters to PKC/NADPH oxidase inhibitors, such as diphenyleneiodonium (DPI), apocynin or Ro-31-8220, result in abolishment of ET release, indicating that the NADPH oxidase-dependent mechanism for ET release is conserved across the animal kingdom (Fuchs *et al.*, 2007; Neeli *et al.*, 2009; Hakkim *et al.*, 2011; Parker, Dragunow, *et al.*, 2012; Gray *et al.*, 2013; Robb *et al.*, 2014).

In the absence of inducers, ET release was observed to occur spontaneously from PMNs in humans and dogs (Fuchs *et al.*, 2007; Maini *et al.*, 2016; Kamoshida *et al.*, 2017). Increasing the concentration of human serum used to nourish human neutrophils correlates with greater ET release in the absence of other stimuli, indicating that spontaneous release does occur (Kamoshida *et al.*, 2017). However, there is no clear explanation for spontaneous ET release and this phenomenon is seldom reported in non-human species (Kamoshida *et al.*, 2017). As neutrophils from human donors display significant spontaneous ET release between individuals, this is an additional factor to consider when studying ET release (Fuchs *et al.*, 2007).

ET release from both vertebrate PMNs and invertebrate haemocytes can also be inhibited by cytoskeleton polymerisation inhibitors such as cytochalasin D or nocodazole (Neeli *et al.*, 2009; Ng *et al.*, 2013; Robb *et al.*, 2014), demonstrating that cytoskeleton remodelling is important for the release of ETs. Both actin and microtubule filaments were observed to regulate the position of the nucleus and facilitate the breakdown of nuclear envelope which occurs prior to ET release, though it is unclear how this exactly (Neeli *et al.*, 2009). However, some studies have found cytochalasin unsuccessful in inhibiting ET release by human neutrophils (Riyapa *et al.*, 2012). Nevertheless, it is believed that some forms of ET release in humans are mediated by actin-mediated cytoskeleton remodelling.

Potent inducers and inhibitors of ET release in mammals have inconsistency in inducing ET release from fish PMNs. For example, PMA is a potent inducer of ET release in many animals (Table 1.7), including some fish such as carp and tongue sole (Pijanowski *et al.*, 2013; Zhao *et al.*, 2017). Conversely, PMA exerts only a weak effect on ET release in zebrafish and fathead minnows (Table 1.7) (Palić, Andreasen, *et al.*, 2007; Palić, Ostojić, *et al.*, 2007; Chi *et al.*, 2015).

PMA and poly IC-induced ET release in carp was inhibited by DPI, but DPI failed to block LPS or zymosan-induced ET release, indicating that carp PMNs can undergo both NADPH oxidase-dependent and independent ET release (Pijanowski *et al.*, 2013). Further similarities of the cellular mechanisms mediating ET release between mammals and fish is demonstrated as the MPO-inhibitor, ABAH and ROS-scavenger, Trolox, inhibited ET release by tongue sole PMNs; collectively indicating that fish PMNs also require ROS signalling and chromatin processing by MPO to release ETs (Zhao *et al.*, 2017). Conversely, Cal is also a very potent inducer of ET release in PMN-enriched cell suspensions of minnows and zebrafish compared to PMA and other PAMPs ( $\beta$ -glucan and LPS) (Palić, Andreasen, *et al.*, 2007; Palić, Ostojić, *et al.*, 2007), which provides evidence for an NADPH oxidase-independent mechanism of ET release in fish PMNs. ET release was also inhibited in zebrafish and fathead minnow PMNs by actin polymerisation inhibitors cytochalasin B, indicating that fish PMNs may also rely on cytoskeleton remodelling for ET release (Palić, Andreasen, *et al.*, 2007; Palić, Ostojić, *et al.*, 2007).

**Table 1.5.** Known chemical and biological inducers of ET release in different animal species.

Inducer	Type / Species	Animal species
<b>Chemical compounds</b>		
<b>Calcium ionophore (Cal) / ionomycin</b>	Chemical	Human (Barrientos <i>et al.</i> , 2013), Cow (Lippolis <i>et al.</i> , 2006), Fish (Palić, Ostojić, <i>et al.</i> , 2007)
<b>Hydrogen peroxide (H<sub>2</sub>O<sub>2</sub>)</b>	Chemical	Chicken (Chuammitri <i>et al.</i> , 2009)]
<b>Monosodium urate</b>	Chemical	Human (Schorn <i>et al.</i> , 2012; Yousefi <i>et al.</i> , 2015)
<b>Phorbol 12-myristate 13-acetate (PMA)</b>	Chemical	Human (Brinkmann <i>et al.</i> , 2004), Cow (Lippolis <i>et al.</i> , 2006), Dog (Jeffery <i>et al.</i> , 2015), Chicken (Chuammitri <i>et al.</i> , 2009), Fish (Pijanowski <i>et al.</i> , 2013; Chi <i>et al.</i> , 2015; Zhao <i>et al.</i> , 2017), Shrimp (Ng <i>et al.</i> , 2013), Crab (Robb <i>et al.</i> , 2014), Mussel (Robb <i>et al.</i> , 2014)
<b>Biological compound</b>		
<b>Cytokines</b>	Biological signal	Human (Brinkmann <i>et al.</i> , 2004), Mouse (Cheng <i>et al.</i> , 2013), Fish (Pijanowski <i>et al.</i> , 2015)
<b>β-glucan</b>	Yeast	Human (Nani <i>et al.</i> , 2015), Fish (Palić, Andreasen, <i>et al.</i> , 2007; Brogden <i>et al.</i> , 2012)
<b>Flagellin</b>	Bacteria	Human (Floyd <i>et al.</i> , 2016)
<b>Lipopolysaccharide (LPS)</b>	Bacteria	Fish (Palić, Ostojić, <i>et al.</i> , 2007), Shrimp (Ng <i>et al.</i> , 2013), Crab (Robb <i>et al.</i> , 2014), Amoebae (Zhang <i>et al.</i> , 2016)
<b>Peptidoglycan</b>	Bacteria	Shrimp (Koiwai <i>et al.</i> , 2016)
<b>Zymosan</b>	Yeast	Seal (Reichel <i>et al.</i> , 2015), Dog (Zhengkai Wei <i>et al.</i> , 2016), Oyster (Poirier <i>et al.</i> , 2014)
<b>Microbial</b>		
<b>Bacteria</b>	<i>Brevibacterium stationis</i>	Oyster (Poirier <i>et al.</i> , 2014)
	<i>Escherichia coli</i>	Baboons (Xu <i>et al.</i> , 2010), Cow (Lippolis, <i>et al.</i> 2006), Shrimp (Ng <i>et al.</i> , 2013)
	<i>Edwardsiella tarda</i>	Fish (Zhao <i>et al.</i> , 2017)
	<i>Enterococcus faecalis</i>	Cow (Lippolis <i>et al.</i> , 2006)
	<i>Helicobacter pylori</i>	Human (Hakkim <i>et al.</i> , 2011)
	<i>Klebsiella pneumoniae</i>	Human (Papayannopoulos <i>et al.</i> , 2010; Wang <i>et al.</i> , 2017), Amoebae (Zhang <i>et al.</i> , 2016)
	<i>Mycobacterium tuberculosis</i>	Human (Ramos-Kichik, <i>et al.</i> 2009)
	<i>Neisseria meningitidis</i>	Human (Lappann <i>et al.</i> , 2013)
	<i>Pseudomonas aeruginosa</i>	Human (Yoo <i>et al.</i> , 2014),
	<i>Pseudomonas fluorescens</i>	Fish (Zhao <i>et al.</i> , 2017)
	<i>Shigella flexneri</i>	Human (Brinkmann <i>et al.</i> , 2004), Mouse (Beiter <i>et al.</i> , 2006)
	<i>Staphylococcus aureus</i>	Human (Brinkmann <i>et al.</i> , 2004; Fuchs <i>et al.</i> , 2007; Von Köckritz-Blickwede <i>et al.</i> , 2008), Cow (Lippolis <i>et al.</i> , 2006)
	<i>Vibrio tasmaniensis</i>	Oyster (Poirier <i>et al.</i> , 2014)
	<i>Vibrio harveyi</i>	Fish (Zhao <i>et al.</i> , 2017)



<b>Protozoa</b>	<i>Besnoitia besnoiti</i>	Cow (Muñoz Caro <i>et al.</i> , 2014)
	<i>Eimeria bovis</i>	Cow (Behrendt <i>et al.</i> , 2010)
	<i>Leishmania amazonensis</i>	Human (Guimarães-Costa, <i>et al.</i> 2009) Cat (Wardini <i>et al.</i> , 2010)
	<i>Neospora caninum</i>	Dog (Zhengkai Wei <i>et al.</i> , 2016)
	<i>Plasmodium falciparum</i>	Human (Abi Abdallah <i>et al.</i> , 2012)
	<i>Toxoplasma gondii</i>	Human (Abdallah <i>et al.</i> , 2012), Seal (Reichel <i>et al.</i> , 2015), Mouse (Abi Abdallah <i>et al.</i> , 2012)
<b>Fungi</b>	<i>Aspergillus fumigatus</i>	Human (Bruns <i>et al.</i> , 2010)
	<i>Candida albicans</i>	Human (Urban <i>et al.</i> , 2006)
<b>Virus</b>	Human immunodeficiency virus	Human (Saitoh <i>et al.</i> , 2012)
	Influenza A virus	Human (Tripathi <i>et al.</i> , 2014)
	Respiratory syncytial virus	Human (Funchal <i>et al.</i> , 2015)

**Table 1.6.** Known chemical and biological inhibitors of ET release in different animal species.

<b>Inhibitor</b>	<b>Type</b>	<b>Animal species</b>
<b>Diphenyleneiodonium (DPI)</b>	NADPH oxidase inhibitor	Human (Ostafin <i>et al.</i> , 2016), Seal (Reichel <i>et al.</i> , 2015), Mussel (Robb <i>et al.</i> , 2014), Crab (Robb <i>et al.</i> , 2014), Oyster (Poirier <i>et al.</i> , 2014)
<b>Cytochalasin</b>	Cytoskeleton inhibitor	Human (Brinkmann <i>et al.</i> , 2004; Neeli <i>et al.</i> , 2009), Crab (Robb <i>et al.</i> , 2014), Shrimp (Ng <i>et al.</i> , 2015), Mussel (Robb <i>et al.</i> , 2014)
<b>N-acetyl cysteine (NAC)</b>	ROS scavenger	Human (Funchal <i>et al.</i> , 2015)
<b>4-aminobenzoic acid hydrazide (ABAH)</b>	MPO inhibitor	Human (Kaplan <i>et al.</i> , 2012), Fish (Zhao <i>et al.</i> , 2017)

**Table 1.7.** Current list of chemical and biological inducers and inhibitors of ET release used in different fish species showing effect of compound, minimum concentration which elicited a response, and earliest time point where a response was reportedly statistically significant

Inducer	Fish species	Lowest effective concentration	Earliest effect	Reference
<b>β-glucan</b>	<i>Pimephales. promelas</i>	50 µg mL <sup>-1</sup>	60 min	(Palić, Ostojčić, <i>et al.</i> , 2007)
	<i>Danio rerio</i>	Unclear, presumably 50 µg mL <sup>-1</sup>	90 min	(Palić, Andreasen, <i>et al.</i> , 2007)
	<i>Cyprinus carpio</i>	200 µg mL <sup>-1</sup>	30 min	(Brogden <i>et al.</i> , 2014)
<b>Cal</b>	<i>Pimephales. promelas</i>	5 µg mL <sup>-1</sup>	10 min	(Palić, Ostojčić, <i>et al.</i> , 2007)
	<i>Danio rerio</i>	5 µg mL <sup>-1</sup>	90 min	(Palić, Andreasen, <i>et al.</i> , 2007)
	<i>Lates calcarifer</i>	Unclear	30 min	(Masterman, 2016)
<b>LPS</b>	<i>Pimephales. promelas</i>	0.5 µg mL <sup>-1</sup>	20 min	(Palić, Ostojčić, <i>et al.</i> , 2007)
	<i>Cyprinus carpio</i>	50 µg mL <sup>-1</sup>	30 min	(Pijanowski <i>et al.</i> , 2013)
	<i>Scophthalmus maximus</i>	1 µg mL <sup>-1</sup>	120 min	(Chi <i>et al.</i> , 2015)
<b>PMA</b>	<i>Pimephales. promelas</i>	0.25 µg mL <sup>-1</sup>	50 min	(Palić, Ostojčić, <i>et al.</i> , 2007)
	<i>Danio rerio</i>	Unclear presumably 0.25 µg mL <sup>-1</sup>	90 min	(Palić, Andreasen, <i>et al.</i> , 2007)
	<i>Cyprinus carpio</i>	1 µg mL <sup>-1</sup>	60 min	(Pijanowski <i>et al.</i> , 2013)
	<i>Lates calcarifer</i>	Unclear	30 min	(Masterman, 2016)
	<i>Cynoglossus semilaevis</i>	1 µg mL <sup>-1</sup>	60 min	(Zhao <i>et al.</i> , 2017)
<b>Polyinosinic:polycytidylic acid (Poly IC)</b>	<i>Cyprinus carpio</i>	25 µg mL <sup>-1</sup>	30 min	(Pijanowski <i>et al.</i> , 2013)
<b>Zymosan</b>	<i>Cyprinus carpio</i>	500 µg mL <sup>-1</sup>	30 min	(Pijanowski <i>et al.</i> , 2013)
<b>Inhibitor</b>				
<b>ABAH (MPO inhibitor)</b>	<i>Cynoglossus semilaevis</i>	100 µM	-	(Zhao <i>et al.</i> , 2017)
<b>NADPH oxidase inhibitor</b>	<i>Cyprinus carpio</i>	50 µM (DPI)	60 min	(Pijanowski <i>et al.</i> , 2013)
<b>Cytochalasin</b>	<i>Pimephales. promelas</i>	2.5 or 5 µg mL <sup>-1</sup>	60 min	(Palić, Ostojčić, <i>et al.</i> , 2007)
	<i>Danio rerio</i>	5 µg mL <sup>-1</sup>	90 min	(Palić, Andreasen, <i>et al.</i> , 2007)
<b>L-NAME (Nitric oxide inhibitor)</b>	<i>Cynoglossus semilaevis</i>	1 mM	Unclear	(Zhao <i>et al.</i> , 2017)
<b>Trolox (ROS scavenger)</b>	<i>Cynoglossus semilaevis</i>	100 µM	Unclear	(Zhao <i>et al.</i> , 2017)

### 1.3.5. Extracellular trap-associated pathogenesis

Despite the advantageous properties of ETs towards eliminating or reducing microbial infection, the ineffective clearance or regulation of ET release is strongly associated with inflammatory disorders and the pathogenesis of several human diseases (Kaplan *et al.*, 2012; Schorn *et al.*, 2012; Zawrotniak *et al.*, 2013; Papayannopoulos, 2017). The inflammatory mediators released during infections can induce the adhesion, degranulation, respiratory burst and ET release from PMNs, while tumour necrosis factor alpha induces differentiation and activation of several leukocytes, which further promotes the inflammatory state (Keshari *et al.*, 2012). Additionally, the antimicrobial peptides that decorate ETs can also exert cytotoxic effects against host cells, and this may lead to progressive host tissue damage if the ETs are not cleared quickly enough (Kaplan *et al.*, 2012). The clearance of ETs within host tissue is performed, in part, by DNases present in host serum (Hakkim *et al.*, 2010) and also by macrophages (Farrera *et al.*, 2013).

In mice, histones can cause epithelial and endothelial death in lung tissue *in vitro*, and administration of histones *in vivo* results in alveolar haemorrhage and microvascular thrombosis (Xu *et al.*, 2010, 2011). Furthermore, the proteases found associated with ETs, such as NE, MPO and LL-37, are also capable of hydrolysing different tissues (Zawrotniak *et al.*, 2013), thus also demonstrating another mechanism underlying the detrimental effects of prolonged exposure to ETs. In addition to direct tissue damage, ETs can promote blood clotting (*i.e.*, thrombosis) within vasculature by acting as a scaffold for the adherence of platelets and other blood cells (Fuchs *et al.*, 2010). Inflammatory cytokines such as IL-8 can promote neutrophil activity and ET release in humans, thus providing a link between inflammation, infection and the detrimental effects of ETs (Brinkmann *et al.*, 2004; Fuchs *et al.*, 2010).

The build-up of DNA and mucus in the sputum is distinctive of cystic fibrosis patients that have impaired ion transport across the epithelium, and the large densities of free DNA found within the sputum contributes to its high viscoelasticity and leads to the accumulation of mucus in the airways (Shah *et al.*, 1996; Henke *et al.*, 2007). The DNA in cystic fibrosis sputum originates mostly from neutrophils and, though it has initially been thought to be derived from necrotic neutrophils, the discovery of ETs has challenged this idea and provides an alternative explanation for the source of the DNA (Manzenreiter *et al.*, 2012). The use of nucleic acid-degrading enzymes such as recombinant human DNase-I promotes the clearance of sputum by degrading the DNA polymers, and this can eliminate or reduce the debilitating symptoms related to this (Shah *et al.*, 1996).

ETs are also implicated in a myriad of autoimmune diseases, as the presence of citrullinated histones in host tissue, which are characteristic of ETs, is highly immunogenic and promotes

the production of autoantibodies (Kaplan *et al.*, 2012). These autoantibodies facilitate immune reactions against the ET aggregates that build up in various diseases such as rheumatoid arthritis, atherosclerosis, small vessel vasculitis, systemic lupus erythematosus, and Felty's syndrome (Xu *et al.*, 2010; Liu *et al.*, 2012; Cheng *et al.*, 2013; Sur Chowdhury *et al.*, 2014). Overall, several inflammatory and autoimmune diseases are associated with ETs that persist in the host tissue for too long and may contribute to host damage, promote inflammation through macrophage activation and neutrophil recruitment, and lead to impaired wound healing (Fadini *et al.*, 2016).

Like mammals, inflammation-induced tissue damage is frequently observed in various salmonid diseases such as vibriosis, red mark syndrome (RMS), bacterial cold water disease, and furunculosis, (Metselaar *et al.*, 2010; Falco *et al.*, 2012; Hickey *et al.*, 2017; Hoare *et al.*, 2017). PMA or LPS-induced ET release in carp also results in the upregulation of the pro-inflammatory cytokines IL-10, IL-1 $\beta$  and TNF- $\alpha$  (Pijanowski *et al.*, 2015). To what extent ETs released by fish cells contributes towards an inflammatory state is uncertain, though it is possible that ETs contribute to the pathogenesis of inflammatory diseases is not limited to mammals.

#### **1.4. Microbial evasion strategies against extracellular traps**

Microbial pathogens demonstrate a breadth of strategies to evade ETs, and these can be broken down to three categories: inhibition of ET release, degradation of ETs, or resistance to killing by ETs (Storisteanu *et al.*, 2017). Group A Streptococcus (GAS) is a well-studied example that exhibits ET evasion strategies within all three of these categories. The haemolytic endotoxin, streptolysin, released by GAS can reduce neutrophil ROS generation, which is required for generation of ETs (Uchiyama *et al.*, 2015). Further downregulation of ROS production in neutrophils is attributed to the hyaluronic acid capsule on GAS, which mimics immunoregulatory proteins and binds to inhibitory neutrophil receptors, Siglec-9, thereby reducing ET formation (Secundino *et al.*, 2016). Also, pro-inflammatory cytokines such as IL-8 can be targeted and cleaved by GAS-produced SpyCEP, which acts to prevent the recruitment of further neutrophils (Zinkernagel *et al.*, 2009). Moreover, the production of extracellular nucleases by GAS, such as streptodornase 1 (Sda 1), is a virulence strategy and these enzymes help to liberate bacterial cells from ETs (Walker *et al.*, 2007). In addition, *S. aureus* evades ETs by producing adenosine synthase A (Ads A), an enzyme that modifies degraded ET products into compounds with apoptosis-inducing activities against macrophages (Thammavongsa *et al.*, 2013).

*P. aeruginosa* resists the antimicrobial actions of ETs by reducing the net negative charge at its cell surface using the aminoarabinose (*arn*) operon. The products of the *arn* operon are

responsible for the covalent addition of aminoarabinose to phosphates of lipid A of the bacterial membranes to mask their negative surface charge, thereby reducing the binding of ETs (Halverson *et al.*, 2015). *P. aeruginosa* also upregulates the surface expression of the cationic protein, spermidine, which contributes to resistance against the activity of antimicrobial peptides and increases bacterial membrane stability (Halverson *et al.*, 2015). A similar method of resistance is reported with *Neisseria meningitides*, whereby they are not killed completely by ETs, but can still replicate after exposure to ETs. *N. meningitides* modifies the lipid A of the LPS to protect against the proteolytic activity of cathepsin G, an antimicrobial protein that decorates the ETs (Lappann *et al.*, 2013). Furthermore, calprotectin in ETs bind zinc or other trace metals, thereby limiting an essential nutrient required for the replication of *Candida albicans* (Urban *et al.*, 2009; Achouiti *et al.*, 2012). However, *N. meningitides* Zinc neisserial outer-membrane transporter (ZnuD) is a high affinity zinc uptake receptor is essential to survival against ETs (Lappann *et al.*, 2013), indicating that there exists a bacterial strategy to combat ET that directly challenges the ion sequestering capability of granules within ETs.

#### **1.4.1. Extracellular nuclease**

In particular, different pathogens can harbour multiple strategies to reduce the antimicrobial effects or trapping by ETs which share similar mechanisms such as surface charge alteration or reducing inflammatory signals. For decades, pathogenic benefit of the production of extracellular nuclease(s) was not clear; although extracellular nucleases were found to have a role in degrading extracellular DNA polymers in the environment to generate nucleotide and phosphate pools that can be used by bacteria as a source of nutrients (Mitchell *et al.*, 1977; Pinchuk *et al.*, 2008; Mcdonough *et al.*, 2016). However, in light of recent evidence surrounding ETs and bacterial trapping showing the association of pathogenesis and infection with extracellular nuclease production, it is clear that extracellular nucleases play a role in ET degradation and evasion to promote pathogenesis (Storisteanu *et al.*, 2017). This simple, yet effective method, is ubiquitously observed in reported ET-resistant pathogens to contribute to ET resistance (Storisteanu *et al.*, 2017), and the direct degradation of ETs observed by extracellular nucleases alone can be a successful strategy to resist trapping (Seper *et al.*, 2011; Brogden *et al.*, 2012; de Buhr *et al.*, 2015; Juneau *et al.*, 2015).

With fish ETs, nuclease production to evade trapping by carp ETs was observed for *A. salmonicida*, (Brogden *et al.*, 2012). Another fish pathogen known to produce nucleases is *Vibrio anguillarum*, the etiological agent of vibriosis, which is a potentially serious disease of salmonid and perciformes finfish and shellfish, and the disease presents as internal and external inflammation and ulceration, flesh rot, dark skin colouration, pale gills, swollen

haemorrhages at the base of the fins, and haemorrhagic septicaemia, while the fish also behave lethargically and show a loss of appetite (Austin *et al.*, 1995; Ackerman *et al.*, 2001; Frans *et al.*, 2011; Novriadi, 2016; Hickey *et al.*, 2017). The extracellular nucleases of *V. anguillarum* are not well characterised, and their role in bacterial fitness is not clear; however, the inflammatory phenotype following *V. anguillarum* infection and their characterised nuclease expression (Austin *et al.*, 1995) eludes to the possibility of the bacteria encountering ETs during its lifecycle and utilising nucleases to resist trapping by ETs.

## **1.5. Aims and Objectives**

The overall aim of this thesis was to confirm and characterise the release of extracellular traps in rainbow trout and to investigate their antimicrobial properties.

This aim was achieved by fulfilling the following objectives:

1. Obtaining enriched cell suspensions of trout PMNs.
2. Validating methods to quantify ET release from PMNs.
3. Confirming the DNA structure and the presence of diagnostic protein markers of ETs
4. Investigating the effect of chemical and biological stimulants on ET release.
5. Characterising and evaluate the roles of extracellular nuclease produced by *V. anguillarum* to mitigate against the ETs
6. Investigating the antimicrobial action of ETs against *V. anguillarum* and determining if their nuclease production may provide resistance against trout ETs.

## Chapter 2: Isolation of polymorphonuclear cells and quantification of extracellular traps

### 2.1. Introduction

Isolation and separation of different blood cell types requires tailored protocols for each fish species due to dissimilarities between species with respect to leukocyte morphologies, relative cell densities and granularities. For example, cyprinids such as goldfish (*Carassius auratus*) and zebrafish (*Danio rerio*) produce polymorphonuclear cells (PMN), which differ morphologically to those of mammals and other fish species (Katzenback *et al.*, 2009), as cyprinid PMNs lack the characteristic lobed nuclei of mammalian or salmonid counterparts (Pettersen *et al.*, 2000; Lieschke *et al.*, 2001; Øverland *et al.*, 2010; Zhu *et al.*, 2012; Collet, 2014). Thus, the unique leukocyte characteristics of different fish species require optimised isolation methods according to species and desired cell type. There are established methods for enriching trout PMNs using antibodies and cell sorting, however, these procedures have a lower throughput and are therefore much slower than separating cells by density gradient centrifugation (Hamdani *et al.*, 1998). Discontinuous Percoll gradients are often used to isolate leukocytes of similar granularity and density, and the use of a specific double-layer discontinuous Percoll gradient has reported proportions of up to 68% pure PMNs from Atlantic salmon head kidney tissue (Øverland *et al.*, 2010); however, protocols for the use of Percoll gradients for isolation of rainbow trout PMNs remain to be well defined.

The proportion of leukocyte types produced by haematopoietic tissue of an organism may be influenced by the organism's weight, and environmental factors, such as diet, light exposure, pH, temperature, and season (Bridges *et al.*, 1976; Lie *et al.*, 1990; Modrá *et al.*, 1998; Ruchin, 2006; Tavares-Dias *et al.*, 2011; Alijagic *et al.*, 2017). This variable proportion has sometimes been termed the leukocyte index, or haematopoietic index (Zhu *et al.*, 2013). Regarding fish, environmental temperature or season can influence the hematopoietic index of the animal. Winter flounder (*Pseudopleuronectes americanus*) have been shown to peak in erythrocyte production during April and May, while their circulating leukocytes reach a peak during the summer months (Bridges *et al.*, 1976). In rainbow trout, season and fish weight have also been shown to influence haematological parameters (Denton *et al.*, 1975). As well as proportions of leukocytes produced, a number of factors can influence immunological responsiveness of leukocytes from rainbow trout, such as altering respiratory burst activity of macrophages (Morgan *et al.*, 2008). Positive correlations with overall leukocyte counts and increased immune function in rainbow trout have, for example, been reported when environmental temperatures were 5 – 10°C above ambient (Bly *et al.*, 1992; Le Morvan *et al.*, 1998). Moreover, macrophage respiratory burst activity, a process regulated by NADPH



oxidase, is affected significantly by temperature (Hardie *et al.*, 1994), and is potentially also affected by fish size (Morgan *et al.*, 2008). Thus, the weight of hatchery trout or rearing temperatures may affect the enrichment methods of PMNs.

Optimal cell culture conditions depend heavily upon the specific demands of different cell types. Studies on extracellular traps (ET) require fresh blood and conditions which yield maximum viability of PMNs during their short (~12 h) lifespan *in vitro* (Payne *et al.*, 1994). In general cell culture practice, serum is often added as a supplement between 10 – 20% of total medium volume to maintain cell viability. The presence of nutrients in the form of vitamins, minerals, carbohydrates, fatty acids, and other survival factors in serum, serve to help inhibit apoptosis and promote cell survival (Brunner *et al.*, 2010). However, heat-resistant nucleases found in foetal calf serum (FCS) can degrade ETs released from human PMNs *in vitro* (Sur Chowdhury *et al.*, 2014). As a result, a fine balance is required when culturing PMNs for studying ETosis and researchers must use minimum serum concentration to maintain high cell viability, at the expense of minimising the potential degradation of ETs by nucleases present in serum (von Köckritz-Blickwede *et al.*, 2010). With respect to rainbow trout, a clear minimum concentration of FCS for maintaining a viable trout PMN-enriched suspension remains to be established. Furthermore, the type of media used to culture cells and their supplementation with pH buffers plays a significant role in determining cell viability, due to different salinities or pH buffer profiles in cell culture (Iscove *et al.*, 1978; Martinelle *et al.*, 2010). For example, the Roswell Park Memorial Institute cell medium (RPMI) preserves human PMN viability significantly better than balanced salt solutions due to their specific formulation (Payne *et al.*, 1994). Bicarbonate buffers such as 4-(2-hydroxyethyl)-1-piperazineethanesulfonic acid (HEPES) are often used in cell culture in the absence of CO<sub>2</sub> incubators to balance pH (Ferguson *et al.*, 1980), as they may assist in balancing pH despite of changes in CO<sub>2</sub> levels, indicated by trout epithelial gill cell recovering from acidosis in the presence of HEPES (Wood *et al.*, 2000). It is not clear whether pH balance is essential for the culture of short-term primary PMN-enriched suspensions in trout, as different cell types require different conditions for maximum viability.

With regards to studying the release of ETs *in vitro*, multiple assays have been established to manipulate and quantify ET release in response to assumed ET-mediating compounds; though currently there is no standardised method. The techniques used to manipulate ET release *in vitro* largely depend on the method used to quantify the ETotic response. The two broad categories of methods used to quantify ET release comprise the measurement of fluorescence from extracellular DNA via fluorescent dyes or antibodies, or the enumeration of the number of physical ET structures, and each method has balanced advantages with disadvantages as summarised in Section 1.3.2 (von Köckritz-Blickwede *et al.*, 2010; Gray *et al.*, 2013; Robb *et al.*, 2014; de Buhr *et al.*, 2016; Jeffery *et al.*, 2016). Careful attention is

required when selecting a method to quantify ET release, and often the limitations of each method are overlooked without further information, or evidence of consideration. A popular method used to quantify ET release *in vitro* includes a fluorimetry-based assay involving the measurement of extracellular DNA fluorescence from fluorescent nucleic acid intercalating dyes, which is used as a proxy for ET release (Gray *et al.*, 2013; Jeffery *et al.*, 2015, 2016). However, fluorescent signals resulting from DNA staining within membrane-compromised cells are not distinguished from ET staining, and thus it is not clear how much impact the stained, membrane-compromised cells have on the overall fluorescence reading. Furthermore, properties of fluorescent readings can depend on the concentration or spread of fluorescent signal which may affect the reliability of the measurement. To circumnavigate this limitation, other methods to quantify ET release *in vitro* include manually counting the ET-like structures after staining with fluorescent dyes. However, these structures are only presumed to be ETs without further confirmation, and the different ET morphologies may lead to inaccuracy in the overall quantification. Validation of the methods used to quantify ETs is required to ensure that appropriate ways to measure ET release are employed. In addition, there is little evidence in the literature as to how fluorescence data behaves at different extremes of data values. For example, how strong is the relationship between fluorescence and ET counts, and is any such relationship directly linear.

The overall aims of the work described in this chapter were to identify a technique that gives enriched populations of viable PMNs from head kidney preparations and to evaluate a method to quantify presumed-ET-like structures *in vitro*. These aims were met by achievement of the following objectives: Comparison of two discontinuous Percoll gradient protocols for enriching PMNs from fish head kidney tissue; evaluation of PMN viability over 24 h in the presence or absence of FCS, or HEPES buffer and in different artificial cell culture media; determination of whether a correlation exists between DNA abundance and SYTOX Green fluorescence; lastly, determination of whether a correlation exists between the abundance of ET-like structures and SYTOX Green fluorescence.

## **2.2. Materials and Methods**

### **2.2.1. Reagents**

The following reagents were purchased from Sigma-Aldrich (Dorset, UK): benzocaine, 10× Hank's balanced salt solution (HBSS) without calcium chloride or magnesium sulphate and sodium bicarbonate, heparin, HEPES, Leibovitz's L-15 media (with L-glutamine and phenol

red, without sodium bicarbonate), penicillin-streptomycin antibiotic (Pen-Strep) 10,000 U penicillin and 10 mg mL<sup>-1</sup> streptomycin (sterile-filtered), Percoll® pH 8.5-9.5 (20°C), phorbol 12-myristate 13-acetate (PMA), trypan blue supplied at 0.4%. The following reagents were purchased from Thermofisher Scientific (Loughborough, UK): Calcium ionophore (Cal) A23187, 4',6-Diamidino-2-Phenylindole, dihydrochloride (DAPI) dilactate, heat-inactivated foetal bovine/calf serum (FCS), Hoechst 33342 trihydrochloride trihydrate, RPMI (different supplementation of RPMI with FCS and antibiotics is defined as RPMI1, 2, or 3<sup>1</sup> [Appendix Table 2], and SYTOX Green. Phosphate buffered saline (PBS) was prepared with 8 g NaCl, 0.2 g KCl, 1.78g Na<sub>2</sub>HPO<sub>4</sub>·H<sub>2</sub>O and 0.24 g KH<sub>2</sub>PO<sub>4</sub> per litre, corrected to pH 7.4 with 1M HCl. All reagents were prepared as per manufacturer's instructions, and aliquots of the reagents were prepared under sterile conditions to reduce contamination, and were discarded after indications of contamination. Self-supplied dH<sub>2</sub>O and PBS were sterilised by autoclaving at 121°C at 15 PSI for 20 minutes.

### **2.2.2. Source of fish and husbandry**

Healthy rainbow trout (*O. mykiss*) from Frandy fish farm were either collected freshly killed or transported live for housing in the flow-through cold-water aquarium at the Institute of Aquaculture (IoA) during June 2014 to September 2017. Water temperature was recorded from tanks on days when fish were sampled, and mean water temperature during the year was 9.76°C (5.7–12.8°C). The fish were fed by hand three to four times daily on a commercial feed (Appendix Table 1). All fish used for experiments weighed between 50–500 g, and were sacrificed according to a Schedule 1 technique (overdose of benzocaine and destruction of the brain) as described in the 1986 Animals Scientific Procedures Act (ASPA). All experiments were approved by the IoA Ethics Committee or the Animal Welfare Ethical Review Board (AWERB).

### **2.2.3. Separation of PMNs rainbow trout head kidney cell suspensions**

Enriched rainbow trout PMN suspensions were prepared by separating head kidney cell (HKC) suspensions by discontinuous Percoll gradient isolation. Two discontinuous Percoll gradient methods were compared with respect to level of purification of populations of PMNs and minimisation of contamination with other leukocyte types. The first method was a double-layer gradient protocol used for enriching PMNs in Atlantic salmon and comprised layers of

---

<sup>1</sup>Roswell Park Memorial Institute-1640 medium: RPMI1 (no FCS, no antibiotics); RPMI2 (1% FCS, 0.5% Penicillin 10,000 U and Streptomycin 10 mg mL<sup>-1</sup>); RPMI3 (1% FCS, no antibiotics)

1.060, and 1.075 g mL<sup>-1</sup> Percoll (Øverland *et al.*, 2010). This was compared to a triple-layer gradient protocol able to enrich PMNs from carp head kidney consisting of 1.060, 1.072, and 1.084 g mL<sup>-1</sup> Percoll (Kemenade *et al.*, 1994). Percoll solutions were prepared aseptically in stock batches (Table 2.1), and were used immediately to form discontinuous gradients in a universal tube, or stored at 4°C for later use for up to three weeks. A discontinuous gradient was formed by layering 5 mL of denser Percoll solutions underneath 5 mL of lesser density Percoll solutions with the aid of an electronic Pipet-Aid XP2 (Drummond, Broomall, USA) to make up a total volume of 10 mL (double-layer) or 15 mL (triple-layer).

**Table 2.1.** Volumes of Percoll, HBSS (10×) and dH<sub>2</sub>O required to make up 10 or 15 mL Percoll solutions as discontinuous double or triple layer gradients in a universal tube.

Target cell; Gradient type	Percoll density (g mL <sup>-1</sup> )	10× HBSS (mL)	dH <sub>2</sub> O (mL)	Percoll (mL)
PMN (Double layer)	1.060	1	4.83	4.17
	1.075	1	3.86	5.32
PMN (Triple layer)	1.06	1	4.83	4.17
	1.072	1	3.91	5.09
	1.084	1	3	6

Each fish was weighed before being bled through caudal venepuncture using a 2.5 mL syringe and 25G × 5/8 needle (Terumo, Surrey, UK). Then the entire head kidney was removed by dissection using 70% isopropanol-disinfected scalpel and tweezers in a Class II flow hood (BS5726; Gelaire, Sydney, Australia). The head kidney was then transferred into a 100-µm mesh cell strainer (Falcon, Fisher Scientific, Loughborough, UK) in a 6-cm Petri dish containing 5 mL of RPMI3 containing an added 5 µL of heparin (final well concentration of 10 U mL<sup>-1</sup>) to prevent clotting, and the tissue was broken up by gently pressing it through the cell strainer with the plunger tip of a 5 mL syringe. Head kidney cells in suspension were overlaid onto the prepared discontinuous Percoll gradient using a sterile Pasteur pipette, and centrifuged at 400 ×g, 35 minutes, 4°C (acceleration: 1, brake: 1) to separate the PMNs from the other leukocytes. A band of enriched PMNs should occur at the interface between 1.060 and 1.072 g mL<sup>-1</sup>, and cells from this band were collected using a sterile Pasteur pipette and transferred into a 50-mL Falcon tube. The PMNs were washed once to remove debris and remaining Percoll solution by adding 20 mL of ice-cooled RPMI3, and centrifuging (800×g, 7 minutes, 4°C, acceleration 8, brake 4), before resuspending the cell pellet in 2 mL of RPMI2. The cells in the nominally PMN-enriched suspension were counted with the aid of a light

microscope and a Neubauer haemocytometer, and adjusted to approximately  $4 \times 10^5$  cells  $\text{mL}^{-1}$  with RPMI2.

#### **2.2.4. Cytospin preparation and RapiDiff staining**

To observe and determine the cell types present in the cell suspension obtained after Percoll enrichment, cytospin slides were prepared from the cell suspension and stained with a commercial Romanowsky histology stain kit (Appendix Section 1.4); TCS Biosciences, Buckingham, UK). The cytospin slides were prepared by placing a glass microscope slide in a cytospin chamber (GMI Inc, Ramsey, MN, USA), and adding the cell collection bucket. To each bucket was added 100  $\mu\text{L}$  of FCS to cushion the cells, and then 100  $\mu\text{L}$  of enriched PMN cell suspension ( $4 \times 10^5$  cells  $\text{mL}^{-1}$ ). The chamber was then centrifuged in a Cytospin 3 centrifuge (1000 revolutions per minute, 5 minutes, room temperature; GMI Inc, Ramsey, MN, USA) and the glass slides were removed and air dried at room temperature for 15 minutes. Three glass Coplin staining jars were filled sufficiently to immerse each slide (excluding the label) with the A, B, and C RapiDiff solutions. The slides were immersed in each jar for 30 s, rinsed gently with tap water, allowed to dry at room temperature for 1 h, and then visualising under a light microscope. Cytospin slides were observed at 20 $\times$  magnification or greater with a compound light microscope (Olympus CH-2 and BX-51; Olympus CH-2, Essex, UK). The BX-51 microscope had an AxioCam MRC camera (Zeiss, Cambridge, UK) attached for imaging, and images were collected with the Axiovision software (v.4.8, Zeiss, Cambridge, UK).

The staining kit employed for cell differentiation consisted of a methanol-based fixative (solution A), an acidic dye (solution B) and a basic dye (solution C). Acidic (or anionic) dyes, such as eosin Y or eosin B, bind to cationic sites on proteins and give an orange-red colour to haemoglobin or eosinophil granules. Basic (or cationic) dyes, such as methylene blue can bind to anionic sites on proteins to give them a dark blue or purple appearance such as chromatin, nucleoproteins, ribosome-rich cytoplasm basophilic granules, as well as a lighter blue appearance for more weakly stained neutrophilic granules (Bain, 2016). Using this kit, the specific staining characteristics of different leukocyte cell types allowed for their differentiation by light microscopy.

#### **2.2.5. Comparing cell proportions from cytospin slide preparations**

Quantification of cell types after enrichment from double and triple-layer Percoll gradient protocols was performed by counting the proportion of cells from at least three randomly-selected fields of view (FOV) from images taken of cytospin slides prepared as in Section

2.2.4. Random FOV were generated by dividing the area of the cells on the slide, and assigning sections as whole integers from 1. A random whole integer generator was used to select FOV from the area. The proportion of PMNs and monocyte/macrophage (Mo/M) cells were calculated as a percentage of the total cells counted in each FOV. Means counts from at least three FOV sections from one cytopsin preparation per fish were calculated. In cytopsin preparations, rainbow trout PMNs (neutrophils) were identified by cells having a lobed, dark purple-stained nucleus, a pink-blue cytoplasm, few purple granules, with a cell diameter of 10 – 20  $\mu\text{m}$ ; appearing similar to trout PMNs (Pettersen *et al.*, 2000; Øverland *et al.*, 2010; Bain, 2016). Macrophages/monocytes were classified as cells containing a kidney-shaped, purple-stained nucleus, grey-blue cytoplasm, no stained granules, and approximately 10 – 15  $\mu\text{m}$  in diameter (Sorensen *et al.*, 1997).

#### **2.2.6. Relationship between PMN proportions, fish weight, and water temperature**

To assess the effect of fish mass on the proportion of trout PMNs enriched from head kidney tissue by the triple layer Percoll gradient approach as above, 6 trout were weighed and PMN proportion determined. PMNs were enriched according to Section 2.2.3 with trout weighing from 168 – 373 g. The PMN proportion from each fish was enumerated by counting the percentage of PMNs from total sampled cells as in Section 2.2.5, and the mass of each fish was correlated with the mean PMN proportions enumerated from the same fish. The tank water temperature was recorded on the morning that each fish was collected for the experiment.

#### **2.2.7. Assessing cell viability with trypan blue exclusion in different culture conditions over time**

To determine the viability of the cells in enriched PMN cell suspensions obtained by triple-layer discontinuous Percoll gradient preparations at a single time point, cells in suspension were examined at  $1 \times 10^6$  cells  $\text{mL}^{-1}$  in RPMI. To 100  $\mu\text{L}$  of cell suspension in a sterile Eppendorf tube, 10  $\mu\text{l}$  trypan blue solution (0.4%) was added and mixed by gentle pipetting. A 10  $\mu\text{L}$  sample of the trypan blue-stained cells were loaded into chambers of a Neubauer haemocytometer and examined immediately under 20 $\times$  magnification on a light microscope. Trypan blue has a negatively-charged chromophore that penetrates and stains the cell only when the membrane is damaged, so cells are considered non-viable if they stain blue. Therefore, the number of trypan blue-stained cells and total cells in the four large haemocytometer quadrants were enumerated and the proportion of viable cells in the cell suspension was then calculated. Counts were performed immediately after staining with

trypan blue, as leaving for >10 minutes can result in false staining of live-cells (Strober, 2015). The percentage of viable cells was calculated as follows:

$$\text{Percentage of viable cells} = [1.00 - (\text{Number of blue cells} \div \text{Number of total cells})] \times 100$$

To determine if FCS concentration affects the viability of trout PMNs, an enriched suspension of PMN cells (isolated, separated and prepared with the triple-layer Percoll gradient according to Section 2.2.3) was adjusted to  $1 \times 10^6$  cells mL<sup>-1</sup> with RPMI1. Five millilitres of this cell suspension was seeded into a sterile 50-mL Falcon tube before 100  $\mu$ L of FCS in RPMI1 was added to give final concentrations of 0.5, 1, 5, and 10% FCS. A negative control group was prepared by making up the final volume of the suspension with RPMI1 only. Then each cell suspension was incubated at 13°C and cell viability in each suspension assessed in triplicate at 0, 24, 48, and 72 h by the trypan blue exclusion method as described above. This experiment was repeated for four individual animals.

In addition, the effect of cell culture media (RPMI or L-15) on viability in PMN-enriched cell suspensions was examined over 0, 24, 48, and 74 h. PMN-enriched cell suspension (isolated, separated, and prepared with the triple-layer Percoll gradient as in Section 2.2.3) were adjusted to  $1 \times 10^6$  cells mL<sup>-1</sup> using RPMI3 or L-15 (supplemented with FCS to 0.5% final concentration) after wash step (as in Section 2.2.3), then pipetted into 50-mL Falcon tubes, and then cell viability determined in quadruplicate readings with trypan blue as above.

As pH control may improve PMN cell viability, the effect of HEPES buffer on viability in PMN-enriched cell suspensions over 0, 24, 48, and 74 h was determined (Olmsted *et al.*, 2005). HEPES is a bicarbonate buffer, it acts to maintain physiological pH without the requirement of a CO<sub>2</sub> incubator. RPMI2 with HEPES buffer (supplied as 25 mM) was used to re-suspend the PMN-enriched suspensions to  $1 \times 10^6$  cells mL<sup>-1</sup> (isolated, separated, and prepared with the triple-layer Percoll gradient) after the wash step, and viability was determined in quadruplicate readings with trypan blue as above. The results were compared to cell viability in RPMI2, without HEPES.

## **2.2.8. Evaluation of a fluorescence microtiter plate assay for high-throughput quantification of ETs**

### **2.2.8.1. Confirmation of correlation between DNA concentration and fluorescence**

To confirm that there was a correlation between DNA concentration in RPMI and SYTOX Green fluorescence, we measured the fluorescence of salmon sperm DNA (0.1, 0.5, 1, 2.5, 5, and 10 ng mL<sup>-1</sup> diluted in dH<sub>2</sub>O) in a 96-well culture plate (Cell+; Sarstedt, Nümbrecht, Germany) after staining with 10 µL of SYTOX Green (final well concentration of 5 µM) for 5 minutes. The concentration and purity of stock salmon sperm DNA was confirmed using the nanodrop reader (ThermoFisher Scientific, Loughborough, UK), and dilutions of DNA were performed in microcentrifuge tubes before adding to wells. To wells containing 50 µL of RPMI2, 10 µL of salmon sperm DNA was added to give final concentrations as stated. The fluorescence from each well was recorded using a spectrofluorimeter (excitation 485 nm, emission 528 nm). Mean fluorescence from five replicate wells represented each treatment group.

#### **2.2.8.2. Assaying *in vitro* ET formation by fluorimetry and fluorescence microscopy**

A 96-well plate assay was used to examine manipulation of ET release, and then the relative amount of ETs released by enriched PMN cell suspensions (obtained by triple-layer discontinuous Percoll gradient preparations) *in vitro* was quantified by spectrofluorimetry according to Section 2.2.8.1. To each well of a flat-bottomed 96-well culture plate, 50 µL of trout PMNs in RPMI2 was transferred at  $4 \times 10^5$  cells mL<sup>-1</sup> under sterile conditions. The plate was incubated (30 min, 15°C) to allow the cells to adhere to the bottom of the wells. The PMNs were subsequently incubated with 10 µL of Cal (final well concentration of 5 µg mL<sup>-1</sup>), a characterised inducer derived from studies of other fish (Palić, Andreasen, *et al.*, 2007; Palić, Ostojić, *et al.*, 2007), or left untreated with 10 µL of RPMI1 as a negative unstimulated control. Plates were wrapped in foil to protect the cells from light and incubated for 1, 3, 6, 9, or 12 h at 15°C, before observation and/or quantification of ET release. Well contents were stained with 10 µL of SYTOX Green (final well concentration of 5 µM), a cell membrane-impermeable dye, for 5 min at room temperature with plates wrapped in foil to protect samples from light exposure. Then, the fluorescence emitted from stained extracellular DNA was measured with a microplate spectrofluorimeter (shaking for 10 s at medium intensity setting, excitation 485 nm, emission 528 nm; BioTek Synergy HT, Swindon, UK). Mean fluorescence was calculated from triplicate wells for each treatment group with wells laid out in a column and avoiding wells at the edge of the plates. Separate plates were loaded for measuring fluorescence at each time point to prevent contamination. Background fluorescence of individual treatment wells was subtracted from a mean fluorescence of triplicate wells at the same time point containing 50 µL of supplemented RPMI2, 10 µL of treatment solution (Cal or RPMI1), stained with 10 µL of SYTOX Green. The stained cells were also observed directly under the Olympus IX-70 (Olympus, Essex, UK) inverted fluorescent microscope through the LUCPlanFLN 20x objective (PH2 Phase Plan Achromat), and images using phase contrast and fluorescent filters



were taken using the Axiovision v.4.8 software paired with the Axiocam MRC camera. Phase contrast and fluorescent images were overlaid and processed using ImageJ v1.50i.

### **2.2.8.3. Relationship between extracellular DNA fluorescence and ET abundance**

The intensity of fluorescent cell membrane-impermeable DNA-intercalating dyes is related to levels of membrane-compromised in cells (Jeffery *et al.*, 2015, 2016; de Buhr *et al.*, 2016). The fluorimetry assay used to quantify *in vitro* abundance of ETs was validated by examining the relationship between *in vitro* fluorometric measurements with representative counts of presumptive ETs from 54 matched samples as another means to quantify ET release. To validate that the SYTOX Green fluorescence recorded in the well of the 96-well plate after staining PMNs (both untreated and induced to release ETs) was representative of the number of ETs present in a well, the mean fluorescence of three replicate wells was compared with the mean number of counted numbers of ETs of total cells from matched fluorescent images; 54 in total. Presumed-ET counts were performed by enumerating the number of ET-like structures in at least three representative images of the well, using a FOV taken at 20x magnification. ET count data were expressed as percentages of ET-forming cells of the total number of cells in a matched phase contrast image. The presumed-ET structures were defined as comet or mesh-like structures which were stained positively with SYTOX Green (Figure 2.7).

To ensure a representative range of ETs were accounted for, we used images and wells which showed both abundant, and very few ET counts. Low ET counts were achieved by counting ETs from incubated unstimulated PMNs while high ET counts were achieved by incubating PMNs using Cal as used in Section 2.2.8.2. Into wells containing 50  $\mu\text{L}$  of PMNs in RPMI2, 10  $\mu\text{L}$  of Cal (final well concentration of 5  $\mu\text{g mL}^{-1}$ ) was added and wells incubated for 1, 3, 6, 9, or 12 h at 15°C. Unstimulated control cells were treated with RPMI1 cell media, which was used to dilute the Cal for the same duration and temperature

### **2.2.9. Statistical analyses**

Statistical analyses were carried out using Prism v.5.1 (GraphPad, La Jolla, USA), and  $p < 0.05$  was considered to indicate a significant difference between groups. The following data were tested for normality by the Shapiro-Wilk test: the comparison of PMN proportions to fish weight or temperature of fish rearing, the relationship between SYTOX fluorescence and salmon sperm DNA concentration, and the relationship between SYTOX fluorescence and ET counts. The Pearson's correlation coefficient was used to determine the statistical significance of these correlation data.

The Kolmogorov-Smirnov test was used to test for normality of data when comparing cell viability in different FCS concentrations, different media, and supplementation with or without HEPES buffer. Two-way ANOVA with Bonferroni's post-hoc test was used to compare differences in mean cell viability in different concentrations of FCS or different media. In all data when applicable, standard error of the mean (s.e.m.) was calculated.

## **2.3. Results**

### **2.3.1. Comparing cell proportions after discontinuous Percoll gradient isolation**

Rapid Romanowsky staining of cytopsin preparations with head kidney cell suspensions after Percoll gradient enrichment allowed for the morphological distinction between leukocyte types and erythrocytes (Figure 2.1). The proportions of PMN and Mo/M cells were compared after enrichment by double or triple-layer Percoll gradient protocols used for isolating fish PMN from head kidney preparations. The double-layer discontinuous gradient approach gave a suspension containing  $34.28 \pm 3.25\%$  ( $\pm$  SEM) PMNs, with  $23.90 \pm 4.97\%$  monocyte/macrophage (Mo/M) observed as a proportion of total cells in the isolated fraction; while the triple-layer approach gave a suspension containing  $57.99 \pm 4.84\%$  PMNs, with  $9.52 \pm 1.71\%$  Mo/M (Table 2.2). The triple-layer gradient resulted in a 1.69-fold improvement in PMN enrichment, and reduced Mo/M contamination compared to the double layer gradient method. Furthermore, erythrocytes and some granulocytes looked similar in appearance to eosinophils (lobed nucleus with darker granules) were found at the Percoll interface of 1.072 and 1.084 g mL<sup>-1</sup> layers in trout (data not shown), suggesting that the triple-layer Percoll gradient method was more successful at filtering out cells of closely-matched densities. These experiments were repeated in diploid Atlantic salmon (with 17 fish) and similar results were obtained (Appendix Table 1).

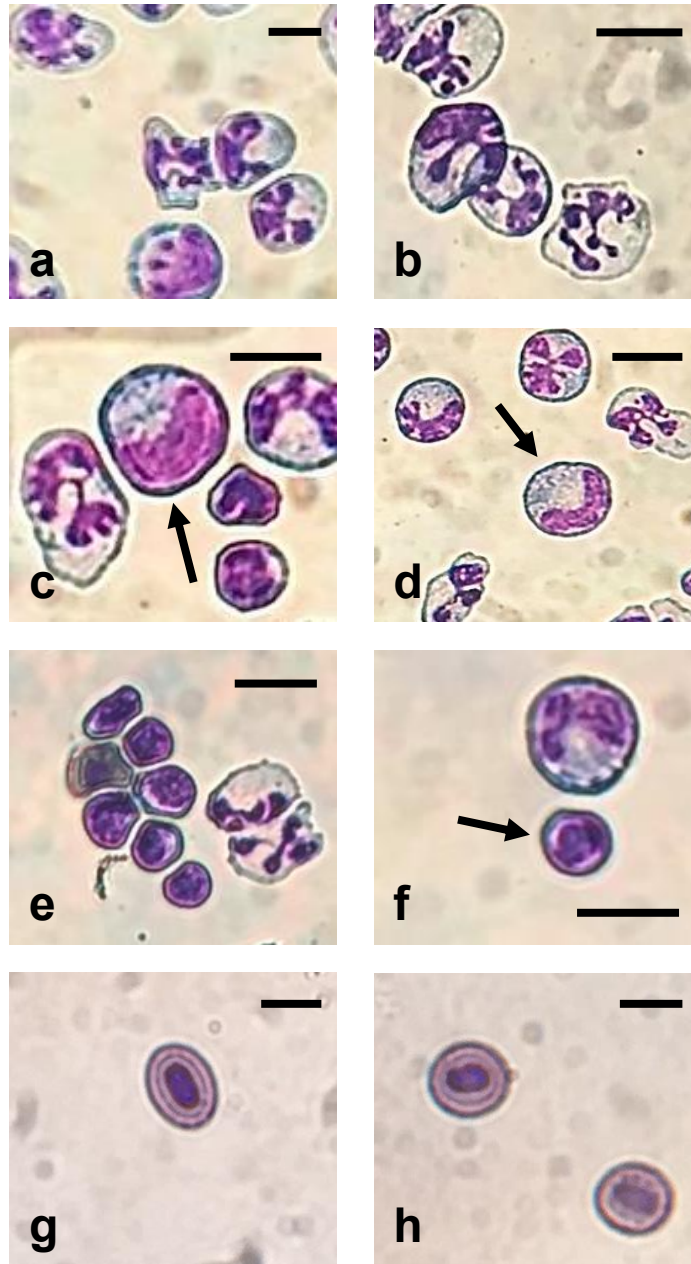


**Figure 2.1.** Representative images showing cytospin preparations from rainbow trout leukocyte cell solutions after rapid Romanowsky staining to show specific cell types based on morphology and staining characteristics. (a,b) Polymorphonuclear cells (PMN) with a dark-purple lobed nucleus; (c,d) Monocyte/macrophages (Mo/M) with a kidney-shaped nucleus, indicated by black arrows, approximately the same size as a PMN; (e,f) Lymphocytes (L) are labelled with black arrows; (g,h) Erythrocytes (E). Scale bar = 10  $\mu$ m.

**Table 2.2** Comparison of proportions of polymorphonuclear cell (PMN) and monocyte/macrophage (Mo/M) cells obtained from double and triple-layer Percoll gradient separation methods in rainbow trout. Cytospin preparations of enriched cell populations were stained with rapid Romanowsky stains to allow classification by microscopic observation of cell morphologies. A minimum count from 5 fields of view (FOV) per fish was made to enumerate cell proportions.

<b>Percoll gradient</b>	<b>Fish type</b>	<b>PMN (%)</b>	<b>Mo/M (%)</b>	<b>No. of fish</b>
<b>Double layer</b>	Rainbow trout	34.28 ± 3.25	23.9 ± 4.97	10
<b>Triple layer</b>	Rainbow trout	57.99 ± 4.84	9.52 ± 1.71	5

### **2.3.2. Relationship between PMN proportions, fish mass and tank temperature**

The proportions of blood types, such as the proportions of different leukocytes, within a fish may be influenced by the mass of the animal and environmental growth conditions (Lie *et al.*, 1990; Tavares-Dias *et al.*, 2011), suggesting that variables such as temperature or maturity can influence PMN proportions. A significant positive correlation between the PMN proportions after triple-layer Percoll gradient enrichment and fish mass was found for 6 rainbow trout between 180–373 g ( $R^2 = 0.8814$ ;  $p < 0.01$ ). The trout were siblings of the same age. The data suggests that a greater proportion of PMNs are produced with mass (Figure 2.2). A significantly negative correlation was observed with PMN proportions attained after triple-layer Percoll gradient enrichment when increasing tank temperature in trout ( $R^2 = 0.8469$ ;  $p < 0.01$ ) (Figure 2.3). These experiments were repeated in diploid Atlantic salmon (with 32 fish) and similar results were obtained (Appendix Figure 1 and Appendix Figure 2).

### **2.3.3. Comparing trout PMN viability in low FCS doses and media supplementation**

The presence of nucleases in FCS can degrade ET structures hence it is important to minimise the concentration of serum in culture medium while not affecting cell viability (von Köckritz-Blickwede *et al.*, 2009, 2010). Supplementation of RPMI cell media with 1% FCS resulted in  $89.09 \pm 3.95\%$  viability of trout PMNs at 24 h, which was not significantly different ( $p > 0.05$ ) compared to a cell culture maintained in the standard 10% FCS supplementation ( $92.25 \pm 1.48\%$  viability; Figure 2.4). However, 0.5% FCS ( $47.48 \pm 7.39\%$ ) and complete absence of FCS ( $56.10 \pm 5.58\%$ ) resulted in significantly lower cell viability ( $p < 0.05$ ) at 24 h compared to 1% FCS (Figure 2.4). Enriched PMN cell suspension viability did not significantly differ at any time point during 48 h in the presence or absence of HEPES buffer (25 mM) ( $p < 0.05$ ). Furthermore, there was no significant difference in cell viability in the enriched PMN cell suspension when culturing the PMNs in L-15 or RPMI up to 24 h ( $p < 0.05$ ) (Figure 2.5).

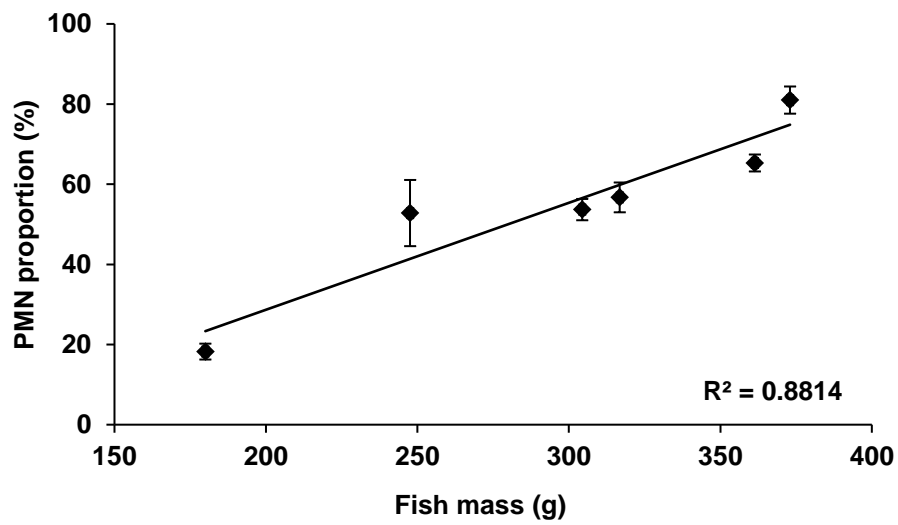


**Figure 2.2.** Scatter plot showing the relationship between rainbow trout mass against the proportion of PMNs attained after isolation with triple-layer Percoll gradients. Each point consists of the mean number of PMNs calculated from three fields of view from cytopsin preparations after enriching trout head kidney tissue for PMNs. There was significant correlation between fish mass and PMN proportion ( $F_{1,4} = 29.73$ ;  $p < 0.05$ ). Error bars represent the s.e.m.  $n = 6$  trout.

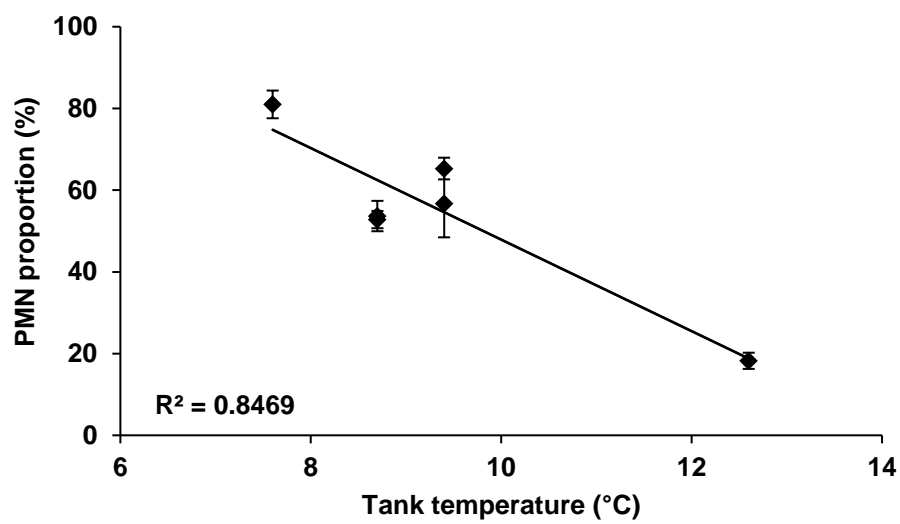


**Figure 2.3.** Scatter plot showing the relationship between tank temperature (°C) at time of sampling and PMN proportions obtained from triple-layer Percoll preparations from rainbow trout. ( $F_{1,4} = 22.13$ ;  $p < 0.05$ ). Error bars represent s.e.m.  $n = 6$  trout.

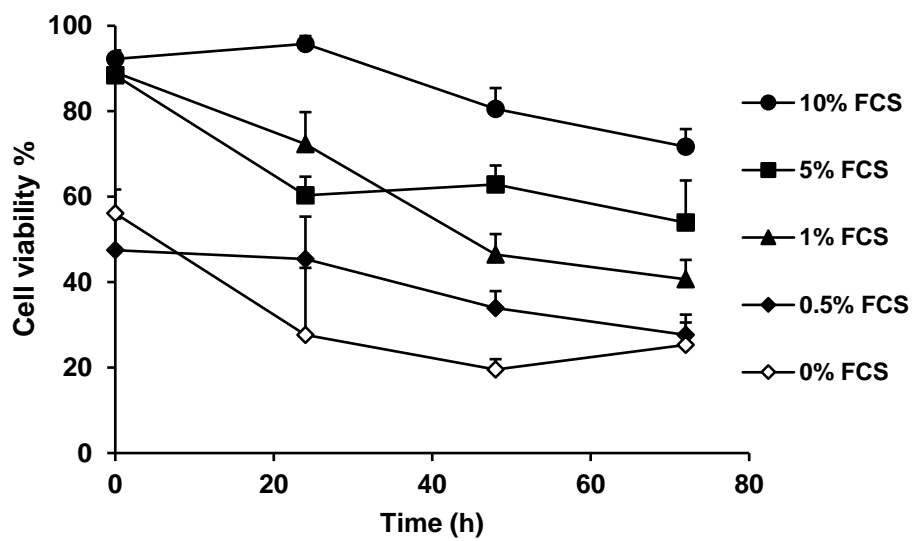


**Figure 2.4.** Viability of cells in PMN-enriched suspensions ( $1 \times 10^6$  cells  $\text{mL}^{-1}$ ) in the absence or presence of 0.5 – 10% FCS supplementation in RPMI cell medium over 72 h at  $13^\circ\text{C}$ , as measured by trypan blue exclusion. Error bars represent s.e.m.  $n = 4$ .



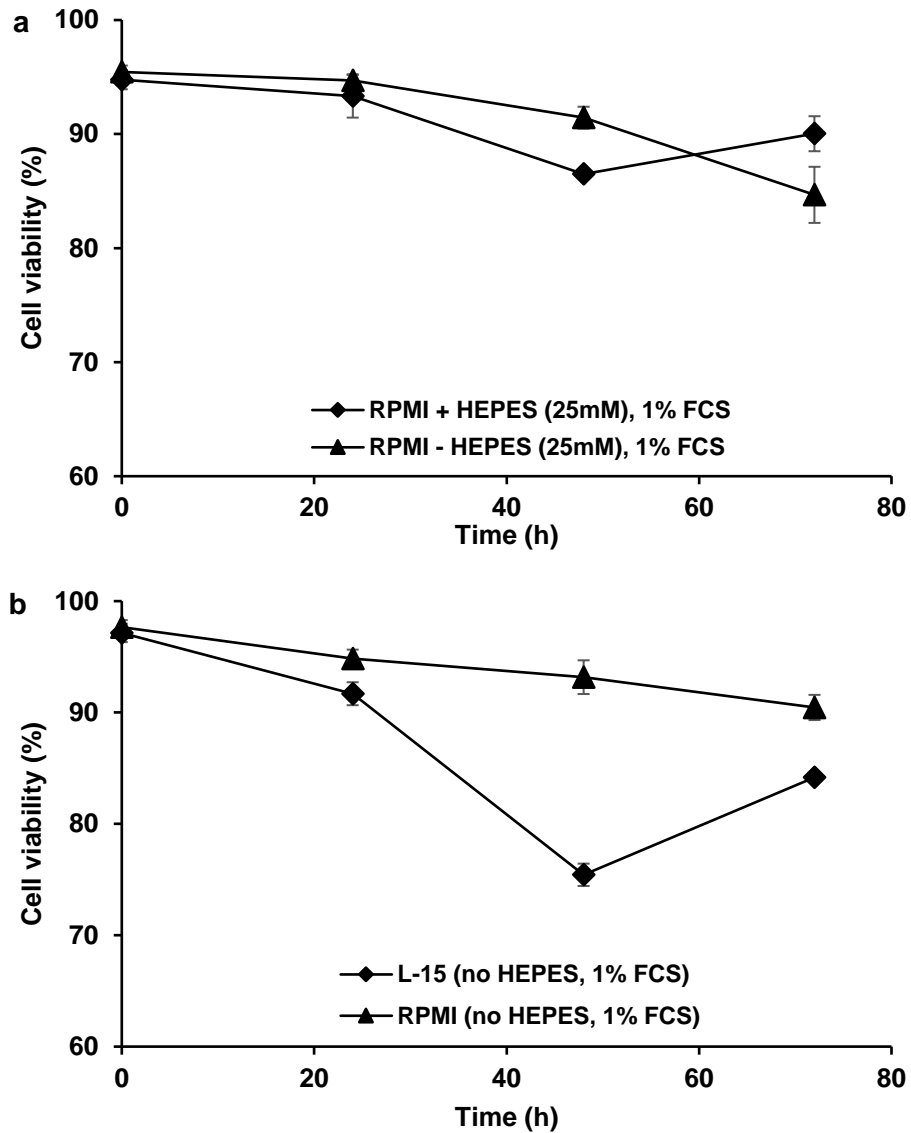


**Figure 2.5.** Viability of cells in PMN-enriched suspensions ( $1 \times 10^6$  cells  $\text{mL}^{-1}$ ) during 72 h in the presence of (a) RPMI3 with and without HEPES buffer (25 mM), which shows no significant difference in cell viability at 0 and 24 h ( $p < 0.05$ ); (b) The use of L-15 or RPMI3 did not show significant differences in cell viability at 0 and 24 h ( $p < 0.05$ ). For both graphs, a significant difference in cell viability was detected between each treatment at 48 and 72 h ( $p > 0.05$ ). Error bars represent s.e.m. (are not visible in all cases).  $n = 4$ .

#### **2.3.4. Confirming DNA concentration is proportional to SYTOX-DNA fluorescence read in a plate reader**

A significant positive correlation was found between SS-DNA concentration and SYTOX Green fluorescence ( $R^2 = 0.9761$ ,  $p < 0.001$ ), indicating fluorescence is proportional to DNA concentration. The greatest fluorescence recorded in arbitrary fluorescence units (AFU) as an indicator of SYTOX-DNA fluorescence was  $5690 \pm 433$  AFU ( $10 \text{ ng mL}^{-1}$  SS-DNA), and the least fluorescence measured was  $141 \pm 1$  AFU ( $0.1 \text{ ng mL}^{-1}$  SS-DNA), giving a large range of expected fluorescence values (Figure 2.6). The SS-DNA stock concentration and purity was confirmed by reading the absorbance of a  $1 \mu\text{L}$  sample (final well concentration of 0.1, 0.5, 1, 2.5, 5, and  $10 \text{ ng mL}^{-1}$  diluted in  $\text{dH}_2\text{O}$ ) using a nanodrop reader.

#### **2.3.5. Use of fluorescence to quantify ETs**

Observing the PMN suspensions in 96-well culture plates with fluorescence microscopy showed that some cells spontaneously released comet-like strand structures that stained positive with SYTOX Green, and these resemble ETs depicted in the literature (Figure 2.7a). Moreover, these presumed-ETs were found in greater densities after incubation of enriched PMNs suspensions with  $5 \mu\text{g mL}^{-1}$  Cal, a known stimulant of ET release in zebrafish and fathead minnow PMN-enriched cell suspensions (Figure 2.7b). Examining the relationship between mean fluorescence and mean presumed-ET counts from 54 matched samples revealed a significant positive linear correlation between extracellular DNA fluorescence and presumed-ET counts,  $R^2 = 0.88$ ,  $p < 0.001$  (Figure 2.8). The fluorescence emitted from extracellular DNA from PMN-enriched cell suspensions ranged from 505 to 5224 AFU, while presumed-ET counts ranged from 0.26 to 31.55% of total cells (Figure 2.8). The presumed-ETs were enumerated from cells treated with and without Cal-treatment, thereby giving a wide range of representative ET abundances (Figure 2.7). Thus, fluorescence is an appropriate method to measure abundance of extracellular DNA and presumptive ET-like structures.

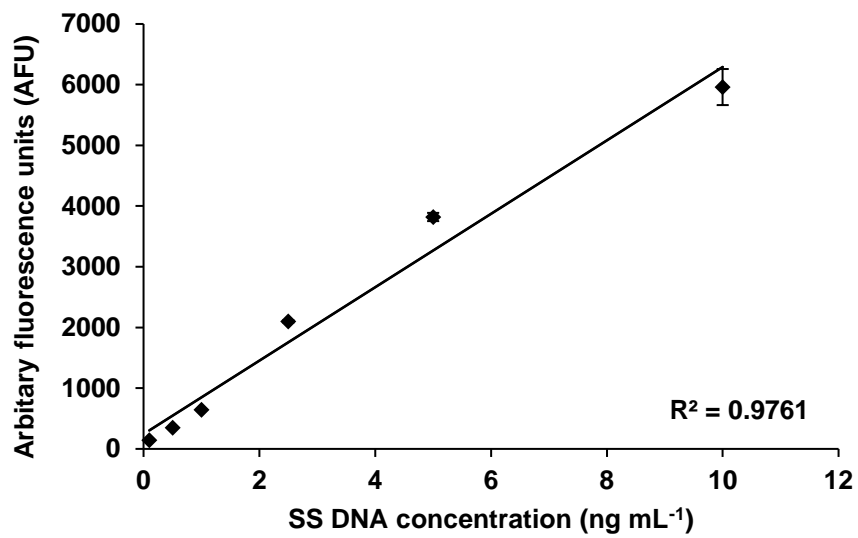


**Figure 2.6.** Scatterplot showing the relationship between salmon sperm DNA (SS-DNA in ng mL<sup>-1</sup>) with SYTOX-stained arbitrary fluorescence (AFU). SYTOX-DNA fluorescence is linearly proportional to SS-DNA concentration in a 96-well plate. Error bars represent s.e.m. but not all are visible. ( $F_{1,16} = 348.7$ ;  $p < 0.05$ );  $n = 5$

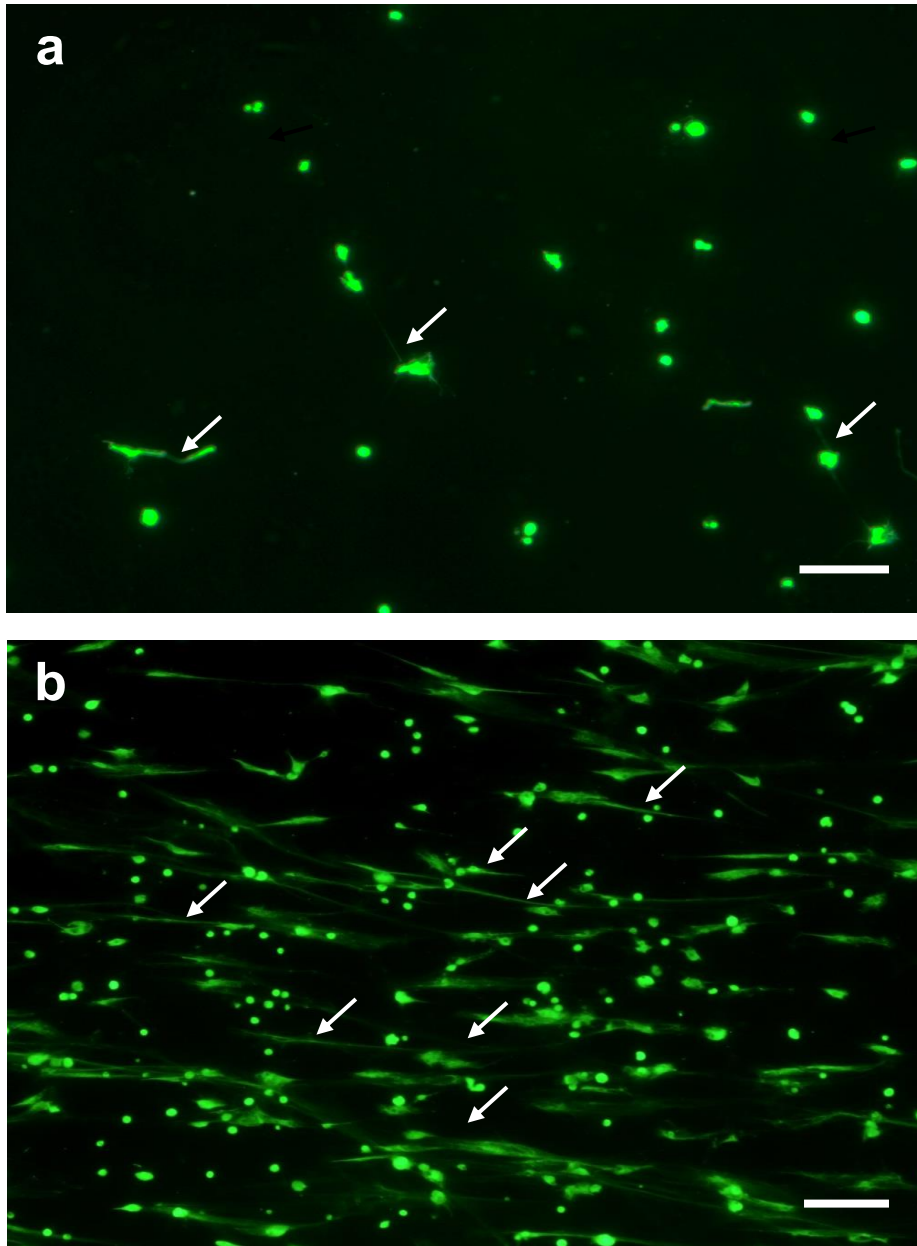


**Figure 2.7.** Representative fluorescence microscopy images of selected presumed trout ETs (white arrows) released by PMN-enriched cell suspensions by triple-layer Percoll gradients ( $4 \times 10^5$  cells  $\text{mL}^{-1}$  in a 96-well plate; 20 $\times$  magnification). (a) Unstimulated controls treated with RPMI1 for 6 h (b) Incubated with Cal ( $5 \mu\text{g mL}^{-1}$ ) for 6 h. Cells were stained with SYTOX Green ( $5 \mu\text{M}$ ) before observing with fluorescence microscopy. The mean count of presumed ETs out of total cells from an image as above was well was compared to the mean fluorescence of triplicate wells containing PMNs enriched cell suspensions. Error bars = 100  $\mu\text{m}$ .

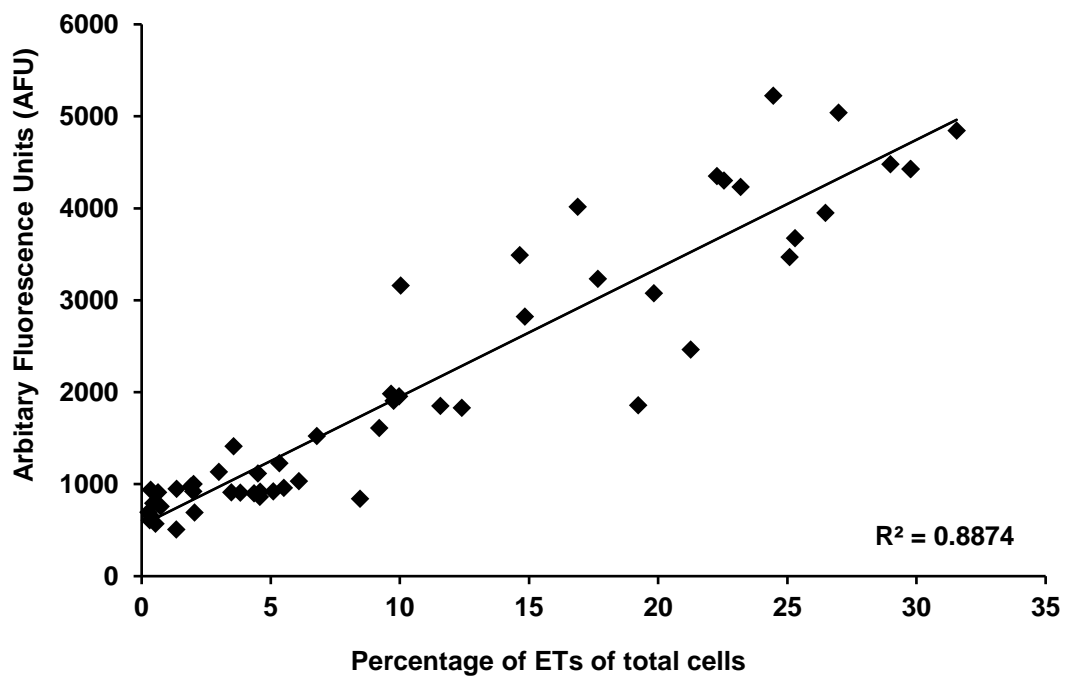


**Figure 2.8.** Scatterplot showing the relationship between mean arbitrary fluorescence units from SYTOX-stained extracellular DNA from enriched PMN cell suspensions *in vitro* (both unstimulated controls and Cal-stimulated), and the mean presumed-ET counts by percentage of total cells in fields of view of matched samples. ( $F_{1,52} = 409.8$ ;  $p < 0.001$ )  $n = 54$ .

## 2.4. Discussion

In this chapter, methods were evaluated for preparing enriched populations of PMNs from trout head kidney tissues and for measuring extracellular DNA release from enriched-PMN cell suspensions. A triple-layer Percoll gradient gave greater PMN enrichment from trout head kidney tissue samples was compared to the two-layer method. There was evidence that larger fish gave greater proportions of PMNs in cell suspensions prepared from head kidney tissue, while lower PMNs proportions were attained on days where the tank water was warmer (Figure 2.3). Trout PMNs in culture with 1% FCS supplementation did not have reduced cell viability compared to more typical cell culture conditions of 10% FCS during the day that the cells were obtained (Figure 2.4) and, as FCS contains nucleases that may degrade ETs (von Köckritz-Blickwede *et al.*, 2009), 1% FCS was used in further experiments. Furthermore, the use of L-15 or RPMI culture media addition of HEPES buffer to control medium pH did not significantly reduce the viability of trout PMNs during culture for 24 h (Figure 2.5). Importantly, spontaneous release of ET-like structures was detected from suspensions of trout PMNs *in vitro* that stained with SYTOX Green, indicating these were of nucleic acid composition. The structures were presumed to be ETs and a fluorimetry-based assay for quantifying these structures was developed. This was achieved by first confirming that a linear relationship existed between SYTOX Green fluorescence and DNA concentration, and then fluorescence was found to correlate significantly with count of presumed-ETs in cell suspensions enriched for PMNs (Figure 2.8). This indicates that measuring the fluorescence of extracellular DNA stained by SYTOX Green can be used to reliably estimate and quantify the presumed-ET structures in suspension, and so was used routinely for this purpose hereon.

The improved enrichment of trout PMNs by switching to a triple-layer Percoll gradient may be explained by slight differences in Percoll density, as the double-layer method used slightly denser solutions ( $1.075 \text{ g mL}^{-1}$ ) rather than the more successful triple-layer gradients ( $1.072 \text{ g mL}^{-1}$ ) (Øverland *et al.*, 2010). It is possible that the triple-layer Percoll gradient allows further separation of cells of similar densities as some granulocytes and erythrocytes were collected at the interface below where the PMNs were found to be enriched. The robustness of the method was tested by comparing double and triple-layer Percoll protocols for enriching PMNs from head kidney preparations of another salmonid species, Atlantic salmon. The results for salmon were similar to trout, with a significant improvement of PMN enrichment from head kidney preparations also being obtained (Appendix Table 3). Therefore, in subsequent chapters, the more successful triple-layer will be used routinely to enrich for PMNs from trout head kidney cell suspensions. Cell sorting was not used for the enrichment of PMNs as these cells are short-lived and require alternative, high throughput methods for immediate isolation and experimentation. For this reason, antibodies were also not used to further enrich the PMN populations after Percoll separation as demonstrated in some studies (Hamdani *et al.*, 1998).

The present study could be refined by additional flow cytometry data to confirm the results indicating populations of cell types after enrichment by discontinuous Percoll gradients. Furthermore, flow cytometry can be used to distinguish cell viability, which may back up the results from the trypan blue viability assay.

The data examining the relationship between fish mass, tank temperature, and PMN proportion, identified a significant positive correlation for more enriched PMN preparations from larger trout and these observations were also confirmed subsequently in Atlantic salmon (Appendix Figure 1). In addition, temperature correlated negatively with PMN enrichment by triple-layer Percoll gradient isolation. Temperature is known to affect humoral immune functions and influence events during the maturation and immunocompetence of immune cells (Avtalion *et al.*, 1973; Le Morvan *et al.*, 1998), which may give some insight to why temperature was observed to influence amount of ET-like structures released by PMN-enriched cell suspensions. These variations in the release of ET-like structures were unexpected and remain unexplained as there is little available evidence in the current literature.

PMNs from mammals and fish are known to remain viable *in vitro* for approximately 12 to 24 h in ideal culture conditions (Hamdani *et al.*, 1998; Oh *et al.*, 2008), but inappropriate medium salinity, and pH can reduce overall viability. The use of serum is also necessary to maintain viability of cells in culture, including short-lived PMNs; however, the minimum concentration necessary to maintain the viability trout PMN-enriched cell suspensions has yet to be defined (Iscove *et al.*, 1978; Brunner *et al.*, 2010). Maintaining cell viability of the PMN-enriched cell suspension within 24 h is critical, as the release of ETs is dependent on the PMNs being viable (Yipp *et al.*, 2013). Often, studies of ETs are compromised by using minimal concentrations of serum to minimise the negative impact of degradative nucleases on ETs (von Köckritz-Blickwede *et al.*, 2010; Zhao *et al.*, 2017). The current data shows that 1% FCS of total culture volume is required to prevent significant losses of viability in trout PMN-enriched suspensions during 24 h (Figure 2.4). Unexpectedly, the use of different cell media (L-15 or RPMI) did not result in significant differences in viability of PMN-enriched suspensions, although L-15 is understood to be formulated for use in CO<sub>2</sub>-free systems, while RPMI usually requires bicarbonate buffering such as with HEPES. Furthermore, the use HEPES buffer in RPMI did not result in any significant differences in cell suspension viability of PMN-enriched suspensions during 24 h compared to RPMI without HEPES supplementation, indicating that there may be no requirement to manage medium pH under these conditions. As pH in cell cultures changes gradually, it is likely that the effect of pH buffering may be more important when used in denser cell suspensions or extended cell culture durations (Skirvin *et al.*, 1986; Kim *et al.*, 2007), explaining the lack of a difference in viability of enriched PMN cultures in the presence of absence of HEPES within 24 h, as these cell suspensions were in relatively low concentrations.

Studies in human and fish PMNs have demonstrated that Cal is a potent inducer of ET release (Palić, Andreasen, *et al.*, 2007; Barrientos *et al.*, 2013). Exposing the enriched PMN cultures to Cal resulted in greater amounts of fibrous ET-like structures that stained positive with SYTOX Green. SYTOX Green intercalates between nucleic acid base pairs, suggesting a nucleic acid content for observed structures.

These structures were presumed to be ETs due to their morphological similarity to ETs described in mammalian and invertebrate studies (Brinkmann *et al.*, 2004; Fuchs *et al.*, 2007; Poirier *et al.*, 2014; Robb *et al.*, 2014; Jeffery *et al.*, 2015). Spontaneous release of these structures was also observed in the unstimulated control enriched PMN suspensions, though to a much lesser extent than when induced by Cal. A significant positive correlation between presumed ET counts and SYTOX Green DNA fluorescence was found, indicating that fluorescence can be used to quantify ET-like structures and therefore release *in vitro*. However, the ability to accurately estimate the amount of ET-like structures was weaker when using fluorimetry to measure ET release. ET-clumping may increase fluorescence readings such that the detection of fluorescence begins to plateau with higher intensity, causing inaccurate measurements of ETs released. As a result, microscopy remains important to confirm the fluorescence readings. In wells containing Cal-induced enriched PMN cultures with large densities of ET-like structures, the greatest measured emitted fluorescence never exceeded 5224 AFU. Expectedly, there was a significant, positive correlation between SS-DNA and fluorescence up to 6000 AFU, therefore fluorescence may be used to reliably determine the relative abundance of ETs released *in vitro*. However, if fluorescence emitted from the wells exceeds 6000 AFU, a reduction in cell density may be required to give accurate measurements. Quantifying the presumed ETs by manual counts also had the disadvantage of not able to clearly distinguish individual ETs, as a cluster of ETs in close proximity may appear as one large ET. The physical appearance of ETs *in vitro* can vary depending on the surrounding media into which it is released, which can result in 'diffuse' or 'comet-like' ETs which may sometimes appear as more than one ET (Fuchs *et al.*, 2007; Hakkim *et al.*, 2011; Yipp *et al.*, 2012). Regardless, the use of different assays to measure ET release depend on the objectives of the experiment. Ultimately, fluorimetry was able to measure the abundance of ET-like structures with high throughput, outweighing the disadvantages of other methods, thus, this method was used to measure the abundance of ET-like structures in later chapters.

In conclusion, the ET-like structures that stained positively with SYTOX Green reported in this Chapter are highly similar to ETs reported in PMN-enriched cell suspensions from mammals and fish; though whether or not these structures are decorated with the granule that is characteristic of ETs remains to be confirmed. Thus, diagnostic confirmation of whether these structures are ETs is still required and was the focus of the next Chapter. Furthermore, there



remains no positive confirmation for which cells within the PMN-enriched cell suspension are responsible for producing these presumed ETs.

.

## **Chapter 3: Confirming release of extracellular traps by polymorphonuclear cells isolated from head kidney of rainbow trout**

### **3.1. Introduction**

In Chapter 2, extracellular nucleic acids resembling the comet-like fibres of extracellular traps (ETs) were observed in cell suspensions enriched for polymorphonuclear (PMN) cells isolated from head kidney tissue by triple-layer Percoll gradients (PMN-enriched cell suspensions). Some of these ET-like structures were released spontaneously from cell suspensions during cell culture and observed at a greater abundance after exposure to calcium ionophore A23187 (Cal), a known potent inducer of ET release in mammals and in other fish species, (Palić, Andreasen, *et al.*, 2007; Palić, Ostojić, *et al.*, 2007; Douda *et al.*, 2015). However, it is unclear which cell types within the suspension are responsible for releasing the ET-like structures. Fluorescence microscopy revealed that these structures appeared to share the ET-like morphology reported by Brinkmann *et al.* (2004) after staining with the membrane impermeable fluorescent nucleic acid stain, SYTOX Green (Brinkmann *et al.*, 2004). Nevertheless, a suite of diagnostic tests needs to be performed to confirm whether these structures do indeed share the features characteristic of ETs released by phagocytes of other cell types (Brinkmann *et al.*, 2004; Fuchs *et al.*, 2007; Robb *et al.*, 2014; Jeffery *et al.*, 2015). Thus, to determine whether the ET-like structures are indeed ETs, it is necessary to confirm that: i) the ET-like structures are not an artefact of the cell isolation methods, or released spontaneously by other cell types isolated from the same tissue; ii) the structures contain nucleic acid (*i.e.*, DNA), confirmed by degradation with deoxyribonuclease-I (DNase-I); iii) histones (*e.g.*, H2A) are present in the structure, confirmed by immunocytochemical labelling with appropriate antibodies; iv) extracellular chromatin co-localises with neutrophil-associated granules such as neutrophil elastase (NE) and myeloperoxidase (MPO), confirmed by immunocytochemical labelling with appropriate antibodies, since the decoration and processing of intracellular chromatin by these granule proteins has been defined as a key process occurring before ET release (Brinkmann *et al.*, 2004; Fuchs *et al.*, 2007; Papayannopoulos *et al.*, 2010; Metzler *et al.*, 2011; Brinkmann and Zychlinsky, 2012; Menegazzi *et al.*, 2012).

The origin of the ET-like structures observed in Chapter 2 can be narrowed down by determining whether these structures are artefacts present within the tissue (head kidney) or caused by the stress associated with cell isolation and culture methods. Erythrocytes are not known to release their DNA in the form of ETs; therefore, erythrocyte suspensions prepared from the same tissue and using the same cell isolation method may be a suitable control for

an exposure to hormones, growth factors or cytokines, which are known to regulate phagocytosis, respiratory burst, and mitogenesis of cells present in the fish head kidney (Harris *et al.*, 2000; Clauss *et al.*, 2008).

In the vertebrates studied, ETs have been reported to be released from neutrophils, other granulocytes, mast cells and macrophages (Wernersson *et al.*, 2006; Von Köckritz-Blickwede *et al.*, 2008; Yousefi *et al.*, 2008; Papayannopoulos *et al.*, 2010; Metzler *et al.*, 2011; Brinkmann and Zychlinsky, 2012; Havixbeck *et al.*, 2015; Pijanowski *et al.*, 2015; Okada, 2017). Regarding the decoration of ETs released by fish PMN-enriched cell suspensions, immunocytochemical staining showed that NE was only detected in carp and turbot, while MPO was only detected in fathead minnows (Table 1.2). Furthermore, the studies in fish suggest use of PMN-enriched cell suspensions rather than pure populations, giving limited evidence as to which specific cell type is responsible for releasing ETs (Palić, Andreasen, *et al.*, 2007; Palić, Ostojić, *et al.*, 2007; Brogden *et al.*, 2012; Pijanowski *et al.*, 2013; Chi *et al.*, 2015). As is the case for humans, the greatest expression of NE in fish is found in PMN cells which was detected at the protein level (Wernersson *et al.*, 2006; Papayannopoulos *et al.*, 2010; Metzler *et al.*, 2011; Brinkmann and Zychlinsky, 2012; Havixbeck *et al.*, 2015; Okada, 2017), and thus the detection of NE and / or MPO in fish ETs may suggest a PMN (*i.e.* neutrophil) origin. It is important to consider that the antibodies used to detect ET-associated proteins such as histone complexes, NE or MPO in the current fish studies were mAbs against mammalian targets. These proteins may have been subject to significant molecular changes throughout evolution that can reduce the effectiveness of mammalian mAbs in detecting the orthologues in fish species. However, due to the lack of available specific mAbs in fish, research groups often compromise by using mammalian antibodies.

Various potent chemical and biological inducers and inhibitors of ET release have been identified from studies conducted mainly on mammalian neutrophils, and many of these have similar effects on ET release from fish and invertebrate PMNs (or cells with PMN function in invertebrates), suggesting that the mechanisms underlying ET release are evolutionarily conserved across the animal kingdom (Palić, Ostojić, *et al.*, 2007; Robb *et al.*, 2014; Lange *et al.*, 2017) (Table 1.5). For example, compounds inducing ET release from zebrafish, fathead minnows, carp, and flatfish PMN-enriched cell suspensions included calcium ionophore (Cal), phorbol 12-myristate 13-acetate (PMA), lipopolysaccharide (LPS), and bacterial suspension (Palić, Ostojić, *et al.*, 2007; Pijanowski *et al.*, 2013; Chi *et al.*, 2015). By contrast, diphenyliodonium (DPI) and cytochalasin inhibited ET release from these cells (Table 1.6) (Palić, Andreasen, *et al.*, 2007; Palić, Ostojić, *et al.*, 2007; Pijanowski *et al.*, 2013; Chi *et al.*, 2015; Zhao *et al.*, 2017).

NADPH oxidase is an enzyme complex commonly found in phagocytic cell membranes which has a role in producing reactive oxygen species (ROS) required for oxidative burst. The requirement for NADPH oxidase in the process of ET release is demonstrated by the fact that the use of inhibitors of NADPH oxidase, such as DPI, results in a reduction of the ROS generation that is required for PMA or pathogen-associated molecular pattern (PAMP)-induced ET release, both in vertebrates and invertebrates (Fuchs *et al.*, 2007; Parker, Dragunow, *et al.*, 2012; Gray *et al.*, 2013; Robb *et al.*, 2014). Exposure of human neutrophils to chemicals such as PMA, or PAMPs such as LPS or flagellin elicits NADPH oxidase-dependent ET release (Gray *et al.*, 2013; Douda *et al.*, 2015; Floyd *et al.*, 2016). Although most compounds (chemical or biological) are known to rely on NADPH oxidase to induce ET release, Cal elicits ET release through an NADPH oxidase-independent mechanism (Parker, Dragunow, *et al.*, 2012; Douda *et al.*, 2015). Conversely, cytochalasin can inhibit ET release independently of NADPH oxidase by inhibiting remodelling of the cytoskeleton (Brinkmann *et al.*, 2004; Neeli *et al.*, 2009; Robb *et al.*, 2014). These studies indicate that there are broadly two conserved systems driving ET release in mammals and invertebrate systems: one dependent upon and one independent of NADPH oxidase activity. However, in contrast with the case for humans, there has not been many published studies surrounding fish ETs, and there is little consistency between the potency of inducers and inhibitors on fish ET release, therefore the signalling mechanism mediating ET release in fish is unclear. For instance, PMA (after correcting for dose) induces poor ET release from fathead minnows and zebrafish, while conversely eliciting higher ET release with carp and tongue sole, even though carp, minnows and zebrafish are all classified within the *Cyprinidae* (Palić, Ostojić, *et al.*, 2007; Pijanowski *et al.*, 2013; Zhao *et al.*, 2017). In zebrafish and fathead minnows, Cal was the most potent inducer of ET release, indicating an NADPH oxidase-independent mechanism for ET release in these fish. However, the use of Cal to induce ET release was not followed up in other fish species (Palić, Andreasen, *et al.*, 2007; Palić, Ostojić, *et al.*, 2007). Exposure of tongue sole PMN-enriched cell suspensions to NADPH oxidase inhibitors resulted in inhibition of PMA-associated, and *Vibrio harveryi*, *Pseudomonas fluorescens*, and *Edwardsiella tarda* bacterial-induced ET release (Zhao *et al.*, 2017). Furthermore, DPI inhibited PMA-induced ET release in carp (Pijanowski *et al.*, 2013), indicating that PMA or bacteria can stimulate ET release in different fish species through an NADPH oxidase-dependent system. To date, there are no studies which test these potential inducers or inhibitors of ET release in the rainbow trout system, and it would be interesting to determine how similarly trout cells respond in comparison to those of other fish species.

Spontaneous ET release and so-called 'background ET release' (Fuchs *et al.*, 2007; Kamoshida *et al.*, 2017), can be highly variable, as has been observed for human neutrophils from healthy donors (Pilszczek *et al.*, 2010; Maini *et al.*, 2016) and dog PMNs (Jeffery *et al.*,

2015). In addition to the spontaneous ET release from human neutrophils, blood collected from different individuals showed that some individuals released significantly more ETs in response to the same PMA induction than others (Fuchs *et al.*, 2007; Maini *et al.*, 2016). In contrast to the case for humans and dogs, this variation in individual response has not often been investigated in fish or smaller animals, due to difficulty of collecting adequate blood samples for sufficient replicates from individual fish, often leading to pooling of samples (Palić, Andreassen, *et al.*, 2007; Palić, Ostojić, *et al.*, 2007; Chi *et al.*, 2015; Zhao *et al.*, 2017). Since individual variability is a key property of immune systems in many organisms, which has ramifications for protection of both the individual and the wider population, the extent of inter-individual variability in ET release in response to treatments is potentially important.

Thus, the aim of the work described in this chapter was to confirm that the SYTOX-stained structures observed to be released from trout PMN-enriched cell suspensions in Chapter 2 were indeed ETs. To achieve this, erythrocytes enriched from the same head kidney tissue were examined for ET-like structures to confirm that the structures were not artefacts of the tissue or cell isolation process. DNase-I was used to determine if the ET-like structures were composed of chromatin. Antibodies against MPO, NE, and histone H2A were used to confirm the presence of these proteinaceous components in association with the extracellular DNA, which is a characteristic of ETs. The association of these components can also confirm if the ETs are released by PMNs, as these cells are known to collectively express MPO and NE. Additionally, scanning laser confocal microscopy was employed to provide images of greater resolution of the ET-like structures. Moreover, a range of chemical and biological compounds known to induce or inhibit ET release in other species, including other fish, was assessed by fluorometric assay for their ability to mediate the release of ET-like structures from trout PMNs *in vitro* over a defined incubation period. Finally, the spontaneous ET release from individual fish was examined by looking at the individual responses to inferred inducers of ET release.

## **3.2. Materials and Methods**

### **3.2.1. Confirming spontaneous release of ET-like structures are specific to PMN-enriched cell suspensions**

To determine that other cell types from the trout head kidney tissue (besides cells within the PMN-enriched cell suspensions) do not spontaneously produce ET-like structures after isolation using a similar Percoll enrichment, a trout erythrocyte-enriched cell suspension was prepared using two-layer discontinuous Percoll (at pH 8.5-9.5 [20°C], Sigma-Aldrich, Dorset,

UK) gradient consisting of 5 mL of 1.085 g mL<sup>-1</sup> Percoll solution overlaid onto 5 mL of 1.108 g mL<sup>-1</sup> Percoll solution (both diluted in dH<sub>2</sub>O). The discontinuous Percoll gradient was prepared in a universal tube and used to enrich for erythrocytes from dissected head kidney tissue collected from trout and processed according to Section 2.2.3. For the 1.085 g mL<sup>-1</sup> Percoll solution: 0.5 mL of 10× Hank's balanced salt solution (HBSS; Sigma-Aldrich, Dorset, UK) and 1.46 mL of sterile dH<sub>2</sub>O was added to 3.04 mL Percoll. While for the 1.108 g mL<sup>-1</sup> Percoll solution: 0.5 mL 10× HBSS and 0.57 mL of sterile dH<sub>2</sub>O was added to 3.93 mL Percoll. Each solution was mixed in a separate 50 mL Falcon tube by gently inverting the tube three times before layering onto each other in the universal tube. The protocol for erythrocyte separation with this gradient was performed as for PMN-enrichment described in Section 2.2.3. The erythrocyte cell suspension (isolated according to Section 2.2.3) was prepared in RPMI2 (Appendix Table 2). Then, 50 µL of erythrocyte suspension (1 × 10<sup>6</sup> cells mL<sup>-1</sup>) was seeded to wells of a 96-well plate (Cell+, Sarstedt, Nümbrecht, Germany), and then incubated for 30 min at 15°C to allow the cells to adhere to the bottom of the well. The Cell+ flat-bottom 96-well culture plates were used throughout this chapter, unless otherwise stated. An additional 10 µL of RPMI1 was added to each well and incubated for 24 h at 15°C.

Chinook salmon embryo cells (CHSE-214) ATCC CRL-1681 (European Collection of Authenticated Cell Cultures, Salisbury, UK) were included as a control for cells that were not isolated from the trout head kidney, and were derived from a different salmonid species. To determine if CHSE-214 can release ET-like structures spontaneously, CHSE-214 cells (1 × 10<sup>6</sup> cells mL<sup>-1</sup>) were prepared in RPMI2, treated the same as the erythrocyte suspension above. Following the 6 and 24 h incubation of trout the erythrocyte suspension or CHSE-214 cells with RPMI2, nucleic acids within the well were fluorescently stained by adding 10 µL of membrane-permeable SYTOX Green (to give final a concentration of 5 µM; Thermofisher Scientific, Loughborough, UK) and membrane-impermeable 4',6-diamidino-2-phenylindole (DAPI; to give final a concentration of 2.5 µM; Thermofisher Scientific, Loughborough, UK) for 5 min at room temperature. The cells were observed for ET release (from the same 96-well plate) at 6 and 24 h, and ET-like structures were counted (as described in Section 2.2.8.3) under fluorescence microscopy (Section 2.2.8.2).

### **3.2.2. Confirming the DNA composition of presumed ETs by digestion with DNase-I**

To further confirm that the SYTOX-positive extracellular structures observed in trout PMN-enriched cell suspensions in Chapter 2 (Section 1.3.6) are composed of nucleic acid, a PMN-enriched cell suspension was induced to form ET-like structures that then could be degraded by DNase-I, an enzyme that cleaves without sequence specificity (Herrera *et al.*, 1994). For this, a PMN-enriched cell suspension (isolated according to Section 2.2.3) was prepared in

RPMI2, then 50  $\mu\text{L}$  of cell suspension was seeded into wells of a 96-well plate at  $4 \times 10^5$  cells  $\text{mL}^{-1}$ , and incubated for 30 min at  $15^\circ\text{C}$ , allowing the cells to settle onto the well surface. Thereafter, to induce the formation of ET-like structures 10  $\mu\text{L}$  of calcium ionophore (Ca; A23187, Thermofisher Scientific, Loughborough, UK) solution diluted in  $\text{dH}_2\text{O}$  was added to give a final well concentration of  $5 \mu\text{g mL}^{-1}$  and the plate was incubated for 3 h at  $15^\circ\text{C}$ . To degrade the presumed ETs that were released, the Cal-exposed ('stimulated') PMN-enriched cell suspensions were treated with 10  $\mu\text{L}$  solutions of DNase-I enzyme (to give final well concentrations of 0.01, 0.1, 1, 10, and  $100 \text{ U mL}^{-1}$ ; Thermofisher Scientific, Loughborough, UK) and incubated for a further 3 h at  $15^\circ\text{C}$ . The stock DNase-I solution had been prepared in DNase buffer (10 mM Tris-HCl [pH 7.5 at  $25^\circ\text{C}$ ], 2.5 mM  $\text{MgCl}_2$ , 0.1 mM  $\text{CaCl}_2$ ) and diluted to desired final concentrations with  $\text{dH}_2\text{O}$ . Control wells were exposed to respective concentrations of buffer diluted in water without DNase-I. After the incubation, the effects of the different concentrations of DNase-I on the digestion of the ET-like structures were measured in each well by adding 10  $\mu\text{L}$  SYTOX Green to each well (final well concentration of  $5 \mu\text{M}$ , 5 min, room temperature) to stain any extracellular DNA and membrane-compromised cells. The fluorescence (excitation 485 nm, emission 528 nm) of each well was recorded (according to Section 2.2.8.2) with a spectrofluorimeter (BioTek Synergy HT, Swindon, UK). Fluorescence values emitted from DNase-I-exposed wells were normalised to the unexposed control (not exposed to DNase-I), giving fold-change fluorescence. This was performed by dividing fluorescence value from each well exposed to the treatment by the mean fluorescence from five wells of non-exposed control treatment.

### **3.2.3. Determining the presence of myeloperoxidase, neutrophil elastase, and histone H2A in ET-like structures by immunocytochemistry**

Immunocytochemical analyses were performed to determine the presence of MPO, NE and H2A proteins in the ET-like structures released from trout PMN-enriched cell suspensions. The primary antibodies used were polyclonal rabbit-anti-MPO IgG1 (final well concentration of 1:20, ab9535, Abcam, Bristol, UK), polyclonal rabbit anti-NE IgG1 (final well concentration of 1:20, ab21595, Abcam, Bristol, UK), and mouse anti-H2A (final well concentration of 1:200) diluted in PBS (without  $\text{Ca}^{2+}$  or  $\text{Mg}^{2+}$  ions), while the secondary antibodies were polyclonal Alexa Fluor 488 goat anti-rabbit IgG (final well concentration of 1:300, A32723) and polyclonal goat anti-mouse IgG (final well concentration of 1:300, A11001), also diluted in PBS (secondary antibodies supplied by Thermofisher Scientific, Loughborough, UK). A PMN-enriched cell suspension was prepared to  $4 \times 10^5$  cells  $\text{mL}^{-1}$  in RPMI2 according to Section 2.2.3. To each well of a 96-well plate was added 50  $\mu\text{L}$  of cell suspension. Then, 10  $\mu\text{L}$  Cal was added to each well to give  $5 \mu\text{g mL}^{-1}$ ) and then the plate was incubated for 3 h at  $15^\circ\text{C}$ . After incubation, the contents of each well were fixed by removing the liquid with a pipette,

then adding 100  $\mu$ L of 4% paraformaldehyde (Sigma-Aldrich, Dorset, UK), incubating for 20 min at room temperature, before washing PBS (without  $\text{Ca}^{2+}$  or  $\text{Mg}^{2+}$  ions). The wash step was performed by removing the culture medium with a pipette, adding 100  $\mu$ L of PBS, and incubating for 5 min at room temperature. After the three consecutive wash steps, blocking was performed to reduce non-specific binding by removing the PBS and adding 100  $\mu$ L of blocking buffer, consisting of 2% goat serum, 2% FCS, and 0.2% Triton X-100 (Sigma Aldrich, Dorset, UK) made up to volume with PBS. The plate was incubated for 30 min at room temperature before the blocking buffer was removed with a pipette, and cells were incubated with 100  $\mu$ L of primary antibody, either  $\alpha$ -MPO,  $\alpha$ -NE, or  $\alpha$ -H2A (90 min, room temperature). After, the cells were washed three more times with PBS as before, and then 100  $\mu$ L of secondary antibodies (Alexa Fluor<sup>®</sup> 488 goat anti-rabbit IgG, or Alexa Fluor<sup>®</sup> 488 goat anti-mouse IgG) were added and the plate was incubated (45 min, room temperature). The wash step was repeated a total of three times before nuclei were stained with DAPI by adding 100  $\mu$ L of DAPI (final well concentration of 1 nM, made up in  $\text{dH}_2\text{O}$ ) and incubated for 5 min at room temperature. Fluorescent photos were taken of each well in FITC (excitation 488 nm, emission 523 nm) and DAPI (excitation 360 nm, emission 460 nm) channels, allowing detection of both Alexa Fluor 488 IgG secondary antibodies using an Olympus IX-73 or 70 microscope (Olympus LUCPlanFLN 40x Objective, PH2 Phase Plan Achromat). Separate channel images were overlaid using ImageJ v1.50i.

#### **3.2.4. Investigating the three-dimensional structure of the ETs**

Confocal microscopy was used to observe the presumed ETs released by PMN-enriched cell suspensions in order to better understand their three-dimensional structure. To prepare samples for confocal microscopy, 100  $\mu$ L of PMN-enriched cell suspension (isolated according to Section 2.2.3, supplemented with 1% FCS and 0.5% Pen-Strep) was seeded into wells of a 4-chamber Ibidi  $\mu$ -slide (Ibidi, Martinsried, Germany) at  $4 \times 10^5$  cells  $\text{mL}^{-1}$ , then incubated for 6 h at 15°C to allow attachment of cells and the spontaneous release of ETs. The  $\mu$ -slide is a chambered coverslip with 4 independent wells which can be removed from the slide after cells are fixed. Contents of each well were fixed by incubating with paraformaldehyde (4% final well concentration, 20 min, room temperature) and washed in the wells by gently removing the media and adding 100  $\mu$ L of PBS, then incubating for 5 min at room temperature. The wash step was repeated a total of three times before the slide chambers on the Ibidi  $\mu$ -slide were removed, and glass coverslips were mounted onto the slide with VECTASHIELD with DAPI (Vector Laboratories, Peterborough, UK) according to the manufacturer's instructions. Samples were observed with a TCS SP2 AOBS Laser Scanning Confocal Microscope (Leica Microsystems, Wetzlar, Germany).



### **3.2.5. Investigating the effect of known ET release inhibitors on ET release from trout PMN-enriched cell suspensions**

Known inhibitors of ET release in other species were assessed for their ability to inhibit ET release from trout enriched-PMN cell suspensions. Specifically, diphenyliodonium chloride (DPI; Sigma-Aldrich, Dorset, UK), which can inhibit the release of reactive oxygen species, and cytochalasin D from *Zygosporium mansonii* (Cyto D; Sigma-Aldrich, Dorset, UK), which is a mycotoxin inhibitor of actin polymerisation. To test this, 50  $\mu\text{L}$  of trout PMN-enriched cell suspension (isolated according to Section 2.2.3) in RPMI2 ( $4 \times 10^5$  cells  $\text{mL}^{-1}$ ) was seeded into each well of a 96-well plate and the plate was incubated for 30 min at  $15^\circ\text{C}$  to allow the cells to adhere to the surface. To each well was added 10  $\mu\text{L}$  of DPI (0.1, 1, 5, 10, and 25  $\mu\text{M}$ ) or Cyto D (0.1, 1, 5, 10, and 20  $\mu\text{M}$ ) solution, with both DPI and Cyto D was diluted using RPMI1 after initial solubilisation as per manufacturer's instructions. Then, the plate was incubated for a further 30 min at  $15^\circ\text{C}$  to allow DPI and Cyto D to take effect on the cells, and to see if this inhibited spontaneous release of ETs. After the 30-min incubation, 10  $\mu\text{L}$  of Cal (final well concentration of 5  $\mu\text{g mL}^{-1}$ ) was added to each well containing the PMN-enriched cell suspension (as Cal is also a known inducer of ET release in other species of fish), then incubated for 1, 3, 6, 9, and 12 h. A different plate was prepared for each time point (*i.e.* non-repeated measures). Extracellular DNA was stained with 10  $\mu\text{L}$  SYTOX Green (final well concentration of 5  $\mu\text{M}$ ) for 5 min, at room temperature. ET release by PMN-enriched cell suspensions in 96-well plates was measured by the fluorimetry according to Section 2.2.8. Fluorescence from three replicate wells were normalised to the mean fluorescence of control groups exposed to RPMI1 instead of DPI or Cyto D to give fold-change fluorescence according to Section 3.2.2. The experiment was repeated four fish in total.

To detect and account for potential nucleic acid contamination present in DPI or Cyto D, 10  $\mu\text{L}$  of each compound (at the same concentrations used as above) was incubated with 50  $\mu\text{L}$  of RPMI2 in wells of a 96-well plate. The well contents were stained with 10  $\mu\text{L}$  SYTOX Green (final well concentration of 5  $\mu\text{M}$ ) for 5 min, at room temperature, and the fluorescence in the well was measured by the fluorimetry assay according to Section 2.2.8. Triplicate wells of each treatment (and of each concentration) was prepared, and the mean fluorescence emitted from the wells without cells (indicating fluorescence of compound alone) was subtracted from fluorescence measured from individual wells containing PMN-enriched cell suspension.

### **3.2.6. Culture and heat-inactivation of *Vibrio anguillarum***

*V. anguillarum* isolates Vib 6 (ATCC 43310, wild type isolated from *Gadus morhua*) and Vib 87 (NCMB 1873I, wild type isolated from *Salmo salar*), were stored in 15:85 glycerol to PBS

at  $1 \times 10^9$  CFU mL<sup>-1</sup> at -70°C (Table 3.1). Tryptone soy agar and broth (TSA/TSB, Thermofisher Scientific, Loughborough, UK) were made up according to manufacturer's instructions and made up to a final concentration of 2% NaCl when culturing *V. anguillarum* before sterilization by autoclaving. Before experimental use, bacteria were recovered onto TSA 2% NaCl plates by spreading thawed isolates with a sterile plastic 10- $\mu$ L inoculation loop (Thermofisher Scientific, Loughborough, UK) and sealed with Parafilm tape (Bemis, Neenah, USA) before incubation (24 h, 22°C, until single colonies have been cultured to a visible size). *Vibrio anguillarum* isolates were confirmed by latex agglutination test, and 16S ribosomal sequencing previously used (McMillan *et al.*, 2015).

Bacteria were cultured in liquid culture (inoculation) by swabbing a single bacterial colony using a sterile inoculation loop and mixing into a universal tube containing 5 mL of TSB 2% NaCl and cultured in a shaking incubator (150 RPM, 16 h, 22°C) to achieve late-exponential phase (derived from experimental growth curves, data not shown). After incubation, bacterial cells were washed by transferring the culture into a 50 mL Falcon tube and pelleted by centrifugation (2600  $\times$  g, 15 min, 4°C). The supernatant was discarded, and the pellet of bacteria was washed by pipetting 5 mL of PBS to the pellet, and vortexing vigorously before another centrifugation step (2600  $\times$  g, 15 min, 4°C). The wash step was repeated a total of three times before the pellet was re-suspended in 5 mL of PBS. Bacterial concentration was measured with a spectrophotometer (CE 2041, Cecil Instruments Ltd, Cambridge, UK) by absorbance at 600 nm wavelength ( $A_{600}$ ), using PBS as a blank reference. Bacterial suspensions were diluted with PBS to desired concentrations in CFU mL<sup>-1</sup> derived from bacterial standard curve data (Appendix Figure 9). Before experimental use, the bacterial concentration was confirmed by plating onto appropriate agar in quadruplicate after serial dilution in a round-bottom 96-well plate (Sarstedt, Nümbrecht, Germany).

The bacterial cell suspension was corrected with sterile PBS to  $1 \times 10^7$  CFU mL<sup>-1</sup>, and then was heat-inactivated by incubating the bacterial suspension in a glass universal tube in a water bath for 25 min at 60°C, and the suspension was subsequently diluted to give three different concentrations of bacteria ( $1 \times 10^3$ ,  $1 \times 10^5$ , and  $1 \times 10^7$  CFU mL<sup>-1</sup>) Heat inactivation was confirmed by absence of colonies forming on tryptone soy agar after incubation for 48 h at 22°C.

**Table 3.1.** Bacterial isolates used in this Chapter. All isolates were stored at -70°C before isolating for experiments as described in Section 3.2.6.

Isolate/Strain	Characteristic	Culture media <sup>a</sup>	Culture temperature	Pathogenicity <sup>b</sup>	Nuclease production	Reference
<b><i>Vibrio anguillarum</i></b>						
Vib 6 (ATCC 43310)	Wild type isolated from <i>Gadus morhua</i>	TSA/TSB 2% NaCl	22°C	+	+	(Austin <i>et al.</i> , 1995)
Vib 87 (NCIMB 1873)	Wild type isolated from <i>Salmo salar</i> , UK	TSA/TSB 2% NaCl	22°C	+ (weak)	-	(Austin <i>et al.</i> , 1995)

<sup>a</sup>TSA (Tryptone soy agar), TSB (Tryptone soy broth), both supplemented with 2% NaCl.

<sup>b</sup>Pathogenicity was suggested by (Austin *et al.*, 1995).

### **3.2.7. Investigating the effect of known ET release inducers on ET release from trout PMN-enriched cell suspensions**

To investigate the ability of known inducers of ET release in fish and other systems, 50  $\mu\text{L}$  of PMN-enriched cell suspension (isolated according to Section 2.2.3) in RPMI2 were seeded in a 96-well culture plate ( $4 \times 10^5$  cells  $\text{mL}^{-1}$ ), and allowed the cells to adhere to the bottom of the wells for 30 min at 15°C. After adherence, 10  $\mu\text{L}$  of Cal (final well concentrations of 0.1, 1, 5, 10, and 25  $\mu\text{g mL}^{-1}$ ), flagellin from *Yersinia ruckeri* (final well concentration of 100  $\text{ng mL}^{-1}$ , flagellin was kindly gifted by Chris Secombes, University of Aberdeen, UK), ultra-pure LPS (pLPS, final well concentrations 0.1, 1, 10, 25, and 50  $\mu\text{g mL}^{-1}$ , Sigma-Aldrich, Dorset, UK), or PMA (final well concentrations 1, 10, 20, 40, and 60 nM, Sigma-Aldrich, Dorset, UK) was incubated with PMN-enriched cell suspensions for up to 12 h (1, 3, 6, 9, and 12 h; and in for Cal at 5  $\mu\text{g mL}^{-1}$ , also 10, 20, 30, 40, 50, and 60 min) at 15°C. To control cell suspensions, equal volumes of RPMI1, was added to dilute all inducers after solubilising by manufacturer's instructions. Heat-inactivated *V. anguillarum* bacteria (isolates Vib 6 and Vib 87, as described in Section 3.2.6), were also tested for capacity to induce ET release as above, by adding 10  $\mu\text{L}$  Vib 6 or Vib 87 ( $\times 10^3$ ,  $\times 10^5$ , or  $\times 10^7$  CFU  $\text{mL}^{-1}$  final well concentration, diluted in sterile PBS) to the seeded cells, and incubating for up to 12 h (1, 3, 6, 9, or 12 h, as above). For all compounds, a different plate was prepared for each time point (i.e. non-repeated measures). To measure the amount of extracellular DNA released in response to each of the inducers, the DNA in each well was stained by adding 10  $\mu\text{L}$  SYTOX Green (final well concentration of 5  $\mu\text{M}$ , 5 min, room temperature) before measuring relative fluorescence as described in Section 2.2.8. Fluorescence from triplicate wells were normalised to the mean fluorescence of the control wells to give fold-change fluorescence according to Section 3.2.2, and this was repeated for four fish in total. In another experiment, two additional fish had their PMN-enriched cell suspensions exposed to DPI (final well concentration of 25  $\mu\text{M}$ ) or PMA (final well concentration of 40 and 60 nM) for up to 12 h as above. To account for potential nucleic acid contamination present in the nucleic acid contamination present in Cal, flagellin, pLPS, PMA and/or whole bacteria, these compounds were incubated with RPMI2 and stained with SYTOX Green as described in Section 3.2.5. Triplicate wells of each treatment (and of each concentration) was prepared, and the mean fluorescence emitted from the wells without cells (indicating fluorescence of compound alone) was subtracted from fluorescence measured from individual wells containing PMN-enriched cell suspension.

### **3.2.8. Examining individual ET release variation between fish**

To examine the relationship between fish mass and spontaneous ET release, PMN-enriched cell suspensions (isolated according to Section 2.2.3) were obtained from 19 trout (wet mass measured: 43.8 to 373.0 g), which were hatched from the same batch of eggs and were

genetically siblings (to minimise genetic variation between individuals). The cells were suspended in RPMI2 and seeded in a 96-well culture plate ( $4 \times 10^5$  cells mL<sup>-1</sup>), and cells were allowed to adhere to the bottom of the wells for 30 min at 15°C. An additional 10 µL was added to the seeded cell suspension, and incubated for 1 h at 15°C, to allow the cells to spontaneously release ETs. To measure the amount of spontaneous extracellular DNA released, the DNA in each well was stained by adding 10 µL SYTOX Green (final well concentration of 5 µM, 5 min, room temperature) before measuring relative fluorescence as described in Section 2.2.8.

### **3.2.9. Statistical analyses**

Statistical analyses were performed using Prism v.5.1 (GraphPad, La Jolla, USA). For comparisons of data from multiple groups of mean fold-change fluorescence, normality and equality of variances were assessed by Kolmogorov–Smirnov and Bartlett’s tests, respectively. When data were normal, one-way ANOVA was performed to compare mean fluorescence against unexposed controls at each time point, and Bonferroni’s *post-hoc* test was applied to allow multiple comparisons between means. Student’s t-test was used when comparing two means of normally distributed data, and Wilcoxon-Mann-Whitney (WMW) test was used if the data were non-normally distributed. For all analyses,  $p < 0.05$  was considered statistically significant. The Pearson’s correlation coefficient was used to determine the statistical significance of these correlation data.

## **3.3. Results**

### **3.3.1. Confirming spontaneous release of ET-like structures are specific to PMN-enriched cell suspensions**

PMN-enriched cell suspensions isolated from trout head kidney tissue using Percoll gradients were observed to spontaneously release ET-like structures when incubated at 15°C. In some cases, the spontaneous release was observed at a high frequency from individual fish within 6 h of incubation at 15°C (Section 2.3.6). Trout erythrocyte suspensions were also isolated from head kidney tissue using a modified Percoll gradient (with different relative densities from that used to obtain PMN-enriched cell suspensions) and were examined for spontaneous release of ET-like structures at 6 and 24 h. Over 24 h incubation, there were no observable ET-like structures released from trout erythrocyte suspensions under fluorescence microscopy, but there were SYTOX-stained erythrocytes indicating residual cell death within

the culture (Figure 3.1). Chinook salmon embryo cells (CHSE-214) was also examined for spontaneous release of ET-like structures as a negative control, and did not produce observable ET-like structures over the 24 h incubation (results not shown). Collectively, the results indicate that the ET-like structures are spontaneously released by PMN-enriched cell suspensions and are not an artefact of the cell culture methods (e.g., media contamination), or processes occurring within the head kidney tissue.

### **3.3.2. Confirming the DNA composition of presumed ETs by digestion with DNase-I**

To determine if the ET-like structures observed by fluorescence microscopy in Chapter 2 were made of chromatin, the ET-like structures released by PMN-enriched cell suspensions were treated with increasing concentrations of DNase-I, which is an endonuclease that degrades nucleic acids. DNase-I was added to PMN-enriched cell suspensions that had been induced to release ET-like structures through exposure to Cal (final well concentration of 5  $\mu\text{g mL}^{-1}$ , 3 h, 15°C), a known inducer of ETs from fish PMNs. SYTOX Green is a cell-impermeable nucleic acid stain that emits fluorescence (excitation: 504 nm, emission: 523 nm) when it binds to DNA and it can be used reliably to quantify extracellular DNA (Section 2.2.8). There was a significant reduction in fluorescence emitted from wells treated with DNase-I at 10  $\text{U mL}^{-1}$  and which displayed a  $0.72 \pm 0.04$ -fold fluorescence of the non-exposed control. Treatment with 100  $\text{U mL}^{-1}$  DNase-I resulted in  $0.79 \pm 0.01$ -fold fluorescence compared to controls lacking DNase-I (both  $p < 0.001$ ), thus indicating a significant reduction in undegraded extracellular DNA (Figure 3.2 and Figure 3.3). No significant reductions in fluorescence were observed after exposure of the ET-like structures to 0.01, 0.1, and 1  $\text{U mL}^{-1}$  DNase-I compared to non-exposed controls, suggesting that these concentrations were insufficient to digest the nucleic acid effectively (Figure 3.2 and Figure 3.3). Treatment with DNase-I at 10 and 100  $\text{U mL}^{-1}$  removed almost all fluorescence, indicating that much of the fluorescent signal detected in these wells was most likely attributable to the presence of ET-like fibres, rather than SYTOX Green-stained nuclei of membrane-compromised (*i.e.* dead) cells.

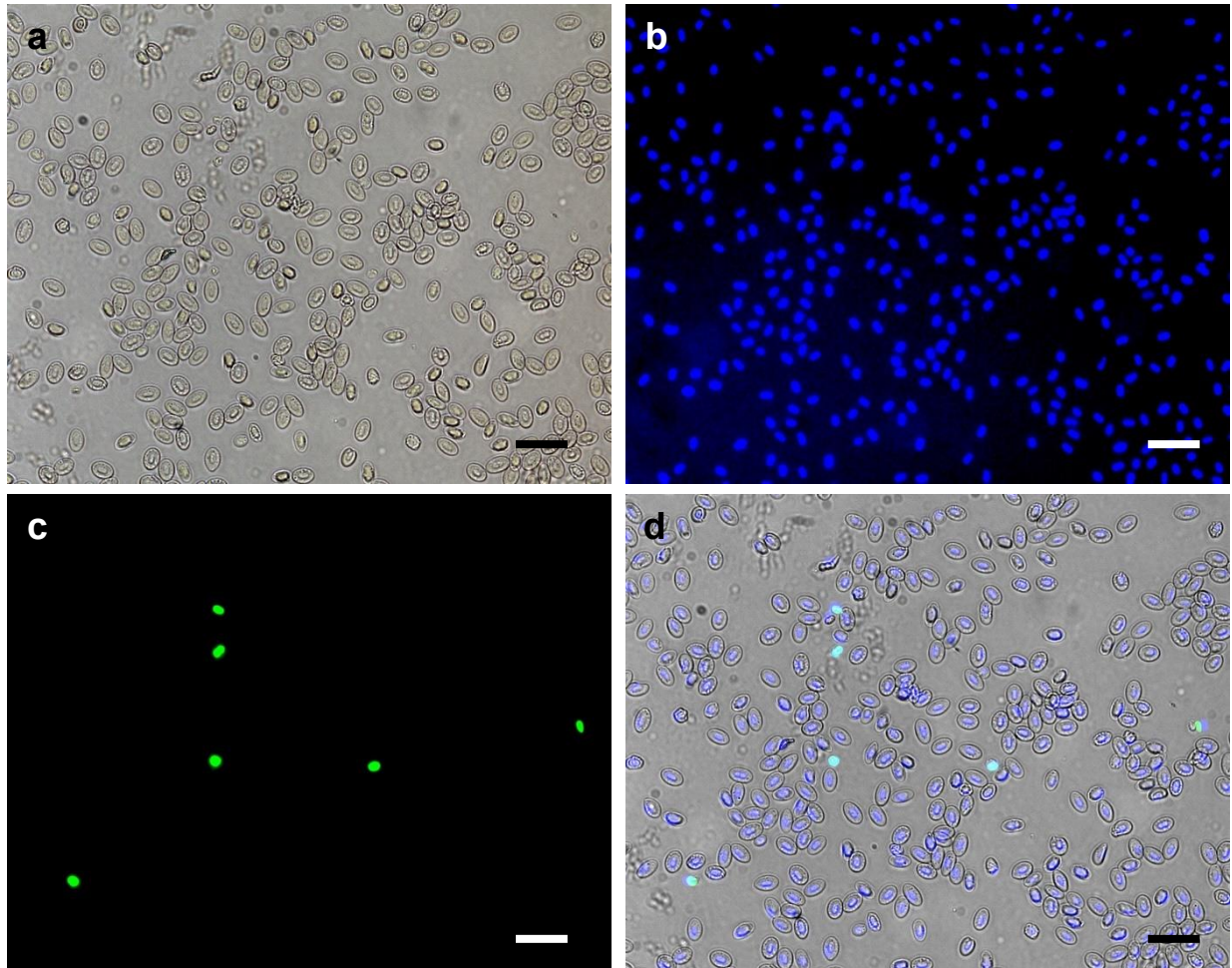


**Figure 3.1.** Representative phase contrast and fluorescence microscopy images showing trout erythrocyte suspensions ( $1 \times 10^5$  cells  $\text{mL}^{-1}$ ) incubated for 24 h at  $15^\circ\text{C}$  exposed to RPMI1, and stained with SYTOX green ( $5 \mu\text{M}$ , 5 min, room temperature) and DAPI ( $1 \mu\text{M}$ , 5 min, room temperature). (a) Phase contrast image showing the morphology of cells within the suspension; (b) DAPI-filter channel showing both intracellular and extracellular nucleic acids stained with DAPI (blue), as DAPI is a membrane-permeable dye; (c) FITC filter channel shows SYTOX Green-stained nucleic acid which only stains extracellular nucleic acids, or membrane compromised cells; (d) Overlay of all three filters. These images show that trout erythrocyte suspensions do not spontaneously release the ET-like structures observed in PMN-enriched cell suspensions. Scale bar =  $50 \mu\text{m}$ .

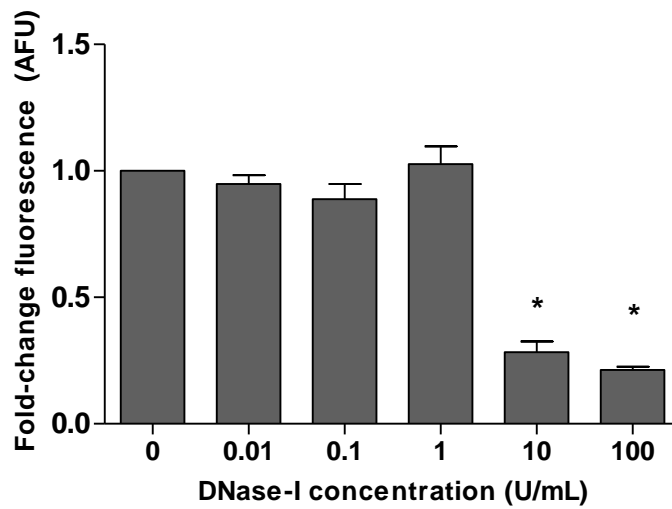


**Figure 3.2.** Bar chart showing the mean fold-change in fluorescence of wells containing trout PMN-enriched cell suspensions ( $4 \times 10^5$  cells  $\text{mL}^{-1}$ ) after initial exposure to Cal ( $5 \mu\text{g mL}^{-1}$ , 3 h,  $15^\circ\text{C}$ ) to stimulate release of ET-like structures, and then to DNase-I (0.01 – 100  $\text{U mL}^{-1}$ ) for 3 h at  $15^\circ\text{C}$ . Exposure of ET-like structures to 10 and 100  $\text{U mL}^{-1}$  DNase-I significantly reduced fluorescence attributed to ET-like structures compared to controls not treated with DNase, indicating ET-like structures are digested by DNA. \* $p < 0.05$  compared to a control not exposed to DNase-I at each time point. Error bars represent s.e.m.  $n = 5$  wells.



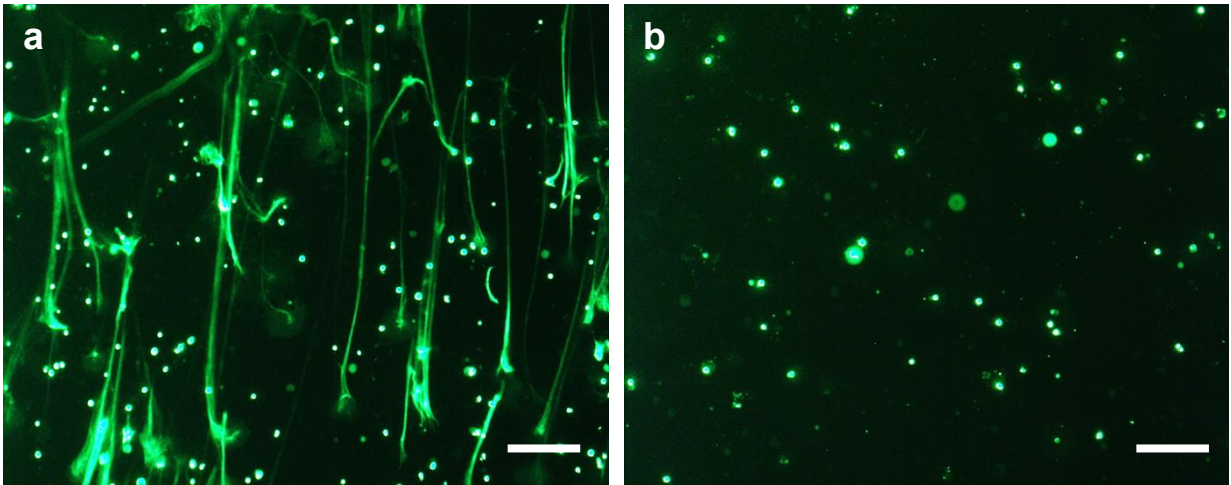


**Figure 3.3.** Representative fluorescence microscopy images of stained ET-like structures released from trout PMN-enriched cell suspensions ( $4 \times 10^5$  cells  $\text{mL}^{-1}$ ) exposed to Cal ( $5 \mu\text{g mL}^{-1}$ , 3h,  $15^\circ\text{C}$ ), treated with (a)  $\text{dH}_2\text{O}$  in DNase buffer, as a negative control for DNase treatment; (b) treated with DNase-I ( $100 \text{ U mL}^{-1}$ , 3 h,  $15^\circ\text{C}$ ), stained with SYTOX Green ( $5 \mu\text{M}$ , 5 min, room temperature). This figure confirms that the ET-like structures in the PMN-enriched cell suspensions were composed of nucleic acids, as they were susceptible to degradation by DNase-I. Scale bars =  $100 \mu\text{m}$ .

### **3.3.3. Determining the presence of myeloperoxidase, neutrophil elastase, and histone H2A in ET-like structures by immunocytochemistry**

The decoration of ET-like structures was probed through the immunocytochemical detection of three diagnostic markers of extracellular traps by using: anti-MPO, anti-NE, and anti-H2A. There was positive detection of MPO (1:20), NE (1:20) and histone H2A proteins (1:200), and each of these respective signals was observed to co-localise with DAPI-stained nucleic acid (Figure 3.4), thus providing further evidence that the ET-like structures released from trout PMN enriched cell suspensions were indeed ETs. Triton X-100 was used to permeabilise the cells during the blocking step before staining with anti-MPO and anti-NE antibodies, and some surrounding cells also staining positive for MPO and NE (observed as concentrated green spots rather than dispersed fibres; Figure 3.4d and Figure 3.4e), indicating the presence of non-ETotic PMNs in the cell suspension. No positive staining was observed in controls lacking primary antibody, indicating that the secondary FITC-conjugated antibodies were specific to the primary markers, and were not cross-reacting with any other non-specific targets within the well.

### **3.3.4. Investigating the three-dimensional structure of the ETs**

Confocal microscopy of fixed, SYTOX-stained trout PMN-enriched cell suspensions exposed to RPMI1 cell media revealed fibrous extracellular nucleic acid strands protruding from a cluster of cells after 6 h incubation (Figure 3.5). The z-stack images taken by confocal microscopy allowed a three-dimensional representation of trout ETs *in vitro*, giving better lateral and axial resolution. A video showing the three-dimensional representation of the ETs released by trout PMNs can be found online in the figure legend (Figure 3.5).

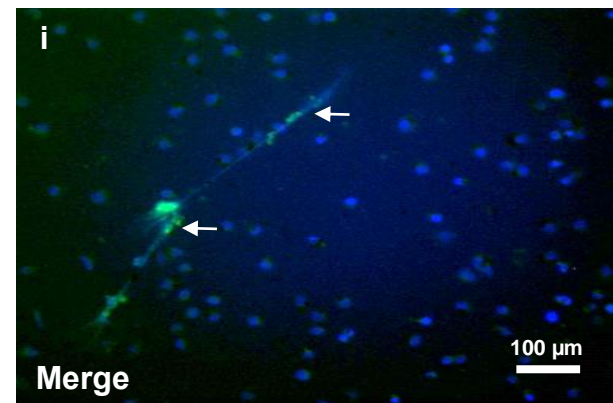
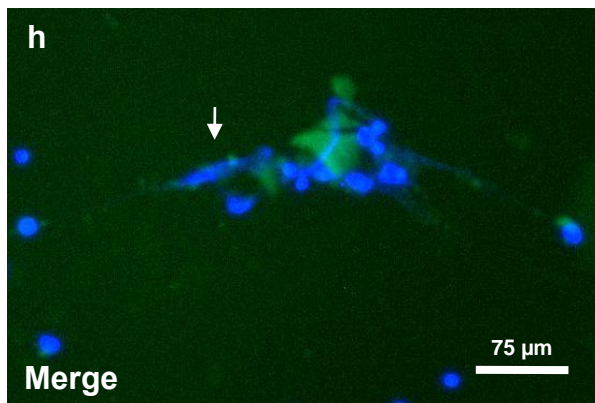
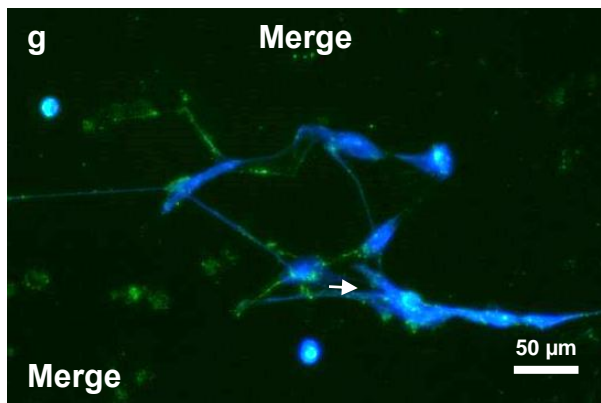
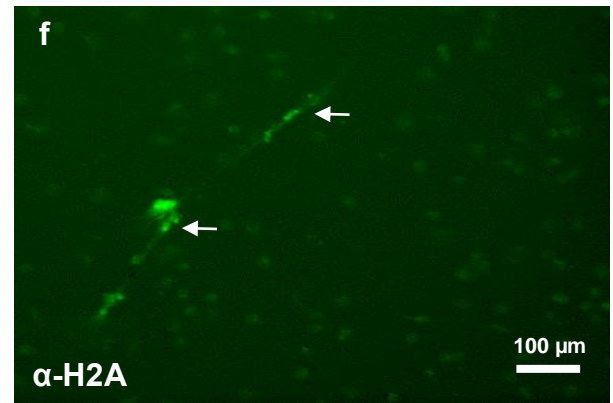
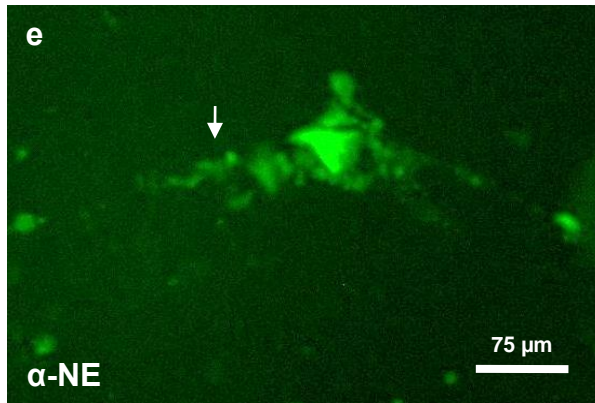
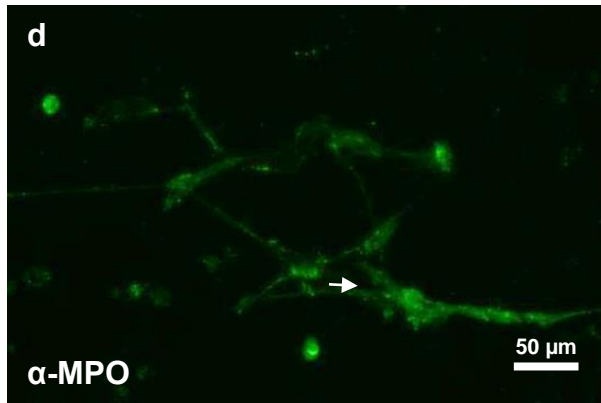
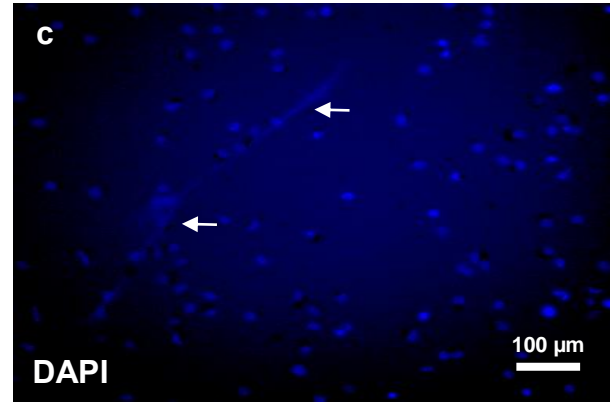
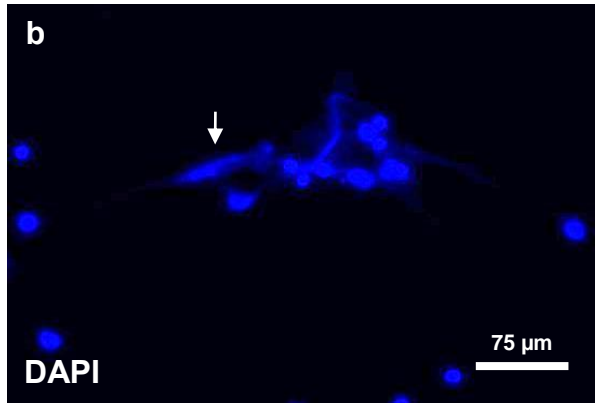
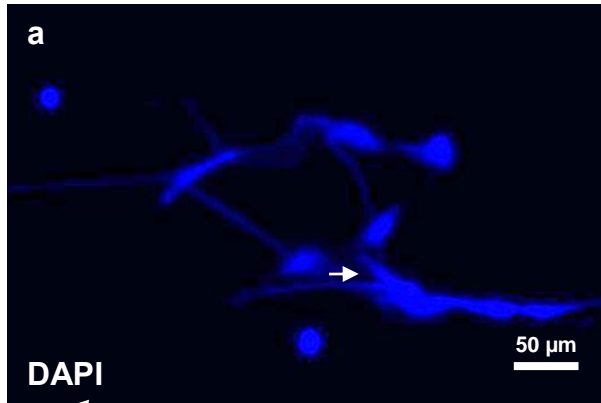


**Figure 3.4.** Representative fluorescence microscopy images of immunocytochemically stained ET-like structures released from trout PMN-enriched cell suspensions ( $4 \times 10^5$  cells mL<sup>-1</sup>) exposed to Cal ( $5 \mu\text{g mL}^{-1}$ , 3h, 15°C), confirming the presence of proteins characteristic for extracellular traps (ETs) in association with extracellular DNA. (a-c) DAPI filter showing the staining of ET-like structures (white arrows) with membrane-permeable nucleic acid-specific DAPI. (d-f) FITC-conjugated anti-myeloperoxidase (MPO, 1:20), neutrophil elastase (NE, 1:20), and histone H2A antibodies (1:2000) demonstrate positive staining which co-localises with the ET-like structures. (g-i) Merged DAPI and FITC channels confirming the co-localisation of ET-like fibres with MPO, NE, and H2A with DAPI-stained DNA fibres, respectively (white arrows).

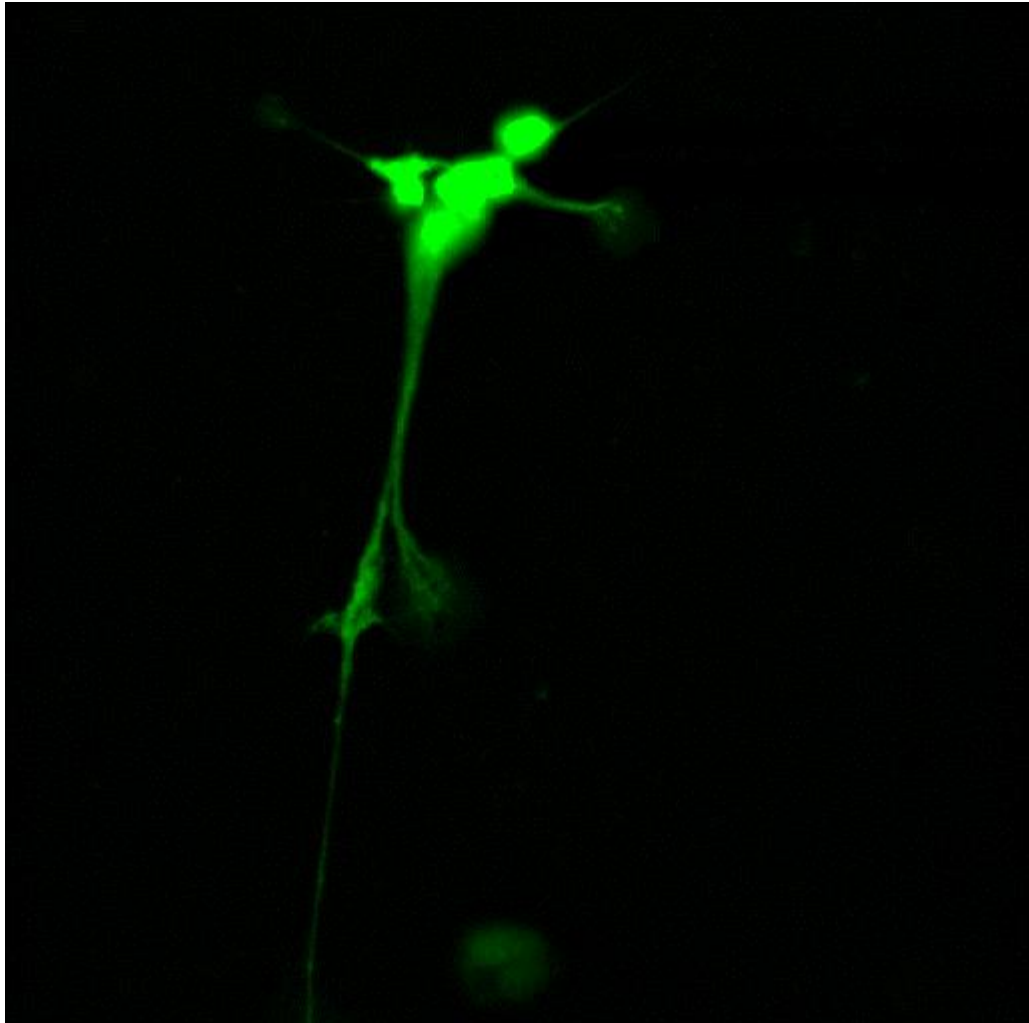


**Figure 3.5.** Confocal microscopy re-constructed 3-dimensional image of SYTOX Green-stained cell suspension (5  $\mu$ M, 5 min, room temperature). Cells within the PMN-enriched cell suspension (incubated for 24 h at 15°C) are shown at the top of the image with DNA, most probably an ET, as indicated by white arrows. A large ET fibre can be observed extending below from the cluster of cells observed above. The full video is found at <https://goo.gl/4RQg2Z>.

### 3.3.5. Investigating the effect of known ET release inhibitors on ET release from trout PMN-enriched cell suspensions

The effect of Cyto D and DPI on ET release from rainbow trout PMN enriched cell suspensions in response to both Cyto D and DPI was determined by measuring fold-changes in SYTOX Green fluorescence (attributable to ET release) compared to non-exposed control cells. Nucleic acid contamination of Cyto D and DPI was checked, and there was no significant difference in fluorescence signal compared to negative controls (data not shown). Incubation of PMN-enriched cell suspensions with Cyto D at all concentrations for 30 min before inducing ET release by incubating with  $5 \mu\text{g mL}^{-1}$  Cal for 1 h did not result in a significant difference in fluorescence from PMN-enriched cell suspensions. At 3 h exposure to Cal, 10 and 20  $\mu\text{M}$  before inducing ET release with  $5 \mu\text{g mL}^{-1}$  Cal for 3 h resulted in a significant,  $0.33 \pm 0.03$  and  $0.37 \pm 0.03$ - fold decrease in fluorescence attributable to ET release from PMN-enriched cell suspensions, respectively (both  $p < 0.05$ ), compared to negative controls not exposed to Cyto D (Figure 3.6). At 3 h, 5  $\mu\text{M}$  Cyto D resulted in a  $0.18 \pm 0.05$ -fold decrease in fluorescence compared to negative controls; however, this did not reach statistical significance (Figure 3.6). At 6 h exposure to 5, 10, and 20  $\mu\text{M}$  Cyto D, the fluorescence was decreased by  $0.28 \pm 0.02$ ,  $0.34 \pm 0.06$ , and  $0.39 \pm 0.04$ -fold compared to negative controls, all reaching statistical significance ( $p < 0.05$ ) (Figure 3.6).

Moreover, observations by fluorescence microscopy confirmed the presence of fewer ETs in Cyto D-treated (5, 10 and 25  $\mu\text{M}$ , 3 h and 6 h,  $15^\circ\text{C}$ ) PMN-enriched cell suspensions compared to negative controls not exposed to Cyto D (Figure 3.7). Notably, nuclear fragmentation characteristic of apoptotic cells was observed at a greater frequency when treated with 10 or 25  $\mu\text{M}$  Cyto D for 3 h (Figure 3.7b) or longer. This indicates that Cyto D may be causing apoptosis of cell in PMN-enriched cell suspensions, or that the cytoskeleton is preventing ETs from being released.

Unexpectedly, DPI alone was found to increase the number of ETs rather than inhibit ET release. At 3 h exposure, 25  $\mu\text{M}$  DPI resulted in a  $2.29 \pm 0.16$ -fold increase in fluorescence attributable to ETs compared to negative controls not exposed to DPI at 3 h ( $p < 0.05$ ) (Figure 3.8). At 6 h exposure, DPI at 10 and 25  $\mu\text{M}$  resulted in a  $2.09 \pm 0.44$ , and  $2.18 \pm 0.40$ -fold increase in fluorescence, respectively, compared to non-exposed controls (both,  $p < 0.05$ ). At 9 h, DPI at 10 and 25  $\mu\text{M}$  resulted in a  $2.70 \pm 0.55$ , and  $3.10 \pm 0.58$ -fold increase in fluorescence, respectively, compared to non-exposed controls (both,  $p < 0.05$ ). At 12 h, DPI at 5, 10, and 25  $\mu\text{M}$  resulted in a  $2.08 \pm 0.41$ ,  $2.43 \pm 0.44$ , and  $1.90 \pm 0.38$ -fold increase in fluorescence, respectively, compared to non-exposed controls (all,  $p < 0.05$ ). These results were confirmed with fluorescence microscopy (Figure 3.9). Collectively, these results that Cyto D has the ability to dose and time-dependently inhibit ET release from trout PMN-enriched cell suspensions, while DPI can induce ET release from these cells.

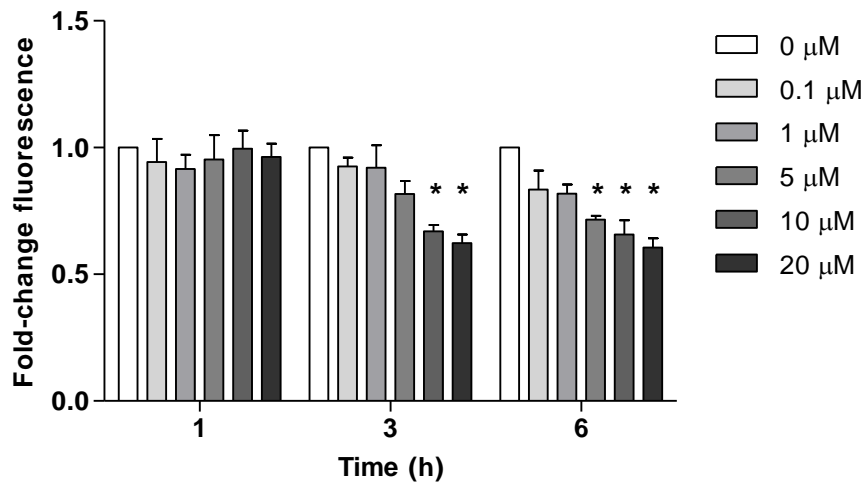


**Figure 3.6.** Bar chart showing the mean fold-change in fluorescence from wells containing trout PMN-enriched cell suspensions ( $4 \times 10^5$  cells  $\text{mL}^{-1}$ ) after initial exposure to Cyto D (0 – 20  $\mu\text{M}$ , 30 min, 15°C), and then induced to form ETs with Cal ( $5 \mu\text{g mL}^{-1}$ ) for up to 6 h at 15°C. Exposure of PMN-enriched cell suspensions to 5, 10, or 20  $\mu\text{M}$  Cyto D resulted significantly less fluorescence (attributable to ETs) compared to controls not exposed to Cyto D at 6 h, indicating that Cyto D is causing the reduction in ET release. \* $p < 0.05$  compared to a control not exposed to Cal at each time point. Error bars represent s.e.m.  $n = 4$  fish.

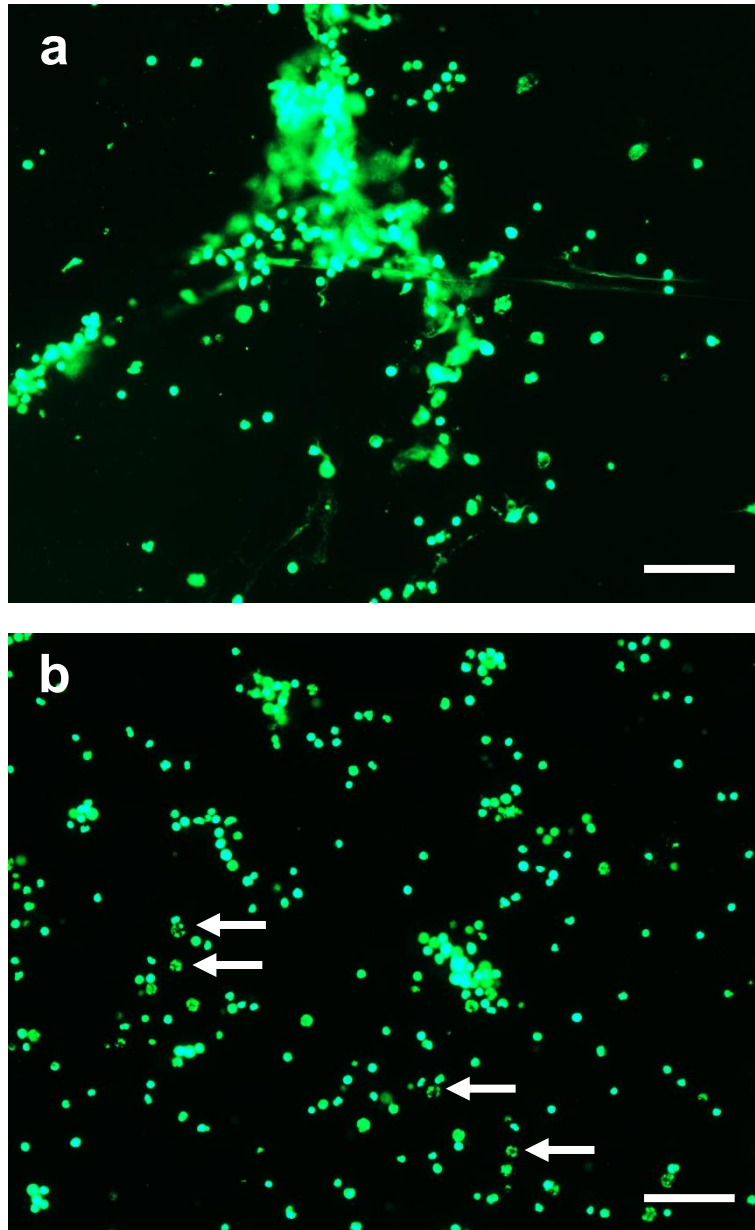


**Figure 3.7.** Representative fluorescence microscopy images of trout PMN-enriched cell suspensions ( $4 \times 10^5$  cells  $\text{mL}^{-1}$ ) stained with SYTOX Green ( $5 \mu\text{M}$ , 5 min, room temperature) after initial 30 min exposure to: (a) RPMI1 negative control (b) Cyto D ( $10 \mu\text{M}$ , 30 min,  $15^\circ\text{C}$ ), followed by exposure to Cal ( $5 \mu\text{g mL}^{-1}$ , 3h,  $15^\circ\text{C}$ ). Exposure to Cyto D before Cal resulted in less ETs released from the PMN-enriched cell suspension compared to cells that were not exposed to Cyto D. Within the cells treated with Cyto D, some membrane-compromised cells with fragmented nuclei resembling apoptotic bodies were observed (white arrows), indicating Cyto D may be inducing apoptosis. Scale bar =  $100 \mu\text{m}$ .



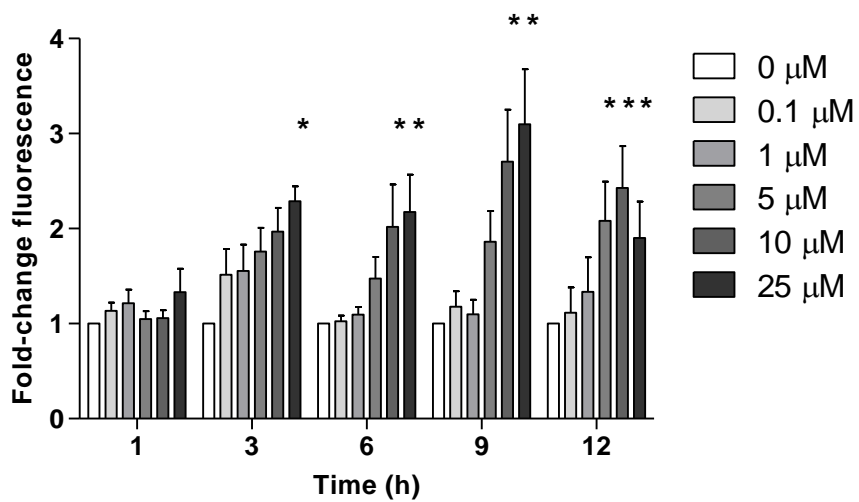


**Figure 3.8.** Bar chart showing the mean fold-change in fluorescence from wells containing trout PMN-enriched cell suspensions ( $4 \times 10^5$  cells  $\text{mL}^{-1}$ ) after exposure to DPI (0.1 – 25  $\mu\text{M}$ ) for up to 12 h at 15°C. Exposure of PMN-enriched cell suspensions to 5, 10, and 25  $\mu\text{M}$  DPI alone resulted significantly greater fluorescence (attributable to ETs) at 12 h compared to controls not exposed to DPI, indicating that DPI can induce ET release. \* $p < 0.05$  compared to a control not exposed to DPI at each time point. Error bars represent s.e.m.  $n = 4$  fish.

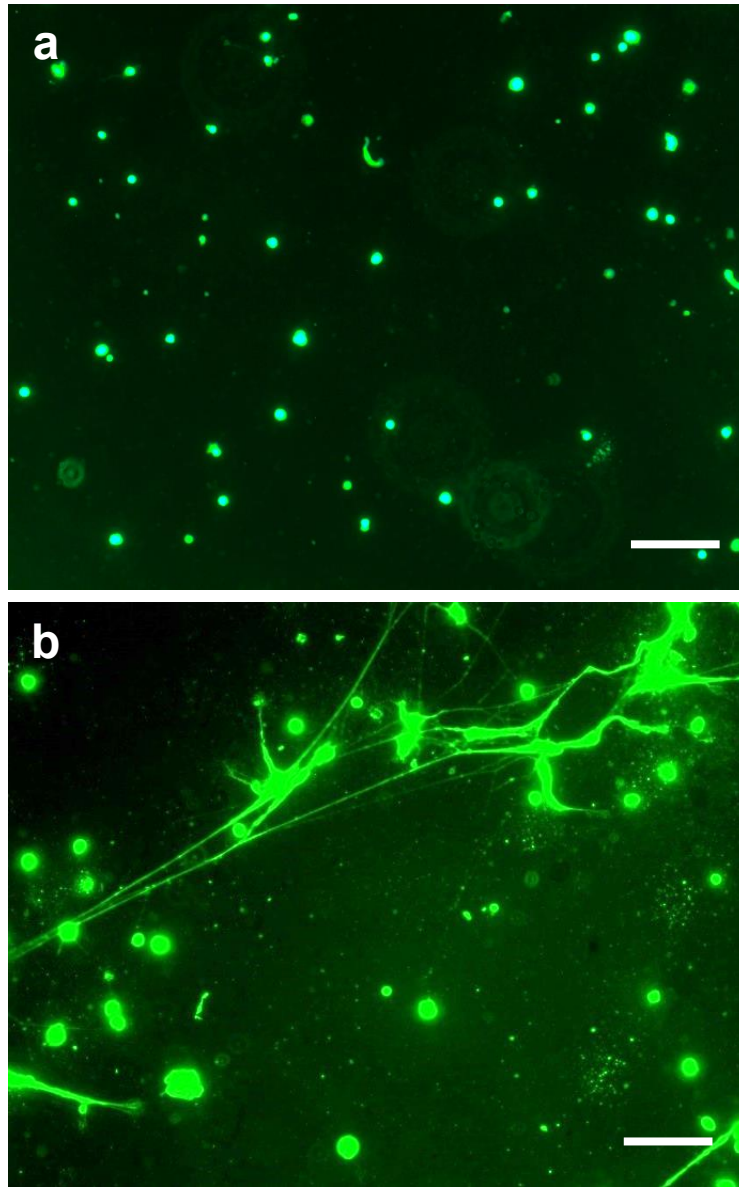


**Figure 3.9.** Representative fluorescence microscopy images of trout PMN-enriched cell suspensions ( $4 \times 10^5$  cells  $\text{mL}^{-1}$ ) stained with  $5 \mu\text{M}$  SYTOX Green ( $5 \mu\text{M}$ , 5 min, room temperature) after exposure to (a) RPMI1 negative control (b) DPI  $10 \mu\text{M}$ , both for 3 h,  $15^\circ\text{C}$ . Exposure to DPI resulted in more visible ETs compared to non-exposed controls. Exposure of cells to DPI resulted in visibly more ET release compared to negative controls. Scale bar =  $100 \mu\text{m}$ .

### 3.3.6. Investigating the effect of known ET release inducers on ET release from trout PMN-enriched cell suspensions

Rainbow trout PMN-enriched cell suspensions were induced to release ETs through exposure to known ET release stimulants: Cal, flagellin, pLPS, and PMA for up to 12 h, and the kinetics of ET release determined by measuring fold-changes in SYTOX Green fluorescence (attributable to ETs) compared to non-exposed control cells. Nucleic acid contamination of Cal, flagellin, pLPS, or PMA was checked, and there was no significant differences in fluorescence signal compared to negative controls (data not shown).

Cal at 0.1, 1, 5, 10, and 25  $\mu\text{g mL}^{-1}$  was tested to induce ET release for up to 12 h exposure. At 1 h exposure, Cal at 1, 5, 10, and 25  $\mu\text{g mL}^{-1}$  resulted in a  $2.38 \pm 0.26$ ,  $3.16 \pm 0.30$ ,  $3.35 \pm 0.21$ , and  $3.33 \pm 0.27$ -fold increase in fluorescence, respectively, compared to negative controls not exposed to Cal at 1 h (all  $p < 0.05$ , Figure 3.10). At 3 h exposure, Cal at 1, 5, 10, and 25  $\mu\text{g mL}^{-1}$  resulted in a  $3.17 \pm 0.32$ ,  $3.19 \pm 0.27$ ,  $3.20 \pm 0.37$ , and  $3.47 \pm 0.27$ -fold increase in fluorescence, respectively, compared to non-exposed controls (all,  $p < 0.05$ ). At 6 h, Cal at 1, 5, 10, and 25  $\mu\text{g mL}^{-1}$ , resulted in a  $3.73 \pm 0.44$ ,  $3.30 \pm 0.25$ ,  $3.12 \pm 0.37$ , and  $3.48 \pm 0.40$ -fold increase in fluorescence, respectively, compared to non-exposed controls (all,  $p < 0.05$ ). At 9 h, Cal at 1, 5, 10, and 25  $\mu\text{g mL}^{-1}$  resulted in a  $3.30 \pm 0.33$ ,  $3.32 \pm 0.35$ ,  $3.46 \pm 0.40$ , and  $3.88 \pm 0.65$ -fold increase in fluorescence, respectively, compared to non-exposed controls (all,  $p < 0.05$ ). At 12 h, Cal at 1, 5, 10, and 25  $\mu\text{g mL}^{-1}$  resulted in a  $3.02 \pm 0.19$ ,  $2.60 \pm 0.13$ ,  $2.75 \pm 0.23$ , and  $3.03 \pm 0.14$ -fold increase in fluorescence, respectively, compared to non-exposed controls (all,  $p < 0.05$ ). These results were confirmed for the presence (or absence) of ETs with fluorescence microscopy (Figure 3.11). Cal at 0.1  $\mu\text{g mL}^{-1}$  did not result in any significant differences in fold-change fluorescence compared to untreated controls at any time point. There was no significant difference in fold-change fluorescence between 5 to 25  $\mu\text{g mL}^{-1}$  Cal ( $p > 0.05$ ), indicating 5  $\mu\text{g mL}^{-1}$  possibly resulted in saturation of ET release by cells capable of releasing ETs by 1 h (Figure 3.10a). Moreover, longer incubation of the PMN-enriched cell suspensions with 5  $\mu\text{g mL}^{-1}$  Cal for 3, 6, and 9 h did not result in significant increases in fold-change fluorescence compared to 1 h ( $p > 0.05$ ), suggesting that all the cells capable of releasing ETs had already done so. Collectively, these results suggest that Cal is a fast and potent inducer of ET release from trout PMN-enriched cell suspensions. Importantly, the ETs appeared to collect at the bottom of the well where the cells have settled (Figure 3.11).

Due to limited availability, recombinant flagellin (kindly donated by Chris Secombes) was only tested to induce ET release at 100  $\text{ng mL}^{-1}$  at 1 h intervals up to 6 h. Flagellin is shown to induce the greatest pro-inflammatory response at 100  $\text{ng mL}^{-1}$  from head-kidney derived macrophages of rainbow trout (Wangkahart *et al.*, 2016). At 1, 2, 3, 4, 5, and 6 h exposure, flagellin at 100  $\text{ng mL}^{-1}$  resulted in a  $3.34 \pm 0.81$ ,  $3.31 \pm 0.311$ ,  $3.56 \pm 0.49$ ,  $3.80 \pm 0.36$ ,  $4.12$

$\pm 0.55$ , and  $2.57 \pm 0.45$ -fold increase in fluorescence, respectively, compared to negative controls not exposed to flagellin at respective times (all  $p < 0.05$ , Figure 3.10). These results were confirmed for the presence (or absence) of ETs with fluorescence microscopy (Figure 3.11); however, flagellin caused the ETs and cells within the suspension to clump together. Therefore, the images taken of cells do not have enough resolution to clearly show the ETs present, and are not representative of the ETs released in culture. This indicates that flagellin may be an inducer of ETs in trout PMN-enriched cell suspensions.

Sterile filtered LPS (purified by phenol extraction) was found to possess abundant nucleic acid contamination, while pLPS (purified by ion exchange chromatography) did not have a significantly greater fluorescence compared to the RPMI1 used for dilution (Appendix Figure 3). Thus, pLPS instead of LPS was tested to induce ET release from trout PMN-enriched cell suspensions for up to 12 h exposure. At 1, 3, 6, 9, and 12 h, exposure of cells to pLPS did not result in a significant difference in fluorescence compared to negative controls not exposed to pLPS ( $p > 0.05$ , Figure 3.10).

PMA at 1, 10, 20, 40, and 60 nM was tested to induce ET release for up to 12 h exposure. At 9 h exposure, PMA at 40, and 60 nM PMA resulted in a  $2.26 \pm 0.72$  and  $2.54 \pm 0.88$ -fold increase in fluorescence, respectively, compared to negative controls not exposed to Cal at 9 h (all  $p < 0.05$ , Figure 3.10). At all other PMA concentrations (1, 10, and 20 nM), PMA did not result in an increase in fluorescence compared to non-exposed controls at all time points. These results were confirmed for the presence (or absence) of ETs with fluorescence microscopy (Figure 3.11). Collectively, these results suggest that PMA is a relatively weaker inducer of ETs in trout compared to that reported in carp, or mammalian counterparts. PMA at 100 nM was also exposed to PMN-enriched cell suspensions for up to 12 h, but no significant increase in fluorescence was observed compared to negative controls, though some ETs were observed to be released spontaneously (Appendix Figure 6). Furthermore, some acute cytotoxicity was noted at 100 nM due to an apparent increased number of SYTOX-stained cells and cell membranes within the cell suspension, suggesting the cells were killed before they could release ETs. However, this cytotoxicity was not represented in the data, as the membrane-compromised cells do not contribute to fluorescence compared to ETs (Appendix Figure 5, and Section 2.3.5). Another morphological distinction are the cell membranes, which appear more irregular compared to the negative controls at 24 h exposure (Appendix Figure 6b, c). Taken together these data suggest that PMA is a weak inducer of ET release in rainbow trout compared to its activity in mammals.

Two isolates of heat-inactivated whole *V. anguillarum* (Vib 6 and Vib 87) bacteria at  $\times 10^3$ ,  $\times 10^5$ , and  $\times 10^7$  CFU mL<sup>-1</sup> was tested to induce ET release for up to 12 h exposure. Each of the bacterial suspensions was confirmed to be heat-inactivated as no growth was observed on

TSA 2% NaCl plates during a 48 h incubation at 22°C. Interestingly, no significant increase of ET release was from trout PMNs was detected after incubation with both isolates over the 12 h compared to untreated controls (all  $p>0.05$ ) (Figure 3.12).

One of the potent inducers of ET release (Cal at 5  $\mu\text{g mL}^{-1}$ ) was followed up to understand the kinetics of ET release within shorter, 10 min intervals over a 60 min incubation. A significant increase in fluorescence was recorded immediately after exposure ( $1.32 \pm 0.04$ -fold change fluorescence compared to negative controls), with a gradual increase in fluorescence thereafter (all  $p<0.05$ , Figure 3.13). Collectively, Cal at 5  $\mu\text{g mL}^{-1}$  demonstrates a potent capacity to significantly induce ET release from trout PMN-enriched cell suspensions

A closer inspection of the data revealed that the PMN-enriched cell suspensions prepared from four fish had different individual responses to PMA and DPI, with two of the four fish responding to PMA or DPI showing significantly greater fluorescence (responding to treatment) compared to negative controls (Figure 3.14 and Figure 3.15). PMA at 40 and 60 nM, and DPI 25  $\mu\text{M}$  was tested again on two additional fish to induce ET release for up to 12 h exposure, and the fold-change fluorescence at 1, 3, 6, 9, and 12 h was recorded and presented to follow the response of the fish. PMA exposure resulted in significant increases of ET release from just two of the six individual fish, while DPI induced ET release in four of the six fish (Figure 3.14). In contrast, ET release was observed from every individual fish when treated with Cal or recombinant flagellin (Appendix Figure 7). The PMN-enriched cell suspension isolated from the same fish (trout 4, in Figure 3.14b) resulted in ET release after exposure or 40 and 60 nM PMA, while cells from trout 1 were not responsive to the same concentrations of PMA (Figure 3.15). This suggests that some fish are consistent responders to the chemicals PMA and DPI.

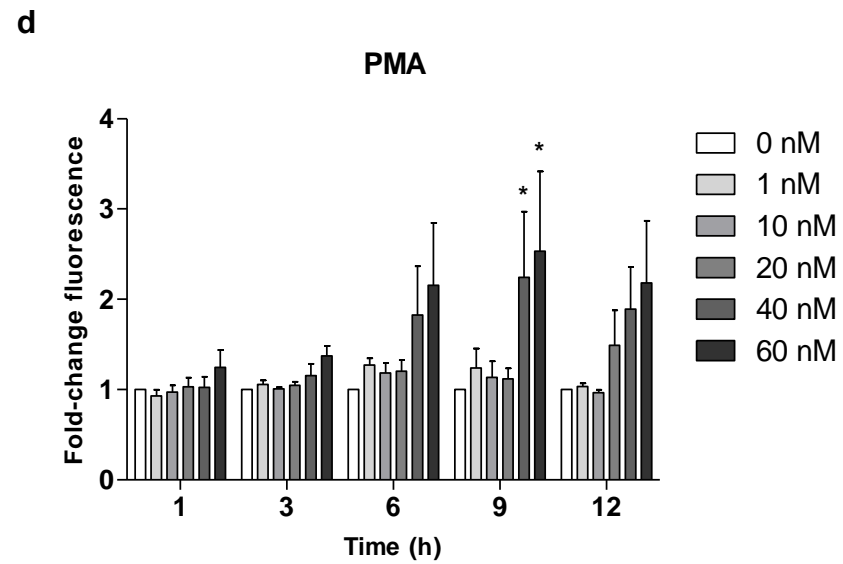
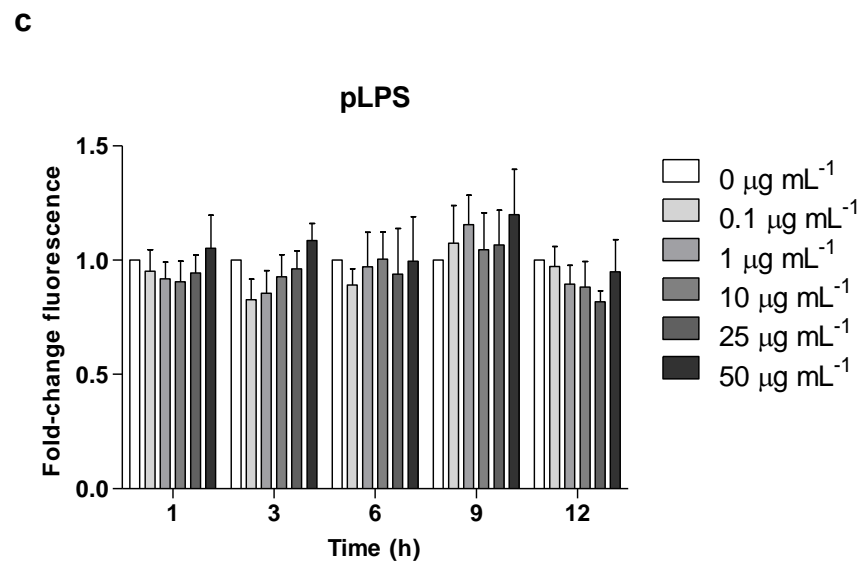
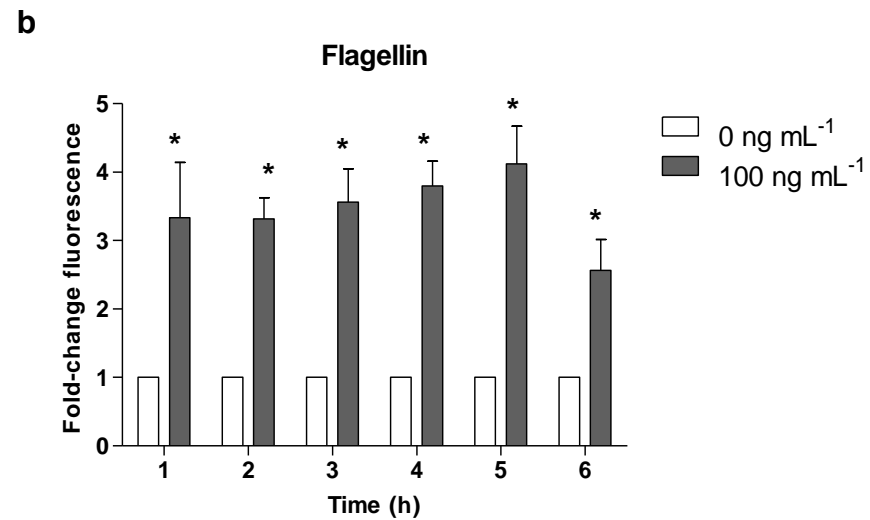
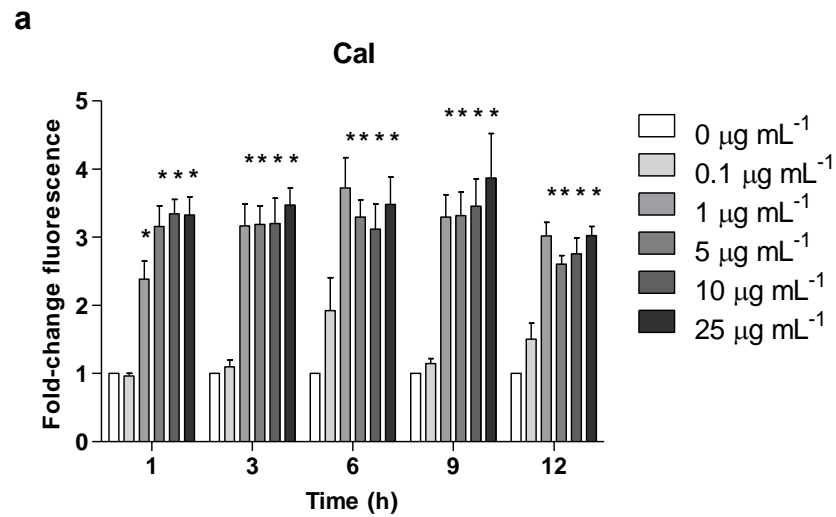


**Figure 3.10.** Bar chart showing the mean fold-change in fluorescence from wells containing trout PMN-enriched cell suspensions ( $4 \times 10^5$  cells mL<sup>-1</sup>) after exposure to: (a) Cal, (b) flagellin, (c) pLPS, (d) PMA for up to 12 h at 15°C, and stained with SYTOX Green (5 µM, 5 min, room temperature). Exposure of PMN-enriched cell suspensions to 1 µg mL<sup>-1</sup> Cal or greater at 1 h; 100 ng mL<sup>-1</sup> flagellin at 1 h, or 40 nM of PMA or greater at 9 h resulted in significantly greater fluorescence (attributable to ETs) compared to negative controls, indicating that Cal, flagellin, and PMA can induce ET release. \* $p < 0.05$  compared to a control not exposed to Cal, flagellin, pLPS, or PMA at each time point. Error bars represent s.e.m.  $n = 4$  fish.

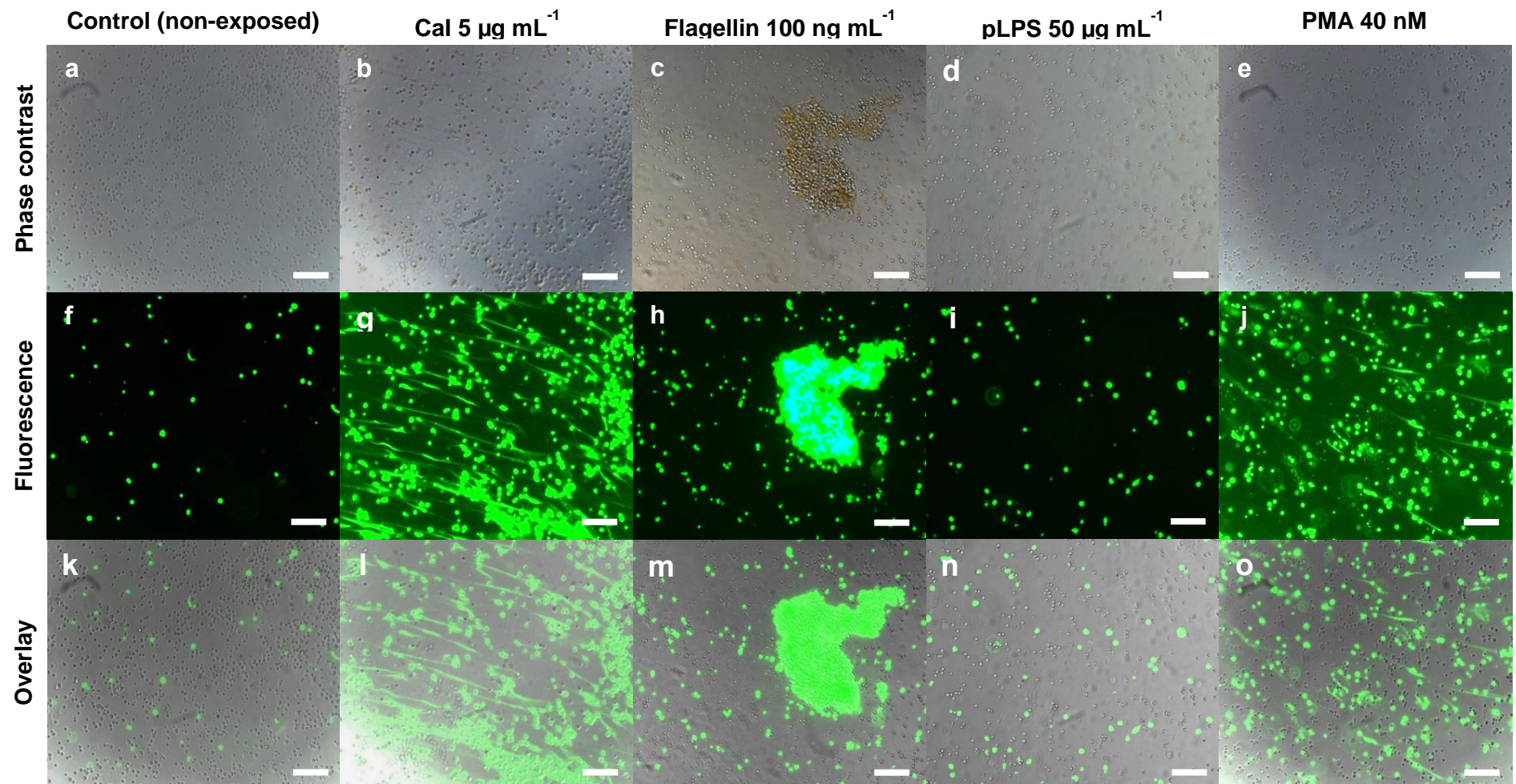




**Figure 3.11.** (a-e) Representative phase contrast images of representative trout PMN-enriched cell suspensions ( $4 \times 10^5$  cells  $\text{mL}^{-1}$ ) exposed to: (a) unexposed control; (b) Cal  $5 \mu\text{g mL}^{-1}$ ; (c) flagellin  $100 \text{ ng mL}^{-1}$ ; (d) pLPS  $50 \mu\text{g mL}^{-1}$ ; (e) PMA  $40 \text{ nM}$ ; (f-j) for 6 h at  $15^\circ\text{C}$ . Paired SYTOX Green-stained cells ( $5 \mu\text{M}$ , 5 min, room temperature) under a FITC filter, showing extracellular DNA and membrane-compromised, non-viable cells. ETs are indicated by white arrows which are absent in unstimulated controls and pLPS-treated PMNs (k-o) Merged overlay of phase contrast images and fluorescence images. Scale bar =  $100 \mu\text{m}$ .

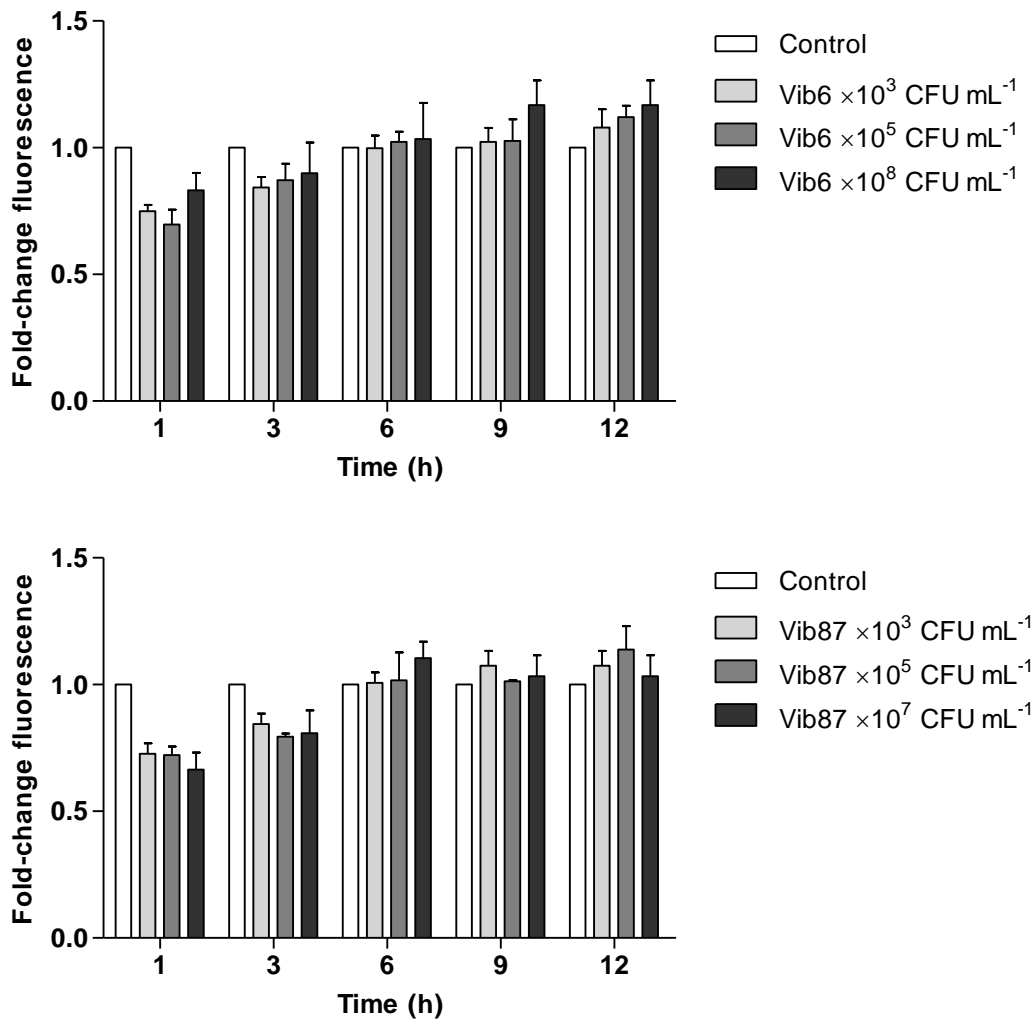


**Figure 3.12.** Bar chart showing the mean fold-change in fluorescence from wells containing trout PMN-enriched cell suspensions ( $4 \times 10^5$  cells mL<sup>-1</sup>) to heat-inactivated *V. anguillarum* (Vib 6 and Vib 87) for up to 12 h at 15°C, then staining with SYTOX Green (5  $\mu$ M, 5 min, room temperature). Exposure of PMN-enriched cell suspensions to heat-inactivated *V. anguillarum* (both Vib 6 and Vib 87) did not result in a significant difference in fluorescence (attributable to ETs) at any time point compared to negative controls, indicating that heat-inactivated *V. anguillarum* does not induce ET release. \* $p < 0.05$  compared to a control not exposed to *V. anguillarum* at each time point. Error bars represent s.e.m.  $n = 4$  fish.

### 3.3.7. Investigating individual variation in spontaneous ET release

Examination of ET release from 19 trout at a range of sizes (wet mass) after incubating PMN-enriched cell suspension with RPMI for 1 h at 15°C showed larger trout (measured in raw wet mass) resulting in significantly less spontaneous unstimulated ET release compared to smaller trout ( $R^2 = 0.4388$ ;  $F_{1,17} = 13.29$ ;  $p < 0.05$ ; Figure 3.16). When removing the 5 large fish weighing 247.6 g – 373.0 g from the dataset, no significant correlation was observed between fish mass and spontaneous ET release ( $R^2 = 0.001$ ;  $F_{1,12} = 0.021$ ;  $p > 0.05$ ; data not shown). The trout used for this study were hatched from the same batch of eggs and are genetically siblings, minimising the genetic variation between individuals. This individual variation of spontaneous ET release by RPMI1-treated PMNs was also detected in a small trial examining diploid and triploid Atlantic salmon. Similar observations were made for the 10 diploid and 10 triploid salmon (Appendix Figure 8).

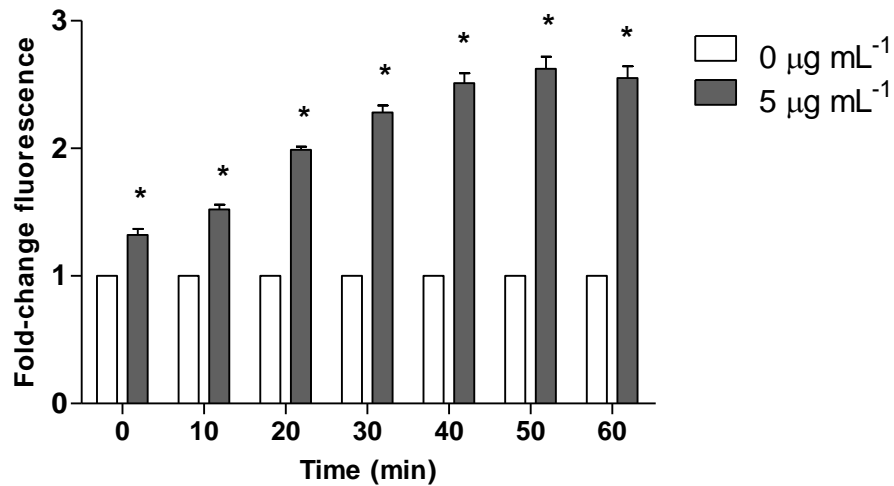


**Figure 3.13.** Bar chart showing the mean fold-change in fluorescence from wells containing trout PMN-enriched cell suspensions ( $4 \times 10^5$  cells mL<sup>-1</sup>) to Cal ( $5 \mu\text{g mL}^{-1}$ ) at 10 min intervals over 60 min at 15°C, then staining with SYTOX Green ( $5 \mu\text{M}$ , 5 min, room temperature). Exposure of PMN-enriched cell suspensions to Cal resulted in a significant difference in fluorescence (attributable to ETs) compared to negative controls at every time point, indicating that Cal induces ET release immediately upon exposure to cells within the PMN-enriched cell suspension. \* $p < 0.05$  compared to a control not exposed to Cal at each time point. Error bars represent s.e.m.  $n = 4$  fish.

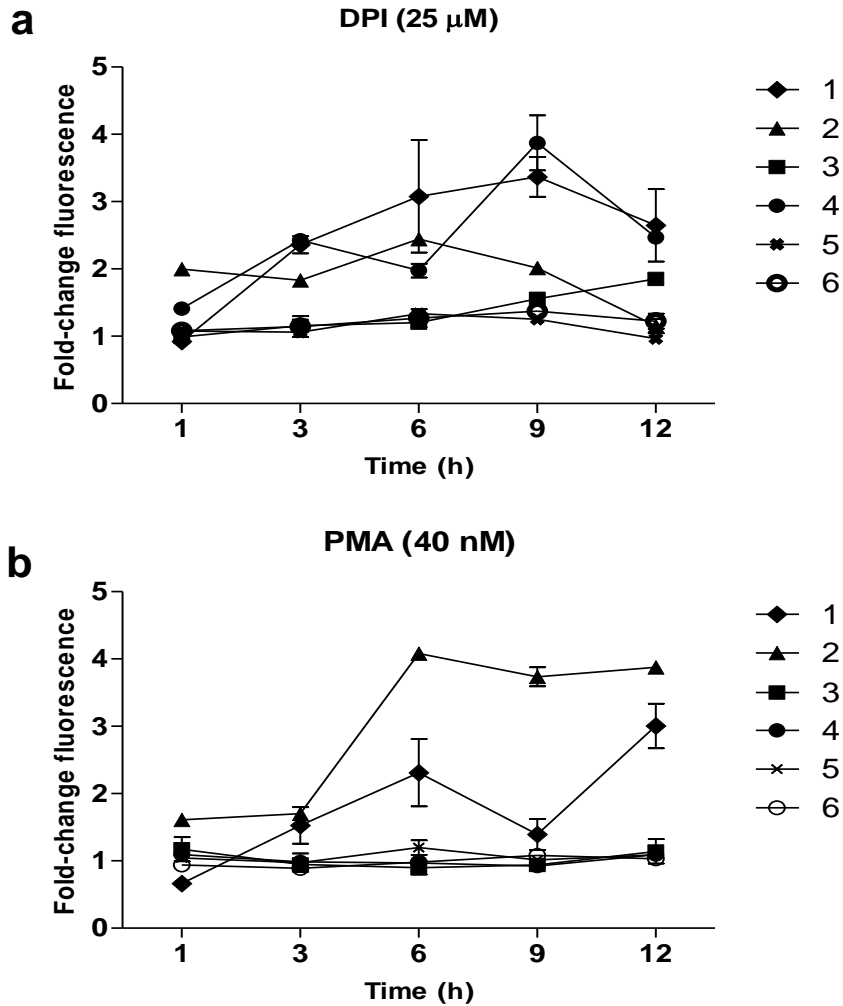


**Figure 3.14.** Scatterplot showing the mean fold-change in fluorescence from wells containing trout PMN-enriched cell suspensions ( $4 \times 10^5$  cells  $\text{mL}^{-1}$ ) from individual fish (labelled 1 to 6) to DPI (25  $\mu\text{M}$ ) or PMA (40 nM) for up to 12 h at 15°C, then staining with SYTOX Green (5  $\mu\text{M}$ , 5 min, room temperature). Each line represents the fluorescence compared to negative controls (being 1-fold) associated with cells from an individual fish. Data from experiment (Figure 3.10) represent labelled fish 1 to 4, and the two additional fish is labelled 5 and 6, (a) DPI (25  $\mu\text{M}$ ) resulted in four out of the six fish (1, 2, 3, and 4) releasing ETs upon stimulation throughout 12 h. (b) Out of six fish tested per treatment, two fish (1 and 2) resulted in a significant response when stimulated with PMA (40 nM) throughout 12 h. Error bars represent s.e.m.  $n = 6$  fish, 3 wells..

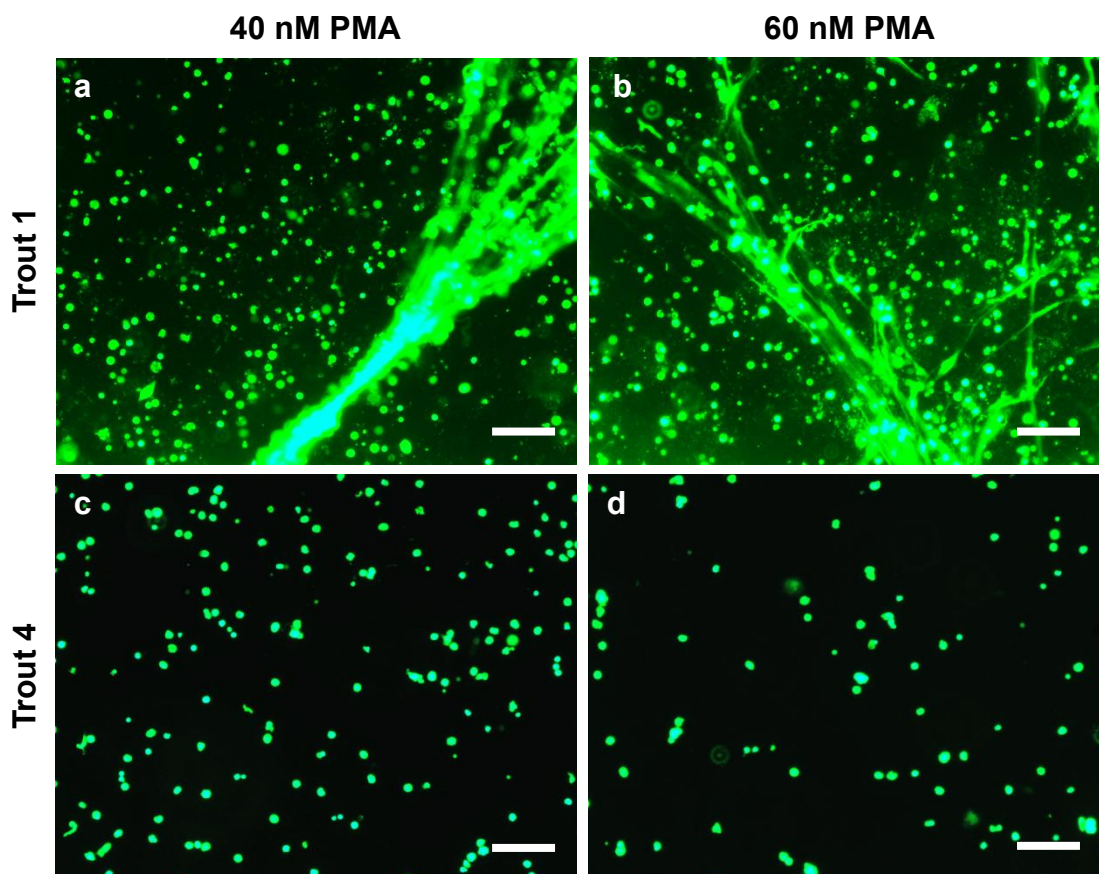


**Figure 3.15.** Representative fluorescence microscopy images of trout PMN-enriched cell suspensions ( $4 \times 10^5$  cells  $\text{mL}^{-1}$ ) isolated from trout numbered in Figure 3.14b, stained with  $5 \mu\text{M}$  SYTOX Green ( $5 \mu\text{M}$ , 5 min, room temperature) after exposure to PMA at 40 or 60 nM for 9 h at  $15^\circ\text{C}$ . These images demonstrate that different fish have a different ET release response when exposed to the same concentration of PMA. (a) Trout number 4 exposed to 40 nM PMA or (b) 60 nM PMA resulting in ET release; (c) Trout number 1 (in relation to Figure 3.14b) exposed to 40 nM PMA (d) 60 nM PMA. Scale bar =  $100 \mu\text{m}$

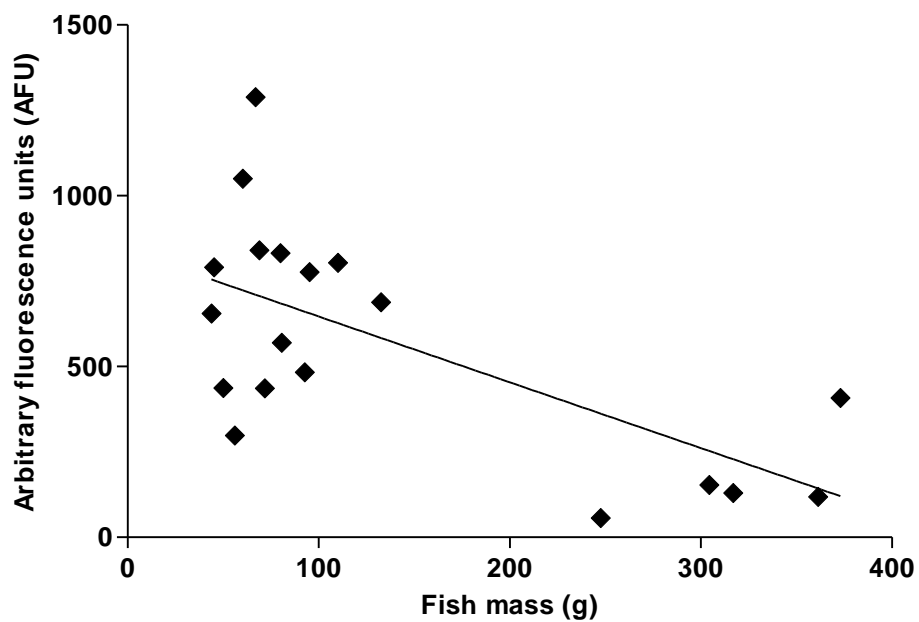


**Figure 3.16.** Scatterplot showing the relationship between trout mass against spontaneous ET release from trout PMN-enriched cell suspensions ( $4 \times 10^5$  cells  $\text{mL}^{-1}$ ) incubated for 1 h at  $15^\circ\text{C}$ , then stained with SYTOX Green ( $5 \mu\text{M}$ , 5 min, room temperature). These data show a significant negative correlation of fluorescence (attributable to ETs), with fish of greater wet mass having lower spontaneous ET release ( $R^2 = 0.4388$ ;  $F_{1,17} = 13.29$ ;  $p < 0.01$ ).  $n = 19$  trout, weighing 43.8 – 373.0 g.

### 3.4. Discussion

This chapter describes for the first time the release of ETs from rainbow trout PMNs *in vitro*. The ET-like structures released spontaneously from PMN-enriched cell suspensions, which stained positively with SYTOX Green in Chapter 2 (Section 2.3.5), were confirmed to be extracellular nucleic acid as these were digested successfully with DNase-I. Crucially, co-localisation of DAPI-stained DNA in the ET-like structures with probes designed to detect three proteins known to be characteristic and diagnostic of ETs, specifically  $\alpha$ -MPO,  $\alpha$ -NE, and  $\alpha$ -H2A, confirmed the presence of ETs in the trout PMN-enriched cell suspensions, also indicating that PMN (neutrophils) are responsible for releasing the ETs. The release of ETs was induced by Cal, flagellin, and PMA, and inhibited by Cyto D, which are known to stimulate and inhibit this process in a similar way in fish and mammals. Unexpectedly, DPI appeared to induce ET release rather than inhibit it.

ET-like structures were observed to be spontaneously released by PMN-enriched cell suspensions, while these were not observed from erythrocyte suspensions isolated from the same tissue (head kidney) using the same method (Percoll gradient), indicating that the ET-like structures are not artefacts of the tissue or the cell isolation and culture methods. Then the ET-like structures were confirmed to be composed of nucleic acids, as they were susceptible to degradation by DNase-I and staining by DNA-intercalating dyes. Additionally, the co-localisation of histones with MPO and NE (PMN-specific granule proteins), satisfies the diagnostic definition of an ET (Brinkmann *et al.*, 2004; Fuchs *et al.*, 2007; Brinkmann and Zychlinsky, 2012; Brinkmann, Goosmann, *et al.*, 2012). All three primary antibodies used in this present study were raised against human immunogens and showed cross-reactivity with rainbow trout MPO, NE, and histone H2A. However, unexpectedly high concentrations of primary antibodies against MPO and NE were required to detect these markers in trout (both used at 1:20 dilution) in comparison to histone H2A (used at 1:200), suggesting that there is greater structural conservation between fish and human histones than between fish and human MPO and NE. More than any other cell type in fish, NE is most heavily expressed in PMNs, and the collective localisation of NE and MPO with extracellular DNA suggests PMNs to be the cell type from where the DNA was most likely released (Wernersson *et al.*, 2006; Papayannopoulos *et al.*, 2010; Metzler *et al.*, 2011; Brinkmann and Zychlinsky, 2012; Havixbeck *et al.*, 2015; Okada, 2017). Furthermore, this is the first time MPO, NE and histone antibody markers of ETs have been used collectively to diagnostically confirm the ETs in a fish species (Table 1.2).

Earlier studies of ETosis in fish did not report the testing of DPI as an ET inhibitor and instead used actin polymerisation inhibitors such as cytochalasin B (Palić, Ostojić, *et al.*, 2007). The use of cytochalasins has been successful for inhibiting induced-ET release in many vertebrate and invertebrate species, and are understood to work by inhibiting the cytoskeleton



remodelling which is a prerequisite to ET release (Palić, Andreasen, *et al.*, 2007; Neeli *et al.*, 2009; Robb *et al.*, 2014; Uchiyama *et al.*, 2015). In human neutrophils, there is contradictory evidence regarding the ability of cytochalasins to inhibit ET release from PMNs (Neeli *et al.*, 2009; Riyapa *et al.*, 2012). While cytochalasin B and D were shown to reduce ET release at 10  $\mu\text{M}$  (Neeli *et al.*, 2009; Palmer *et al.*, 2012), conflicting studies in humans have described similar concentrations of cytochalasin D (10 – 20  $\mu\text{M}$  / 5.26 – 10.52  $\mu\text{g mL}^{-1}$ ) that failed to block PMA-induced ETosis (Riyapa *et al.*, 2012). It is likely that inhibition of ET release with cytochalasin D in trout was successful as it targets one of the final steps of ET release, cytoskeleton remodelling, which leads to release of an ET. Conversely, the effect of DPI on inhibiting NADPH oxidase activity to inhibit ET release lies upstream of the cytoskeletal changes required to release ETs.

PMA is understood to induce ET release by activating protein kinase C (PKC), which then promotes formation of an active NADPH oxidase complex responsible for generating intracellular ROS, leading to ET release (Doussiere *et al.*, 1992; Gray *et al.*, 2013). DPI is able to inhibit ET release by binding to NADPH oxidase subunits and preventing electron flow leading to ROS production (Doussiere *et al.*, 1992). It is uncertain why DPI induced ET release in only four of the six trout examined, and why PMA shows such subtle ET inducing capacity in two of the six trout examined. The use of DPI to inhibit ET release in fish species was only described in one study with carp (Pijanowski *et al.*, 2013), while DPI is a potent inhibitor of NADPH-oxidase-dependent ET release in both mammals and invertebrates (Poirier *et al.*, 2014; Robb *et al.*, 2014; Reichel *et al.*, 2015; Ostafin *et al.*, 2016). This is inconsistent with the results from trout, as DPI alone resulted in a positive effect on ET release (Figure 3.8). One explanation as to why DPI was unable to inhibit ET release in trout could be that the mechanism controlling ET release is less dependent on NADPH-oxidase activity and ROS signalling. In support of this notion, PMA (a potent inducer in mammalian systems) was also only a weak inducer of ET release, while Cal resulted in a strong and rapid ET release response in all trout tested (Appendix Figure 7). Furthermore, Cal successfully induced ET release in all trout and is known to induce ET release by generating ROS through an NADPH oxidase-independent system (Parker, Dragunow, *et al.*, 2012; Arai *et al.*, 2014; Douda *et al.*, 2015). Furthermore, studies of vertebrate PMNs and invertebrate haemocytes found PMA to be a potent inducer of ET release, with the exception of oysters (Poirier *et al.*, 2014; Robb *et al.*, 2014), and therefore it was surprising to find PMA showing little activity against trout PMNs. The current data suggest that the mechanism mediating ET release in trout may be less dependent on NADPH-oxidase activity.

The unexpected DPI-induced ET release remains unexplained, but it could be due to DPI exerting stress on the cell. To support this, there was an indication of weak cytotoxic activity by DPI at 10  $\mu\text{M}$  or greater (data not shown). DPI at 10  $\mu\text{M}$  is known to target several

flavoenzymes in humans in addition to NADPH oxidase, and impairs the activity of NADP-dependent enzymes. One consequence of this is the inhibition of the pentose phosphate pathway, which is one of the main antioxidant pathways operating in most cells (Riganti *et al.*, 2004; Aldieri *et al.*, 2008). Reduced intracellular antioxidant activity can lead to an overall increase in oxidative stress, which may explain a source for the stress that may lead to ET release in trout PMN-enriched cell suspensions. Further research is required to confirm whether DPI is successful in inhibiting NADPH oxidase in trout, or instead produces a greater overall oxidative stress on the trout cell that leads to the induction of ET release.

The use of biological inducers of ET release in fish (such as LPS in carp and flatfish) have been demonstrated to be more potent at inducing ET release compared to chemical inducers (Pijanowski *et al.*, 2013, 2015; Chi *et al.*, 2015; Zhao *et al.*, 2017). However, biological compounds were used with caution in this present study as many studies have used SYTOX Green fluorescence as a measurement of ET release, but have not openly addressed or reported mitigation for the potential of additional fluorescence signals deriving from abundant nucleic acid contamination in some biological compound preparations (Jeffery *et al.*, 2016). In instance, LPS was shown to induce ET release in carp at 50 µg mL<sup>-1</sup>; however, there was a signal from the nucleic acid contaminants within LPS that may have indicated greater ET release (Pijanowski *et al.*, 2015). A strong positive correlation was found with LPS concentration and SYTOX Green fluorescence (Appendix Figure 4); thus, a purer form of LPS was tested (pLPS, purified by ion exchange chromatography) for its capability to induce ET release from trout PMNs. pLPS was demonstrated to not fluoresce after exposure to SYTOX Green (Appendix Figure 3), though ETs were not observed to be released upon exposure and incubation with trout (present study) or carp PMNs, suggesting pLPS is unable to induce a response in carp and trout (Pijanowski *et al.*, 2015). The lack of ET release in response to pLPS could be due to the lack of TLR4 response, the receptor that recognises LPS as a PAMP in trout (Sepulcre *et al.*, 2009).

Recombinant flagellin from *Yersinia ruckeri* was a potent inducer of ET release from trout PMNs. Flagellin is a TLR-5 activator in humans and can induce the expression of many pro-inflammatory genes in the rainbow trout, including IL-6, IL-8 and TNF-α isoform (Wangkahart *et al.*, 2016), and therefore known to be an immunostimulatory compound. Additionally, the trout PMN-enriched cell suspensions released ETs which appeared to clump significantly due to the flagellin. Thus, a flagellin dose response may clarify if flagellin truly induces an ET-release response from these cells. Using whole heat-inactivated *V. anguillarum* (a Gram-negative fish pathogen) failed to induce ET release from trout PMN-enriched cell suspensions. Perhaps the heat-inactivation process (albeit only for 25 min at 60°C) denatures the epitopes to an extent dulls recognition by TLRs on trout PMNs, which are then unable to induce ET release. Thus, inactivation by other methods such as UV-radiation may be a more suitable

option to inactivate bacteria before testing as an ET inducer. However, live *V. anguillarum* (Vib 87) was unable to induce ET release from trout PMN-enriched cell suspensions (data not shown).

The level of ET release by PMNs isolated from individual trout upon exposure to PMA (40 nM or greater) and DPI (25  $\mu$ M) remained the same over time per individual despite non-repeated measures, indicating individual responders and non-responders (Figure 3.14). Conversely, exposure to Cal (1  $\mu$ g mL<sup>-1</sup> or greater) resulted in the most reproducible ET release response, as PMN-enriched cell suspensions was observed from all individuals (Appendix Figure 7). This is an interesting finding because it suggests that some individual trout have a predisposition to release ETs in response to PMA or DPI. Individual responses have been previously suspected and observed in humans (Fuchs *et al.*, 2007; Maini *et al.*, 2016) and dogs (Jeffery *et al.*, 2015), though all the individuals (humans and dogs) were shown to release ETs at different levels and did not find any individuals which did not respond to inducers of ET release. Conversely, there have been no previous reports with respect to a fish species. The challenge of collecting adequate cells (such as PMNs) from small animals often results in pooling of samples, thus limiting the possibility to study individual responses (Palić, Ostojić, *et al.*, 2007; Chi *et al.*, 2015; Masterman, 2016; Zhao *et al.*, 2017). One explanation for the unexpected response to PMA or DPI is that the cell culture conditions were not adequate to elicit a response to PMA or DPI-induced ET release (or inhibition). In instance, studies in humans have found that neutrophils can be primed with cytokines to be more responsive to compounds which induce ET release (Clark *et al.*, 2007), indicating that co-stimulatory factors may be important to enhance the ET release response. This co-stimulation of ET release by PMNs in fish with cytokines has not been identified and warrants further research.

The variation of spontaneous ET release observed from the 19 trout (siblings) suggests that PMNs isolated from fish with lower mass are more likely to release ETs spontaneously, and these results were also reflected in 10 diploid and 10 triploid Atlantic salmon that were examined. Indeed, Atlantic salmon also showed strikingly large variation in spontaneous ET release, with respect to diploid and triploid fish (Appendix 1.4). The cause of such variation in spontaneous ET release observed from trout and salmon remains unclear. The genetic contribution to this variation may be limited as these trout and salmon sourced suppliers were hatched in the same batch of eggs and are therefore genetically siblings. Collectively, the reported spontaneous release of ETs from individual fish within this Chapter needs to be considered for future research.

In summary, this chapter presented evidence that trout PMNs release ETs that resemble ETs released by other organisms. Additionally, compounds were identified that induce and inhibit

ETs release by trout PMN-enriched cell suspensions, and some of these compounds showed a similar effect on ET release in other vertebrate and invertebrate organisms. As ETs are antimicrobial defences, it will be intriguing to see whether bacterial pathogens of trout have virulence mechanisms that enable them to counteract the effect of ETs, and this subject was the focus of Chapter 4.

## Chapter 4: Extracellular nuclease activity of *Vibrio anguillarum*

### 4.1. Introduction

Nucleases are a diverse group of enzymes and catalytic RNA (ribozymes) which cleave phosphodiester bonds of nucleic acids. They are involved in various biological processes, including genome maintenance and repair, recombination, regulating genetic transformation, regulating apoptosis (Minion *et al.*, 1986; Nishino *et al.*, 2002; Ambur *et al.*, 2009; Lenhart *et al.*, 2012). Different roles of the nuclease leads to unique structure, properties, and distribution of the enzyme (Pohl *et al.*, 1982). Depending on their roles, nucleases such as the intracellular zinc-finger nucleases may have 5'-3' exo- and endonuclease activity in the case of removing RNA primers during DNA replication, or 3'-5' exonuclease activity in the case of genomic proofreading (Yang, 2011). Some nucleases show substrate specificity which can be divided into DNase or RNase, yet there are many nucleases which are sugar non-specific which cleave both DNA and RNA, such as *Vibrio cholerae* periplasmic nuclease Vvn (Hsia *et al.*, 2005). Furthermore, most nucleases can cleave nucleic acid whether single- or double-stranded (Li *et al.*, 2003; Yang, 2011; Dang *et al.*, 2016), though there are some nucleases in the S1 nuclease of *Aspergillus oryzae* which prefer single-stranded substrates (Desai *et al.*, 2003). Membrane-bound nucleases of *Streptococcus pneumoniae* are known to regulate their ability to uptake DNA from outside the cell for transformation (Puyet *et al.*, 1990). Some extracellular nucleases from *Vibrio cholerae* (*dns* and *xds*) are over or under expressed to switch between states of high and low transformation frequency in response to different bacterial cell densities (Blokesch *et al.*, 2008).

The advantage of extracellular nucleases in bacteria has remained unclear for decades (Sumbly *et al.*, 2005). One hypothesis is that these nucleases played a role in freeing up nucleotides from extracellular DNA to be utilised as a nutrient source, or recycling DNA from necrotic cells (Mitchell *et al.*, 1977). This feature is demonstrated by *Mycoplasma spp.* which can degrade DNA polymers and absorb free nucleotides and nucleosides from the environment as a nutrient, as they lack the biosynthetic capacity for *de novo* synthesis of nitrogenous bases (McIvor *et al.*, 1978; Minion *et al.*, 1986). In marine and freshwater environments where dissolved DNA is ubiquitous (ranging from 4.03  $\mu\text{g mL}^{-1}$  to 871  $\mu\text{g mL}^{-1}$ ), it is likely that it is utilised by many microbes (Karl *et al.*, 1989). However, given the recent research within the microbial interactions with ETs, the role of microbial extracellular nucleases has been linked to combating trapping by ETs (Ferrieri *et al.*, 1980; Singer *et al.*, 1992; Pinchuk *et al.*, 2008; Wang *et al.*, 2009; Seper *et al.*, 2011).

Several respiratory pathogens such as *S. pneumoniae* and *Staphylococcus aureus* require extracellular nuclease activity to establish successful infections and evade ETs (Sumbly *et al.*,

2005; Buchanan *et al.*, 2006; Thammavongsa *et al.*, 2013). Within the *Vibrio* spp., nuclease inactivity of *V. cholerae*, and the two extracellular nucleases *dns* and *xds*, can degrade ETs released by human neutrophils, and regulate bacterial transformation (Blokesch *et al.*, 2008; Seper *et al.*, 2013).

One of the most prevalent diseases in finfish aquaculture, vibriosis, is caused by *Vibrio anguillarum*, and these bacteria are detected abundantly in the fish skin mucus (Carda-Diéguez *et al.*, 2017). The life cycle of *V. anguillarum* can be divided into the free-living non-obligate stage (i.e. on surfaces, sediment, or in water), and a pathogenic or infectious stage (Frans *et al.*, 2011). Whole genome sequencing and preliminary phenotype studies have revealed *V. anguillarum* to possess at least one extracellular nuclease and one membrane-associated nuclease (Austin *et al.*, 1995; Naka *et al.*, 2011; Hickey *et al.*, 2017). However, there is relatively little understanding of the roles and enzyme activities of these *V. anguillarum* nucleases (Maeda *et al.*, 1976). Furthermore, most isolates of *V. anguillarum* express extracellular nucleases, and some are inferred by their DNA sequence to be membrane-bound or associated (Muroga, 1985; Focareta, 1989; Austin *et al.*, 1995; Li *et al.*, 2003; Blokesch *et al.*, 2008; Frans *et al.*, 2011; Seper *et al.*, 2013; Hickey *et al.*, 2017). Though the role of extracellular nuclease in *V. anguillarum* remains unclear, some studies of closely related species suggest that *V. anguillarum* may also utilise the enzyme to generate nucleotide or phosphate pools from extracellular DNA during its free-living stage for nutrients (Blokesch *et al.*, 2008; McDonough *et al.*, 2016). During the infectious stage of the lifecycle, *V. anguillarum* upregulates expression of genes which promote survival within the host. For example, extracellular metalloproteases and mucinase activity are known to be upregulated which promotes mucus degradation, and infection through mucosal surfaces (Norqvist *et al.*, 1990).

The primary point of entry of *V. anguillarum* during the infection stage is still debated, but there is evidence suggesting that the bacteria can enter directly through the skin (Norqvist *et al.*, 1990; Hickey *et al.*, 2017). Skin mucus serves as a protective barrier to infections; however, *V. anguillarum* nucleases may assist in the thinning of mucus viscosity by digestion of DNA. Proteases, exopolysaccharides and flagellin expressed by *V. anguillarum* collectively promote the binding of this bacterium to fish skin mucus (Croxatto *et al.*, 2007; Frans *et al.*, 2011; Benhamed *et al.*, 2014). As a result, infection of the fish may occur through damaged or weakened skin, whereby these virulence factors assist in attachment, and tunnelling through the mucus barrier and skin to infect the host (Norqvist *et al.*, 1990; Milton *et al.*, 1996; Hickey *et al.*, 2017). Still, other researchers suggest that *V. anguillarum* infects the host through the mucosal surfaces of the gastrointestinal tract and gills (Lumsden *et al.*, 1994; Frans *et al.*, 2011). Mucus harbours a collection of glycoproteins (such as mucin), as well as DNA polymers, and studies of human cystic fibrosis patients have indicated that the integrity of the DNA present in mucus in the lungs contributes to its rheology (Shak *et al.*, 1990; Shah *et al.*,

1996), suggesting that nucleases produced by bacteria could reduce the viscosity of the mucus through degradation of the DNA polymers. Thus, this could be an important mechanism that compromises mucosal barriers, such as on fish skin and in the gastrointestinal tract, allowing easier access of pathogens to the skin to initiate an infection.

Bacteria can escape ETs released by human neutrophils by degrading the DNA polymers with extracellular nucleases (Sumbly *et al.*, 2005; Beiter *et al.*, 2006; Juneau *et al.*, 2015). Evidence that nuclease-producing strains or isolates of *V. anguillarum* grow better in the presence of DNA, and the presence of DNA-uptake machinery such as type IV pili and membrane ATPase (Frans *et al.*, 2011, 2013; Seitz *et al.*, 2013), support the possibility that *V. anguillarum* may also use nucleases to assist in infection, growth, or survival following successful infection of the host (McDonough *et al.*, 2016). Nevertheless, few studies have implicated a role for bacterial nucleases in establishing infection within fish, though it is likely that nucleases might contribute to degrading chromatin ETs (Seper *et al.*, 2013; de Buhr *et al.*, 2015; Storisteanu *et al.*, 2017).

There are limited studies surrounding *V. anguillarum* extracellular nucleases, and their roles are poorly understood. Additionally, few studies have investigated the physicochemical conditions under which nuclease activity is greatest, or if these enzymes may play a role in virulence (Maeda *et al.*, 1976). The thermostability of nucleases is typically less than 41°C (Lodish *et al.*, 2000); however, some nucleases present in foetal calf serum, or bacterial species adapted to extreme conditions have thermostable secondary structures which allow their catalytic activity to persist in greater temperatures (Kauzmann, 1959; Napirei *et al.*, 2009; von Köckritz-Blickwede *et al.*, 2009; Kiedrowski *et al.*, 2014; Juneau *et al.*, 2015). As well as exposure to absolute temperature, enzymes in solution lose activity after undergoing freeze-thaw cycles, due to ice-induced partial unfolding of proteins (Cao *et al.*, 2003). Additionally, enzymatic function is influenced by the pH and salinity of the solution it is suspended in, as these physicochemical parameters also disrupt the bonds responsible for the secondary structure of the protein (Lodish *et al.*, 2000). Specifically to nucleases (including DNase-I), catalytic activity is limited by the availability of cations such as Ca<sup>2+</sup> and Mg<sup>2+</sup> (Cuatrecasas *et al.*, 1967; Frank *et al.*, 1975; Moore, 1981; Yang, 2011). Ion-chelating agents, like the aminopolycarboxylic acids such as ethylenediaminetetraacetic acid (EDTA) can limit the free divalent cations required for the catalytic activity of some nucleases (Moore, 1981). As the environmental conditions that result in greatest nuclease activity can vary depending on the enzyme (Pohl *et al.*, 1982), testing the nuclease activity of a range of environmental conditions (i.e. different temperature, pH, NaCl concentration, and cation availability) may provide a better understanding of *V. anguillarum* nucleases and the conditions under which they exhibit greatest activity. In turn, this may give insight into the conditions where the bacterium is

utilising the nucleases. Testing the activity of nucleases in different environmental conditions requires a reliable method to measure nuclease activity.

Different methods have been established to measure the nuclease activity within solutions, including spectrophotometry and fluorimetry which measures the fluorescence emitted from intact DNA content after degradation with nuclease; electrophoresis, which compares DNA fragment size after degradation with nuclease; or a semi-quantitative method which examines digestion of deoxyribonuclease (DNase) agar (Kunitz, 1950). In the latter, DNase agar contains DNA that can be hydrolysed by nuclease in a test solution, and this is indicated by clear zones forming in the otherwise opaque agar after addition of hydrochloric acid. The size of the clear zones correlates directly with nuclease activity, thus providing a useful metric for nuclease activity (Ferrieri *et al.*, 1980; Macanovic *et al.*, 1997). Prior to using the DNase agar assay to screen solutions or bacteria colonies for nuclease activity, it is necessary to determine sensitivity (i.e., the lowest detectable activity) and the reproducibility of the assay (i.e., variation between repeated assays), and confirm the range of activities for which a linear relationship exists between nuclease activity and clear zone area.

The aim of this Chapter is to investigate if the extracellular nuclease activity produced by the fish pathogen *V. anguillarum* has a potential role as an infection or virulence factor through DNA degradation. To achieve this, a simple quantitative assay that measures the clear zone areas of DNase agar was used to screen for relative nuclease activity from a collection of *V. anguillarum* isolates. A comparison of clear zone area with known concentrations of recombinant human DNase-I enzyme was performed to confirm if this method was suitable for assessing the relative nuclease activity of unknown solutions (i.e., nucleases present in culture filtrates of *V. anguillarum*). *V. anguillarum* cells were separated from the culture filtrate and nuclease activity within this filtrate was measured to determine if extracellular nucleases were produced. Then, extracellular nuclease activity detected in the *V. anguillarum* culture filtrate was examined under a range of environmental conditions, and to see if nuclease activity was conserved after numerous freeze-thaw cycles. Finally, the functional activity of the bacterial culture filtrate was examined for the ability to degrade DNA from trout PMNs in the form of ETs, or DNA within the skin mucus. Collectively, these data may provide a better understanding of *V. anguillarum*, and if they can utilise extracellular nucleases to assist in establishing infection in fish.



## 4.2. Materials and Methods

### 4.2.1. Bacterial culture and confirmation of nuclease activity of *Vibrio anguillarum* isolates

*V. anguillarum* (Vib 6 and Vib 87) and *Yersinia ruckeri* (YR 1) isolates (Table 4.1) were stored and cultured according to Section 3.2.6. Tryptone soy agar and broth (TSA/TSB; Thermofisher Scientific, Loughborough, UK) were made up according to manufacturer's instructions, and supplemented with 1.5% NaCl to make a final concentration of 2% NaCl when culturing *V. anguillarum*. Bacterial CFU mL<sup>-1</sup> was estimated with a spectrophotometer (CE 2041, Cecil Instruments Ltd, Cambridge, UK) by absorbance at 600 nm wavelength ( $A_{600}$ ), using PBS as a blank reference. Bacterial suspensions were diluted with PBS to desired concentrations in CFU mL<sup>-1</sup> derived from a standard curve (Appendix Figure 9) and CFU mL<sup>-1</sup> confirmed by plating onto appropriate agar in quadruplicate after serial dilution in a round-bottomed 96-well plate (Sarstedt, Nümbrecht, Germany).

A collection of *V. anguillarum* isolates (Appendix Figure 1) have been previously screened for relative nuclease activity from using a similar quantitative DNase agar digestion method according to Section 4.2.2 below (Appendix Figure 10). Most of the *V. anguillarum* isolates gave detectable clearance zones on DNase agar, isolate *V. anguillarum* Vib 87 showed no detectable nuclease activity, while Vib 6 was as a strong nuclease producer (Appendix Figure 10). The measurement of relative nuclease activity from *V. anguillarum* Vib 87 and Vib 6 was again repeated to confirmation the previous observation from the larger screen. Cultures of Vib 87 and Vib 6 were freshly isolated and cultured to late-exponential phase, then corrected with PBS to  $A_{600}$ : 0.7. Five microliters of the Vib 87 and Vib 6 suspension (isolated as described above) was assayed for nuclease activity in triplicate at 24 h at 22°C according to Section 4.2.2. As a negative control for a flagellated strain of bacteria known not to show nuclease activity, and a non-*V. anguillarum* bacterial species, the fish pathogen *Y. ruckeri* (YR 1) was used in addition to *V. anguillarum*.

**Table 4.1.** Table showing the bacterial isolates/strains used in this Chapter. All isolates/strains were stored at -70°C before isolating for experiments as described in Section 4.2.1.

Isolate/Strain	Characteristic	Culture media <sup>a</sup>	Culture temperature	Pathogenicity <sup>b</sup>	Nuclease production	Reference
<b><i>Vibrio anguillarum</i></b>						
Vib 6 (ATCC 43310)	Wild type isolated from <i>Gadus mouhua</i>	TSA/TSB 2% NaCl	22°C	+	+	(Austin <i>et al.</i> , 1995)
Vib 87 (NCIMB 1873)	Wild type isolated from <i>Salmo salar</i> , UK	TSA/TSB 2% NaCl	22°C	+ (weak)	-	(Austin <i>et al.</i> , 1995)
NB 10	Wild type Sweden	TSA/TSB 2% NaCl	22°C	+	+	(Norqvist, 1989)
<b><i>Yersinia ruckeri</i></b>						
YR 1	Wild type isolated from <i>O. mykiss</i> , UK	TSA/TSB	22°C	+	-	(Tinsley <i>et al.</i> , 2011)

<sup>a</sup>TSA (Tryptone soy agar), TSB (Tryptone soy broth).  
<sup>b</sup>Pathogenicity was suggested by (Austin *et al.*, 1995).

#### 4.2.2. Quantification of nuclease activity by DNase agar

In the DNase agar digestion assay, the relationship between clear zone area and nuclease activity needed to be described to confirm that the clear zone area was proportional to the quantity of nuclease activity. To determine the relationship between the clear zone area on the DNase agar to give an indication of relative nuclease activity, 15 mL of DNase agar (prepared according to manufacturer's instructions) was poured into each 9-cm diameter petri dish. The DNase agar formulation, volume, and thickness were kept as uniform as possible to minimise the variability in the agar hydrolysis, then allowed to dry overnight at room temperature. DNase agar plates were always used within four days to minimise any variations in zone size caused by alterations in agar moisture content. Solutions of DNase-I (Thermofisher Scientific, Loughborough, UK) were prepared in DNase buffer (final well concentration of 10 mM Tris-HCl, 2.5 mM MgCl<sub>2</sub>, 0.1 mM CaCl<sub>2</sub>, Thermofisher Scientific, Loughborough, UK) and sterile dH<sub>2</sub>O to 5, 10, 25, 50, 100, 200, 300, 400, 500, and 600 units (U) mL<sup>-1</sup> in sterile Eppendorf tubes. Then, 5 µL of each DNase-I solution was added to 2-mm diameter wells that had been punched into the surface of the agar using a biopsy punch (Stiefel, Brentford, UK). This was repeated on individual wells across three separate DNase agar plates. DNase plates were sealed with Parafilm tape (Bemis, Neenah, USA) to limit evaporation and the plates were incubated upright at room temperature for 24 h before use. To visualise the area of DNase agar that had been digested by nucleases (clear zone area), 5 mL of 1 M hydrochloric acid (HCL; VWR, Radnor, USA) was poured onto the agar surface and incubated for 1 min at room temperature. Relative nuclease activity was quantified by measuring the diameter (*d*) of each clear zone area to the nearest half of a millimetre, such that the clear zone area could be calculated from the mean of the perpendicular diameters (*d*<sup>1</sup> and *d*<sup>2</sup>, Figure 4.1). The formula to calculate 'Clear zone': *Clear zone* =  $\pi r^2$ . The radius (*r*) is calculated from a mean of the two perpendicular diameters, as shown:  $r = \frac{(d^1 + d^2)}{4}$ . The area of the 2-mm diameter well (3.14 mm<sup>2</sup>) was not included in the total clear zone area, and thus subtracted from the 'Total clear zone area', giving the formula:

$$\text{Total clear zone area} = \pi \left( \frac{(d^1 + d^2)}{4} \right)^2 - 3.14$$

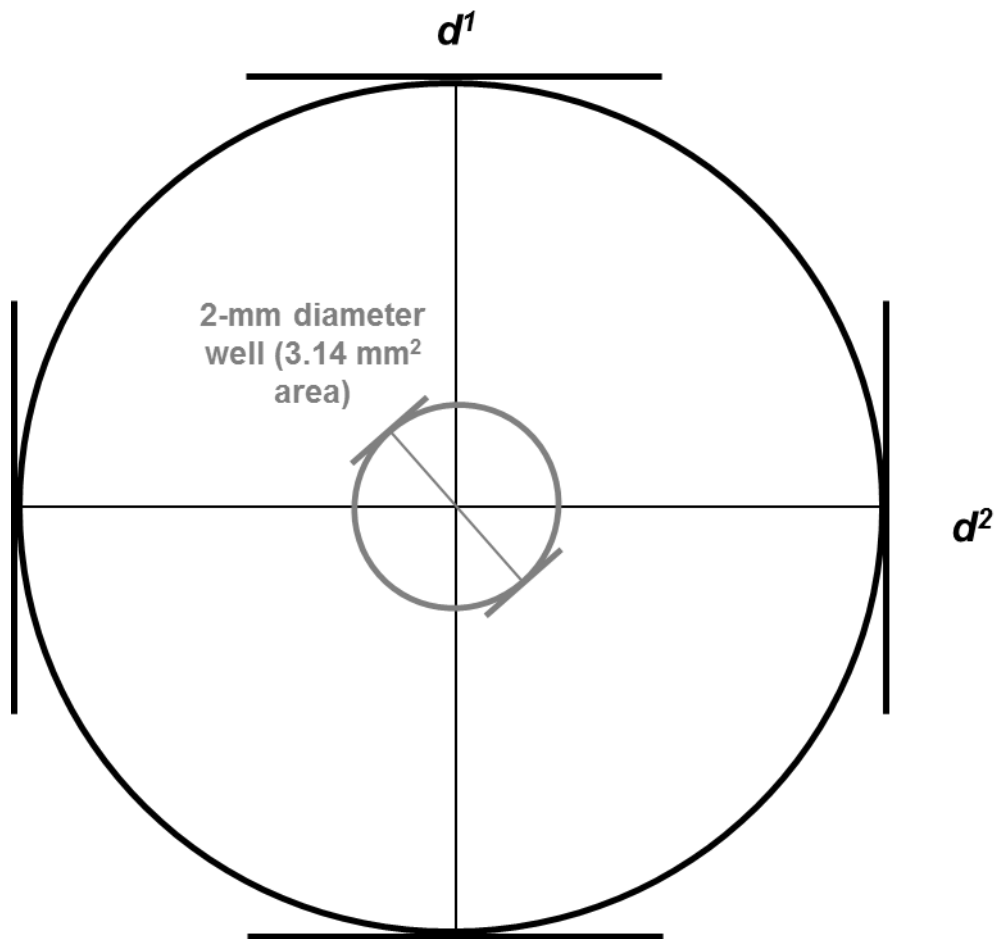


**Figure 4.1.** The total clear zone area after incubation (with the agent being examined for nuclease activity) was calculated from the mean of perpendicular diameters ( $d^1$  and  $d^2$ ) measured after 24 h incubation with at 22°C. The area (3.14 mm<sup>2</sup>) from the 2-mm diameter holes punched in the DNase agar was subtracted from the total clear zone area.

#### **4.2.3. Detection of nuclease activity in cell-free *Vibrio anguillarum* supernatant**

To confirm that *V. anguillarum* Vib 6 showed extracellular nuclease activity, a single colony was cultured to late-exponential phase in TSB 2% NaCl according to Section 4.2.1. Then 5 mL of bacterial suspension was centrifuged (2600 × g, 15 min, 4°C) and the supernatant passed through a 0.22-µm syringe filter (NML syringe filter; Sartorius, Gottingen, Germany) to remove any bacterial cells and debris, before this culture filtrate was collected in a sterile bijoux bottle, collecting approximately 1.2 mL. The sterility of the culture filtrate was confirmed by plating 10 µm across TSA and TSA 2% NaCl and incubating at 22°C for 48 h, and then checking for the absence of bacterial colonies. The nuclease activity present in unconcentrated filtrate may be too weak to form visible clear zones within the DNase agar digestion assay; thus, the culture was concentrated with a rotating vacuum condenser (DNA SpeedVac, Model no: DNA110-240, Savant instruments, Farmingdale, USA). One millilitre of culture filtrate was divided equally between sets of five sterile Eppendorf tubes (per time point), and all the tubes were placed into the rotating vacuum condenser and concentrated for 10, 20, 30, 40, 50, and 60 min, and the rotating vacuum condenser was set to 'medium' (~35°C). After 10 min has elapsed, a group of five tubes were removed from the condenser kept on ice. This was repeated every 10 min until the remaining tubes completed condensing. Each group of culture filtrate was combined back into a single Eppendorf tube, resulting in a single tube per time point. The splitting culture filtrate into smaller volumes was necessary for the rotating vacuum condenser to perform as designed. From here, the nuclease activity of 5 µL of culture filtrate at each time point was measured by the DNase agar assay according to Section 4.2.2, performed in triplicate across three different DNase agar plates

#### **4.2.4. Standardisation of culture filtrate by concentration**

To increase nuclease activity of the culture filtrate, the suspension was concentrated by rotary evaporation. Measuring the relative mass of the culture filtrates before and after evaporation gives an estimation of how much the filtrate was concentrated. *V. anguillarum* culture filtrate was isolated and concentrated with rotary evaporation according to Section 4.2.3, and the differences in mass measured in grams (g) was recorded before and after rotary evaporation (to four decimal places), then used to calculate the 'concentration factor' (*Cf*) shown in (Equation 4.1). *Cf* is a fraction that represents how much the filtrate was concentrated; for example, a *Cf* of 0.2 indicates that the filtrate was concentrated to 20% of its original mass. In simple terms, *Cf* is the concentrated filtrate weight divided by the original filtrate weight before condensing. The *Cf* can be used to dilute/adjust a solution of concentrated filtrate to a new, desired *Cf* value using sterile dH<sub>2</sub>O (Equation 4.3).

$$Cf = \frac{(b - y)}{(a - y)}$$

**Equation 4.1.** Concentration factor (*Cf*) is determined using the equation above. Weight of unconcentrated filtrate in Eppendorf tube (*a*); Weight of concentrated filtrate in Eppendorf tube (*b*); Weight of empty Eppendorf tube (*y*).

The following formula (Equation 4.3) is used to calculate the volume of  $\mu\text{L}$  to add to the sample for dilution to 0.2 concentration factor:

$$v = (0.2 \times B - A) \times 1000$$

**Equation 4.2.** Calculation for the volume required (*T*) to adjust concentration factor of nuclease filtrate to 0.2 using sterile  $\text{dH}_2\text{O}$ . Volume of  $\text{dH}_2\text{O}$  in  $\mu\text{L}$  to add to achieve a desired 0.2 concentration factor (*v*): mass of unconcentrated filtrate without Eppendorf: *A* = (*a* - *y*); mass of concentrated filtrate without Eppendorf: *B* = (*b* - *y*). In this case, a *Cf* of 0.2 would mean the mass is 20% of the original mass. This formula assumes the mass of water is equivalent to the mass of filtrate.

$$v = (0.2 \times B - A) \times 1000$$

**Equation 4.3.** Calculation for the volume required (*T*) to adjust concentration factor of nuclease filtrate to 0.2 using sterile  $\text{dH}_2\text{O}$ . Volume of  $\text{dH}_2\text{O}$  in  $\mu\text{L}$  to add to achieve a desired 0.2 concentration factor (*v*): mass of unconcentrated filtrate without Eppendorf: *A* = (*a* - *y*); mass of concentrated filtrate without Eppendorf: *B* = (*b* - *y*). In this case, a *Cf* of 0.2 would mean the mass is 20% of the original mass. This formula assumes the mass of water is equivalent to the mass of filtrate.

#### **4.2.5. Inhibition of *Vibrio anguillarum* Vib 6 culture filtrate nuclease activity**

To determine if ion-chelating agents that sequester free divalent cations can inhibit the nuclease activity of *V. anguillarum* Vib 6 culture filtrate, the isolate was cultured in broth according to Section 4.2.1., and the filtrate was filtered, condensed, and adjusted to a *Cf* of 0.1 according to Sections 4.2.3 and 4.2.4. The *V. anguillarum* Vib 6 filtrate was mixed 1:1 with EDTA solution (at 2, 20, or 50 mM; Thermofisher Scientific, Loughborough, UK) in an Eppendorf tube (giving final well concentrations of 1, 10, or 25 mM EDTA), resulting in *Cf* of 0.2 final concentration factor before assaying for nuclease activity by DNase agar digestion assay according to Section 4.2.2 for 24 h at 22°C. EDTA was diluted with sterile  $\text{dH}_2\text{O}$ , and a negative control was incubated with sterile  $\text{dH}_2\text{O}$  as a substitute for EDTA. The mixture was

vortexed, centrifuged, and incubated for five min at room temperature before being measured for nuclease activity by the DNase agar digestion assay (Section 4.2.2). This was performed in triplicate across three separate DNase agar plates.

This was repeated in a separate experiment, except a range of DNase-I concentrations was also included to determine the relative nuclease activity of concentrated *V. anguillarum* Vib 6 filtrate (incubated with and without EDTA) in relation to known concentrations of DNase-I. Here, *V. anguillarum* Vib 6 filtrate (Cf: 0.2) was collected and examined for nuclease activity with and without exposure to 25 mM EDTA as above, and DNase-I was prepared according to Section 4.2.2.

#### **4.2.6. Freeze-thaw stability of *Vibrio anguillarum* Vib 6 culture filtrate nuclease activity**

To assess the freeze-thaw activity stability of the extracellular nuclease activity present in the concentrated *V. anguillarum* Vib 6 filtrate (adjusted to Cf: 0.2, and isolated according to Section 4.2.3 and 4.2.4), was split into four Eppendorf tubes (100 µL per tube) representing different treatment groups: negative control (not subjected to freezing, kept on ice during the experiment after isolation), 1x, 2x, and 3x freeze-thaw cycles. The 1x, 2x, and 3x tubes were frozen (-20°C) simultaneously. For the first freeze-thaw cycle, the 3x tube was removed and completely thawed at room temperature. This was repeated two more times to complete the three cycles. All three tubes were removed simultaneously from -20°C, and the nuclease activity was assessed by the DNase agar digestion assay according to Section 4.2.2. Triplicate tubes were prepared per group, and each tube was assayed for nuclease activity three times. Replicates were performed in different DNase agar plates to reduce the effect of plate variation.

#### **4.2.7. Assaying stability of *Vibrio anguillarum* Vib 6 culture filtrate nuclease activity in different temperature, pH and NaCl concentration**

To assess the stability of nuclease activity in *V. anguillarum* Vib 6 culture filtrates in a range of temperatures over 60 min, condensed *V. anguillarum* Vib 6 filtrate (isolated and concentrated to Cf: 0.2 according to Section 4.2.3 and 4.2.4), were divided into six treatment groups (incubation at 4, 15, 28, 37, 50, and 60°C) into Eppendorf tubes (100 µL per tube) for each time point (10, 20, 30, 40, 50, and 60 min). All tubes of *V. anguillarum* Vib 6 filtrate were simultaneously incubated in heat blocks for 60 min, removing one set every 10 min, and kept on ice until all were removed after 60 min. The relative nuclease activity was determined according to Section 4.2.2. Each time point, and temperature were performed in triplicate across different DNase agar plates.

The effect of pH and NaCl concentration on *V. anguillarum* Vib 6 nuclease activity present in the filtrate or from the whole bacteria was assayed by supplementing the DNase agar with acid (HCl), base (NaOH), or salt (NaCl) before sterilisation by autoclaving. Nuclease activity from the bacteria (*V. anguillarum* Vib 6) was also assessed in addition to the filtrate, to determine the difference of activity between the filtrate and the whole bacteria. *V. anguillarum* Vib 6 cultures were cultured, washed, and adjusted to  $A_{600}$ : 1.6 according to Section 3.2.6. To adjust the pH of DNase agar, a magnetic bead was placed in the dissolved agar to stir the agar while titrating with 1 M NaOH or 1 M HCl to achieve the desired pH (6.5, 7, 7.5, 8, 8.5, 9, 9.5, 10, 10.5, and 11). The pH of the DNase agar was measured with a pH probe. NaCl was used to adjust the salinity of the DNase agar to 0.5 (negative control), 1, 1.5, 2, 2.5, 3, 3.5, and 4% final well concentration (stock DNase agar is formulated with 0.5% NaCl). The agar was prepared according to Section 4.2.2, and *V. anguillarum* Vib 6 was cultured according to Section 3.2.5., and culture filtrate was isolated and condensed to *Cf*: 0.2 according to Section 4.2.3 and 4.2.4. Five microliters of the *V. anguillarum* Vib 6 filtrate, or bacterial solution ( $A_{600}$ : 0.7), was assayed for clear zones by the DNase agar digestion assay using the modified DNase agar (for pH or NaCl concentration), incubating for 24 h at 22°C. Each treatment was replicated in single wells across three different DNase agar plates for the pH experiment, while the NaCl concentration experiment was replicated in single wells across six plates, and the clear zone area representing nuclease activity of the filtrate or the bacteria was measured according to Section 4.2.2.

#### **4.2.8. Investigating the production of extracellular nuclease during *Vibrio anguillarum* Vib 6 growth**

To determine if *V. anguillarum* Vib 6 is constitutively expressing extracellular nuclease, the nuclease activity of the filtrate was measured during the culture of *V. anguillarum* Vib 6. *V. anguillarum* Vib 6 was inoculated and cultured overnight in a universal tube containing 5 mL of TSB 2% NaCl at 22°C shaking at 150 RPM. The culture was washed by transferring to a 15-mL Falcon tube and pelleting the bacteria (2600 × g, 10 min, 4°C), then discarding the supernatant and resuspending the pellet in 5 mL of PBS, repeating the wash for a total of three times. The washed culture was corrected to the  $A_{600}$ : 0.8 with PBS, equating to approximately  $10^9$  CFU mL<sup>-1</sup> according to *V. anguillarum* Vib 6 standard curve formula ( $y = 2.83 \times 10^9x - 6.64 \times 10^8$ ; Appendix Figure 4.2). TSB 2% NaCl was fully dissolved in dH<sub>2</sub>O before separating into a sterile 500-mL conical flask. Non-absorbent cotton wool was placed in the top of the flask and covered with aluminium foil before autoclaving for sterilisation. One millilitre of the culture of *V. anguillarum* Vib 6 was inoculated into a 500-mL conical flask containing 200 mL TSB 2% NaCl aliquot, and cotton wool was placed back on. A single negative control flask containing 200 mL of TSB 2% NaCl was inoculated with 1 mL of PBS



(that was also used to correct the *V. anguillarum* Vib 6 suspension), while the *V. anguillarum* Vib 6-inoculated flasks were performed in quadruplicate. The flasks were mixed thoroughly by swirling. The bacterial culture was sampled from the flask at 60 min intervals as above and continued until optical density plateaued (indicating that culture has reached stationary phase of growth). The culture was sampled using a sterile 10-mL pipette, whereby 5 mL of culture was taken and transferred into a sterile Bijoux bottle. The cotton wool was placed straight back into flask as soon as culture was removed and returned to the orbital shaker at 150 RPM, 22°C.

From the 5 mL sampled culture, 1 mL was used to record the growth of the culture by measuring  $A_{600}$  against TSB 2% NaCl as the blank. The remaining 4 mL of the *V. anguillarum* Vib 6 suspension was transferred into a 15-mL Falcon tube, and centrifuged ( $2600 \times g$ , 10 min, 4°C). Approximately 500 – 700  $\mu\text{L}$  was filtered through 0.22- $\mu\text{m}$  syringe filter into a pre-weighed (to nearest 1/10000 of a gram) sterile Eppendorf tube. The bacterial filtrate in Eppendorf tubes was weighed before freezing at -20°C for storage. The filtrates were thawed at room temperature before condensing by rotary evaporation and corrected to Cf: 0.2 according to Section 4.2.4, then the nuclease activity was measured by clear zone area in triplicate as described in Section 4.2.2. The mean nuclease activity present in the filtrate was expressed on a scatter graph to demonstrate the relationship with the mean  $A_{600}$  of *V. anguillarum* Vib 6 (indicating bacterial growth). To demonstrate the clear zone area (*i.e.*, nuclease activity) per  $A_{600}$ , the mean clear zone area from the 4 biological replicates was divided by the mean  $A_{600}$  of the bacterial culture.

#### **4.2.9. Investigating if *Vibrio anguillarum* Vib 6 culture filtrate can degrade ETs released by rainbow trout PMNs**

To determine if the extracellular nuclease produced by *V. anguillarum* Vib 6 exhibits a dose-dependent ability to degrade ETs produced from trout polymorphonuclear (PMN) cells, rainbow trout PMN-enriched cell suspensions isolated by the triple-layer discontinuous Percoll gradient method (Section 2.2.3), were stimulated to release ETs *in vitro* with 10  $\mu\text{L}$  of calcium ionophore A23187 (Cal; Thermofisher Scientific, Loughborough, UK; 5  $\mu\text{g mL}^{-1}$ , 3 h, 22°C) in a well of a 96-well plate (50  $\mu\text{L}$  of PMNs per wells at  $4 \times 10^5$  cells  $\text{mL}^{-1}$ ) as described in Section 2.2.8.2. As a negative control (*i.e.*, without ETs), the generated ETs were degraded with 10  $\mu\text{L}$  DNase-I (final well concentration of 10 U  $\text{mL}^{-1}$ ) in DNase buffer (final well concentration of 10 mM Tris-HCl, 2.5 mM  $\text{MgCl}_2$ , 0.1 mM  $\text{CaCl}_2$ ) diluted in  $\text{dH}_2\text{O}$ , while positive controls were incubated with  $\text{dH}_2\text{O}$  in DNase buffer. Five replicate wells were made per treatment.

*V. anguillarum* Vib 6 and Vib 87 culture filtrates were prepared to a Cf of 0.2 according to Section 4.2.4. To the wells containing ETs, 40  $\mu\text{L}$  of *V. anguillarum* Vib 6 culture filtrate (Cf

0.2, 0.4, or undiluted) was added to determine if various concentrations of Vib 6 culture filtrate could degrade ETs. As a control, an isolate known not to produce extracellular nucleases, *V. anguillarum* Vib 87, was used in this study. The *V. anguillarum* Vib 87 culture filtrate (Cf 0.2) was prepared according to Section 4.2.4, and was included as a separate treatment. The positive control (with ETs) was incubated with 40 µL of dH<sub>2</sub>O instead of culture filtrate, while the negative control (without ETs) was incubated with DNase (10 U mL<sup>-1</sup>). The 96-well plate was incubated for 30 min at 22°C before staining all wells with 10 µL of SYTOX Green (final 5 µM final well concentration, 5 min, room temperature; Thermofisher Scientific, Loughborough, UK). The fluorescence emitted from SYTOX Green was used as a proxy of presence of ETs and was measured using the plate reader (Synergy HT; BioTek, Swindon, UK) according to Section 2.2.8. To account for background fluorescence, wells without cells containing 60 µL RPMI3 (Appendix Table 2), 10 µL dH<sub>2</sub>O, and 40 µL of *V. anguillarum* Vib 6 filtrates (at each concentration) were stained with 10 µL SYTOX Green (as above), and the fluorescence was recorded. To control for background fluorescence emitted from SYTOX-stained culture filtrate (as this contains nucleic acids which can be stained by SYTOX), the mean fluorescence of the 5 replicate wells from one treatment containing the culture filtrate without cells was subtracted from the values obtained from wells containing the culture with cells (*i.e.*, matched treatment groups). The remaining fluorescence after this correction will be due to cells or extracellular DNA (*i.e.*, ETs), rather than the nucleic acids present in the culture filtrate.

#### **4.2.10. Investigating if nucleic acids within Atlantic salmon skin mucus are susceptible to degradation by *Vibrio anguillarum* Vib 6 culture filtrate**

To determine if the nucleic acids present in fish skin mucus is susceptible to degradation by *V. anguillarum* Vib 6 extracellular nuclease, Atlantic salmon *Salmo salar* skin mucus was collected from freshly killed fish (housed at Buckieburn fish farm) by a Schedule 1 technique (overdose of benzocaine (Sigma-Aldrich, Dorset, UK) and destruction of the brain) as described in the 1986 Animals Scientific Procedures Act (ASPA). Atlantic salmon were used in this experiment due to limitations in availability. All animal experiments were approved by the IoA Ethics Committee or the Animal Welfare Ethical Review Board (AWERB). Fish weighing between 300 – 500 g, were placed in polyurethane bag containing 5 mL of PBS and gently massaged around the body and fins to liberate the mucus from the skin. Mucus in PBS was collected into 15-mL Falcon tubes as a crude sample and centrifuged to remove debris such as scales and faecal matter (2800 × g, 20 min, 4°C), and then the supernatant was collected in Bijoux bottles and stored in -20°C. Before use, the mucus was thawed at room temperature (~22°C), collected in a 5-mL syringe, and filtered through a 0.22-µm syringe filter. Fifty microliters of filtered mucus was seeded into a well of a 96-well plate, and 10 µL of *V.*

*anguillarum* Vib 6 or Vib 87 culture filtrate (Cf. 0.2; collected by methods according to Section 4.2.3 and 4.2.4) or DNase-I (10 U mL<sup>-1</sup> final well concentration) was added to wells and incubated (30 min, room temperature). Negative controls were incubated with sterile PBS, and triplicate wells were made per treatment. The nucleic acid in each well was stained with 10 µL SYTOX Green (5 µM final well concentration) and fluorescence was recorded by a plate reader. Data were represented as mean fluorescence from triplicate wells per treatment. To account for background fluorescence, triplicate wells containing 50 µL PBS (instead of mucus) and 10 µL of *V. anguillarum* Vib 6 or Vib 87 culture filtrate (Cf. 0.2) was stained with SYTOX Green as above. The mean fluorescence from triplicate wells was subtracted from individual measurements per treatment, as described in Section 4.2.9.

#### **4.2.11. Assaying growth of *Vibrio anguillarum* in mucus**

To determine if *V. anguillarum* isolates: Vib 6, Vib 87, and NB10 (used as a control, as preliminary experiments found NB10 to be an intermediate nuclease producer between *V. anguillarum* Vib 6 and Vib 87) can metabolise the nucleic acids in Atlantic salmon mucus for growth, 50 µL double-strength TSA 2% NaCl was seeded into wells of a 96-well plate. Atlantic salmon mucus was collected and filtered according to Section 4.2.10, and made up to 20, 40, 60, and 80% solution of mucus diluted in sterile dH<sub>2</sub>O before adding 50 µL to the well containing TSB 2% NaCl (as a 1:1 dilution results in final mucus concentrations of 10, 20, 30, and 40%). Vib 6, Vib 87, and NB 10 were inoculated and cultured to late exponential phase and corrected with PBS to 1 × 10<sup>8</sup> CFU mL<sup>-1</sup> according to Section 4.2.1. A negative control was included using sterile dH<sub>2</sub>O instead of mucus. Bacteria were corrected using standard curve (Vib 6 and 87:  $y = 2.83 \times 10^9x - 6.64 \times 10^8$ ; NB 10:  $y = 1.34 \times 10^9x$ ), and 10 µL of bacteria were inoculated into six replicate wells per treatment. A negative control well lacking bacterial suspension was prepared by substituting the 10 µL of bacteria with the same PBS used to dilute the bacterial cultures.

#### **4.2.12. Statistical analyses**

Statistical analyses were performed using Prism v5.1 (GraphPad, La Jolla, USA). For comparisons of relative nuclease activity (mean clear zone area), normality and equality of variances were assessed by Kolmogorov–Smirnov test and Bartlett’s tests, respectively. When data were normally distributed, two-way ANOVA was used to determine statistical significance between means of each group at each time point with Bonferroni’s test applied to account for multiple comparisons.

Regarding data examining the effect of *V. anguillarum* nucleases on degrading ETs released by PMN-enriched cell suspensions, and when examining the effect of *V. anguillarum* nucleases (and DNase-I) on degrading nucleic acids within fish mucus, the normality and equality of variances were assessed with tests as above, respectively. When data were normal, one-way ANOVA was performed to compare mean fluorescence of ETs after exposure to *V. anguillarum* nucleases, while two-way ANOVA was performed to compare mean fluorescence of mucus after exposure to *V. anguillarum* nucleases or DNase-I. Bonferroni's post-hoc test was used to account for multiple comparisons. For all analyses,  $p < 0.05$  was considered statistically significant.

## **4.3. Results**

### **4.3.1. Quantification of nuclease activity by DNase agar**

A quantitative DNase agar digestion assay was used to determine the relationship between clear zone area and concentration of DNase-I, and clear zone area was plotted against DNase-I concentrations. A strong positive correlation was found between clear zone area of DNase agar digestion and DNase-I concentration ( $R^2 = 0.9443$ ) (Figure 4.2). DNase agar was unable to detect nuclease activity of DNase at  $5 \text{ U mL}^{-1}$  ( $0.005 \text{ U}$  total in the  $2 \text{ }\mu\text{L}$  assayed) (Figure 4.2). Overall, a linear relationship between DNase-I concentration and area of DNase agar digestion was found, and this DNase agar digestion assay can be used to measure and estimate relative nuclease activity.

### **4.3.2. Confirmation of nuclease activity of *Vibrio anguillarum* isolates**

The variation in nuclease activity was confirmed by previous projects which screened a range of isolates for relative nuclease production (Appendix Figure 10). *V. anguillarum* generally considered to possess nuclease activity, though differences in nuclease production were found between different specific strains or isolates from different geographical regions. *V. anguillarum* Vib 6 was confirmed to possess strong nuclease activity as colonies cultured on DNase agar, while *V. anguillarum* Vib 87 lacked any detectable nuclease activity (Figure 4.3). As a control for lack of nuclease activity and known nuclease-negative species of bacteria, *Y. ruckeri* YR 1 also resulted in no clear zones. The average clear zone area digestion from  $5 \text{ }\mu\text{L}$  of Vib 6 at  $A_{600} = 0.7$  was  $338.31 \pm 19.88 \text{ mm}^2$ .

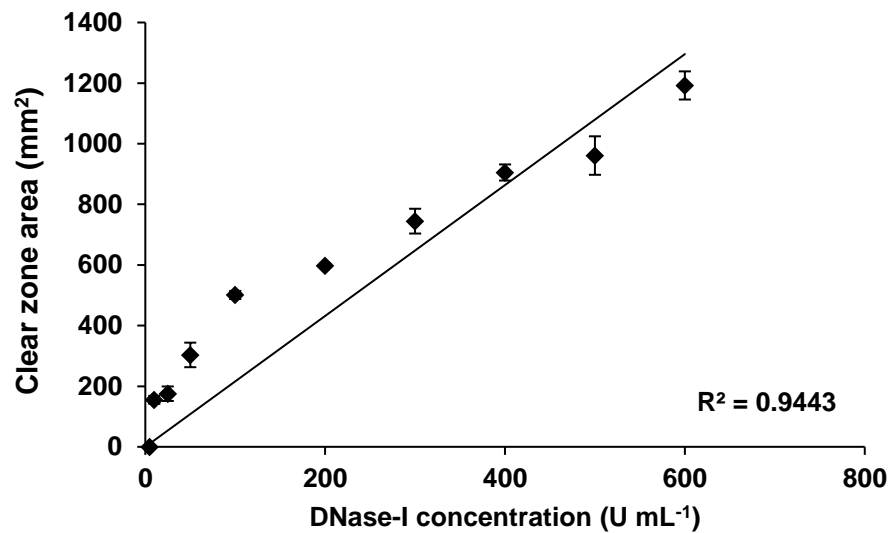


**Figure 4.2.** Scatterplot showing the relationship between DNase-I concentration (U mL<sup>-1</sup>) against mean clear zone area (mm<sup>2</sup>) of the DNase agar, indicating relative nuclease activity. This graph shows there is a strong relationship ( $R^2 = 0.9443$ ) between DNase-I concentration in 2-mm diameter wells in DNase agar and nuclease activity.  $y = 1.7522x + 169.86$ . All concentrations of DNase-I except 5 U mL<sup>-1</sup> gave a visibly detectable digestion of DNase agar. Error bars represent s.e.m.  $n = 3$ .

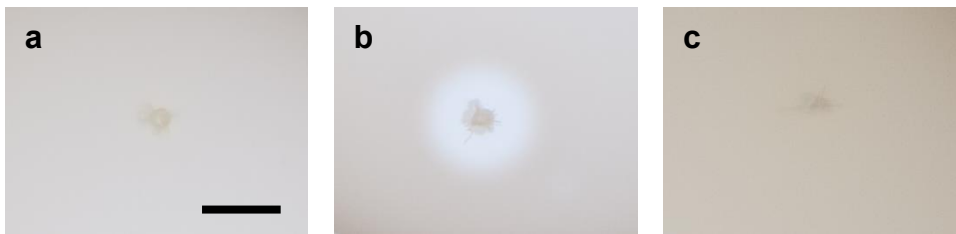


**Figure 4.3.** Representative images of DNase agar digestion by (a) *V. anguillarum* Vib 87, (b) *V. anguillarum* Vib 6, and (c) *Y. ruckeri* YR 1 bacterial solutions after growth on DNase agar for 24 h at 22°C. Clear zone area indicates digestion of DNase agar caused by nuclease activity present in the solution containing the bacteria. All bacteria were cultured in a shaking incubator (150 RPM, 16 h, 22°C) adjusted to  $A_{600}$ : 0.7 before inoculating into 2-mm diameter wells on DNase agar. Scale bar = 6 mm.

#### 4.3.3. Detection of nuclease activity in cell-free *Vibrio anguillarum* supernatant

Many *V. anguillarum* strains are now known to produce nucleases; however, whether the nuclease is membrane-tethered or extracellular is still unclear. Here, the supernatant of the strong nuclease producer, *V. anguillarum* Vib 6, was passed through 0.22- $\mu\text{m}$  pore filters to remove bacterial cells, and the nuclease activity from the filtrate was measured using the quantitative DNase agar digestion assay as above. The nuclease activity of the uncondensed filtrate did not give a detectable clear zone from the DNase agar plates (data not shown), thus, the filtrate was concentrated by rotary vacuum evaporation for 60 min to determine if nuclease activity could be detected. The *V. anguillarum* Vib 6 filtrate showed greater nuclease activity as it was concentrated, which was confirmed by measuring the clear area (Figure 4.4), indicating that Vib 6 has at least one extracellular nuclease. Incubating the culture filtrate on TSA 2% NaCl did not show growth after 48 h at 22°C, confirming that the filtration was successful at removing the bacterial cells from the culture filtrate.

#### 4.3.4. Inhibition of *Vibrio anguillarum* Vib 6 culture filtrate nuclease activity

EDTA has a high affinity for metal ions and is often used to inhibit the activity of cation-dependent nucleases by chelating free  $\text{Ca}^{2+}$  or  $\text{Mg}^{2+}$  ions into a metal complex (Kunitz, 1950). Incubation of condensed *V. anguillarum* Vib 6 culture filtrate (*Cf.* 0.2) with EDTA at 10 and 25 mM significantly reduced mean area of clear zone area ( $296.68 \pm 86.13 \text{ mm}^2$ , and  $188.3 \pm 17.81 \text{ mm}^2$ , respectively) compared to negative controls ( $512.40 \pm 69.99 \text{ mm}^2$ ,  $p < 0.05$ ), indicating that DNA digestion by the nuclease(s) in the culture filtrate is dependent on the presence of free cations (Figure 4.5). No significant difference in mean nuclease activity was observed between 1 mM EDTA-exposed Vib 6 culture filtrate ( $583 \pm 7.13 \text{ mm}^2$ ) and in negative controls ( $p < 0.05$ ) (Figure 4.5), indicating 1 mM EDTA does not sufficiently chelate cations to prevent activity from the nucleases within the culture filtrate. The nuclease activity of *V. anguillarum* Vib 6 culture filtrate (with and without EDTA 25 mM) was also examined in relation to relative to known concentrations of DNase-I (5 – 600 U mL<sup>-1</sup>). The activity of concentrated Vib 6 filtrate at *Cf* 0.2 resulted in a mean DNase agar digestion area of  $528.18 \pm 20.22 \text{ mm}^2$  (Figure 4.6), equivalent to 131.58 U mL<sup>-1</sup> DNase-I ascertained by using the regression equation attained from the standard curve of DNase-I activity, and approximately 26.316 U mL<sup>-1</sup> when uncondensed (Figure 4.2).

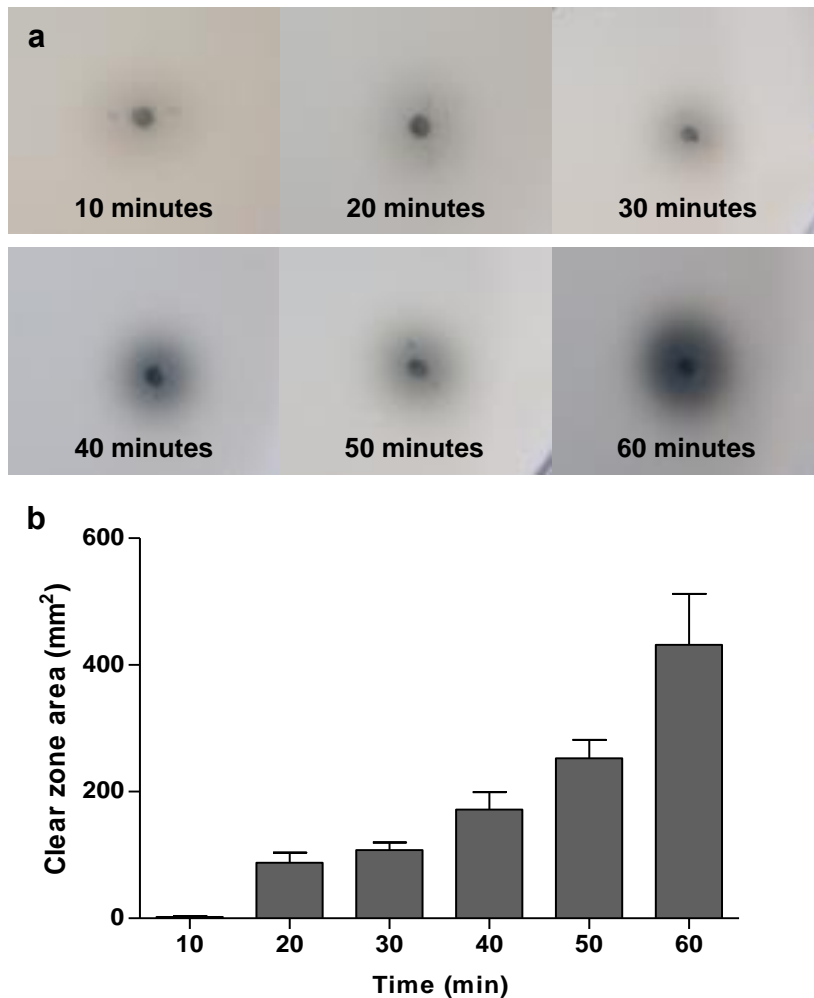


**Figure 4.4.** (a) Representative images of clear zones in the DNase agar *V. anguillarum* Vib 6 culture filtrate after 24 h at 22°C, with the clear zone relative nuclease activity. Bacteria was cultured in a shaking incubator (150 RPM, 16 h, 22°C), bacteria were removed with a 0.22- $\mu$ m syringe filter. The culture filtrate was condensed with rotating vacuum evaporation (35°C) up to 60 min (removing some for assay every 10 min), and the culture filtrate was assayed by inoculating into 2-mm<sup>2</sup> diameter wells on DNase agar. (b) Bar chart showing *V. anguillarum* Vib 6 culture filtrate nuclease activity measured by mean clear zone area (mm<sup>2</sup>) on DNase agar after 24 h at 22°C incubation. Culture filtrate was concentrated with rotating vacuum evaporation (medium temperature setting) over 60 min, showing as the culture filtrate becomes more concentrated, nuclease activity increases. The nuclease activity of the filtrate was assayed at 10 min condensing intervals, by inoculating into 2-mm diameter wells on DNase agar. Error bars represent s.e.m.  $n = 3$



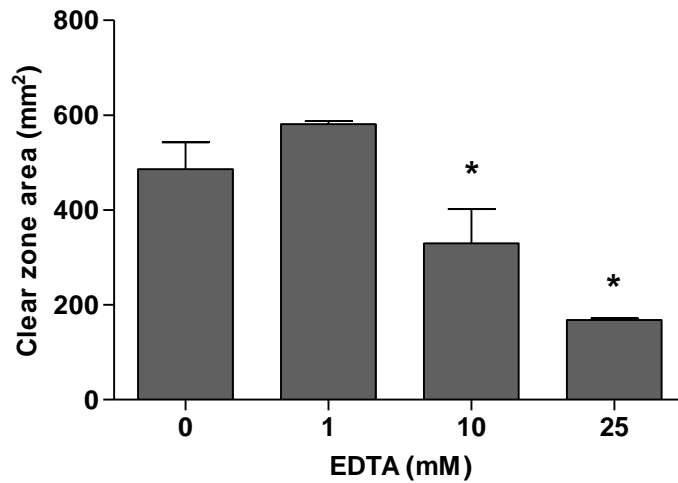


**Figure 4.5.** Bar chart showing *V. anguillarum* Vib 6 culture filtrate (Cf: 0.2) nuclease activity after exposed to EDTA (0 – 25 mM, 24 h at 22°C), measured by mean clear zone area (mm<sup>2</sup>) on DNase agar. Incubation with 10, and 25 mM EDTA, but not 1 mM, was sufficient to limit free cations required for nuclease activity within the *V. anguillarum* Vib 6 culture filtrate compared to non-exposed controls. \* $p < 0.05$ . Error bars represent s.e.m.  $n = 3$

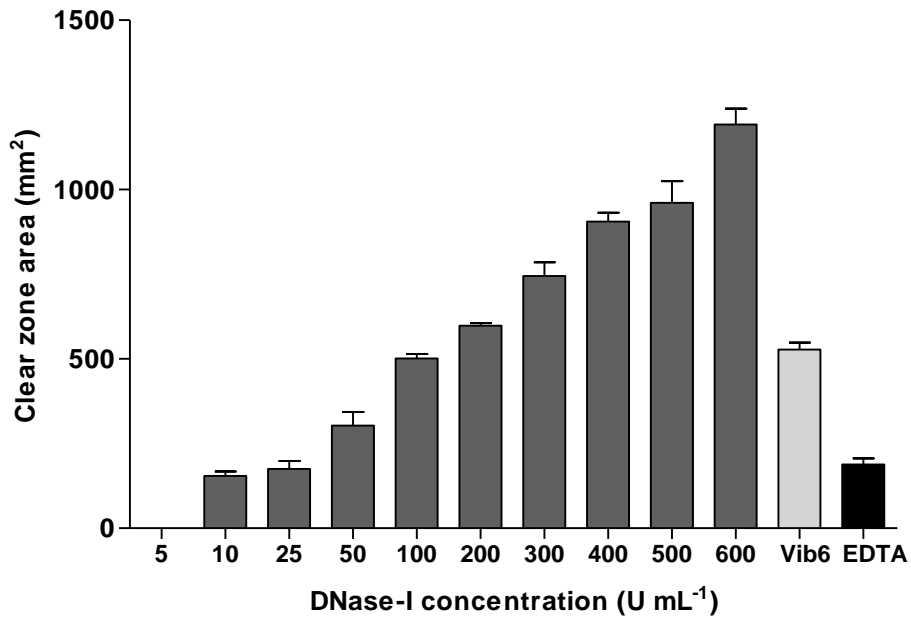


**Figure 4.6.** Bar chart showing *V. anguillarum* Vib 6 culture filtrate (Cf: 0.2) nuclease activity (light grey bars) in the presence of EDTA (25 mM, black bars), against DNase-I (5 – 600 U mL<sup>-1</sup>; grey bars), measured by mean clear zone area (mm<sup>2</sup>) on DNase agar after 24 h at 22°C incubation. The *V. anguillarum* Vib6 filtrate nuclease activity was calculated to be equivalent to 131.58 U mL<sup>-1</sup> at Cf: 0.2, and ~26.32 U mL<sup>-1</sup> when uncondensed. Error bars represent s.e.m. *n* = 3

#### **4.3.5. Freeze-thaw stability of *Vibrio anguillarum* Vib 6 culture filtrate**

The activity of DNases reduces when subjected to freeze-thaw cycling, due to losses in protein integrity (Cao *et al.*, 2003). Thus, the resistance of the nucleases in *V. anguillarum* Vib 6 filtrate was assessed by subjecting the concentrated filtrate solution to three freeze-thaw cycles (-20°C to room temperature), but no significant change in nuclease activity was detected after the first ( $413.25 \pm 28.00 \text{ mm}^2$ ) or second cycle ( $400.55 \pm 11.78 \text{ mm}^2$ ) compared to the control ( $400.42 \pm 5.96 \text{ mm}^2$ ) that had been incubated at 22°C for the experiment, though a statistically insignificant ( $p > 0.05$ ) loss in activity was detected after the third cycle ( $343.61 \pm 16.69 \text{ mm}^2$ ), (Figure 4.7).

#### **4.3.6. Stability of *Vibrio anguillarum* Vib 6 culture filtrate nuclease activity in different temperature, pH, and NaCl concentration**

Nuclease activity can vary in optimum temperature, pH and NaCl concentration (Pohl *et al.*, 1982; Dutta *et al.*, 2006). Incubation of the *V. anguillarum* Vib 6 culture filtrate (Cf: 0.2) for 10 min at 50 and 60°C for 10 min abolished all detectable nuclease activity (Figure 4.8), indicating denaturation of the enzyme(s) after 10 min. No significant difference of mean clear zone area was found at any time point between 4 – 37°C (Figure 4.8). Nuclease activity of the *V. anguillarum* Vib 6 culture filtrate and whole bacteria was examined over pH (6.5 – 11), and the greatest nuclease activity for was observed at pH 8.5 for both the filtrate and whole bacteria (Figure 4.9). Increasing NaCl concentration resulted in a negative correlation between NaCl concentration and nuclease activity (Figure 4.10). As with pH, the nuclease activity of the culture filtrate was proportionally less than the whole bacteria (Figure 4.10). Filtrate nuclease activity at 3.5% - 4% was difficult to detect, though whole bacteria still displayed nuclease activity at these salinities (Figure 4.10). Adding acid (HCl), base (NaOH), or NaCl to the agar did not observably affect the setting of the agar, though pH 10 and greater began to show darker discolouration of the agar. Expectedly, the nuclease activity of culture filtrate was proportionally less than the nuclease activity of the whole bacteria when compared (Figure 4.9 and Figure 4.10).

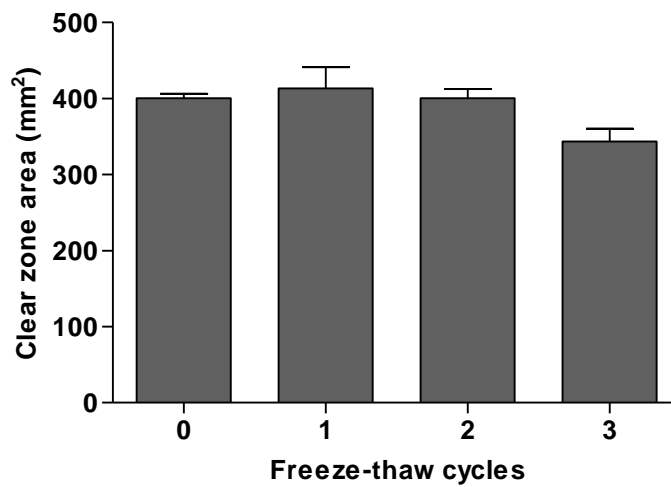


**Figure 4.7.** Bar chart showing *V. anguillarum* Vib 6 culture filtrate (Cf: 0.2) nuclease activity after three freeze-thaw cycles from -20°C to thawing at room temperature, measured by mean clear zone area (mm<sup>2</sup>) on DNase agar after 24 h at 22°C incubation. No statistically significant differences were observed between mean nuclease activity between the three cycles compared to the control indication robustness of the nuclease in the filtrate. Error bars represent s.e.m.  $n = 3$ .

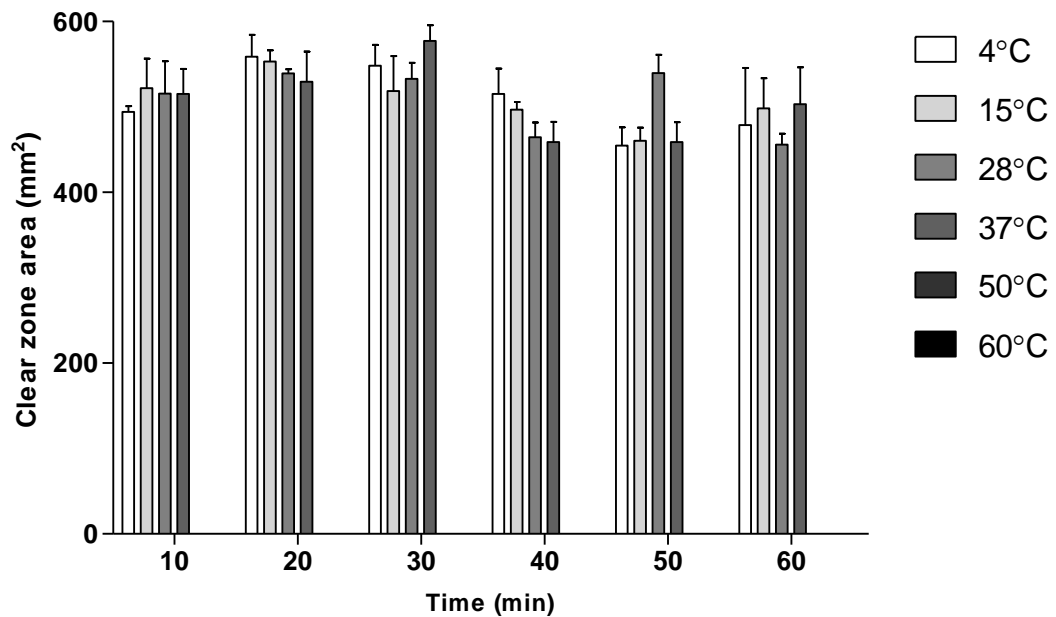


**Figure 4.8.** Bar chart showing *V. anguillarum* Vib 6 culture filtrate (Cf. 0.2) nuclease activity after exposure to heat blocks with temperatures ranging from 4°C to 60°C, for up to 60 min, measured by mean clear zone area (mm<sup>2</sup>) on DNase agar after 24 h at 22°C incubation. Nuclease activity was abolished between 0 – 10 min of incubation at 50°C and 60°C, while the activity of the nuclease remains constant at other temperatures and time points. There was no statistical difference between nuclease activity at every time point or temperature. Not all bars visible as no clear zones were detected in some instances. Error bars represent s.e.m.  $n = 3$ .

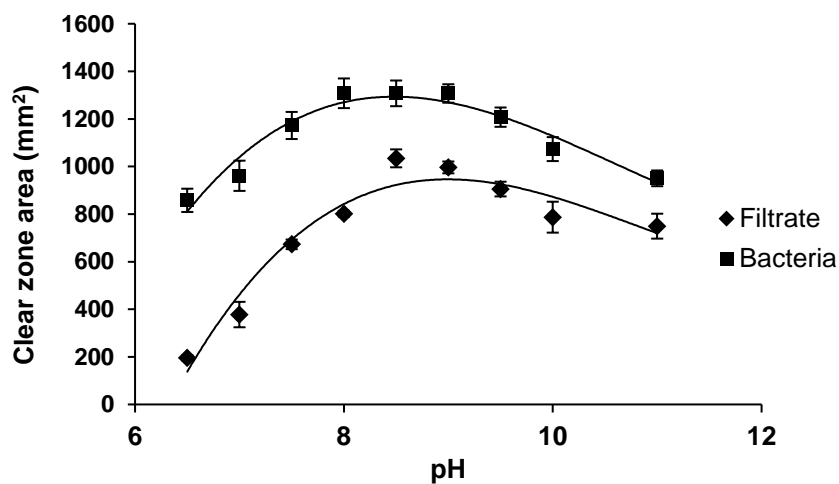


**Figure 4.9.** Scatterplot showing the relative nuclease activity by mean DNase agar digestion area (mm<sup>2</sup>) after 24 h, 22°C incubation with Vib 6 nuclease filtrate (◆) and whole bacteria (■) over different pH (6.5 – 11). Bacteria was prepared to A<sub>600</sub>: 1.6. The optimum pH for nuclease activity was observed at 8.5. For filtrate:  $y = 14.754x^3 - 469.33x^2 + 4777x - 14462$ ,  $R^2 = 0.9374$ ; for bacteria  $y = 16.409x^3 - 531.85x^2 + 5584.7x - 18199$ ,  $R^2 = 0.9412$ . Error bars represent s.e.m.  $n = 3$ .

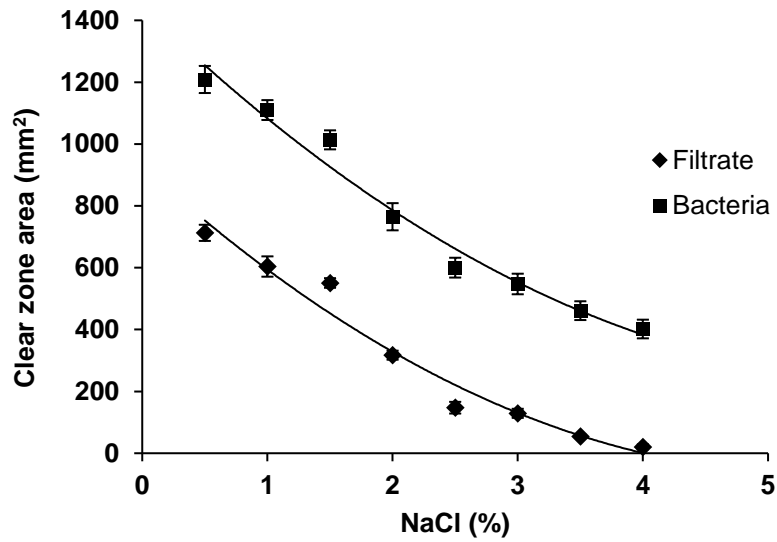


**Figure 4.10.** Scatterplot showing the relative nuclease activity by mean DNase agar digestion area (mm<sup>2</sup>) after 24 h, 22°C incubation with Vib 6 nuclease filtrate (◆) and whole bacteria (■) over different salinities (0.5 – 4%). Whole bacteria was prepared to A<sub>600</sub>: 1.6. For filtrate:  $y = 34.115x^2 - 368.36x + 928.39$ ,  $R^2 = 0.9665$ ; bacteria:  $y = 31.838x^2 - 392.21x + 1443$ ,  $R^2 = 0.9778$ . Error bars represent s.e.m.  $n = 6$ .

#### **4.3.7. Investigating the production of extracellular nuclease during *Vibrio anguillarum* Vib 6 growth**

Results above demonstrate that extracellular nuclease(s) is expressed by *V. anguillarum* Vib 6 at 16 h; however, it is unknown if the nuclease is expressed constitutively, or expressed differentially during culture. Examining the clear zone area digestion from *V. anguillarum* Vib 6 culture filtrate at every hour during *V. anguillarum* Vib 6 culture showed clear zones first detected at 5 h, during the early phase of exponential growth at 22°C (Figure 4.11). The clear zone area was divided by the  $A_{600}$  of the bacteria, and the nuclease activity of culture filtrate was found to not change throughout culture after 5 h (Figure 4.11). Up to 5 h, there was no detection of nuclease activity from the filtrates, but the nuclease activity is likely still present within the filtrate during early bacterial growth, though not completely detected due to the sensitivity of the DNase agar assay (Figure 4.11). Original data can be found in (Appendix Figure. 3).

#### **4.3.8. Investigating if *Vibrio anguillarum* Vib 6 culture filtrate can degrade ETs released by rainbow trout PMNs**

The *V. anguillarum* Vib 6 culture filtrate was tested for the ability to degrade ETs released by rainbow trout PMN-enriched cell suspensions. The culture filtrate was concentrated to 20% of its original mass (Cf: 0.2) and designated 'Vib 6 filtrate (concentrated)'. Treating the ETs with *V. anguillarum* Vib 6 culture filtrate (Cf: 0.2) showed degradation of ETs ( $249 \pm 47.60$  AFU), resulting in a 76.95% decrease in fluorescence compared to negative controls with ETs still present (Control + ETs), which had mean fluorescence of  $1081 \pm 115.69$  AFU ( $p < 0.05$ ), (Figure 4.12). To determine the fluorescence emitted of wells when ETs were degraded, a positive control was incubated with  $10 \text{ U mL}^{-1}$  DNase-I (Control - ETs), resulting in a fluorescence value of  $207 \pm 22.62$  AFU (Figure 4.12).

The degradation of ETs by *V. anguillarum* Vib 6 culture filtrate was dose-dependent, as a dilution of the concentrated culture filtrate (Cf: 0.4) resulted in a 55% reduction in fluorescence ( $482 \pm 79.16$  AFU) compared to negative controls ( $1081 \pm 115.69$  AFU), ( $p < 0.05$ ). Exposing the ETs with unconcentrated *V. anguillarum* Vib 6 culture filtrate resulted in a 29% reduction in fluorescence ( $767.6 \pm 50.14$  AFU) compared to negative controls ( $1081 \pm 115.69$  AFU); however, this did not reach statistical significance within 30 min incubation ( $p > 0.05$ ) (Figure 4.12). Culture filtrate *V. anguillarum* Vib 87 (Cf: 0.2) was included as a control, as this isolate is known to not possess extracellular nuclease activity in their culture filtrate. No significant decrease in fluorescence was found compared to positive controls ( $964.4 \pm 129.34$  AFU,  $p > 0.05$ ) (Figure 4.12). All results were confirmed for the presence of ETs in the wells with fluorescence microscopy (data not shown).



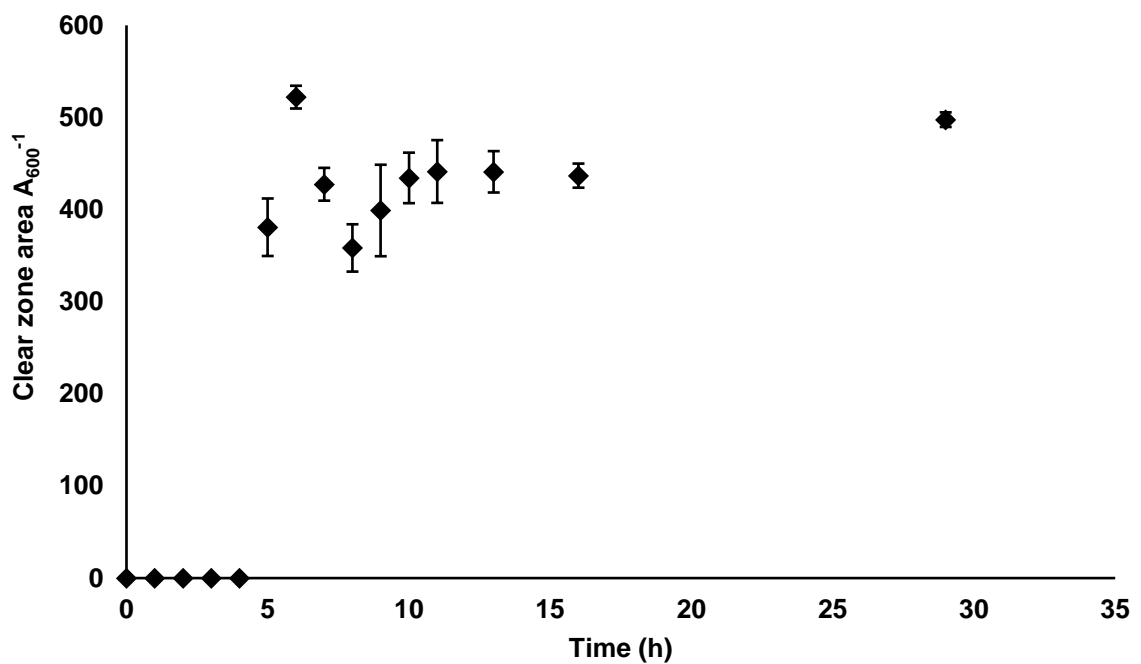


**Figure 4.11.** Scatterplot showing liquid culture of *V. anguillarum* Vib 6 in TSB 2% NaCl (150 RPM, 22°C) over 29 h (x-axis), against nuclease activity per bacteria, expressed by mean clear zone area (mm<sup>2</sup>) over absorbance ( $A_{600}$ ) (y-axis). This shows that at 5 h, *V. anguillarum* Vib 6 produces enough nuclease to be detected by the DNase agar assay. During *V. anguillarum* Vib 6 culture, the bacteria expresses a consistent amount of extracellular nuclease activity. Error bars represent s.e.m. (present with  $A_{600}$ , but too small to be observed).  $n = 4$  biological replicates.

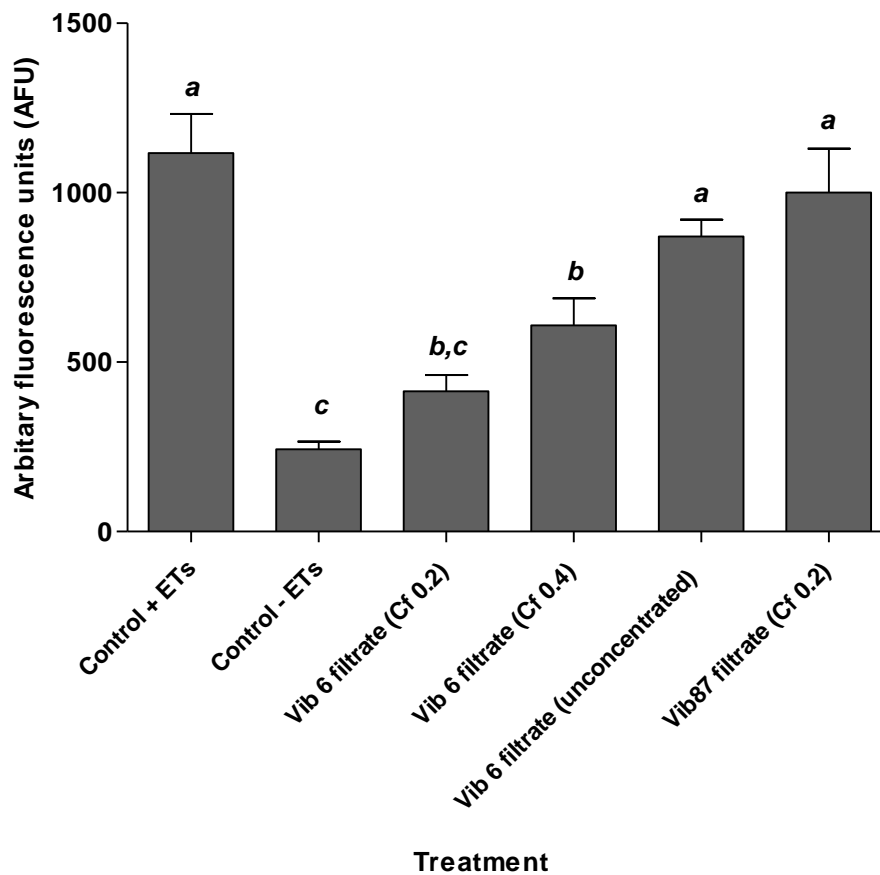


**Figure 4.12.** Bar chart showing the amount fluorescence emitted from wells containing PMN-enriched cell suspensions ( $4 \times 10^5$  CFU mL<sup>-1</sup>) induced to form ETs with Cal ( $5 \mu\text{g mL}^{-1}$ , 3 h, 15°C), stained with SYTOX Green ( $5 \mu\text{M}$ , 5 min, room temperature). The fluorescence is indicative of the amount of extracellular nucleic acid polymers (including ETs) are present. The ETs within each well was exposed to different treatments: 'Control + ETs' contained PMN-enriched cell suspensions induced to form ETs with Cal and incubated with dH<sub>2</sub>O and DNase buffer (1×). 'Control - ETs' contained PMN-enriched cell suspensions induced with Cal and incubated with DNase 10 U mL<sup>-1</sup> diluted with dH<sub>2</sub>O, and DNase buffer (1×). 'Vib 6 filtrate (Cf: 0.2, 0.4, unconcentrated)' contained the contained PMN-enriched cell suspensions induced with Cal and incubated with difference concentrates of *V. anguillarum* Vib 6 culture filtrates. 'Vib 87 filtrate (Cf: 0.2)' is the same treatment as above, using a nuclease-deficient isolate. Letters indicate statistical differences ( $p < 0.05$ ). Error bars represent s.e.m.  $n = 5$  wells.

#### **4.3.9. Investigating if nucleic acids within Atlantic salmon skin mucus are susceptible to degradation by *Vibrio anguillarum* Vib 6 culture filtrate**

Staining nucleic acids in Atlantic salmon skin mucus with SYTOX Green and measuring the fluorescence with SYTOX (Figure 4.13), or observation under fluorescence microscopy suggests that mucus contains nucleic acids (data not shown). The filtered Atlantic salmon mucus was exposed to *V. anguillarum* Vib 6 culture filtrate nuclease for 30 min and the fluorescence of the mucus reduced significantly ( $606.33 \pm 68.42$  AFU) by 65% compared to mucus exposed to dH<sub>2</sub>O only ( $1732.67 \pm 52.26$  AFU) ( $p < 0.05$ ), indicating the presence of nucleic acids in skin mucus that is susceptible to degradation by *V. anguillarum* Vib 6 culture filtrate (Figure 4.13). Exposing DNase-I ( $10 \text{ U mL}^{-1}$ ) to mucus resulting in a significant, 81% reduction in fluorescence ( $322.00 \pm 7.93$  AFU) to a similar degree as concentrated *V. anguillarum* Vib 6 filtrate ( $p < 0.05$ ). Meanwhile the concentrated *V. anguillarum* Vib 87 culture filtrate did not significantly reduce fluorescence ( $1633.00 \pm 136.10$  AFU) compared to negative controls ( $p > 0.05$ ) (Figure 4.13).

#### **4.3.10. Growth of *Vibrio anguillarum* in Atlantic salmon skin mucus**

As nuclease produced by *V. anguillarum* Vib 6 digested nucleic acids from Atlantic salmon skin mucus, perhaps *V. anguillarum* utilises nucleotides from digested nucleic acids to assist in growth. Incubation of nuclease-producing and deficient isolate (*V. anguillarum* Vib 6 and Vib 87) with culture media supplemented with 0 – 40% filtered Atlantic salmon skin mucus did not result in differences in growth rate (Figure 4.14). However, a separate nuclease-producing *V. anguillarum* strain (NB 10) was found to grow better in 40% mucus to a small degree, though not reaching statistical significance (Figure 4.14).

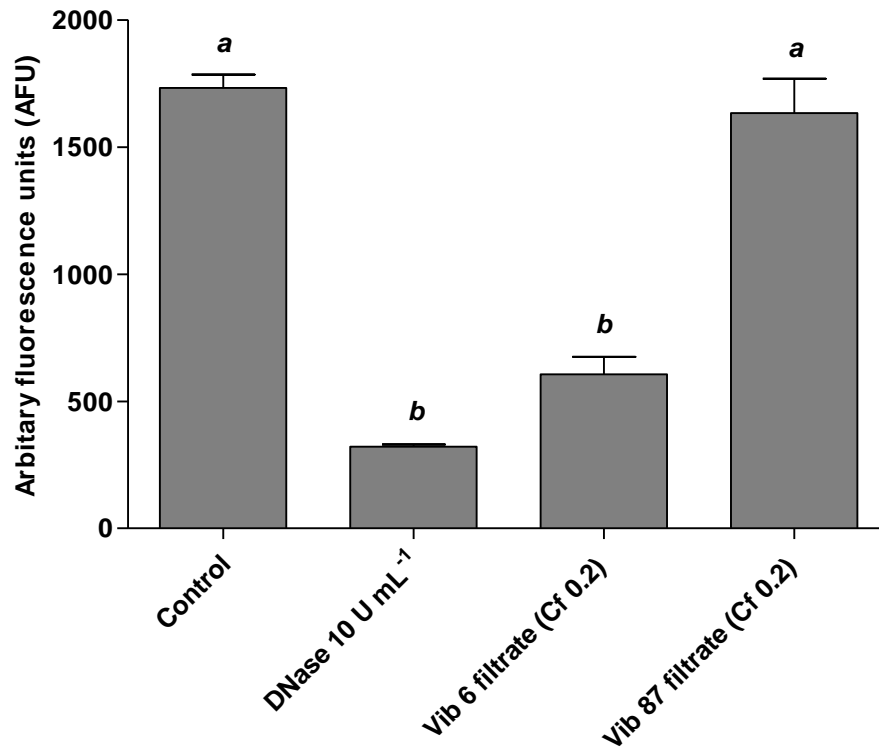


**Figure 4.13.** Bar chart showing the amount fluorescence emitted from wells containing 0.22- $\mu$ m-filtered fish skin mucus stained with SYTOX Green (5  $\mu$ M, 5 min, room temperature). The fluorescence is indicative of the nucleic acid polymers present within the mucus. The mucus in the wells were treated with DNase-I (10 U mL<sup>-1</sup>), *V. anguillarum* Vib 6, or Vib 87 culture filtrate (both condensed to 20% of original mass/ Cf: 0.2), compared to negative controls treated with dH<sub>2</sub>O. Letters indicate statistical differences ( $p < 0.05$ ). Error bars represent s.e.m.  $n = 3$  wells.

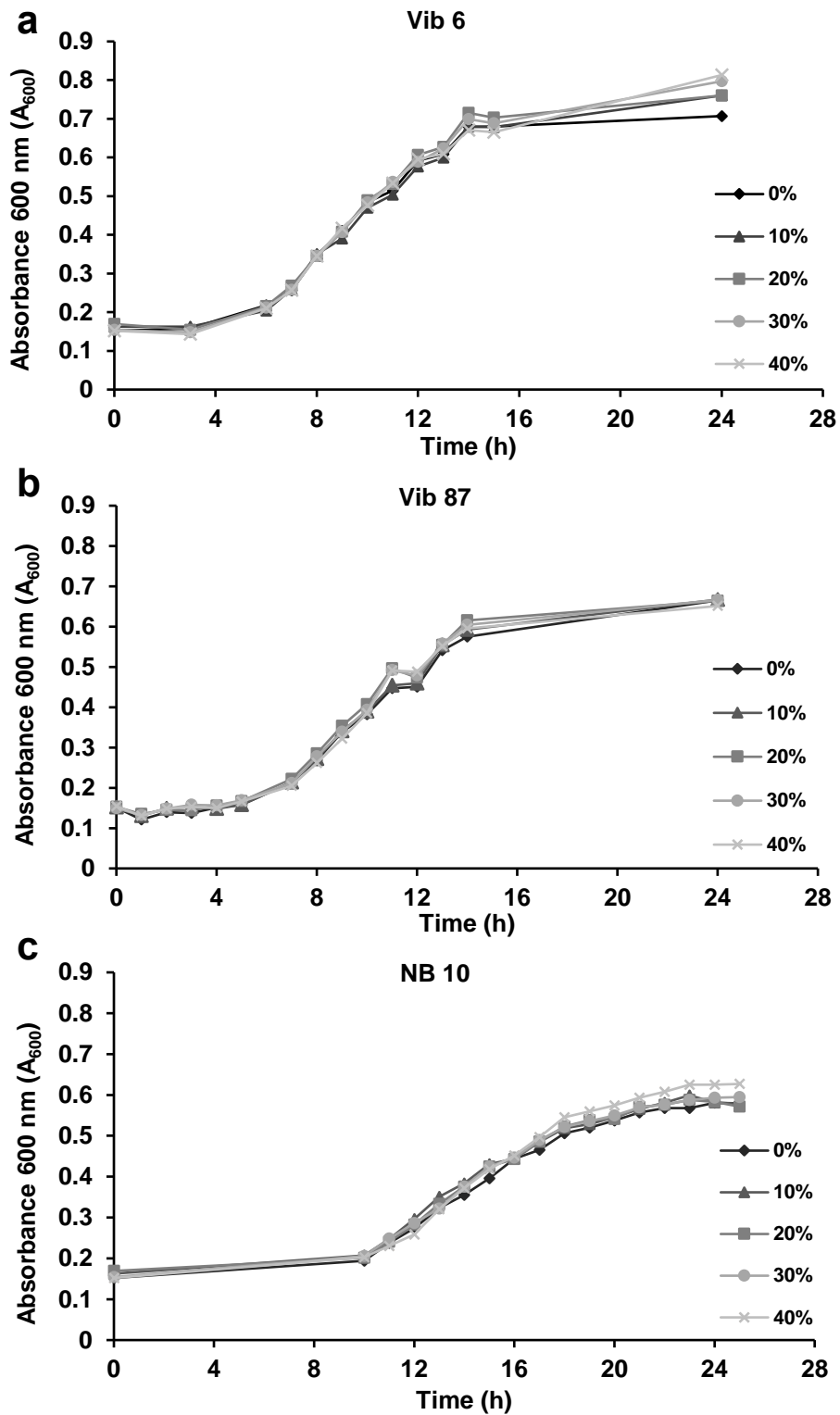


**Figure 4.14.** Scatterplot showing culture of *V. anguillarum* strains in TSB 2% NaCl supplemented with 10, 20, 30, and 40% Atlantic salmon skin mucus, 150 RPM, 22°C. (a) Vib 6, (b), Vib 87, (c) NB 10 Error bars not shown to improve graph clarity.  $n = 6$ .

#### 4.4. Discussion

The aim of this Chapter was to investigate the potential role of extracellular nucleases produced by the fish pathogen, *V. anguillarum*, in nutrition and in virulence. A DNase agar digestion assay was used to examine the relative nuclease production from a collection of *V. anguillarum* isolates. *V. anguillarum* Vib 6 produced the greatest nuclease activity, while *V. anguillarum* Vib 87 showed no detectable activity (Figure 4.3). The nuclease activity was also present in the filtered supernatant of the *V. anguillarum* Vib 6 (*i.e.*, culture filtrate), and activity increased with greater concentration (Figure 4.4). Additionally, the culture filtrate of *V. anguillarum* Vib 6 showed characteristic properties of known nucleases including the reduction or loss of activity at greater temperature, salinity, extreme pH, and requirement for cations (Section 4.3.6), suggesting extracellular nuclease enzyme is responsible for the detected nuclease activity. The nuclease activity in the culture filtrate was similar on a per cell-basis throughout *V. anguillarum* Vib 6 culture (Figure 4.11), indicating that the bacterium might produce the enzymes constitutively. Lastly, and most importantly, the *V. anguillarum* Vib 6 culture filtrate degraded ETs released from trout PMN-enriched cell suspensions (Figure 4.12) and nucleic acids within fish mucus (Figure 4.13), while the filtrate derived from *V. anguillarum* Vib 87 filtrate; indicating some potential biological roles for *V. anguillarum* extracellular nucleases.

The suitability of the DNase agar digestion assay used to screen for nuclease activity was first validated by confirming a significant positive correlation between DNase-I concentration and clear zone area within the agar ( $R^2 = 0.9443$ ), and overall, there was high reproducibility (Figure 4.2). Variables such as formulation and volume of agar, well size, and concentration of the nuclease were standardised in the assay to allow comparison between experiments. Expectedly, this method did not give a detectable clear zone with low concentrations of DNase-I, as  $5 \text{ U mL}^{-1}$  (0.005 U total) was likely too weak to digest the DNA within the DNase agar. Still, this method was preferred as it quick and semi-quantitative, requires small volumes of solutions, and the formulation of the agar could be modified by supplementation, allowing simpler testing of nuclease activity at different pH or salinities.

In this present study, the nuclease activity from *V. anguillarum* Vib 6 culture filtrate was investigated in different environmental conditions. Expectedly, the culture filtrate nuclease activity was abolished between 37 and 50°C (Figure 4.8) and displayed an asymmetric bell-shaped curve of nuclease activity across different pH, with greatest activity at pH 8.5 (Figure 4.9), and a slightly diminished activity was observed after three freeze-thaw cycles (Figure 4.7). Unexpectedly, the nuclease activity of *V. anguillarum* Vib 6 culture filtrate did not reduce sharply with greater alkalinity as observed with greater acidity (Figure 4.9). This may be due to the DNase agar having reduced viscosity, affecting the gel setting due to the pH, indicating that this DNase agar digestion assay can be sensitive to different pH formulations.

Additionally, nuclease activity within the *V. anguillarum* Vib 6 culture filtrate showed a negative relationship with increasing NaCl concentration (Figure 4.10). Furthermore, sequestering free divalent metal ions with 25 mM EDTA was successful at reducing Vib 6 filtrate nuclease activity by 64.43% (Figure 4.5), collectively indicating the need for metal cations for enzymatic activity. Taken together, these results show that the nuclease activity within *V. anguillarum* Vib 6 filtrate displaying properties of many other characterised nucleases, including similar optimum temperature, salinity and pH (Ferrieri *et al.*, 1980; Pohl *et al.*, 1982) and requirement for metal cations (Pohl *et al.*, 1982; Derré-Bobillot *et al.*, 2013).

The production of nucleases by bacteria serves multiple functions, for instance, *V. cholerae* extracellular nucleases can degrade the nucleic acids that are abundant in the marine environment (Paul *et al.*, 1984; Thomsen *et al.*, 2016; Stoeckle *et al.*, 2017) in order to generate free nucleotide and phosphate pools as a nutrient source (McDonough *et al.*, 2016). Additionally, the primary point of entry of *V. anguillarum* during the infection stage is still debated, but there is evidence that the bacteria can enter directly through the skin with the use of proteases which may break down mucus integrity (Norqvist *et al.*, 1990; Hickey *et al.*, 2017). As these extracellular nucleases can promote the presence of nutrients for *V. anguillarum*, bacterial survival may be enhanced at mucosal surfaces, considering that nucleic acids are abundantly present in fish mucus (Tkachenko *et al.*, 2013; Benhamed *et al.*, 2014; Carda-Diéguez *et al.*, 2017; Minniti *et al.*, 2017).

Fish skin mucus also serves as a protective barrier to pathogenic organisms which may be attributed, in part, to its viscosity (Benhamed *et al.*, 2014; Carda-Diéguez *et al.*, 2017; Thompson, 2017), and the presence of antimicrobial peptides such as lysozyme and histones (a chromatin component) within the mucus (Fernández *et al.*, 2002; Thompson, 2017). The contribution of nucleic acids to the integrity and viscosity of fish mucus remains to be clarified, though studies in human cystic fibrosis patients have found a relationship between DNA concentration and sputum mucus viscosity, as treatment with aerosol nucleases can reduce the symptoms of the disease by degrading DNA polymers (Shah *et al.*, 1996; Henke *et al.*, 2007). In this present study, the fluorescent nucleic acid dye SYTOX Green positively-dyed Atlantic salmon skin mucus, and treatment of the mucus with DNase-I resulted in an 81% reduction in fluorescence (Figure 4.13), indicating that there is an abundance of nucleic acids in fish skin mucus. The *V. anguillarum* Vib 6 culture filtrate significantly reduced the fluorescence emitted from SYTOX Green-stained fish skin mucus by 65% (Figure 4.13), indicating that *V. anguillarum* Vib 6 culture filtrate can degrade nucleic acids in fish skin mucus. However, there is currently little evidence in the literature demonstrating nucleic acid abundance with fish skin viscosity. To better understand this relationship, future experiments should examine if the viscosity of the mucus (i.e., acting as a physical barrier) is reduced by degrading the nucleic acids present. Nuclease-producing strains of bacteria could be

assessed for their abilities to penetrate fish mucus, as this would determine if the bacterial nucleases, or other factors such as proteases, may assist with burrowing through mucosal surfaces (Benhamed *et al.*, 2014; Carda-Diéguez *et al.*, 2017; Thompson, 2017).

The viscosity of fish skin mucus may be lost during the method used to process the mucus within this thesis, as filtering (to sterilise the mucus) may remove large aggregations or polymers of proteins and nucleic acid which contribute to the mucus viscosity. Therefore, future methods to extract fish mucus should have a focus on preserving mucus integrity. Otherwise, methods using highly sensitive rheological analysis may distinguish the viscosity of small volumes of mucus.

Understanding if nuclease-producing *V. anguillarum* isolates can grow faster in mucus may give a better insight to other functions of the nuclease. Some *Vibrio* species utilise nucleotides for growth (sometimes in the form of phosphates), and mutants deleted for both of extracellular nuclease genes exhibit a severe growth defect when DNA is supplied as the sole source of phosphate (Seper *et al.*, 2011; Mcdonough *et al.*, 2016), suggesting that *V. anguillarum* may utilise the products of degraded nucleic acids within fish skin mucus for growth. The three strains of *V. anguillarum* used had relatively distinct nuclease activity (high, medium, and absent), though the high nuclease producer (*V. anguillarum* Vib 6), and nuclease deficient strain (*V. anguillarum* Vib 87) showed no difference in growth in 0 – 40% mucus supplementation in broth, suggesting that nucleic acids are not the most important factor for *V. anguillarum* growth. Interestingly, the intermediate nuclease-producing strain *V. anguillarum* NB 10 replicated slightly better in 40% mucus, suggesting other more important mechanisms are utilised for growth. Perhaps, the growth benefit may have been present but not adequately detected, as antibacterial factors (such as piscidins, pleurocidins, and histones) found in fish mucus may reduce the growth benefit from the additional nutrition (Fernández *et al.*, 2002; Bergsson *et al.*, 2005; Smith *et al.*, 2010, 2015).

Molecular evidence and understanding of the other species in the *Vibrio* family suggests that *V. anguillarum* produces more than one nuclease, and some may be membrane associated (Muroga, 1985; Focareta, 1989; Austin *et al.*, 1995; Li *et al.*, 2003; Blokesch *et al.*, 2008; Frans *et al.*, 2011; Seper *et al.*, 2013; Hickey *et al.*, 2017). The results from this chapter has focused on the extracellular nuclease of *V. anguillarum*, and the presence of membrane-bound nucleases was not examined. The current understanding from other species suggests that the membrane-bound nucleases are involved in DNA uptake and genetic transformation (Bergé *et al.*, 2013; Liechti *et al.*, 2013), while extracellular nucleases play a more prominent role in the degradation of ETs (Seper *et al.*, 2013). Further investigation is warranted, and characterisation of the nuclease through a molecular approach may improve our understanding of the roles of extracellular nuclease in *V. anguillarum*.



Importantly, *V. anguillarum* Vib 6 culture filtrate was able to dose-dependently degrade the ETs released by trout PMNs, indicating the potential ability to evade or resist trapping by ETs. This may be important for the successful infection within the host, as the bacterium must persist and survive when exposed to ETs and other components of the innate immune system to establish a successful infection (Beiter *et al.*, 2006; Seper *et al.*, 2011, 2013; Brinkmann and Zychlinsky, 2012). However, the degradation of ETs by crude, unconcentrated *V. anguillarum* Vib 6 filtrate resulted in a small, but insignificant decrease in fluorescence compared to the negative controls lacking nuclease-active filtrate treatment (Figure 4.12), indicating ETs were degraded. In biological context, perhaps only small amounts of nuclease are required, or that the bacteria may already produce sufficient nucleases to locally free itself when trapped in ETs. Thus, the next chapter focuses on investigating the antimicrobial action of the ETs, and if these nucleases can assist the bacteria to prevent trapping or to escape ETs.

## Chapter 5: Investigating the antimicrobial properties of rainbow trout extracellular traps

### 5.1. Introduction

Extracellular traps (ETs) released by human PMNs can trap various microbes including bacteria (Brinkmann *et al.*, 2004), fungi (Urban *et al.*, 2006), viruses (Saitoh *et al.*, 2012), and unicellular protozoans (Guimaraes-Costa *et al.*, 2009), but whether these microbes are killed by ETs remains under debate (Menegazzi *et al.*, 2012). The negative electrostatic charge of the DNA that composes an ET promotes the attraction of microbes and may aid trapping (Yipp *et al.*, 2013), while various peptides that decorate the ETs such as histones have antimicrobial properties *in vitro*, and could facilitate killing of the entrapped microbes (Fernández *et al.*, 2002; Patat *et al.*, 2004; Zou *et al.*, 2007; Young *et al.*, 2011; Parker, Albrett, *et al.*, 2012; Perera *et al.*, 2012; Branzk *et al.*, 2014; Neumann *et al.*, 2014; Halverson *et al.*, 2015; Smith *et al.*, 2015). Bactericidal histones and other ET-associated peptides have been confirmed to decorate ETs released by cyprinids, flatfish, and salmonids (Brogden *et al.*, 2012; Chi *et al.*, 2015), (Section 3.3.3); thus, it is possible that entrapped microbes may be killed by the membrane destabilizing properties of these proteins and peptides (Richards *et al.*, 2001; Fernández *et al.*, 2002; Palić, Ostojić, *et al.*, 2007; Pijanowski *et al.*, 2013; Chi *et al.*, 2015).

A simple and effective method to demonstrate the antimicrobial activity by ETs involves pre-inducing the release of ETs from cells *in vitro* (using a biological or chemical stimulant) to generate large concentrations of ETs in suspension, before co-incubating with a bacterium of interest (Young *et al.*, 2011; Brogden *et al.*, 2012; Chi *et al.*, 2015; Reichel *et al.*, 2015). Then, at defined times thereafter, the bacterial colony forming units (CFU) enumerated from the co-incubation provides an indication for bacterial viability. A CFU is formed when a single viable bacterium (or a clump formed by bacterial cell aggregations) multiplies via binary fission on agar surfaces. The data achieved under these conditions is compared to control conditions where ETs are digested with exogenous DNase-I prior to the addition of bacteria (Menegazzi *et al.*, 2012). A significant reduction in CFU compared to the control conditions may indicate attachment of the bacteria to the ET (which can cause bacterial clumping) or direct killing of the bacteria by the ET. In many studies, ETs are pre-induced by biological or chemical compounds such as phorbol 12-myristate 13-acetate (PMA) before bacteria is added to the ET suspension (Urban *et al.*, 2006; Young *et al.*, 2011), and a further control must be performed to confirm that this compound itself does not affect the viability of the bacteria. In this present study, calcium ionophore (Cal) has been shown to be the most potent inducer of ET release from trout PMN-enriched cell suspensions (Section 3.3.4), though this chemical can exert bactericidal activity (Guyot *et al.*, 1993). Thus, when studying ET trapping by the

method outlined above, the viability of the bacteria in the presence of relevant concentrations of the reagents used to manipulate the ETs (*i.e.*, the Cal used to induce ET release, inhibitors, or the DNase-I used to degrade the ETs) must be verified to ensure appropriate experimental control.

One limitation of studying microbial trapping by ETs measuring bacterial CFU is the contribution of phagocytic activity by the PMNs to any reductions in CFU. To reduce phagocytosis, PMNs are typically exposed to actin polymerisation inhibitors, such as cytochalasin D, as these agents block phagocytosis meaning that reductions in CFUs can be more reliably attributed solely to the antimicrobial properties of the ETs in suspension (Urban *et al.*, 2006; Wartha *et al.*, 2007; Brinkmann and Zychlinsky, 2012; Seper *et al.*, 2013). However, one drawback with using cytochalasin D is that it can also inhibit ET release (Robb *et al.*, 2014) (Section 3.3.5). Moreover, primary cell cultures of PMNs induced to release ETs with chemical inducers has resulted in abolishment of phagocytosis 1 h after induction, making the use of cytochalasin to block phagocytosis not always necessary (Fuchs *et al.*, 2007). Low-speed centrifugation can be applied to sediment the bacteria within wells, promoting contact of bacteria with pre-induced ETs *in vitro* (Chi *et al.*, 2015; Zhao *et al.*, 2017). As the ETs in culture are usually found settled at the bottom of the well (observed in Chapter 3, Section 3.3.6). However, centrifugation at high speeds in the presence of cultured cells result in cell lysis, especially as PMNs are easily perturbed resulting in activation of the cell, including release of different cytokines and favouring a more motile state (Naccache *et al.*, 2016).

With respect to fish, microbial trapping by ETs has been demonstrated for PMN-enriched cell suspensions of European carp (*Cyprinus carpio*) (Brogden *et al.*, 2014), turbot (*Scophthalmus maximus*), and tongue sole (*Cynoglossus semilaevis*) (Chi *et al.*, 2015; Zhao *et al.*, 2017) (Table 1.4). However, the fate of these microbes remained uncertain, as the experimental design examining microbial trapping in flatfish ETs does not liberate the entrapped microbes to distinguish conclusively whether the microbes were still viable. In the flatfish studies, co-incubation of released ETs with *Vibrio harverii* and *Escherichia coli*, but not *Edwardsiella tarda* resulted in a significant change of CFU compared to controls with ETs pre-degraded with DNase-I, indicating trapping (Zhao *et al.*, 2017). The carp study confirmed trapping of *Aeromonas hydrophilla* on the ETs by fluorescent microscopy, as fluorescently-labelled bacteria were observed to be entangled on the ETs released by carp PMNs (Brogden *et al.*, 2014). Fluorescent labelling and electron microscopy has been used previously to demonstrate microbial trapping on ETs, and protocols to show microbial trapping by ETs released by PMNs of different animal species has been developed (Poirier *et al.*, 2014; Robb *et al.*, 2014; Reichel *et al.*, 2015; de Buhr *et al.*, 2016; Tran *et al.*, 2016; Zhang *et al.*, 2016; Zhengkai Wei *et al.*, 2016).

Exogenous addition of recombinant DNase-I mimics the pathogens ability to produce nuclease, which is a strategy implemented by various microbial pathogens to escape entrapment by ETs (Sumbly *et al.*, 2005; Beiter *et al.*, 2006; Brogden *et al.*, 2012; Seper *et al.*, 2013; Neumann *et al.*, 2014; de Buhr *et al.*, 2015). Many *Vibrio* species produce nucleases, and co-incubation of a *Vibrio cholerae* mutant with deleted extracellular nucleases are more susceptible to trapping by human ETs compared to the wild-type strain (Seper *et al.*, 2013). In Chapter 4, a suite of *Vibrio anguillarum* isolates was shown to produce extracellular nuclease activity that can degrade ETs, though whether this enzyme action could influence bacterial trapping by ETs remains unclear.

Therefore, this Chapter aimed to investigate whether ETs produced from PMN-enriched cell suspensions of rainbow trout can interact with the fish pathogen, *V. anguillarum*, and to determine if microbial nuclease production could influence the trapping ability of the ETs. To achieve this, a wild-type, nuclease-deficient isolate of *V. anguillarum* that lacks detectable nuclease activity (Section 4.2.2) was incubated with pre-induced ETs released by trout PMN-enriched cell suspensions *in vitro*, and abundance of live bacteria (*i.e.*, bacterial CFU) after incubation was compared to the CFUs recovered when DNase-I was added to break up the ETs. Furthermore, the ability of a wild-type *V. anguillarum* isolate with extracellular nuclease activity to be trapped by the ETs was compared to number of CFU from co-incubations of the extracellular nuclease deficient isolate with ETs. Finally, direct observation of fluorescently stained bacteria interacting with the ETs will be attempted, as this method can demonstrate interaction between microbes and ETs, providing support for the CFU trapping experiments (de Buhr *et al.*, 2016).

## **5.2. Materials and Methods**

### **5.2.1. Effect of calcium ionophore and DNase-I on viability of *Vibrio anguillarum***

In the previous Chapter (Section 3.3.5), Cal (Thermofisher Scientific, Loughborough, UK) was identified as a potent inducer of ET release from trout PMN-enriched cell suspensions (prepared from triple-layer Percoll gradients according to Section 2.2.3), and ETs can be degraded by DNase-I (Thermofisher Scientific, Loughborough, UK). Thus, Cal and DNase-I needed to be confirmed to have no effect on bacterial viability for use as appropriate experimental controls. To assess whether *V. anguillarum* viability was affected in the presence of the concentrations of Cal (a potent inducer of ET release from trout PMN-enriched cell suspensions) and DNase-I (a nuclease able to degrade the ETs; Section 3.3.2) to be used in

the experiments, each compound was incubated with the bacteria (at  $1 \times 10^3$ ,  $10^4$ , and  $10^5$  CFU mL<sup>-1</sup>) for up to 4 h in wells of a flat-bottom 96-well polystyrene culture plate (Cell+, Sarstedt, Nümbrecht, Germany). Separate wells were made up for each time point. The number of viable *V. anguillarum* Vib 87 CFU was measured after incubation in 5 µg mL<sup>-1</sup> Cal. To do this, *V. anguillarum* Vib 87 was cultured from a single colony to exponential phase in a shaking incubator (150 RPM, 16 h, 22°C) according to Section 4.2.2. The bacteria were collected by centrifugation (2600 × g, 10 min, 4°C), and then the supernatant was poured off and discarded. The bacterial pellet was washed by resuspending in 5 mL sterile PBS by vigorous agitation on a vortex and centrifuged again as before. After three identical washes, the bacterial suspension was diluted to achieve final well concentrations of  $3.33 \times 10^3$ ,  $10^4$ , and  $10^5$  CFU mL<sup>-1</sup> in PBS in bijoux bottles, and incubated on ice until use. In a flat-bottom 96-well plate, 50 µL of bacterial suspension at each concentration was added to individual wells that already contained 90 µL of PBS and 10 µL of Cal (diluted in dH<sub>2</sub>O and to give a final well concentration of 5 µg mL<sup>-1</sup>). In the negative control wells the Cal was substituted for PBS.

To assess whether *V. anguillarum* viability was affected in the presence of the concentrations of 10 U mL<sup>-1</sup> DNase-I, *V. anguillarum* Vib 6 and Vib 87 ( $1 \times 10^4$  CFU mL<sup>-1</sup>) were cultured in the same way using the same method as above, and then incubated for up to 4 h in 96-well microtitre plates at 15°C. In each well, 200 µL of bacterial suspension was added to DNase-I (diluted in 16 µL dH<sub>2</sub>O) and 24 µL DNase buffer (final well concentration of 10 mM Tris-HCl, 2.5 mM MgCl<sub>2</sub>, 0.1 mM CaCl<sub>2</sub>; Thermofisher Scientific, Loughborough, UK). No DNase-I was included in the negative control group.

Each treatment was repeated in triplicate wells. For both experiments, microtitre plates were removed from the incubator and the bacteria were sampled from the appropriate wells by gently pipetting the well contents up and down to mix them (aspirating), and then 10 µL of this suspension was spread onto TSA 2% NaCl plates before incubation (48 h, 22°C) and enumeration of CFUs. When required, serial dilutions (1:10) were prepared in round bottom 96-well plates (Sarstedt, Nümbrecht, Germany) before plating onto the agar.

### **5.2.2. Effect of centrifugation on sedimentation of *Vibrio anguillarum* in 96-well culture plates**

To investigate whether low-speed centrifugation of *V. anguillarum* could be effective in bringing the bacteria to the bottom of the well in a 96-well plate, 140 µL of exponential-phase *V. anguillarum* Vib 87 or Vib 6 (suspended in PBS to  $1 \times 10^5$  CFU mL<sup>-1</sup>) was added to wells and centrifuged (510 × g, 10 min, 4°C). Then, 10 µL from the very top or very bottom of the liquid suspension in the well was taken. Each 10 µL sample was serially diluted (1:10) in PBS before plating onto TSA 2% NaCl agar according to Section 4.2 or 3.2.6. Negative control

wells contained the same suspensions as prepared above, except that these microtitre plates were incubated for 10 min at 4°C without centrifugation. Each treatment group was replicated in five wells. The agar plates were incubated for 48 h at 22°C before enumerating CFUs, and comparison was made between CFUs recovered from control wells and from top and bottom of experimental wells.

### **5.2.3. Investigating the effect of ETs on abundance of *Vibrio anguillarum* CFU after co-incubation with bacteria**

To investigate whether the number of viable CFU of *V. anguillarum* is reduced after exposure to ETs released by trout PMN-enriched cell suspensions, *V. anguillarum* Vib 6 and Vib 87 was exposed ETs in wells of a flat-bottom 96-well microtitre plate for up to 4 h. Trout PMN-enriched cell suspensions (isolated by triple-layer Percoll gradients according to Section 2.2.3), were prepared in RPMI2 were seeded to  $4 \times 10^5$  cells mL<sup>-1</sup> in each well (100 µL per well). The PMN-enriched cell suspension was incubated for 30 min at 15°C to allow cells to adhere to the bottom of the polystyrene wells before inducing ET release by addition of 20 µL of Cal solution in dH<sub>2</sub>O (to give a final well concentration of 5 µg mL<sup>-1</sup>) and incubating for a further 3 h. In each well, 24 µL of dH<sub>2</sub>O and 16 µL DNase buffer (final well concentration of 10 mM Tris-HCl, 2.5 mM MgCl<sub>2</sub>, 0.1 mM CaCl<sub>2</sub>) was added and incubated with the plate for 10 min at 15°C. Then, 80 µL of *V. anguillarum* Vib 87 at  $1 \times 10^2$  CFU mL<sup>-1</sup>, or with *V. anguillarum* Vib 6 at  $1 \times 10^3$  CFU mL<sup>-1</sup> (prepared as Section 4.2.2.) was gently pipetted into appropriate wells and the plate was centrifuged (510 × g, 10 min, 4°C). This treatment was designated as (+ ETs), as the ETs were not degraded. An ET-negative treatment group (*i.e.*, - ETs) was included to determine if degrading ETs with DNase-I results in greater number of CFUs recovered. In this well, the PMN-enriched cell suspension was seeded into the well and incubated with Cal as described above, then in each well, 24 µL of DNase-I (final well concentration 10 U mL<sup>-1</sup> diluted in dH<sub>2</sub>O) and 16 µL DNase buffer (same concentration as above) was added before finally adding 80 µL of *V. anguillarum* Vib 87 as above. To control for DNase-I and Cal affecting number of CFUs recovered, a control group (*i.e.*, Vib 87 + Cal + DNase) containing 100 µL of RPMI2 was incubated with 20 µL of Cal, 40 µL of DNase-I, and 80 µL of *V. anguillarum* Vib 87 was prepared as described above. Lastly, to control for and account for the number of bacteria recovered without the presence of cells or reagents, another a control group (*i.e.*, Vib 87 only) containing 100 µL of RPMI2 was incubated with 60 µL of dH<sub>2</sub>O, and 80 µL of *V. anguillarum* Vib 87 was prepared as described above. After centrifugation, the abundance of CFUs in each well was enumerated by aspirating the well contents before plating this across a TSA 2% NaCl plate. Plates were incubated for 24 h at 22°C to allow CFU to form and then, these were counted. Separate wells were made for each time point (including all controls), and CFUs were enumerated before centrifugation (pre-spin), immediately after centrifugation

(0 h), at 1 h and where required additionally at 4 h after incubation 15°C. Triplicate wells were prepared for each treatment. To determine if the nuclease-producing *V. anguillarum* Vib 6 isolate would make any difference to CFUs recovered, this experiment was repeated as above for both *V. anguillarum* Vib 6 and Vib 87 (final well concentration  $1 \times 10^3$  CFU mL<sup>-1</sup>).

#### **5.2.4. Staining and observation of *Vibrio anguillarum* under fluorescence microscopy**

It was desirable to observe directly the interaction of *V. anguillarum* Vib 6 and Vib 87 with trout ETs. To enable this, a strategy was selected to stain the bacteria with the blue fluorescent stain, 4',6-diamidino-2-phenylindole (DAPI; Thermofisher Scientific, Loughborough, UK) while the ETs would be stained separately with the green fluorescent stain, SYTOX Green (Thermofisher Scientific, Loughborough, UK), and then the interaction of bacteria with ETs could be observed by fluorescence microscopy. A PMN-enriched cell suspension was prepared in RPMI2 ( $4 \times 10^5$  cells mL<sup>-1</sup>) and this was used to seed wells of a flat-bottom 96-well culture plate with 100  $\mu$ L of suspension per well. The PMN-enriched cell suspension was incubated for 30 min at 15°C to allow cells to adhere on the polystyrene well surface before inducing ET release with 20  $\mu$ L of Cal (final well concentration of 5  $\mu$ g mL<sup>-1</sup>, 3 h, 15°C). Single colonies of *V. anguillarum* Vib 6 and Vib 87 were inoculated, cultured, and bacterial cell suspensions prepared in PBS as Section 4.2.2. The membrane-permeable nucleic acid stain, DAPI was added to bacterial cultures at exponential growth phase (final well concentration of 1  $\mu$ M) and incubated for 30 min in the dark on ice (Goldmann et al., 2004). Then the DAPI-stained bacteria were pelleted by centrifugation (3000  $\times$  g, 10 min, 4°C) before discarding the supernatant, and washing to remove any unbound DAPI by discarding the supernatant, resuspending the pellet in 5 mL of PBS and centrifuging as before. After three washes, the pellet was resuspended in sterile PBS, the  $A_{600}$  was recorded, and a suspension prepared to  $1 \times 10^8$  CFU mL<sup>-1</sup> in PBS. PMN-enriched cell suspensions that had been induced to form ETs were exposed to *V. anguillarum* Vib 6 or Vib 87 by gently pipetting 80  $\mu$ L of the bacterial suspension into the well, to give a final well concentration of  $4 \times 10^7$  CFU mL<sup>-1</sup>, centrifuging to promote contact (512  $\times$  g, 10 min, 4°C), and then incubating (1 h, 15°C). Extracellular DNA in the wells (*i.e.*, ETs) were stained with 20  $\mu$ L of 55  $\mu$ M SYTOX Green (final well concentration of 5  $\mu$ M). To demonstrate that bacteria were stained with DAPI, a negative control well lacking the PMN-enriched cell suspension (substituted with RPMI2) was included. To confirm that there was no unbound DAPI left in the solution that could stain the PMNs and ETs in suspension, another negative control was included with the well containing PMNs (induced to form ETs as above) incubated with 80  $\mu$ L of bacterial supernatant collected after the final wash. Triplicate wells were prepared per treatment, and the plate was observed using fluorescence microscopy (Olympus IX-70 inverted microscope, Olympus, Essex, UK).

Representative fluorescent images were collected for each of the treatment groups (in DAPI and FITC wavelength channels) and this was achieved with an AxioCam MRC camera paired with the Axiovision (v.4.8) imaging software (Zeiss, Cambridge, UK). Subsequently, images from the different channels were merged using ImageJ (v.1.50i; National Institutes of Health, USA) biological-image analysis software. To directly observe real-time interactions of the bacteria with ETs, real-time videos of *V. anguillarum* Vib 87 co-incubated with ETs in the wells were recorded under phase contrast microscopy with an Olympus IX-70 microscope at  $\times 40$  magnification, using CamStudio software (v.2.7; Techsmith, USA).

### 5.2.5. Statistical analyses

Statistical analyses were performed with Prism v.5.1 (GraphPad, La Jolla, USA). Data from all experiments involving CFU enumeration were tested for normality and equality of variances using the Kolmogorov–Smirnov and Bartlett’s tests, respectively. When data were normal, the Student’s t-test (two-tailed) was performed to compare differences in mean bacteria CFUs recovered after incubation with Cal and DNase-I at each time point, and to calculate significant differences in mean bacteria CFUs recovered before and after low-speed centrifugation from the top and bottom of the wells. A One-Way ANOVA with Bonferroni’s post-hoc test was used to compare differences in mean CFUs recovered at each time point after incubation with ETs. For all analyses,  $p < 0.05$  was considered statistically significant.

## 5.3. Results

### 5.3.1. Effect of calcium ionophore and DNase-I on viability of *Vibrio anguillarum*

The concentrations of reagents used to induce and degrade ETs for the subsequent experiments were checked for their effect on bacterial viability. Incubation of *V. anguillarum* Vib 87 ( $1 \times 10^3$ ,  $10^4$ , and  $10^5$  CFU mL<sup>-1</sup>) in 5  $\mu$ g mL<sup>-1</sup> Cal for 1, 2, and 4 h did not result in a significant difference in mean bacterial CFUs recovered compared to incubations lacking Cal (Figure 5.1). Also, incubation of *V. anguillarum* Vib 6 and Vib 87 ( $1 \times 10^3$  CFU mL<sup>-1</sup>) in 10 U mL<sup>-1</sup> DNase-I also did not result in a significant difference in CFUs mean recovered compared to incubations lacking DNase-I (Figure 5.2).



### 5.3.2. Investigating the effect of centrifugation on *Vibrio anguillarum* sedimentation in 96-well culture plates

Low speed centrifugation (510 x g, 15 min, 4°C) of *V. anguillarum* Vib 87 ( $\times 10^5$  CFU mL<sup>-1</sup>) in flat-bottom 96-well plates resulted in significantly greater ( $p < 0.05$ ) abundance of CFU at the bottom of the well ( $1.58 \times 10^5 \pm 4.73 \times 10^4$  CFU mL<sup>-1</sup>) by 2.34 times compared to the bottom wells from the plate that had not been centrifuged ( $4.72 \times 10^4 \pm 6.80 \times 10^3$  CFU mL<sup>-1</sup>), (Figure 5.3). At the top of the wells, there was significantly fewer ( $p < 0.05$ ) abundance of CFU ( $2.44 \times 10^3 \pm 4.84 \times 10^2$  CFU mL<sup>-1</sup>) containing 3/50 bacteria compared to the top of wells from the plate that had not been centrifuged ( $4.00 \times 10^4 \pm 8.82 \times 10^2$  CFU mL<sup>-1</sup>), (Figure 5.3). Taken together, these results show that low speed (510 x g) centrifugation successfully collects *V. anguillarum* bacterial cells to the bottom of the wells in flat-bottom 96-well plates.

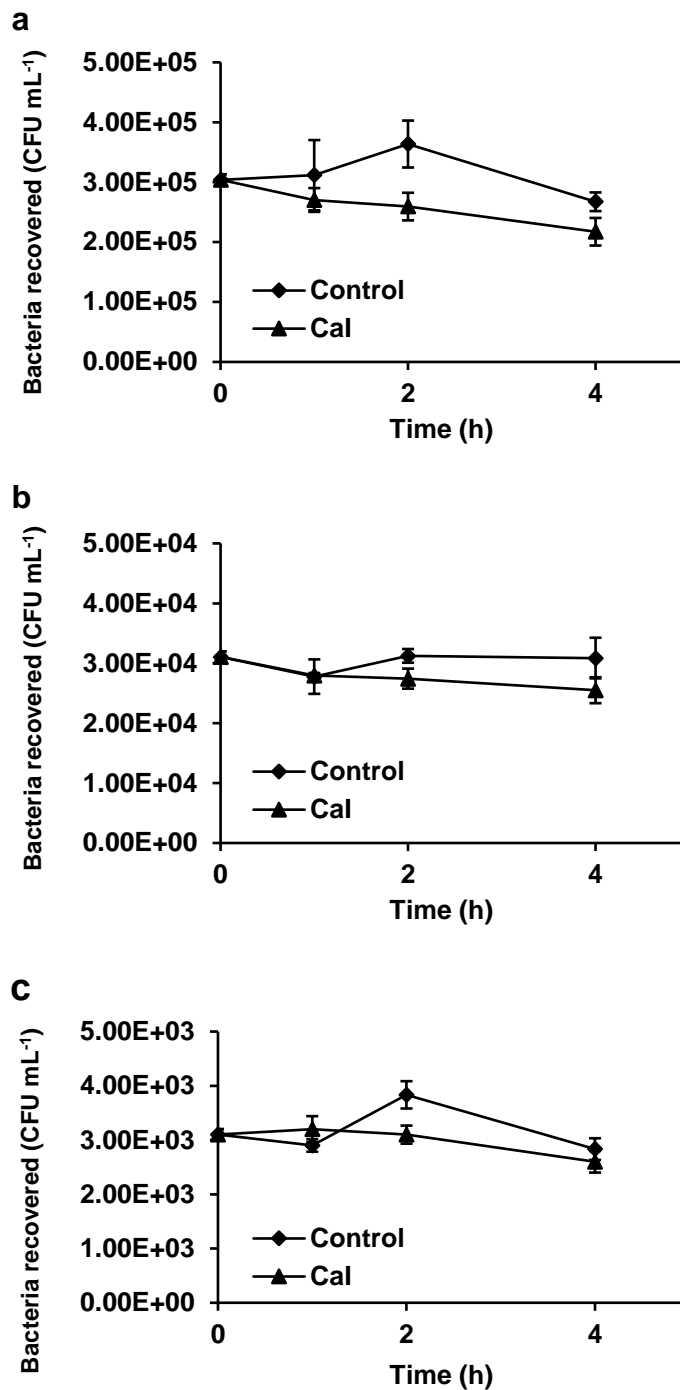


**Figure 5.1.** Scatterplot showing the relationship between *V. anguillarum* Vib 87 viability over time (as measured by mean CFU recovered from the well) in the presence or absence of Cal ( $5 \mu\text{g mL}^{-1}$ , 4 h,  $22^\circ\text{C}$ ). Suspensions of *V. anguillarum* Vib 87 in PBS were tested at (a)  $10^5 \text{CFU mL}^{-1}$ ; (b)  $10^4 \text{CFU mL}^{-1}$ ; and (c)  $10^3 \text{CFU mL}^{-1}$ . No significant differences were detected between mean CFU recovered from wells with and without Cal at each bacterial concentration and time point ( $p < 0.05$ ). Error bars represent s.e.m.  $n = 3$

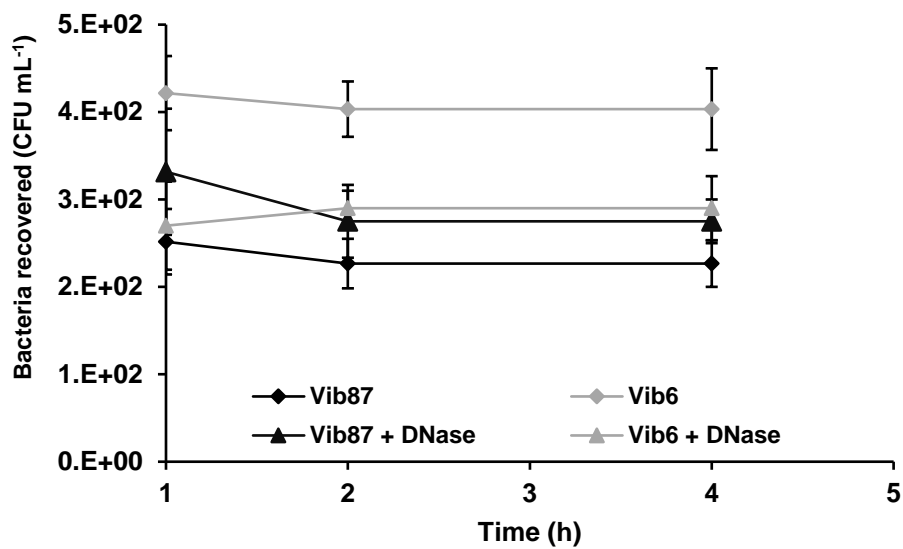


**Figure 5.2.** Scatterplot showing the relationship between *V. anguillarum* Vib 87 and Vib 6 ( $10^3$  CFU mL<sup>-1</sup>) viability over time (as measured by mean CFU recovered from the well) in the presence or absence of DNase-I ( $100$  Ut mL<sup>-1</sup>, 4 h, 22°C). No significant differences were detected between mean CFU recovered from wells with DNase-I or control treatments (dH<sub>2</sub>O with DNase buffer) at each time point ( $p > 0.05$ ). Error bars represent s.e.m.  $n = 3$ .

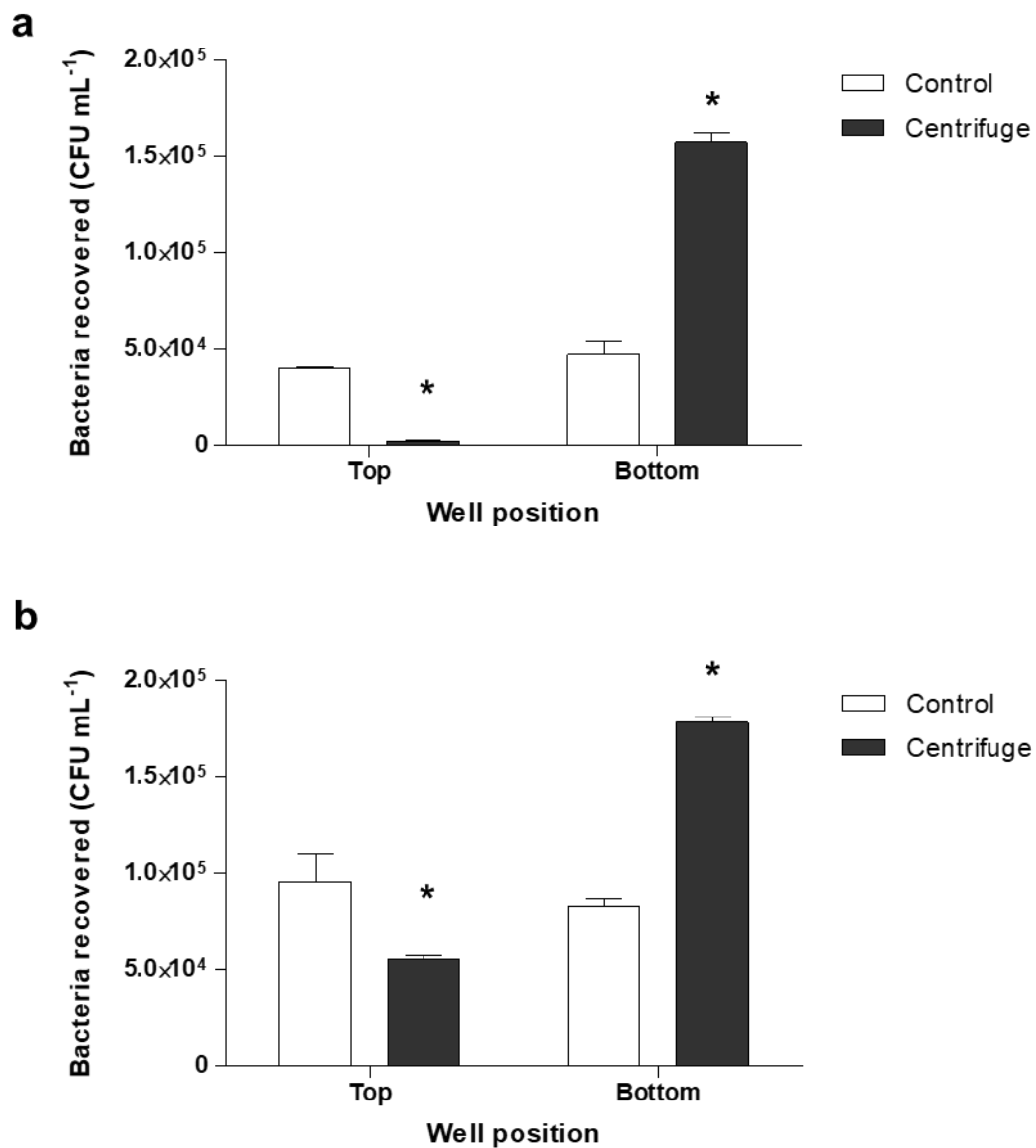


**Figure 5.3.** Bar graph showing (a) *V. anguillarum* Vib 87, (b) *V. anguillarum* Vib 6 ( $10^4$  CFU mL<sup>-1</sup>) bacterial CFU recovered from different positions within a well of a 96-well plate after centrifugation (510 × g, 10 min, 22°C). Wells subjected to centrifugation had significantly fewer CFU recovered at the top of the well compared to the top of non-centrifuged control wells; while significantly greater CFU was recovered from the bottom of centrifuged wells compared to the bottom of non-centrifuged control wells. \* $p < 0.05$ . Error bars represent s.e.m.  $n = 3$ .

### 5.3.3. Investigating the effect of ETs on abundance of CFU after co-incubation with bacteria

Incubation of the nuclease-deficient *V. anguillarum* Vib 87 with pre-induced trout ETs resulted in 0.27 times lower CFUs recovered from the wells at 0 h ( $78 \pm 7$  CFU) compared to wells treated with exogenous DNase-I ( $10 \text{ U mL}^{-1}$ ) to digest ETs ( $107 \pm 11$  CFU),  $p < 0.05$  (Figure 5.4). A similar pattern was observed at 1 h, where 0.26 times less CFUs were recovered when wells contained intact ETs ( $85 \pm 10$  CFU) compared to wells treated with DNase-I ( $115 \pm 9$  CFU)  $p < 0.05$  (Figure 5.4). Conversely, there was no significant difference between CFUs recovered from wells with DNase-treated ETs compared to control wells with only the bacteria at 0 and 1 h, indicating DNase-I was sufficient to degrade the ETs and preventing bacteria trapping in the ETs,  $p > 0.05$  (Figure 5.4). Without centrifugation, the 'pre-spin' treatment group did not show any significant difference in CFUs recovered between treatments,  $p > 0.05$  (Figure 5.4), indicating centrifugation was required to promote interaction between the ETs and bacteria. Overall, the reduced number of CFUs recovered in wells with ETs is indicative of trapping action, though the results do not confirm if the ETs are killing or merely trapping the bacteria.

As exogenous DNase-treatment could prevent the reduced the amount of CFUs recovered (indicating no trapping) after co-incubating the nuclease-deficient *V. anguillarum* Vib 87 with ETs (Figure 5.4), the nuclease-producing *V. anguillarum* Vib 6 was tested to see if its natural production of extracellular nuclease activity was sufficient reduce bacterial CFU recovery (*i.e.*, prevent trapping). Both *V. anguillarum* Vib 6 and Vib 87 ( $10^3$  CFU) were incubated with pre-induced ETs for 0, 1 and 4 h, and the amount of CFUs recovered was compared to after degrading the ETs with DNase-I ( $10 \text{ U mL}^{-1}$ ). *V. anguillarum* Vib 87 was used to confirm that the ETs exerted ability to reduce CFUs recovered at each time point  $p < 0.05$  (Figure 5.5a). With *V. anguillarum* Vib 6, no significant differences between CFU recovery was observed at each time point when ETs were present compared to when ETs were degraded by DNase-I,  $p > 0.05$  (Figure 5.5b). Collectively, these data suggest that trapping, but not killing of the *V. anguillarum* Vib 87 by the ETs occurs within 4 h, while *V. anguillarum* Vib 6 were not affected by the ETs.

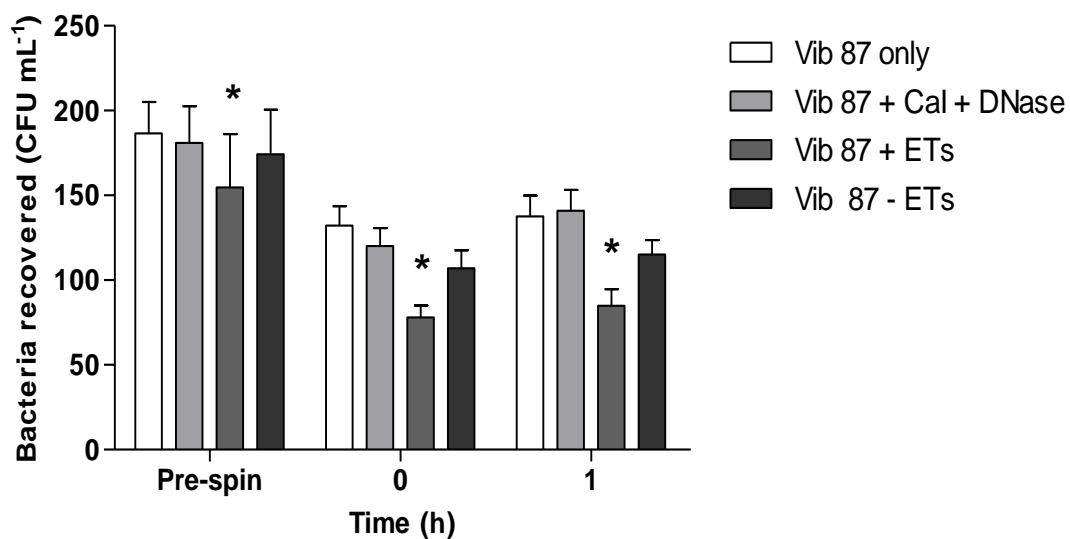


**Figure 5.4.** Bar graph showing the amount of *V. anguillarum* (Vib 87) CFUs recovered after incubation with trout extracellular traps (released from PMN-enriched cell suspensions after incubation with Cal 5  $\mu\text{g mL}^{-1}$ ) at 15°C. CFUs was sampled before centrifugation (pre-spin), immediately after centrifugation (0 h), and 1 h at 15°C. *V. anguillarum* Vib 87 was incubated with cell media as a control (Vib 87 only), with Cal and DNase (Vib 87 + Cal + DNase), in the presence of ETs (Vib 87 + ETs), and with DNase-degraded ETs (Vib 87 - ETs). No significant differences of CFUs were found between all treatments before centrifugation (pre-spin). Immediately after centrifugation (0 h), the Vib 87 + ETs treatment resulted in significantly less CFUs recovered than *V. anguillarum* Vib 87 – ETs; which was also observed after 1 h incubation. \* $p < 0.05$ . Error bars represent s.e.m.  $n = 6$ .

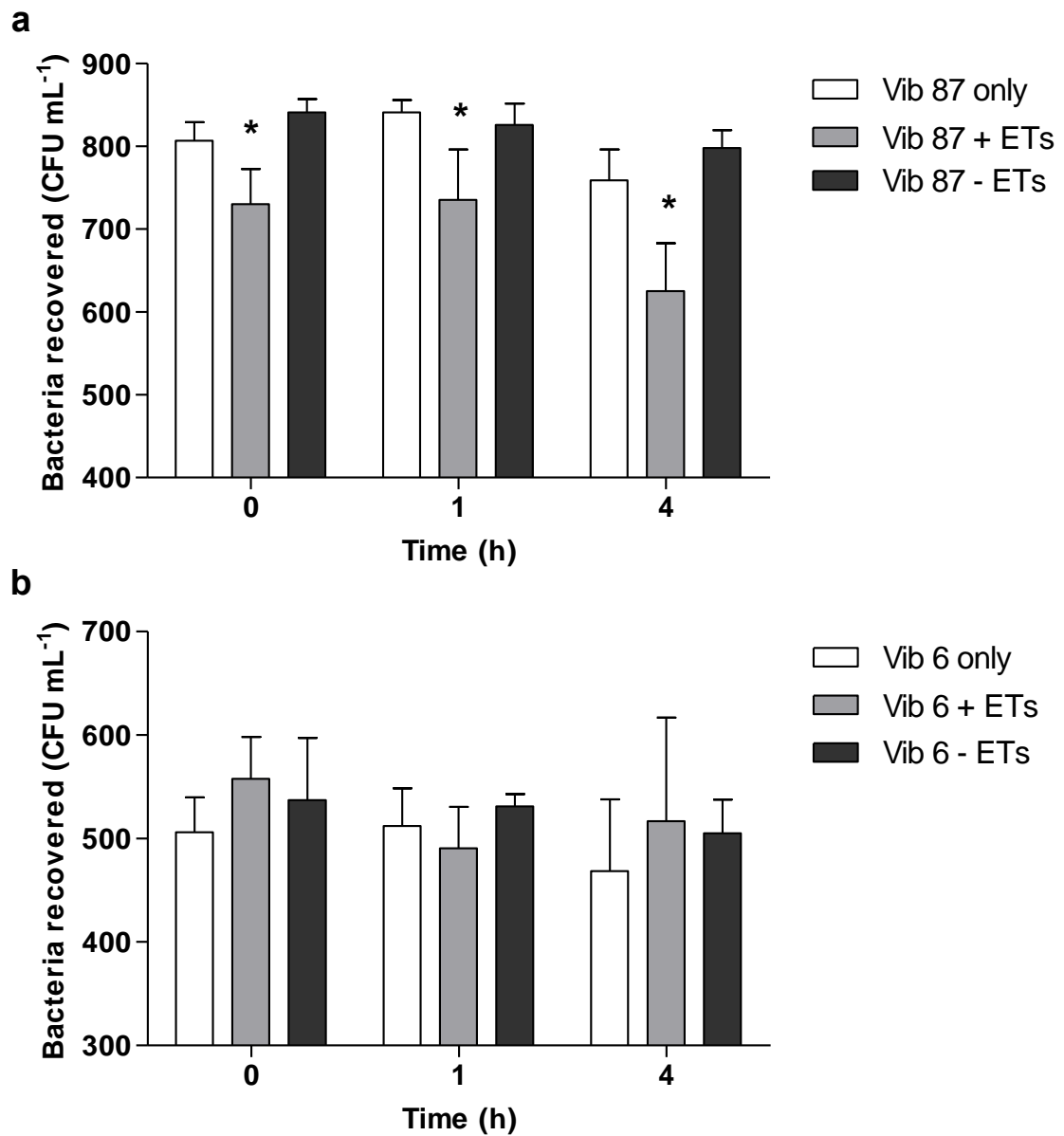


**Figure 5.5.** Bar graph showing the amount of *V. anguillarum* CFUs recovered (comparing Vib 87 and Vib 6) after incubation with trout extracellular traps (released from PMN-enriched cell suspensions after incubation with Cal 5  $\mu\text{g mL}^{-1}$ ) at 15°C. (a) *V. anguillarum* Vib 87 CFUs recovered after incubation with ETs (Vib + ETs) resulted in significantly less CFUs at 0, 1 and 4 h at 15°C when compared to incubation with DNase-digested ETs (Vib - ETs) and controls without cells (Vib 87 only). (b) Vib 6 CFUs recovered after incubation with ETs (Vib 6 + ETs) was not significantly different from the DNase-digested ETs (Vib 6 - ETs) and Vib 6 only controls at 0, 1, and 4 h at 15°C. \* $p < 0.05$ . Error bars represent s.e.m.  $n = 3$ .

#### 5.3.4. Confirming *Vibrio anguillarum* interaction with ETs by microscopy

To observe interaction between the bacteria and the ETs, bacteria and ETs were separately stained with DAPI (1  $\mu$ M) and SYTOX Green (5  $\mu$ M), respectively, before adding bacteria to pre-induced ETs *in vitro*, and directly observing the interaction with fluorescence microscopy. The wells containing *V. anguillarum* Vib 87 and ETs showed distinct ET fibres that occasionally formed aggregated meshes (Figure 5.6, Figure 5.7). Co-localisation between *V. anguillarum* Vib 87 and ET fibres was observed, as there was a visibly more abundant amount of DAPI-stained bacteria overlapping the SYTOX Green-stained ET fibres (Figure 5.6, Figure 5.7). Conversely, ETs fibres appeared to be broken up when incubated with the nuclease-producing *V. anguillarum* Vib 6 isolate (Figure 5.7). These wells appeared to contain fragmented extracellular DNA that shows no cohesive structure (Figure 5.7) compared to the ETs incubated with the nuclease-deficient *V. anguillarum* Vib 87 (Figure 5.7). Collectively, this suggests that the nuclease produced by *V. anguillarum* Vib 6 is responsible for degrading the ETs. The removal of residual DAPI after staining was confirmed as the supernatant of DAPI-stained *V. anguillarum* Vib 87 after the final wash did not stain ETs (Figure 5.6).

Finally, video recordings were taken of live *V. anguillarum* Vib 87 incubated with Cal-induced trout ETs under phase contrast microscopy (magnification  $\times 20$ ) to demonstrate the interaction live bacteria with the ETs. The real-time videos recordings showed highly abundant bacteria appearing stuck to, and entirely covered the ET fibres, with the thinner ET strands appearing to be mechanically perturbed by the locomotive force of the bacteria's flagellum. In areas without fibres, bacteria were much less abundant and free-swimming in solution (Figure 5.8).



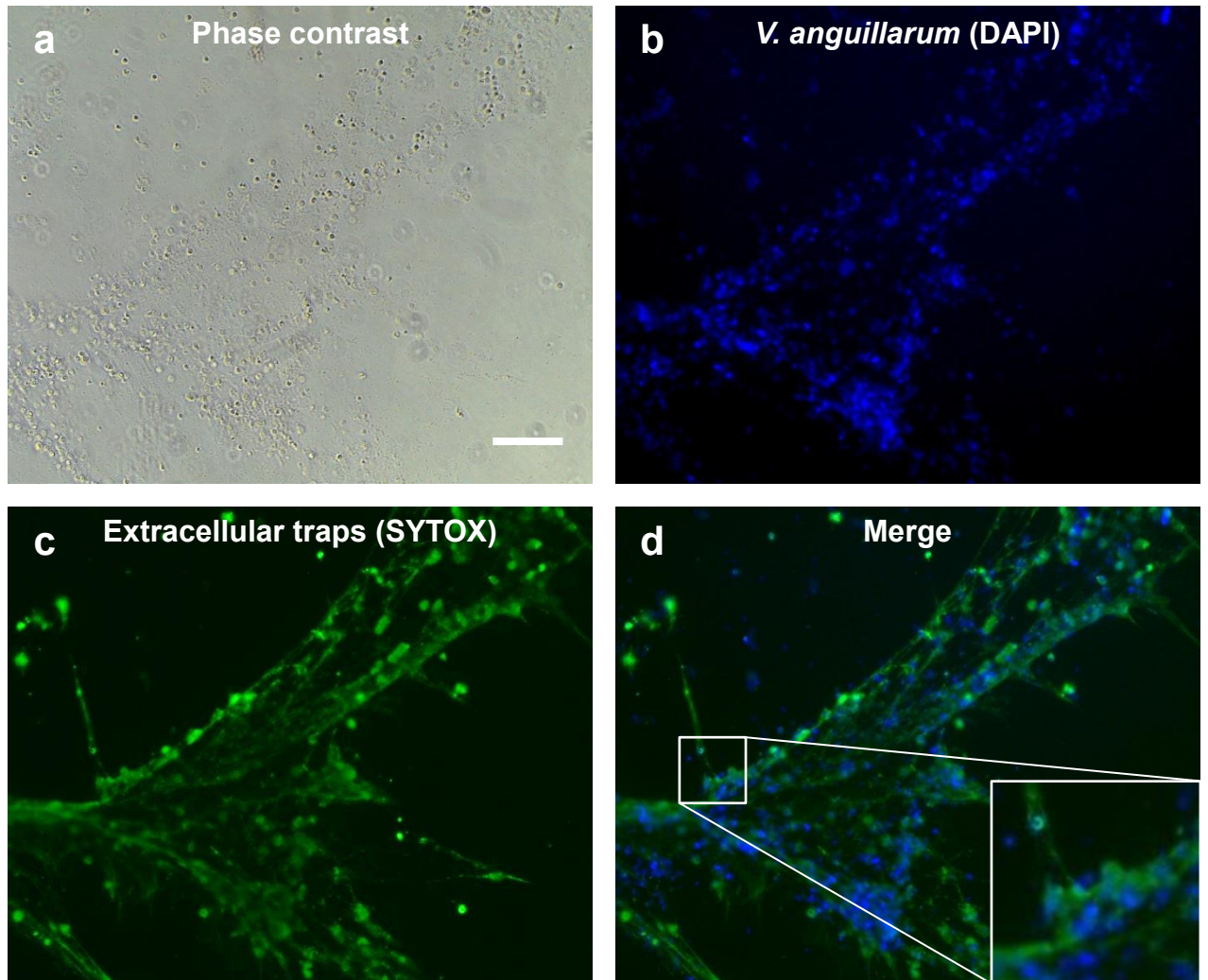


**Figure 5.6.** Representative phase contrast and fluorescent images showing co-localisation of *V. anguillarum* Vib 87 stained by DAPI (1  $\mu$ M) incubated with trout ETs ( $4 \times 10^7$  CFU mL<sup>-1</sup>, 1 h, 15°C) generated from Cal-induced PMN-enriched cell suspensions ( $4 \times 10^5$  CFU mL<sup>-1</sup>, 30 min, 15°C). ETs were stained with SYTOX Green (5  $\mu$ M, 5 min). (a) Trout PMNs and *V. anguillarum* Vib 87 under phase contrast; (b) DAPI channel showing DAPI-stained *V. anguillarum* Vib 87 in blue; (c) FITC channel showing a mesh of trout ETs stained with SYTOX Green; (d) Merged DAPI and FITC images which show *V. anguillarum* Vib 87 in blue co-localising with ETs in green. The magnified section shows a distinction between staining of the bacteria and extracellular traps, confirming no counterstaining was occurring between the DAPI and SYTOX Green. Scale bar = 100  $\mu$ m, all images were taken at the same magnification.

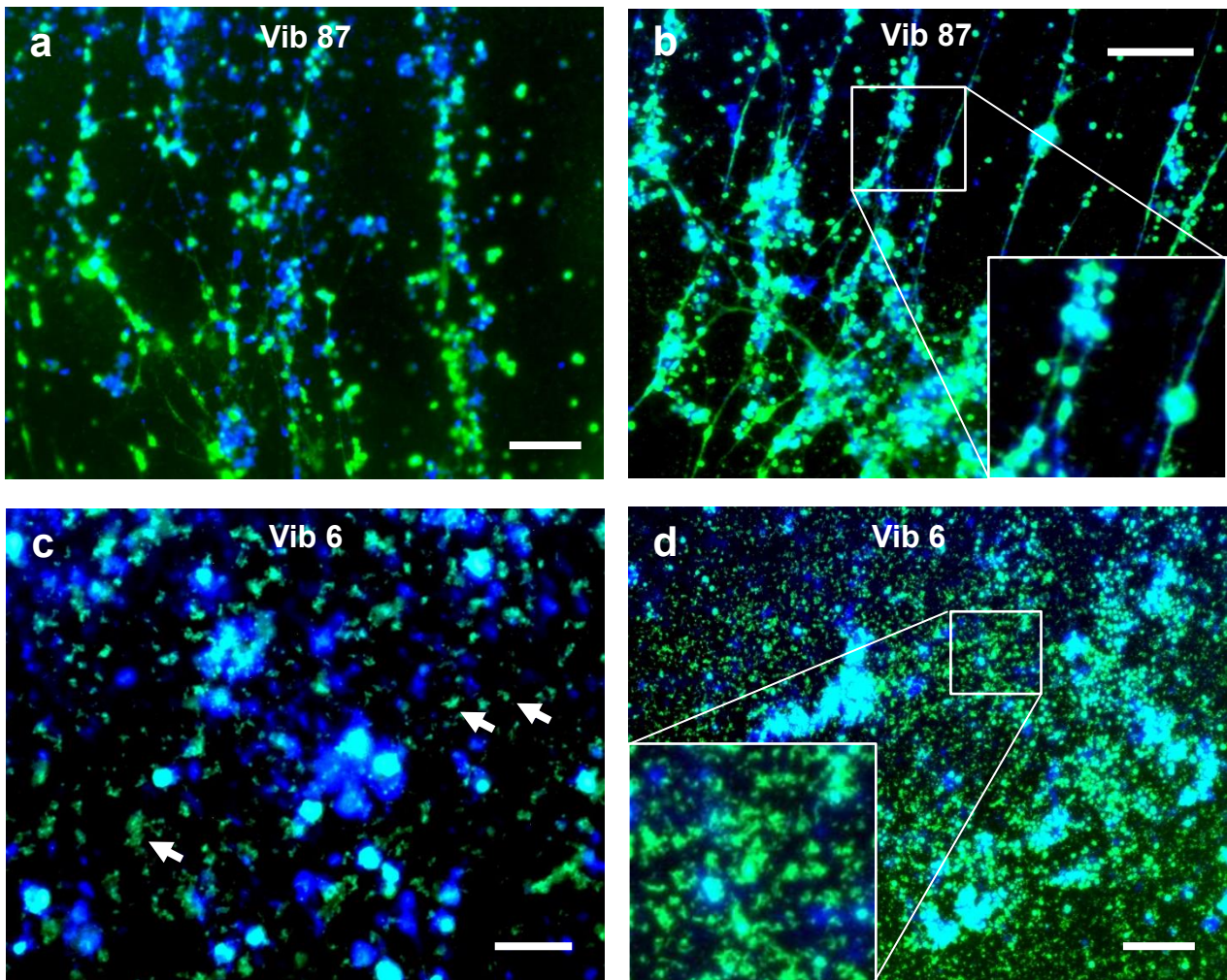


**Figure 5.7.** Representative fluorescent microscopy images with both DAPI and FITC channels merged together showing wells containing *V. anguillarum* Vib 87 or Vib 6 co-incubated with trout ETs ( $4 \times 10^7$  CFU mL<sup>-1</sup>, 1 h, 15°C) released from Cal-induced PMN-enriched cell suspensions ( $4 \times 10^5$  cells mL<sup>-1</sup>, 30 min, 15°C). *V. anguillarum* was stained blue by DAPI (1 μM) while ETs were stained green by SYTOX Green (5 μM). (a-b) Shows nuclease-deficient *V. anguillarum* Vib 87 co-incubated with ET fibres which were still intact after incubation for 1 h; while (c-d) shows nuclease-producing *V. anguillarum* Vib 6 co-incubated with ET fibres which appeared fragmented without cohesive structure, suggesting the action of the nuclease is responsible for degrading the ETs. White arrows (c) indicate the remaining fragments of DNA which do not hold a fibrous structure, indicating nuclease from *V. anguillarum* Vib 6 degrades the ETs. Scale bars = 100 μm



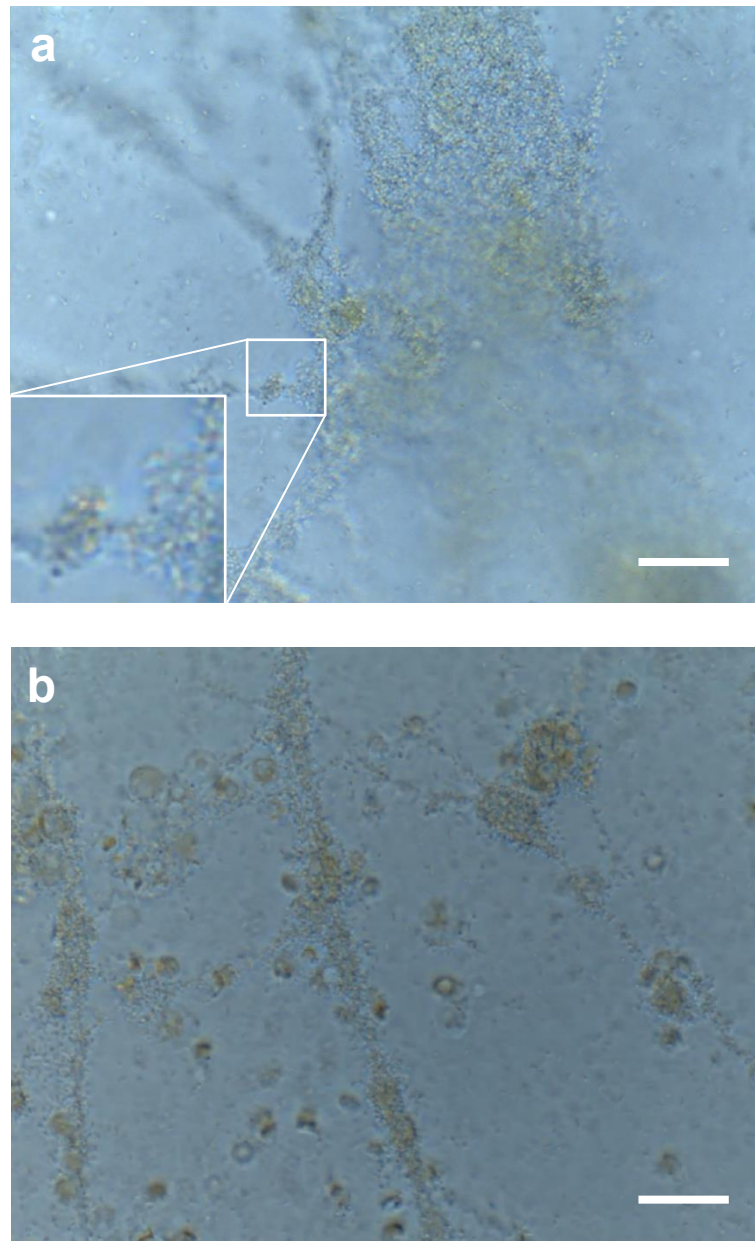


**Figure 5.8.** Representative screen-captures from phase contrast videos showing wells containing *V. anguillarum* Vib 87 co-incubated with trout ETs ( $4 \times 10^7$  CFU mL<sup>-1</sup>, 1 h, 15°C) released from Cal-induced PMN-enriched cell suspensions ( $4 \times 10^5$  cells mL<sup>-1</sup>, 30 min, 15°C). Videos (a) and (b) were taken from different wells, both showing the highly motile *V. anguillarum* Vib 87 appearing stuck to, and entirely covered the ET fibres. Free-swimming bacteria can also be observed in the video. The magnified section shows a close-up of an ET appeared to be covered in the grainy-looking bacteria. Magnification  $\times 20$ ; scale bar = 100  $\mu$ m. Videos can be found online using links of Video (a): <https://goo.gl/GQGpHo> ; Video (b) <https://goo.gl/qXYDSb>

## 5.4. Discussion

The data generated in this Chapter is the first to show that *V. anguillarum* can utilise extracellular nuclease(s) to evade trapping by trout ETs, which may potentially contribute to pathogenesis. ETs released from trout PMN-enriched cell suspensions significantly reduced bacterial CFUs after co-incubation with an extracellular nuclease-deficient *V. anguillarum* isolate (Vib 87) compared to controls, indicating a trapping or killing function for the ETs. Meanwhile, degradation of the ETs with the addition of exogenous DNase-I negated this reduction in CFUs. Co-incubation of a nuclease-producing *V. anguillarum* isolate (Vib 6) with ETs did not lead to a significant reduction in CFU compared to controls, suggesting a possible role for nuclease against trapping or killing by ETs. Microscopic observation revealed that *V. anguillarum* Vib 87 appeared to co-localise with ETs, while *V. anguillarum* Vib 6 appeared to degrade the ETs and not co-localise with ETs.

The reduction in recovered *V. anguillarum* Vib 87 CFUs may result from either the ETs killing the bacteria or trapping the bacteria on or within the structure, thus aggregating the bacteria and meaning that subsequent suspensions may appear to contain fewer CFU. In support of this, video recordings under the light microscope showed highly motile *V. anguillarum* Vib 87 had stuck to, and entirely covered the ET fibres, with thinner ET strands being mechanically perturbed by the locomotive force of the bacteria's flagellum (Figure 5.8). Addition of exogenous DNase-I to degrade to ETs before addition of the bacteria resulted in more CFU counts, indicating that the nuclease activity of DNase-I degraded the DNA polymers that provides the structural integrity and trapping properties to the ETs. Thus, *V. anguillarum* Vib 87 did not have an ET scaffold to bind to and result in a lower CFU. Similarly, the co-culture of *V. anguillarum* Vib 6 also resulted in more CFU counts compared to controls without ETs, and the extracellular nuclease produced by *V. anguillarum* Vib 6 is also presumed to degrade the ETs. In support of these data, observations of co-cultures of bacteria with ETs by fluorescent microscopy showed that *V. anguillarum* Vib 87 co-localised with intact ET fibres (Figure 5.6 and Figure 5.7), while co-cultures of nuclease-producing *V. anguillarum* Vib 6 with ETs under the same conditions showed the ETs to be degraded (Figure 5.7), thereby confirming the degradation of ETs by extracellular nuclease. Furthermore, *V. anguillarum* Vib 87 appeared to stick to and aggregate on and within the ET fibres when observed under phase contrast microscopy (Figure 5.8). Taken together, these data demonstrate that trout ETs released by PMNs can trap the nuclease-deficient *V. anguillarum* Vib 87 but not *V. anguillarum* Vib 6, which may evade trapping by way of extracellular nuclease activity that degrades the ET fibres.

The reduced CFU recovery (*i.e.*, trapping) measured with co-cultures of *V. anguillarum* Vib 87 and ETs was not as prominent as expected (Figure 5.6 and Figure 5.7). One explanation for the difficulty of detecting reduced CFU recovery could be that the ET may have been saturated

by the bacteria. This problem could be resolved by generating greater ET density through increasing the concentration of PMNs in the suspension; however, direct observation of released ETs *in vitro* showed that ETs tend to clump heavily when greater densities of PMNs were used (data not shown), which might reduce the surface area of ETs to size ratio which bacteria can attach. Another explanation can be attributed by the variability of ET fibre morphology produced *in vitro*, which might influence the trapping efficacy of the ETs (Sollberger *et al.*, 2016); however this was not examined and warrants further investigation. Fluorescent images of SYTOX Green-dyed ETs trapping DAPI-stained *V. anguillarum* Vib 87 show web-like ETs in some cases (Figure 5.6), though smaller, comet-like ETs (Figure 5.7a, b) might be less effective at trapping in comparison due to a smaller relative surface area (Sollberger *et al.*, 2016). Additionally, the physical structure of the ETs was delicate and sensitive to movement in culture plates, as knocking or perturbing the plates often resulted in the ETs detaching from the surface of the wells and shrinking (probably due to elastic properties), and this was confirmed by direct microscopic observation (data not shown). Thus, the data showing CFU recovered from the well after co-incubation with released ETs may not completely reflect the trapping potential of ETs, as trapping is difficult to quantify and often leads to the use of qualitative data to support and demonstrate bacterial interaction (de Buhr *et al.*, 2016).

Short-duration centrifugation at relatively low speeds ( $510 \times g$ ) that caused the *V. anguillarum* to collect at the bottom of wells in a 96-well plate was a crucial step when examining the possible trapping and killing of bacteria by the ETs *in vitro*. This was demonstrated as CFUs of *V. anguillarum* Vib 87 did not reduce in the presence of ETs when centrifugation was not used (Figure 5.4), and the centrifugation likely promotes contact between bacteria and ETs as the latter are also mostly located at the bottom of the wells when released from PMNs (observed in Chapter 3, Section 3.3.6).

The rapid and simple method used to stain *V. anguillarum* and trout ETs separately with DAPI and SYTOX Green was adapted from the method described above by von Köckritz-Blickwede, *et al.* (2010) but instead was used in this Chapter for qualitative analysis. In this Chapter, *V. anguillarum* was successfully labelled with DAPI and the supernatant of DAPI-stained *V. anguillarum* did not stain ETs (Figure 5.6). Other methods to quantify *V. anguillarum* trapping were considered, such as staining bacteria and ETs separately with fluorescent markers, and then determining the co-localisation by measuring the ratio of the different markers as an indicator of trapping (von Köckritz-Blickwede *et al.*, 2010; Brogden *et al.*, 2014). However, the frequent wash steps required in this method can remove unbound bacteria and disrupt the ETs, thereby impacting negatively on the accuracy and reliability of the data (von Köckritz-Blickwede *et al.*, 2010). Quantifying the trapping as performed by von Köckritz-Blickwede, *et al.* (2010) may be additionally complicated due to the variation in results caused by clumping

of ETs, which may artificially increase the fluorescence emitted (Waters, 2009). The typical method to visualise bacterial interaction with ETs requires immunostaining, though the availability of antibodies to specific bacteria or markers of fish cells are limited (Randelli *et al.*, 2008). Using nucleic acid stains rather than antibodies may be a suitable alternative when performing larger trapping screens on several different species of bacteria by eliminating the need for bacteria-specific fluorescent markers. However, one drawback is that DAPI is non-specific for the nucleic acids that it stains, meaning any contamination of the culture can result in a false positive.

Although ETs contain a range of antimicrobial peptides (at least histones and neutrophil elastase in trout) that are known to directly kill microbes, from the results from this present study it is not possible to conclude whether the ETs can kill *V. anguillarum*, and killing by ETs has been difficult to confirm (Yipp *et al.*, 2013). Studies in flatfish used reductions in bacterial CFU as evidence of trapping and supported these data with scanning electron microscopy, showing bacteria co-localising with ETs (Chi *et al.*, 2015; Zhao *et al.*, 2017). Both *Pseudomonas fluorescens* and *E. coli* were susceptible to trapping by tongue sole ETs (Zhao *et al.*, 2017). Trapping was more effective with *E. coli* as a significant reduction in CFUs compared to controls were detected much earlier (1 h) than with *Pseudomonas fluorescens* (at 4 h and later) (Zhao *et al.*, 2017). In contrast, *E. tarda* showed no significant susceptibility to trapping by tongue sole ETs and the authors proposed that *E. tarda* has an undefined mechanism to resist the antimicrobial effect of ETs (Zhao *et al.*, 2017). In this Chapter, the ETs were pre-degraded with DNase-I before *V. anguillarum* was added, thus, the bacteria were never exposed to intact ETs and the fate of *V. anguillarum* (*i.e.*, trapping or killing) cannot be concluded. Future experimental designs would aim to co-culture bacteria with ETs and subsequently liberate the entrapped bacteria with DNase-I to determine if the trapped *V. anguillarum* Vib 87 were indeed killed by ETs.

When investigating the trapping and killing effect of ETs on *V. anguillarum*, phagocytosis was not blocked because chemical inhibitors of phagocytosis such as cytochalasin D can inhibit ET release and induce cell death of trout PMN-enriched cell suspensions (Section 3.3.4). A similar observation is found in human neutrophils, as incubation with chemical ET inducers also abolished phagocytic activity without the use of phagocytosis inhibitors within 1 h (Fuchs *et al.*, 2007). This is likely due to the fact that many of the cells are dying when releasing ETs, thus leaving few cells alive to phagocytose the bacteria (Fuchs *et al.*, 2007). In this Chapter, Cal was used to induce ET release before the addition of *V. anguillarum*, and Cal can induce a high proportion of cells in rainbow trout PMN-enriched cell suspensions to release ETs and therefore lyse (Section 3.3.5). As a result, it is likely that most of the cells within the PMN-enriched suspensions die from exposure to Cal and cannot participate in phagocytosis. This is supported by the lack of reduction in *V. anguillarum* Vib 6 or Vib 87 CFUs from wells

containing DNase-degraded ETs compared to control wells containing only bacteria. A reduction in CFUs observed in wells containing DNase-degraded ETs (released by PMN-enriched cell suspensions) might be explained by phagocytosis rather than due to ETs, though no reduction in *V. anguillarum* CFU was observed in these conditions.

Nuclease production by human microbial pathogens was previously found to degrade ETs which can contribute to pathogenesis in mammalian models (Seper *et al.*, 2013; de Buhr *et al.*, 2015; Storisteanu *et al.*, 2017). With respect to fish, nucleases produced by the fish pathogen, *Aeromonas hydrophila*, was found to degrade ETs released by carp PMN enriched cell suspensions (Brogden *et al.*, 2012). However, the pathogenic significance of this was not initially clear until a recent study showed that nuclease-deficient *Aeromonas hydrophila* mutants were more susceptible to killing by blunt-snout bream (*Megalobrama amblycephala*) head kidney leukocyte suspensions compared to the nuclease-producing wild-type strain (Ji *et al.*, 2015). In addition, challenging the fish with the nuclease-deficient *A. hydrophila* also resulted in greater survival compared to wild-types (Ji *et al.*, 2015); though these authors did not show whether degradation of ETs within the fish was responsible for the greater virulence. Nevertheless, these studies signify a link between nuclease production and ET resistance, and it is likely that nuclease production by *V. anguillarum* may also contribute to pathogenesis in fish through degrading ETs, though future work will have to investigate the relationship between the degradation of ETs by *V. anguillarum* and virulence of this pathogen in fish.

## Chapter 6: General Discussion

Aquaculture plays a salient role in global food production and can reduce the pressures on wild fisheries (Forti, 2017). Salmonids are one of the most valuable fish for consumption and these species contribute 17% of total exports by value, and farmed salmonids exceeds 2 million tonnes per year compared to 700,000 tonnes supplied from wild fisheries (FAO, 2017). However, infectious microbial diseases continue to cause considerable economic losses on farms, with associated negative impacts on animal welfare (Lafferty *et al.*, 2015; Ababouch *et al.*, 2016). Antibiotics and the introduction of vaccines have helped to combat infectious diseases, though there remains diseases for which successful or commercially-available vaccines are unavailable (Birkbeck *et al.*, 2002; Metselaar *et al.*, 2010; Hoare *et al.*, 2017). Importantly, the overuse of antibiotics has led to the development of bacterial resistance, which can render certain antibiotics ineffective (Cabello, 2006; Watts *et al.*, 2017). To address this issue, there is a need to better understand the immune systems of fish and their interaction with microbial pathogens, as this may lead to the development novel and alternative therapeutics to treat infectious diseases in aquaculture.

The aim of this thesis was to characterise extracellular traps (ETs) from rainbow trout (*Oncorhynchus mykiss*) and to investigate their antimicrobial properties. Initially, suitable methods to isolate and enrich for trout polymorphonuclear cells (PMNs; *i.e.*, the neutrophil-like cells in fish) and to measure the release of ET-like structures from enriched cell suspensions had to be selected, developed and validated (Chapter 2). The ET-like structures observed to be released in PMN-enriched cell suspensions were confirmed to be ETs by the detection of a suite of diagnostic ET-associated protein markers. Furthermore, an array of known ET-inducers and inhibitors were evaluated to identify those with similar actions reported previously, and these experiments provided insight into the possible cell signalling mechanisms involved ET release from trout PMNs (Chapter 3). A collection *Vibrio anguillarum* isolates were screened for extracellular nuclease activity and one highly active isolate was used to demonstrate that the bacterial-derived nuclease activity can degrade the nucleic acid structure of the ETs and the DNA in fish skin mucus (Chapter 4). Moreover, trout ETs displayed antimicrobial activity through trapping a nuclease-deficient isolate of *V. anguillarum*; though, importantly, the production of extracellular nuclease activity did allow *V. anguillarum* to evade this trapping effect; though we do not know whether this prevents pathogenicity of disease development (Chapter 5). The present study provides a platform for further research leading to investigations on the *in vivo* significance of ET release in trout.

The aim of Chapter 2 was to evaluate and validate repeatable and high throughput methods to obtain enriched populations of viable PMNs from rainbow trout head kidney samples and to quantify ET-like structures *in vitro*. A discontinuous Percoll gradient similar to one used to



enrich for PMNs from Atlantic salmon (*Salmo salar*) (Øverland *et al.*, 2010) was used on trout head kidney tissue, and gave cell suspensions containing up to 58% PMNs. Exposure of PMN-enriched cell suspensions to SYTOX Green, a membrane-impermeable dye specific for nucleic acids, revealed ET-like structures under fluorescence microscopy; however, these were not yet confirmed to be ETs because this necessitated the identification of diagnostic markers associated with the structure. The abundance of these ET-like structures in the wells correlated significantly with the fluorescence signal emitted from SYTOX Green-stained cell suspensions, indicating that a fluorometric assay would be suitable for quantifying ET release. Measuring the release of ETs with a fluorometric assay was favoured over counting ETs by fluorescence microscopy due to greater throughput and objectivity (Maini *et al.*, 2016).

The aim of Chapter 3 was to confirm that the ET-like structures observed in Chapter 2 were indeed ETs, and to test whether inhibitors and inducers of ET release from other fish species were similarly effective against PMN-enriched cell suspensions from rainbow trout. The ET-like structures were degraded in a dose-dependent manner by recombinant deoxyribonuclease-I (DNase-I), which confirmed a nucleic acid structure. These nucleic acid structures were determined to be chromatin released from PMNs due to co-localisation of histone subunits (H2A) and the granule proteins, neutrophil elastase (NE) and myeloperoxidase (MPO), and the presence of these granule and nuclear proteins on the extracellular DNA satisfies the diagnostic definition of ETs (Brinkmann *et al.*, 2004; Fuchs *et al.*, 2007). Thus, the presence of histones in trout ETs indicates their nuclear origin, suggesting that the PMN underwent a lytic form of ET release resulting in cell death (Yousefi *et al.*, 2008; Yipp *et al.*, 2012, 2013).

An intracellular influx of reactive oxygen species (ROS) is a ubiquitous and crucial step prior to ET release (Figure 1.3) (Papayannopoulos *et al.*, 2010; Kaplan *et al.*, 2012; Arai *et al.*, 2014; Morshed *et al.*, 2014; Jorch *et al.*, 2017), but how exactly intracellular ROS influx initiates the steps leading to ET release remains unclear, though the mechanisms that lead to the generation of intracellular ROS are now better understood (Fuchs *et al.*, 2007; Douda *et al.*, 2015). The majority of inducers of ET release promote intracellular ROS influx leading to ET release through the enzyme complex, nicotinamide adenine dinucleotide phosphate oxidase (NADPH oxidase). For instance, phorbol 12-myristate 13-acetate (PMA) is a well-known chemical protein kinase C (PKC) activator and inducer of ET release in mammals, and this compound potently promotes the formation of active NADPH oxidase complexes responsible for generating superoxide (a form of ROS) and ultimately ET release (Riganti *et al.*, 2004; Hakkim *et al.*, 2011). In addition to PMA, biological compounds like lipopolysaccharide (LPS) and whole microorganisms (Brinkmann *et al.*, 2004; Urban *et al.*, 2006; Saitoh *et al.*, 2012; Uchiyama *et al.*, 2015) can induce ET release through the activation of PKC, *i.e.*, ET release is triggered by an NADPH oxidase-dependent mechanism

(Papayannopoulos, 2017). Alternatively, intracellular calcium ( $\text{Ca}^{2+}$ ) influx caused by exogenous addition of calcium ionophore (Cal) may also promote mitochondrial ROS generation that leads to ET release (Douda *et al.*, 2015; Görlach *et al.*, 2015).

Three results from Chapter 3 suggest that ET release from rainbow trout PMNs is less dependent on NADPH oxidase activation compared to mammals and other fish species. First, PMA, a potent inducer of ET release in mammals, carp, zebrafish (*Danio rerio*) and tongue sole (*Cynoglossus semilaevis*) (Palić, Andreassen, *et al.*, 2007; Pijanowski *et al.*, 2013; Hoppenbrouwers *et al.*, 2017; Zhao *et al.*, 2017), surprisingly did not potently and reproducibly induce ET release from trout PMN-enriched cell suspensions, as PMA (at 40 nM and 60 nM) induced ET release from only two out of six trout tested (Section 3.3.6). Second, Cal can induce ET release independently of any NADPH oxidase activity, and was a potent inducer of ET release in all individual trout within 10 min of incubation (Section 3.3.6). Furthermore, the actin polymerisation inhibitor cytochalasin D, a potent inhibitor of ET release in many species, was effective (Section 3.3.5), indicating that the cells were responsive to other inducer and inhibitors of ET release that act independently of NADPH oxidase signalling. Third, and most importantly, the NADPH oxidase-inhibitor, diphenyleneiodonium (DPI), failed to inhibit ET release from rainbow trout PMN-enriched cell suspensions, and instead acted as an inducer of ET release (Section 3.3.6). In contrast, flagellin induced ET release from trout PMN-enriched cell suspensions (Section 3.3.6). Flagellin is a pathogen associated molecular pattern (PAMP) that binds toll-like receptor 5 (TLR5) on rainbow trout phagocytes (Wangkahart *et al.*, 2016). TLRs, including TLR5, signal through the adaptor protein MyD88, which can activate PKC (Hayashi *et al.*, 2001), thus suggesting the involvement of NADPH oxidase during flagellin-induced ET release (Floyd *et al.*, 2016; Kim *et al.*, 2016). This result contradicts the notion of ET release by trout PMN-enriched cell suspension relying less on activation of NADPH oxidase. Perhaps the release of ETs by DPI could be explained by DPI acting as a general stressor to the cells, as demonstrated with pH (Naffah de Souza *et al.*, 2018), and thereby causing ET release through an undefined mechanism. The cell signalling pathways underlying ET release in trout PMNs warrants further investigation to understand the cell signalling pathway which controls ET release in trout, as they appear to be distinct from the activation mechanisms in other fish species such as carp and tongue sole. Future work should examine the effects of a broader range of NADPH oxidase inhibitors, and include ROS and MPO inhibitors, as the identification of a potent inhibitor will be a useful tool towards elucidating the signalling pathway(s) underlying ET release in trout. Unfortunately, these results did not detect an increase of ET release when exposed to heat-inactivated cultures of *V. anguillarum*. This result may be explained by the denaturation of the pathogen-associated molecular patterns (PAMPs) when heat-inactivating the bacterial suspension. Exposing the PMN-enriched cell suspensions to live *V. anguillarum* bacteria did not result in observable

increases in ET release, though perhaps the method determining ET release in response to solutions needs to be improved when bacteria are used.

The aim of Chapter 5 was to investigate whether ETs released by trout PMN-enriched cell suspensions could trap bacteria. As expected, trout ETs reduced bacterial CFU when incubated with *V. anguillarum* (Vib 87), an isolate lacking extracellular nuclease activity, indicating contribution possible role of trout ETs in innate immunity against bacterial pathogens. In contrast, extracellular nuclease activity allowed another isolate of *V. anguillarum* (Vib 6) to degrade and liberate itself from trout ETs (Section 5.5.3). These observations were supported with microscopic observations showing that fluorescently-stained *V. anguillarum* Vib 87 co-localised with the ETs, while *V. anguillarum* Vib 6 appeared to degrade the ET fibres and did not co-localise with the chromatin. Taken together, these *in vitro* results confirm that ETs released from trout PMN-enriched cell suspensions can ensnare microbes, though the production of extracellular nucleases by *V. anguillarum* could degrade the ETs and prevent trapping, therefore implicated these enzymes may serve a potential role in virulence. Whether or not *V. anguillarum* Vib 87 was killed when trapped on the ETs remains uncertain, as the method used did not distinguish between trapping and killing. Thus, future work should be confirming the trapping ability of ETs with different microbial species with a wider spectrum of activity, as this present study focused on one bacterial species.

The nuclease activity screen in Chapter 4 identified the majority of *V. anguillarum* isolates positive for nuclease activity, suggesting that they may play an important role for the bacteria during their lifecycle. Although some *V. anguillarum* isolates produce extracellular nucleases (Austin *et al.*, 1995), their interaction with the immune system has not been investigated until now. Research of extracellular nucleases from other bacterial species, including *Vibrio cholerae*, has shown that extracellular nucleases have roles in regulating bacterial transformation, generating nucleotide or phosphate nutrient pools from extracellular DNA, and more recently, degrading ETs (Blokesch *et al.*, 2008; Seper *et al.*, 2013; Kiedrowski *et al.*, 2014; Mcdonough *et al.*, 2016). Understanding the *V. anguillarum* lifecycle may give insight into the purpose of extracellular nuclease production. During the free-living, aquatic stage of the bacteria, the degradation of extracellular nucleic acids may generate nucleotide/phosphate nutrient pools (Mcdonough *et al.*, 2016); while during the infection stage, nucleases may assist in burrowing through the mucosal surfaces of gill or skin to enter the host (Frans *et al.*, 2011). Once within the host, the bacteria need to combat the immune system to allow successful propagation within the host which might include resisting or avoiding trapping by ETs. The extracellular nuclease activity was consistent throughout *V. anguillarum* culture *in vitro*, thus indicating that the bacteria may produce extracellular nucleases throughout its lifecycle. Furthermore, the extracellular nuclease activity produced by the bacteria was able to degrade DNA within fish skin mucus and that composing trout ETs

(Section 4.3.8 and 4.3.9), suggesting that this might be a strategy implemented by *V. anguillarum* to infect through mucosal surfaces or evading trapping by ETs.

The next logical step would be to confirm the presence of trout ETs *in vivo* and assess their ability to ensnare or kill bacteria during infection. A study in turbot (*Scophthalmus maximus*) demonstrated fewer recovered *Pseudomonas fluorescens* CFUs from kidney and spleen tissue after injecting the fish with co-cultures of bacteria and pre-induced ETs, compared to co-cultures of bacteria and DNase-digested ETs, indicating the *in vivo* antimicrobial effect of ETs in fish (Chi *et al.*, 2015). Despite this important finding, ET release from PMNs during infection *in vivo* and their protective effect against such a challenge has yet to be shown in a fish system. Furthermore, Chi and Sun (2015) did not report how the injected co-cultures of bacteria and ETs affected the health status of the fish compared to DNase-treated co-cultures. Thus, future studies should investigate if fish can release ETs in response to fish pathogens and if the ETs can trap or kill these pathogens *in vivo*.

Regarding the *in vivo* significance of ETs, the initial discovery of ET release has associated this process as a defensive innate immune response; however, recent evidence has shown ETs to directly underlie several diseases or ailments associated with the inflammatory response and autoimmunity (Kaplan *et al.*, 2012; Cheng *et al.*, 2013; Kahlenberg *et al.*, 2013). There is strong evidence that ETs promote adverse skin inflammation (Keijsers *et al.*, 2014), sepsis (Xu *et al.*, 2010), vascular disorders (Phillipson *et al.*, 2011), and inflammatory bowel disease (IBD) (Bennike *et al.*, 2015) in mice and humans. These inflammatory symptoms are believed to be exacerbated by the action of the potentially cytotoxic peptides (e.g., histone fragments, NE or MPO) and other molecules (such as ROS) that decorate the ETs (Saffarzadeh *et al.*, 2012), which are cytotoxic to host cells and can lead to direct degradation of cells and tissues, or the activation of neutrophils by the pro-inflammatory cytokines liberated during ET release (Hahn *et al.*, 2011; Kaplan *et al.*, 2012; Cheng *et al.*, 2013; Yang *et al.*, 2016). Moreover, several peptides decorating the ETs are auto-antigens for systemic autoimmune disorders in humans, such as the anti-neutrophil cytoplasmic antibody (ANCA) that contributes to systemic vasculitis (Nakazawa *et al.*, 2012). As such, ETs may be both beneficial and detrimental to the host, as they serve as an antimicrobial defence but are also a putative source of molecules that promote inflammatory and autoimmune responses. Some therapeutics prescribed to humans and others tested in mice models target ET-derived DNA to alleviate the disease symptoms. For instance, the vicious sputum of cystic fibrosis obstructs breathing, but the use of DNase aerosols successfully reduces symptoms in some patients, as DNA provides structural integrity to mucus and increases viscosity (Shak *et al.*, 1990). Also, DNase treatment can prevent deep vein thrombosis in mice by degrading ETs that act as scaffolds within blood vessels to promote blood clotting (Fuchs *et al.*, 2010). Blocking NE proteases in mice suffering from atherosclerosis also reduces overall inflammation and the

mice develop smaller atherosclerotic lesions (Warnatsch *et al.*, 2015). Overall, it is becoming abundantly clear that although ETs can facilitate microbial pathogen trapping, the clearance of ETs within host tissues is also important to reduce potential negative symptoms of inflammatory diseases. Also, there is an increasing amount of research that has found treating the disease symptoms rather than treating the pathogen as a successful method to improve animal or patient welfare. It is likely that future therapeutics will target ETs in some diseases. Some of these may include ROS scavengers which can suppress ET release; exogenous DNases which can break down ETs; or MPO and protease inhibitors which can reduce the detrimental effects of granule proteins.

The research surrounding fish ETs has not yet investigated if ET release within fish can have similar negative consequences similar to those observed in humans and mammals. However, the upregulation of pro-inflammatory cytokines was detected when carp PMN and macrophage-enriched cell suspensions released ETs (Pijanowski *et al.*, 2015). In addition, the combination of pro-inflammatory cytokines and PAMPs in carp can induce further ET release (Pijanowski *et al.*, 2015). Considering the contribution of ETs towards inflammation and autoimmune diseases in mammals, it would therefore not be surprising to find that ETs are involved in the pathogenesis of similar diseases in fish. Microbial infections causing severe inflammation are good candidates for further investigation. For example, red mark syndrome (RMS) in trout is likely caused by a Rickettsia-like organism (RLO) and results in multiple skin lesions with histological confirmation of inflammation and high abundances of neutrophils (Metselaar *et al.*, 2010). Furunculosis caused by *Aeromonas salmonicida* infection results in external and internal haemorrhaging, septicaemia and inflammation of the lower intestine (Wiklund *et al.*, 1998; Mutoloki *et al.*, 2006). Furthermore, several fish viruses such as viral haemorrhagic septicaemia virus (VHSV) and piscine orthoreovirus results in severe haemorrhaging of internal organs, skin and muscle, along with heart and skeletal muscle inflammation (Arnfinn Aunsmo *et al.*, 2015; Olsen *et al.*, 2015). Moreover, autoimmunity disorders have been described in fish and it is possible that these may be caused by ETs as observed with mammals. For example, rainbow trout and chinook salmon (*Oncorhynchus tshawytscha*) suffering from glomerulonephritis in bacterial kidney disease caused by *Renibacterium salmoninarum* infection was found to be associated with antibody-antigen complexes within the kidney (Sami *et al.*, 1992; Lumsden *et al.*, 2008). These immune complexes can lead to a type III hypersensitivity reaction, giving rise to inflammatory responses that may lead to host tissue damage (Afonso *et al.*, 1998; Phillipson *et al.*, 2011; Papayannopoulos, 2017). Hence, it may be desirable to moderate the release of ETs in fish after considering their potential contribution towards inflammatory pathogenesis of several diseases. Therefore, an apt direction for future work would investigate if ETs released within the host contributes to the pathogenesis of inflammatory diseases, which may lead to new

classes of therapeutants that could be used to reduce disease outbreaks on fish farms. Alternatively, perhaps the presence of ETs are beneficial to fish as they may trap microbial pathogens without contributing to inflammatory status and diseases as reported in mammals. Taken together, an improved *in vivo* understanding of ETs would identify their immunological significance and indicate their benefits and any associated detriments to fish.

In summary, the present study is the first to demonstrate that ETs are released from PMN-enriched cell suspensions from rainbow trout. These ETs were decorated with neutrophil granule proteins NE, MPO, and histone H2A, which serve as diagnostic markers of ETs. The ETs could trap the bacterial fish pathogen *V. anguillarum in vitro*, thus suggesting a role in defence against bacterial challenges. Understanding how to successfully enhance this general immune response to increase protection against pathogens may lead to the development of alternative broad-spectrum antimicrobial therapies and reducing the need for antibiotics in aquaculture. Understanding the immunological role of ET release in fish is an important step forward towards reducing infectious diseases in salmonid and finfish aquaculture to ensure these industries continue to provide a source of healthy food for a growing global population.

## Appendix

### 1.1. Trout commercial feed

**Appendix Table 1.** Formulation of commercial feed used for trout husbandry. Trout were fed two to three times per day.

**Trout feed: Micro 50P LR – 25 kg/100**

Vitamins E671 Vitamin D3	2100 IU/kg
<b>Trace elements</b>	
E1 Iron-Fe (ferrous sulphate monohydrate)	170 mg/Kg
E2 Iodine-I (calcium iodate anhydrous)	5 mg/kg
E4 Copper-Cu (cupric sulphate pentahydrate)	24 mg/kg
E5 Manganese-Mn (manganous sulphate monohydrate)	113 mg/kg
E6 Zinc-Zn (zinc sulphate monohydrate)	330 mg/kg
3b8 10 Selenium-Se (selenised yeast inactivated)	100 mg/kg
<b>Analytical constituents</b>	
Oil	22.0%
Protein	48.0%
Fibre	1.8%
Ash	8.3%
Calcium	1.6%
Sodium	0.1%
Phosphorous	1.0%

## 1.2. RPMI media supplementation

**Appendix Table 2.** The different RPMI variants showing supplementation used within throughout this thesis. \*Unless otherwise states, FCS (sterile filtered) was used at 1% (v/v), supplied by Thermofisher Scientific (Loughborough, UK). #Used at 1% (v/v), with stock solution containing: 10,000 U penicillin and 10 mg mL<sup>-1</sup> streptomycin (sterile-filtered), supplied by Sigma-Aldrich (Dorset, UK)

<b>Name</b>	<b>Foetal calf serum (FCS)*</b>	<b>Antibiotics#</b>
<b>RPMI1</b>	-	-
<b>RPMI2</b>	+	+
<b>RPMI3</b>	+	-



### 1.3. Trypan blue exclusion protocol

Cell viability was calculated by dividing the number of viable cells by the total number of cells within the grids on the Neubauer hemacytometer. If cells take up trypan blue, they are considered non-viable.

1. Determine the cell density of your cell line suspension using a haemocytometer.
2. Prepare a 0.4% solution of trypan blue in buffered isotonic salt solution, pH 7.2 to 7.3 (*i.e.*, phosphate-buffered saline).
3. Add 0.1 mL of trypan blue stock solution to 1 mL of cells.
4. Load a haemocytometer and examine immediately under a microscope at low magnification.
5. Count the number of blue staining cells and the number of total cells. Cell viability should be at least 95% for healthy log-phase cultures.

$$\% \text{ viable cells} = [1.00 - (\text{Number of blue cells} \div \text{Number of total cells})] \times 100$$

To calculate the number of viable cells per mL of culture, use the formula below. Remember to correct for the dilution factor.  $\text{Number of viable cells} \times 10^4 \times 1.1 = \text{cells mL}^{-1} \text{ culture}$

## 1.4. Rapid Romanowsky staining protocol

Description: A set of three different stains for the rapid staining of smears for cytological and haematological microscopy. Results will be similar to Romanowsky stained smears.

Reagents:

- A. Fixative Solution A – 500ml or 250ml (contains thiazine dye in methanol)
- B. Solution B – 500 mL or 250 mL (contains eosin Y dye in phosphate buffer)
- C. Solution C – 500 mL or 250 mL (contains polychromed methylene blue in phosphate buffer)

Preparation:

1. Dispense an aliquot of each solution into a Coplin staining jar
2. Prepare a solution of phosphate buffer solution pH 6.8 in a wash bottle.
2. Immerse in Solution A for 30 seconds.
3. Transfer, without rinsing or drying, to Solution B, and immerse for 30 seconds.
5. Transfer slide to Solution C without rinsing or drying, and repeat staining as for B above.
6. Rinse slide in phosphate buffer solution pH 6.8 and allow to dry before examining under the microscope.

## **1.5. Atlantic salmon**

Diploid Atlantic salmon were used alongside rainbow trout to test the robustness of the discontinuous Percoll gradient protocols used to enrich PMNs from fish head kidney tissue.

### **1.5.1. Methods**

#### **1.5.1.1. Source of fish and husbandry**

Healthy pre-smolt Atlantic salmon from AquaGen were housed in the aquarium at the Institute of Aquaculture during October 2015 to October 2016. Water temperature was recorded from tanks on days when fish were sampled, and mean water temperature during the year was 9.76°C (5.7–12.8°C). All fish used for experiments weighed between 23–158 g, and were sacrificed according to a Schedule 1 technique (overdose of benzocaine and destruction of the brain) as described in the 1986 Animals Scientific Procedures Act (ASPA). All experiments were approved by the IoA Ethics Committee or the Animal Welfare Ethical Review Board (AWERB).

#### **1.5.1.2. Comparing cell proportions from discontinuous Percoll gradient isolation**

Atlantic salmon head kidney tissue was dissected and enriched for PMNs by double and triple-layer Percoll gradients as prepared according to Section 2.2.3. The proportions of cells in suspension attained after Percoll gradient enrichment was determined by counting the proportions of PMNs and Mo/M cells from fixed samples of end-product cell suspensions fixed onto glass microscopy slides (fixation by Cytospin, and staining with the RapiDiff protocol, as described in Section 2.2.4).

#### **1.5.1.3. Relationship between PMN proportion, fish weight, and water temperature**

To assess the effect of fish mass on the proportion of salmon PMNs enriched from head kidney tissue by the triple-layer Percoll gradient approach as above, 32 pre-smolt Atlantic salmon were weighed and PMN proportion determined. PMNs were enriched according to Section 2.2.3 with salmon weighing from 23 – 158 g. The PMN proportions were achieved by counting according to Section 2.2.5, and mass of each fish was correlated with the mean PMN proportions. The tank water temperature was recorded on the morning that each fish was collected for the experiment.

## 1.5.2. Results

### 1.5.2.1. Comparing cell proportions from discontinuous Percoll gradient isolation

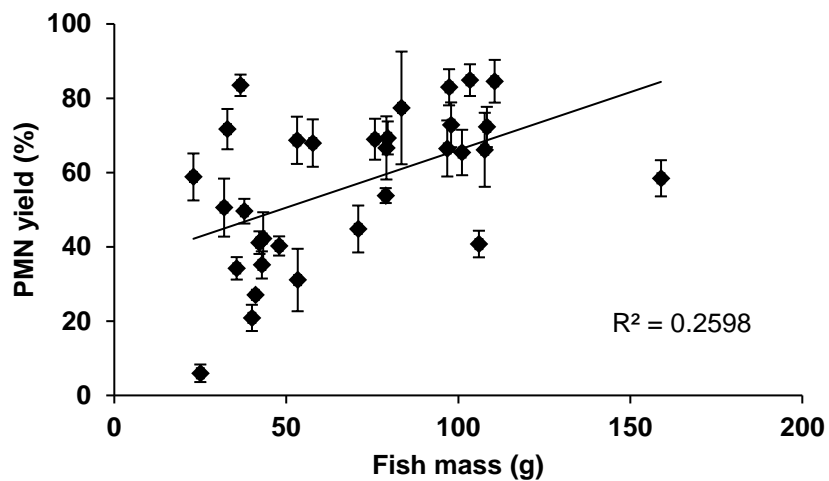
The proportions of PMN and Mo/M cells enriched were compared after enrichment by the double or triple-layer Percoll gradient protocols used for isolating Atlantic salmon PMNs from head kidney preparations. The double-layer discontinuous gradient approach gave a  $32.97 \pm 4.13\%$  PMN enrichment, with the presence of  $24.04 \pm 5.50\%$  Mo/M observed as a proportion of total cells in the isolated fraction; while the triple-layer approach gave a  $59.06 \pm 4.91\%$  PMN enrichment, with  $3.25 \pm 1.20\%$  Mo/M (Appendix Table 3). The triple-layer gradient resulted in a 1.69-fold improvement in PMN enrichment, and reduced Mo/M contamination compared to the double layer gradient method.

**Appendix Table 3.** Comparison of proportions of polymorphonuclear cell (PMN) and monocyte/macrophage (Mo/M) cells obtained from double and triple-layer Percoll gradient separation methods in diploid Atlantic salmon. Cytospin preparations of enriched cell populations were stained with rapid Romanowsky stains to allow classification by microscopic observation of cell morphologies. A minimum count from 5 fields of view (FOV) per fish was made to enumerate cell proportions.

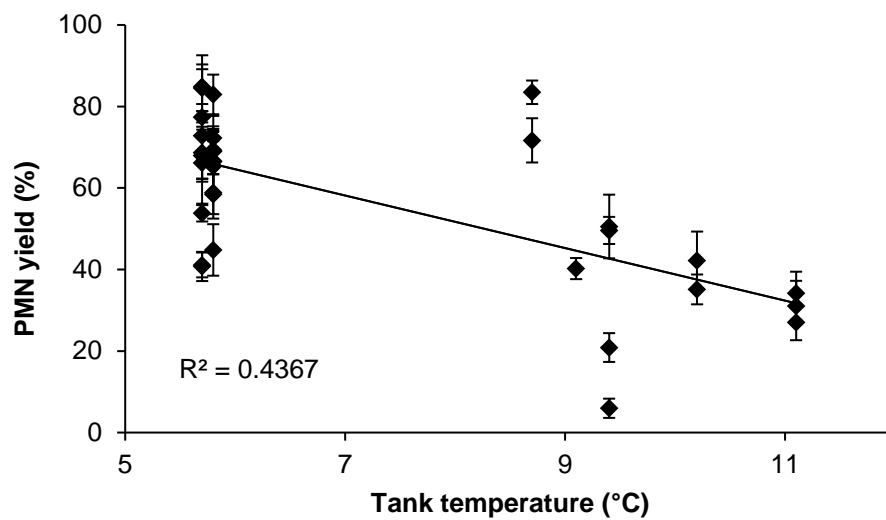
Percoll gradient	Fish type	PMN (%)	Mo/M (%)	No. of fish
<b>Double layer</b>	Atlantic salmon	$32.97 \pm 4.13$	$24.04 \pm 5.50$	7
<b>Triple layer</b>	Atlantic salmon	$59.06 \pm 4.91$	$3.25 \pm 1.20$	10

#### **1.5.2.2. Relationship between PMN proportions, fish mass and tank temperature**

Out of 32 pre-smolt Atlantic salmon, there was a significant positive correlation between the PMN yield and fish mass in Atlantic salmon weighing between 23 – 158 g ( $R^2 = 0.2598$ ;  $p < 0.01$ ). The salmon were siblings of the same age, as they were from the same hatch. The data suggest that a greater proportion of PMNs are produced with relative mass (Appendix Figure 1). A significantly negative correlation was observed with PMN yield when increasing tank temperature in Atlantic salmon ( $R^2 = 0.4367$ ;  $p < 0.01$ ) (Appendix Figure 2).



**Appendix Figure 1.** A scatter plot showing the relationship between Atlantic salmon mass against the yield of PMNs attained after isolation. Each point consists of the mean number of PMNs calculated from three fields of view (FOV) from cytospin preparations after enriching salmon head kidney tissue for PMNs with triple layer Percoll gradients. There was no significant correlation between fish weight and PMN yield ( $F_{1,30} = 10.53$ ;  $p < 0.05$ ). Error bars represent s.e.m.  $n = 32$  salmon.

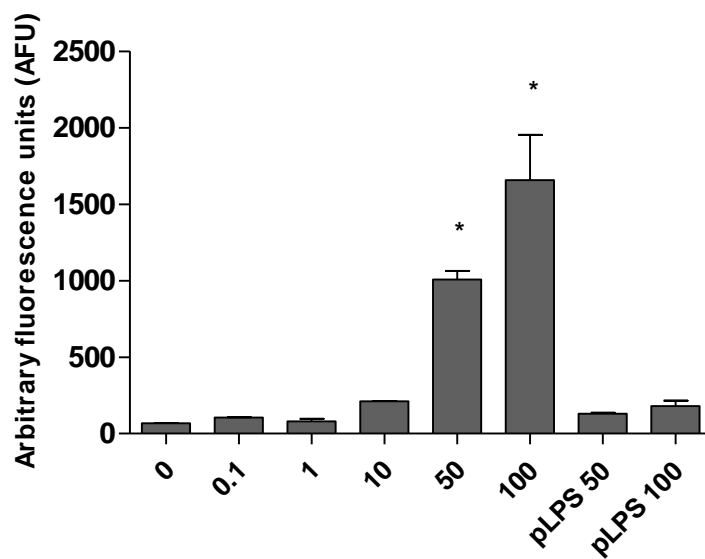


**Appendix Figure 2.** Scatterplot showing the correlation between tank temperature (°C) at time of sampling and PMN proportions obtained from triple-layer Percoll preparations from Atlantic salmon showing that tank temperature may affect the proportions of PMNs obtained ( $F_{1,30} = 23.26$ ;  $p < 0.05$ ). Error bars represent s.e.m.  $n = 32$  salmon.

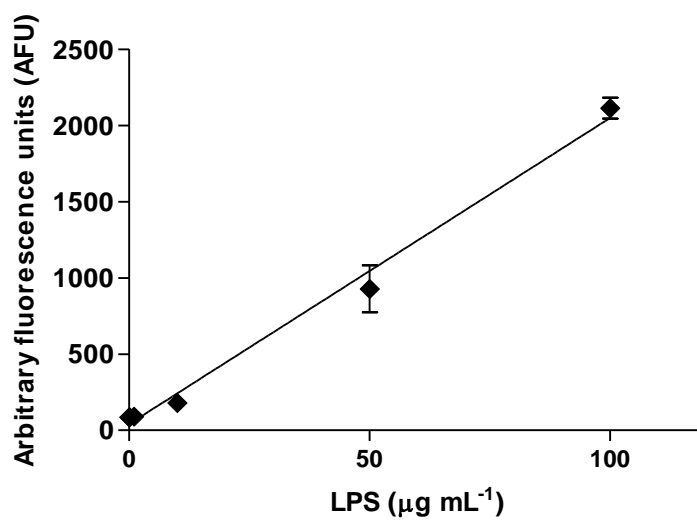
## 1.6. Background fluorescence of compounds used as ET inducers

Extraction of PAMPs such as LPS, zymosan, and  $\beta$ -Glucan from microbes is a crude process, which does not remove many molecular contaminants. Other methods such as ion-exchange chromatography during the extraction of ultra-pure LPS (pLPS) is better at removing unwanted by products still present in solution after phenol extraction. The method used to measure fluorescence from LPS and pLPS was described in Section 3.2.5. Measuring the fluorescence of SYTOX-stained LPS showed a relationship between concentration of LPS and fluorescence, while pLPS did not show this effect (Appendix Figure 3, Appendix Figure 4), suggesting that the phenol extraction process fails to remove nucleic acid contamination. Other compounds where this nucleic acid contamination was observed was zymosan, and  $\beta$ -Glucan. Furthermore, preliminary results showed incubation of trout PMN-enriched cell suspensions with zymosan and  $\beta$ -Glucan did not result in ET release over 12 h, after observation with fluorescence microscopy (data not shown). Direct subtraction of the fluorescence of these compounds at the same concentration used to stimulate ET release does not have a proportional effect on fluorescence (data not shown). Subtraction of the PAMP's fluorescence from cells incubated with the PAMP results in a negative number; likely due to the interaction between the cells, and properties of the PAMP. For example, PAMPs have agglutination properties which can clump cells and DNA together, artificially increasing the fluorescence by density.



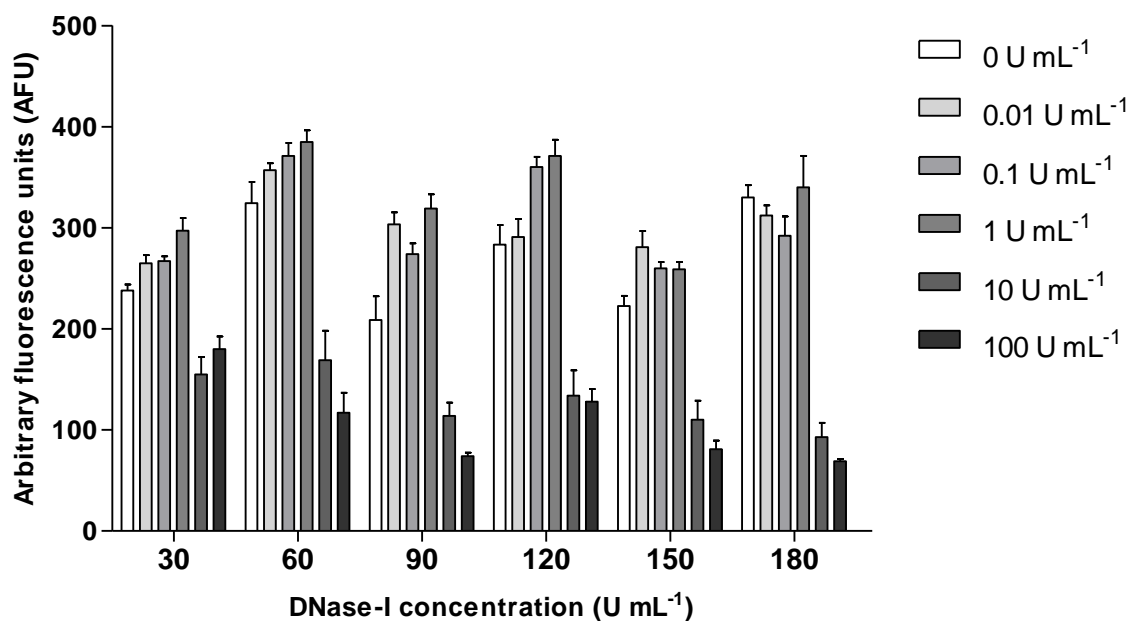


**Appendix Figure 3.** Bar chart showing mean fluorescence of wells containing LPS (0.22  $\mu\text{m}$  sterile filtered) fluorescence after staining with SYTOX Green (5  $\mu\text{M}$ , 5 min, room temperature). The fluorescence is indicative of nucleic acid contamination. pLPS at 50 and 100  $\mu\text{g mL}^{-1}$  was included to confirm the lack of nucleic acid contamination. \* $p < 0.05$  compared to a control without DNase-I. Error bars represent s.e.m.  $n = 5$  wells.



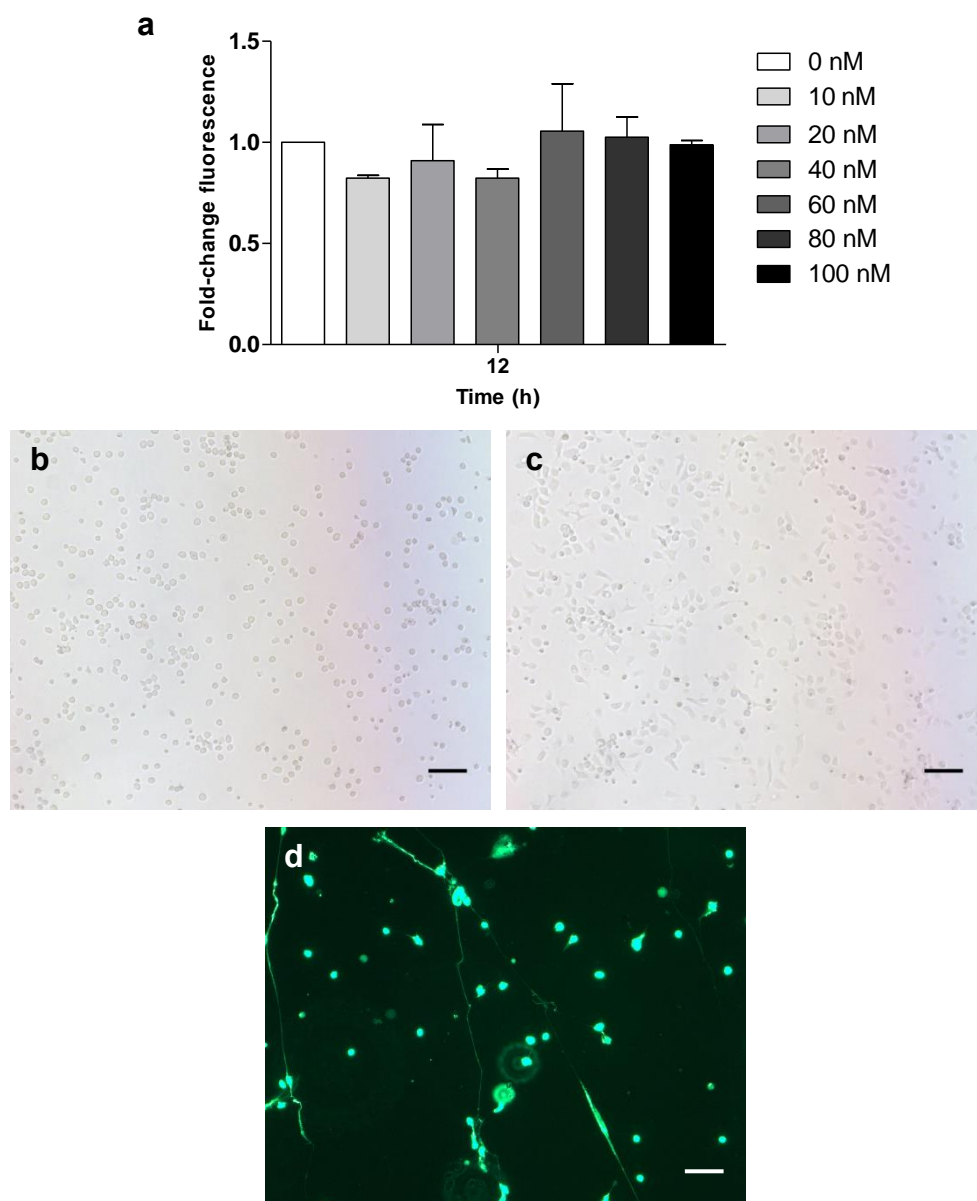
**Appendix Figure 4.** Scatter plot showing mean fluorescence of wells containing LPS (0.22 μm sterile filtered) fluorescence after staining with SYTOX Green (5 μM, 5 min, room temperature). The results indicate a strong positive relationship between LPS concentration and fluorescence attributable to nucleic acid contamination ( $R^2 = 0.9365$ ;  $F_{1,46} = 678.5$ ;  $p < 0.05$ ).

## 1.7. Degrading ETs with DNase-I



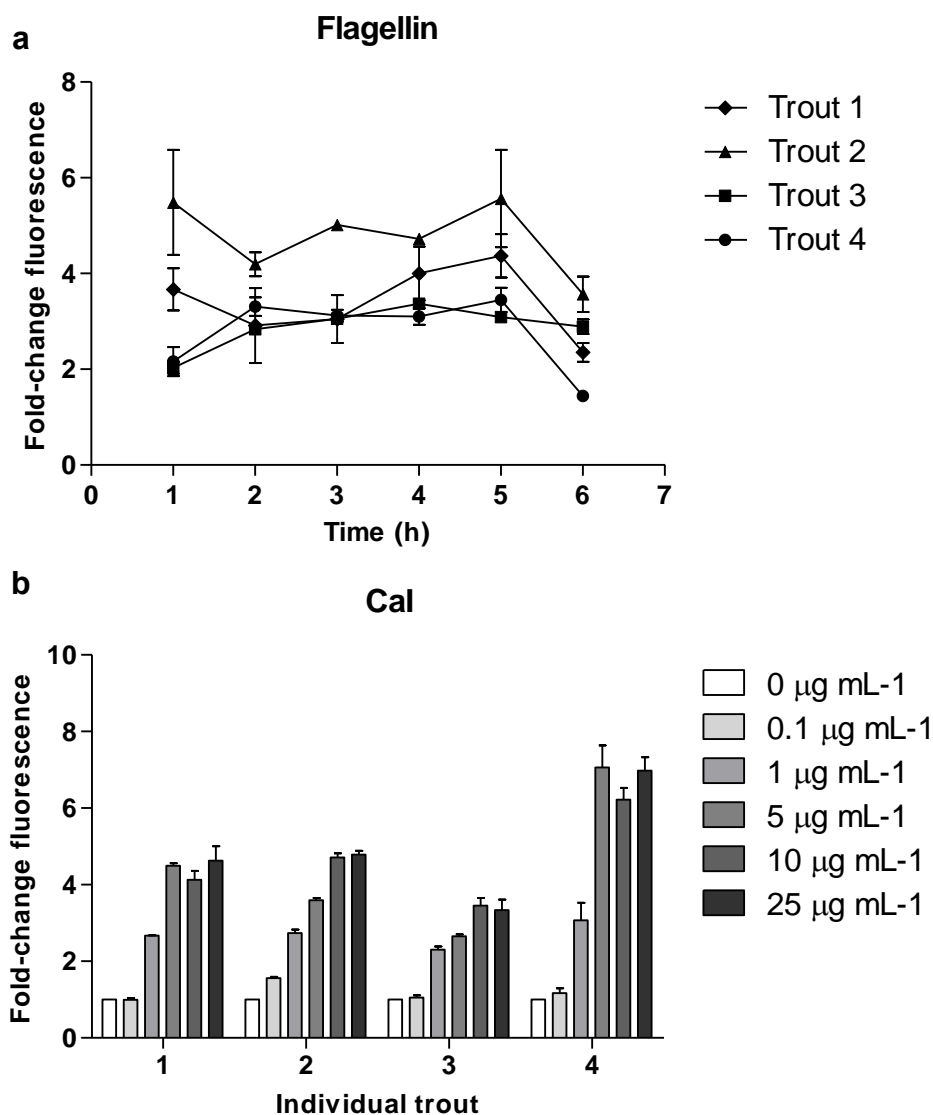
**Appendix Figure 5.** Bar chart showing the mean fluorescence of wells containing trout PMN-enriched cell suspensions ( $4 \times 10^5$  cells mL<sup>-1</sup>) after initial exposure to Cal ( $5 \mu\text{g mL}^{-1}$ , 3 h, 15°C) to stimulate release of ET-like structures, and then to DNase-I (0.01 – 100 U mL<sup>-1</sup>) over 180 min at 15°C. Exposure of ET-like structures to 10 and 100 U mL<sup>-1</sup> DNase-I significantly reduced fluorescence attributed to ET-like structures compared to controls not treated with DNase. The remaining fluorescence is attributable to membrane-compromised cells which the DNase-I cannot access. \* $p < 0.05$  compared to a control not exposed to DNase-I at each time point. Error bars represent s.e.m.  $n = 5$  wells.

## 1.8. Examining cell morphology within PMN-enriched cell suspension following exposure to PMA at 100 nM



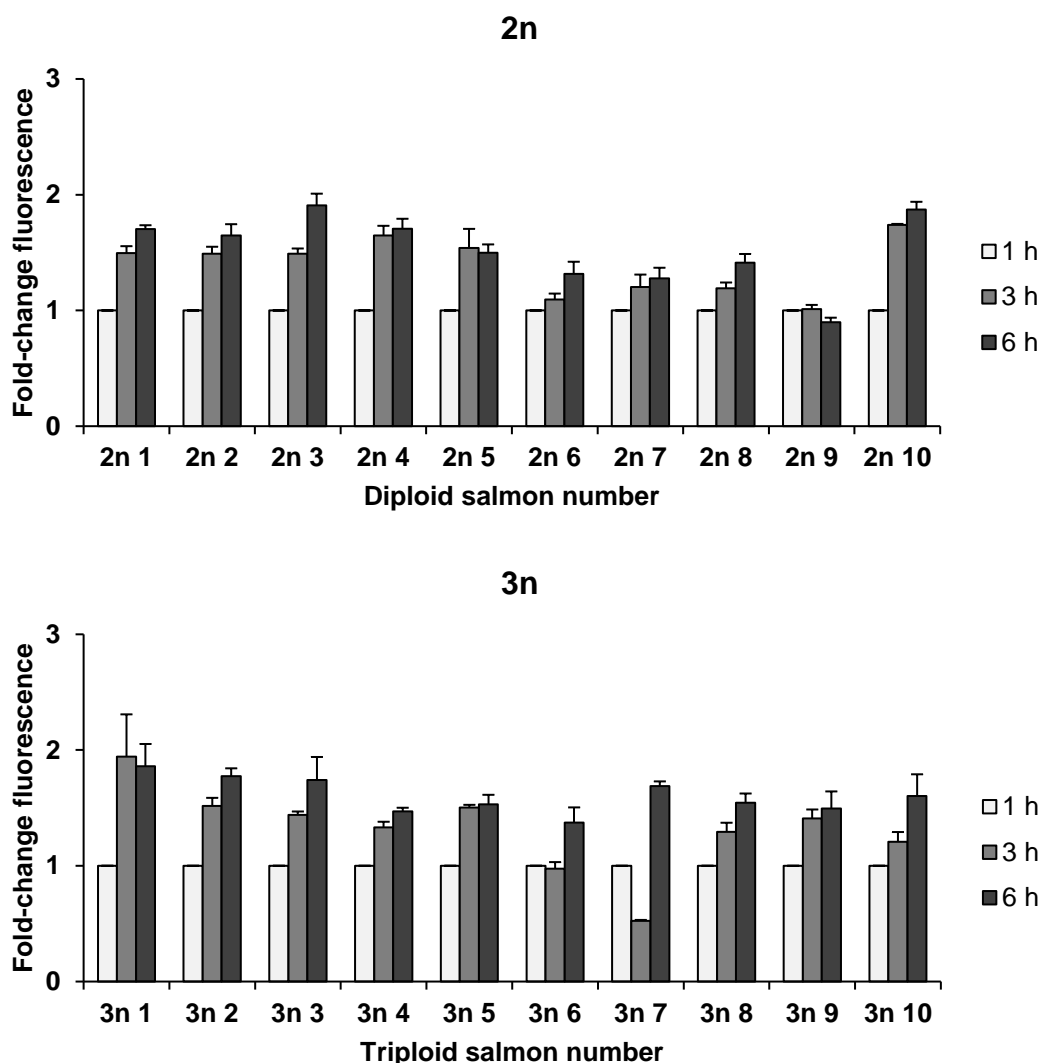
**Appendix Figure 6.** (a) Bar chart showing the mean fold-change fluorescence of wells containing trout PMN-enriched cell suspensions ( $4 \times 10^5$  cells  $\text{mL}^{-1}$ ) after exposure to PMA (12 h,  $15^\circ\text{C}$ ). Mean fluorescence for each treatment was not significantly different compared to unexposed controls ( $*p < 0.05$ ). Error bars represent s.e.m.  $n = 5$  wells. (b) Representative phase contrast images of PMN-enriched cell suspensions exposed to RPMI, or (c) PMA 100 nM, for 24 h at  $15^\circ\text{C}$ . (d) Fluorescence microscopy image of PMN-enriched cell suspensions exposed PMA 100 nM, for 12 h at  $15^\circ\text{C}$ . Scale bar =  $40 \mu\text{m}$ .

## 1.9. Examining individual fish response to flagellin or PMA



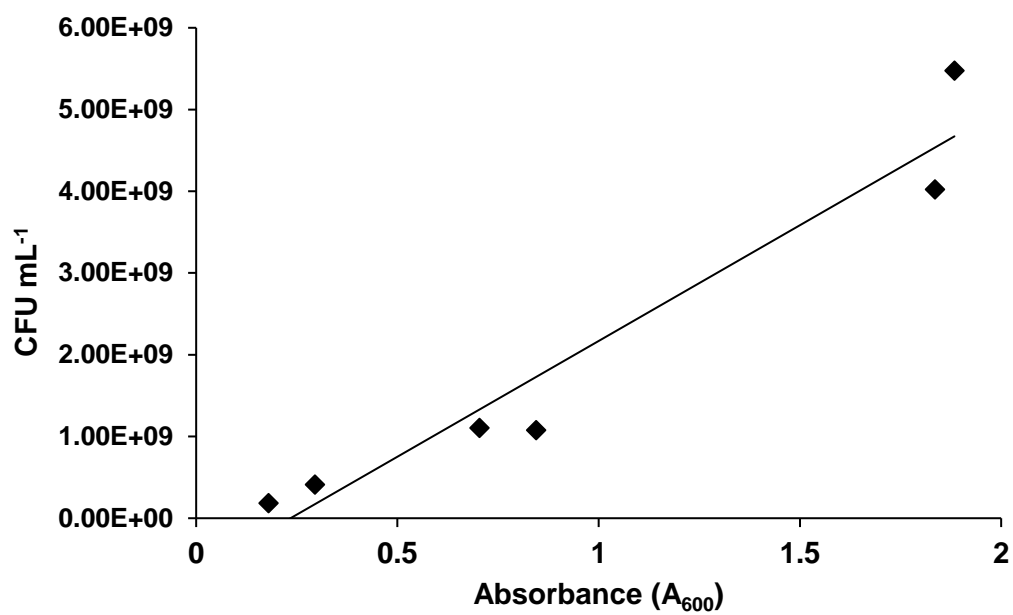
**Appendix Figure 7.** (a) Scatterplot showing the mean fold-change fluorescence of PMN-enriched cell suspensions ( $4 \times 10^5$  cells  $\text{mL}^{-1}$ ) from individual trout (1 to 4) exposed to flagellin for up to 6 h (b) Bar chart showing the mean fold-change fluorescence of PMN-enriched cell suspensions ( $4 \times 10^5$  cells  $\text{mL}^{-1}$ ) from individual trout (1 to 4 different from trout in [a]) exposed to Cal (0 to 25  $\mu\text{g mL}^{-1}$ ) for 1 h. All wells were stained with SYTOX Green (5  $\mu\text{M}$ , 5 min, room temperature) before measuring fluorescence. These graphs indicate that all fish released ETs (indicated by greater fluorescence) in response to treatment with flagellin ( $100 \text{ ng mL}^{-1}$ ) or Cal.

## 1.10. Spontaneous ET release variation of ten diploid and ten triploid Atlantic salmon



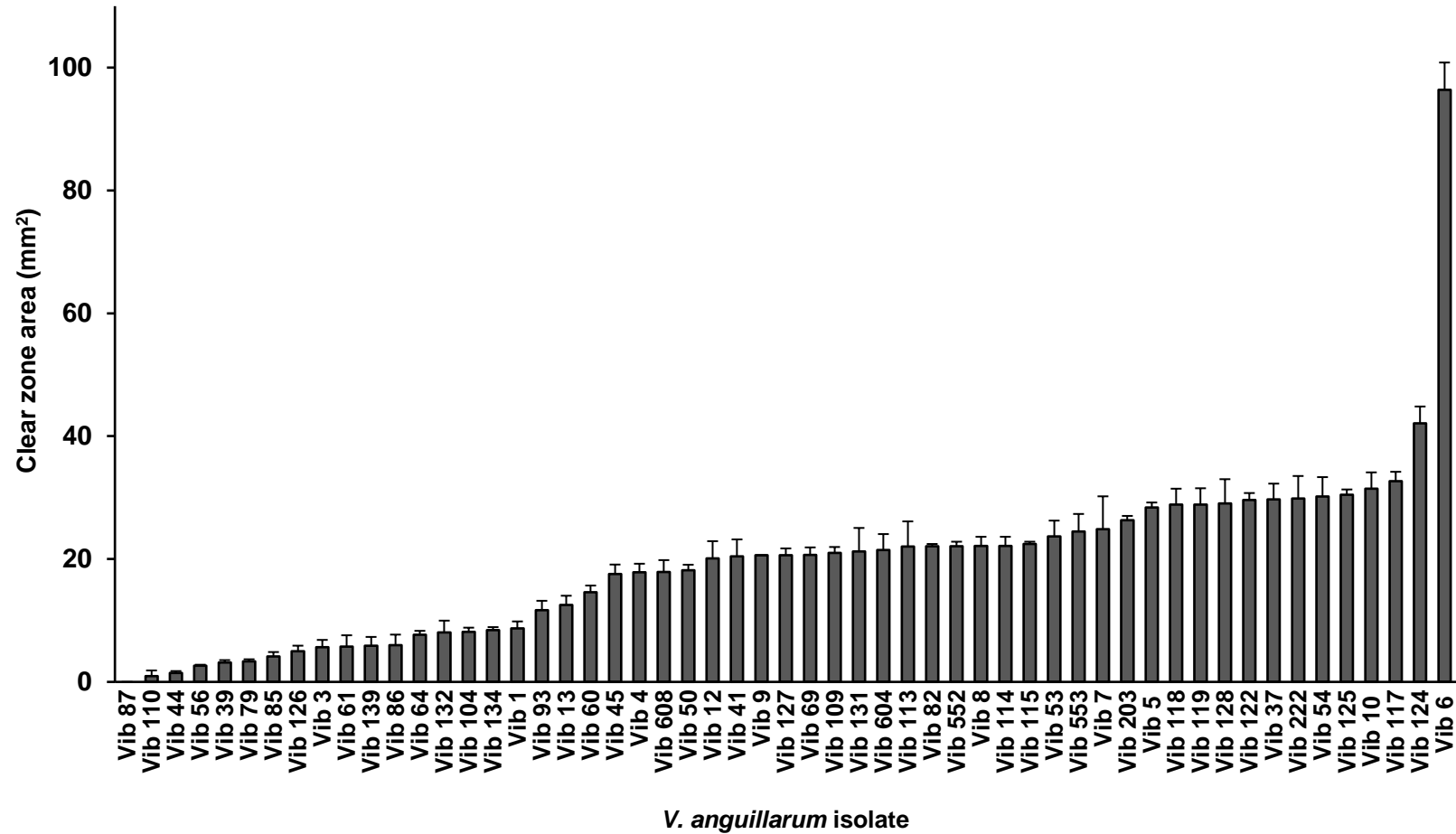
**Appendix Figure 8.** Bar chart showing the mean fold-change fluorescence of PMN-enriched cell suspensions ( $4 \times 10^5$  cells  $\text{mL}^{-1}$ ) from individual pre-smolt diploid (2n) and triploid (3n) Atlantic salmon exposed to RPMI1 for up to 6 h, then stained with SYTOX Green ( $5 \mu\text{M}$ , 5 min, room temperature), with fluorescence normalised to 1 h. Confirmation using fluorescence microscopy found the relative fluorescence was reflected by the density of ETs observed from SYTOX-stained PMN-enriched cell suspensions (data not shown). Some fish had a large background level of ET release such as 2n3, 4, 5, and 6; others had moderate to contrastingly low levels. The triploid values have been normalised for DNA content by dividing raw fluorescence by 1.5. Fish weighed  $74.02 \pm 8.68$  g for diploids and  $99.15 \pm 8.55$  g for triploids. Error bars represent s.e.m.

## 1.11. Bacterial culture and standard curve



**Appendix Figure 9.** Scatter plot representing the relationship between optical density at 600 nm ( $OD_{600}$ ) of *V. anguillarum* Vib87 in PBS with colony forming units (CFU) plotted against optical density.  $y = 2.83 \times 10^9 x - 6.64 \times 10^8$ ;  $R^2 = 0.934$ .

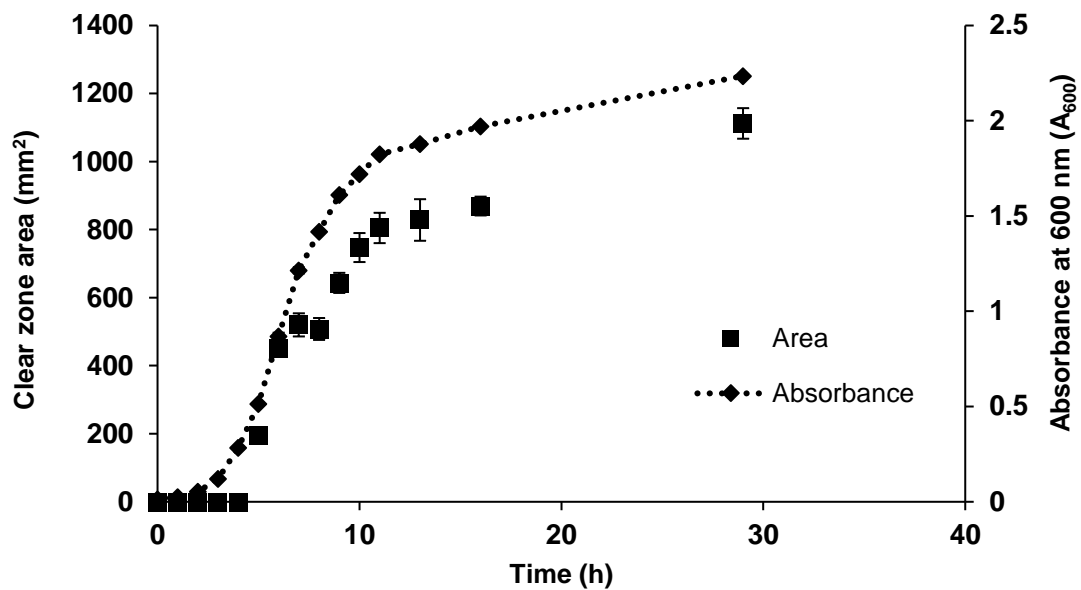
1.12. Nuclease activity screen of *Vibrio anguillarum* isolate



**Appendix Figure 10.** Histogram showing nuclease activity from 55 *V. anguillarum* isolates measured by mean DNase agar digestion area (mm<sup>2</sup>) after 24 h at 22°C. Total means of clear zones range from 0 mm<sup>2</sup> to 96.359 mm<sup>2</sup>. Error bars represent s.e.m. *n* = 3.



### 1.13. Nuclease activity of *Vibrio anguillarum* Vib 6 during culture



**Appendix Figure 11.** Scatterplot showing mean *V. anguillarum* Vib 6 culture ( $A_{600}$ ) against mean clear zone area due to nuclease activity within the culture filtrate, measured by mean DNase agar digestion area ( $\text{mm}^2$ ) on DNase agar over 29 h, 150 RPM, 22°C. The graph shows that nuclease activity within the *V. anguillarum* Vib 6 culture filtrate is produced proportionally to the growth of culture. Error bars represent s.e.m. (present with  $A_{600}$ , but too small to be observed).  $n = 4$  biological replicates.

## References

- Ababouch, L., Alder, J., Anganuzzi, A., Barg, U., Bartley, D., Bernal, M., Bianchi, G., Boccia, M., Camilleri, M., Chomo, V., Farmer, T., Franz, N., Fuentevilla, C., Funge-Smith, S., Garibaldi, L., Gee, J., Hasan, M., Hilborn, R., Hishamunda, N., Laurenti, G., Lem, A., Lovatelli, A., Mannini, P., Metzner, R., Sanders, J., Soto, D., Stankus, A., Suuronen, P., Torrie, M., Turner, J., Vannuccini, S., Ye, Y., Zhou, X., Taconet, M., Tsuji, S., Aguilar-Manjarrez, J., Liermann, C. R., Lymer, D., Fluet-Chouinard, E., McIntyre, P., Bartley, D., Kalikoski, D., Suuronen, P., Siar, S., Franz, N., Barg, U., Marttin, F., D'Andrea, M. E., Bueno, P., Soto, D., G. Marmulla, J. Caffrey, Dick, J., Gallagher, C., Lucy, F., Toppe, J., Poulain, F., Metzner, R., Barg, U., Farmer, T. and Vannuccini, S. (2016) *The state of world fisheries and aquaculture*.
- Abdallah, D. S. A., Lin, C., Ball, C. J., King, M. R., Duhamel, G. E. and Denkers, E. Y. (2012) 'Toxoplasma gondii triggers release of human and mouse neutrophil extracellular traps', *Infection and Immunity*, 80(2), pp. 768–777. doi: 10.1128/IAI.05730-11.
- Abi Abdallah, D. S. and Denkers, E. Y. (2012) 'Neutrophils cast extracellular traps in response to protozoan parasites', *Frontiers in Immunology*, 3(382), pp. 1–6. doi: 10.3389/fimmu.2012.00382.
- Achouiti, A., Vogl, T., Urban, C. F., Röhm, M., Hommes, T. J., van Zoelen, M. A. D., Florquin, S., Roth, J., van 't Veer, C., de Vos, A. F. and van der Poll, T. (2012) 'Myeloid-Related Protein-14 Contributes to Protective Immunity in Gram-Negative Pneumonia Derived Sepsis', *PLoS Pathogens*, 8(10), p. e1002987. doi: 10.1371/journal.ppat.1002987.
- Ackerman, P. A. and Iwama, G. K. (2001) 'Physiological and Cellular Stress Responses of Juvenile Rainbow Trout to Vibriosis', *Journal of Aquatic Animal Health*, 13(173), pp. 173–180. doi: 10.1577/1548-8667(2001)013<0173.
- Afonso, A., Lousada, S., Silva, J., Ellis, A. E. and Silva, M. T. (1998) 'Neutrophil and macrophage responses to inflammation in the peritoneal cavity of rainbow trout *Oncorhynchus mykiss*. A light and electron microscopic cytochemical study', *Diseases of Aquatic Organisms*, 34(1), pp. 27–37. doi: 10.3354/dao034027.
- Ainsworth, A. J. (1992) 'Fish granulocytes: Morphology, distribution, and function', *Annual Review of Fish Diseases*, 2, pp. 123–148. doi: 10.1016/0959-8030(92)90060-B.
- Aldieri, E., Riganti, C., Polimeni, M., Gazzano, E., Lussiana, C., Campia, I. and Ghigo, D. (2008) 'Classical Inhibitors of NOX NAD(P)H Oxidases Are Not Specific', *Current Drug Metabolism*, 9(8), pp. 686–696. doi: 10.2174/138920008786049285.
- Alijagic, A. and Suljevic, D. (2017) 'Haematopoietic potential of tench (*Tinca Tinca*)

pronephros in relation to ambient temperature and relative condition factor', *Bulgarian Journal of Veterinary Medicine*, 20(2), pp. 110–117. doi: 10.15547/bjvm.985.

Alter, G., Malenfant, J. M. and Altfeld, M. (2004) 'CD107a as a functional marker for the identification of natural killer cell activity', *Journal of Immunological Methods*, 294(1), pp. 15–22. doi: <https://doi.org/10.1016/j.jim.2004.08.008>.

Ambur, O. H., Davidsen, T., Frye, S. A., Balasingham, S. V., Lagesen, K., Rognes, T. and Tønjum, T. (2009) 'Genome dynamics in major bacterial pathogens', *FEMS Microbiology Reviews*, 33(3), pp. 453–470. doi: 10.1111/j.1574-6976.2009.00173.x.

Ángeles Esteban, M. (2012) 'An Overview of the Immunological Defenses in Fish Skin', *ISRN Immunology*, 2012, pp. 1–29. doi: 10.5402/2012/853470.

Arai, Y., Nishinaka, Y., Arai, T., Morita, M., Mizugishi, K., Adachi, S., Takaori-Kondo, A., Watanabe, T. and Yamashita, K. (2014) 'Uric acid induces NADPH oxidase-independent neutrophil extracellular trap formation', *Biochemical and Biophysical Research Communications*, 443(2), pp. 556–561. doi: 10.1016/j.bbrc.2013.12.007.

Arnfinn Aunsmo, Tonje C. Osmundsen, T. M. Pettersen, F.O. Mardones and Karl Rich (2015) 'Controlling emerging infectious diseases in salmon aquaculture', *Scientific and Technical Review*, 34(3), pp. 923–938.

Austin, B., Alsina, M., Austin, D. A., Blanch, A. R., Grimont, F., Grimont, P. A. D., Jofre, J., Koblavi, S., Larsen, J. L., Pedersen, K., Tiainen, T., Verdonck, L. and Swings, J. (1995) 'Identification and Typing of *Vibrio anguillarum*: A Comparison of Different Methods', *Systematic and Applied Microbiology*, 18(2), pp. 285–302. doi: 10.1016/S0723-2020(11)80400-5.

Avtalion, R. R., Wojdani, A., Malik, Z., Shahrabani, R. and Duczyminer, M. (1973) 'Influence of Environmental Temperature on the Immune Response in Fish', in *Current Topics in Microbiology and Immunology*. Berlin, Heidelberg: Springer Berlin Heidelberg, pp. 1–35.

Baggiolini, M. and Clark-Lewis, I. (1992) 'Interleukin 8, a chemotactic and inflammatory cytokine', *FEBS letters*, 307(1), pp. 97–101.

Bain, B. J. (2016) *Preparation and Staining Methods for Blood and Bone Marrow Films*. Twelfth Ed, *Dacie and Lewis Practical Haematology: Twelfth Edition*. Twelfth Ed. Elsevier Ltd. doi: 10.1016/B978-0-7020-6696-2.00004-7.

Baker, V. S., Imade, G. E., Molta, N. B., Tawde, P., Pam, S. D., Obadofin, M. O., Sagay, S. A., Egah, D. Z., Iya, D., Afolabi, B. B., Baker, M., Ford, K., Ford, R., Roux, K. H. and Keller, T. C. (2008) 'Cytokine-associated neutrophil extracellular traps and antinuclear antibodies in

*Plasmodium falciparum* infected children under six years of age', *Malaria Journal*, 7(1), p. 41. doi: 10.1186/1475-2875-7-41.

Barrientos, L., Marin-Esteban, V., Chaisemartin, L. De, Le-Moal, V. L., Sandré, C., Bianchini, E., Nicolas, V., Pallardy, M. and Chollet-Martin, S. (2013) 'An improved strategy to recover large fragments of functional human neutrophil extracellular traps', *Frontiers in Immunology*, 4(166), pp. 1–10. doi: 10.3389/fimmu.2013.00166.

Behrendt, J. H., Ruiz, A., Zahner, H., Taubert, A. and Hermosilla, C. (2010) 'Neutrophil extracellular trap formation as innate immune reactions against the apicomplexan parasite *Eimeria bovis*', *Veterinary Immunology and Immunopathology*, 133(1), pp. 1–8. doi: 10.1016/j.vetimm.2009.06.012.

Beiter, K., Wartha, F., Albiger, B., Normark, S., Zychlinsky, A. and Henriques-Normark, B. (2006) 'An endonuclease allows *Streptococcus pneumoniae* to escape from neutrophil extracellular traps', *Current Biology*, 16(4), pp. 401–407. doi: 10.1016/j.cub.2006.01.056.

Benhamed, S., Guardiola, F. A., Mars, M. and Esteban, M. Á. (2014) 'Pathogen bacteria adhesion to skin mucus of fishes', *Veterinary Microbiology*, 171, pp. 1–12. doi: 10.1016/j.vetmic.2014.03.008.

Bennike, T. B., Carlsen, T. G., Ellingsen, T., Bonderup, O. K., Glerup, H., Bøgsted, M., Christiansen, G., Birkelund, S., Stensballe, A. and Andersen, V. (2015) 'Neutrophil extracellular traps in ulcerative colitis: A proteome analysis of intestinal biopsies', *Inflammatory Bowel Diseases*, 21(9), pp. 2052–2067. doi: 10.1097/MIB.0000000000000460.

Bergé, M. J., Kamgoué, A., Martin, B., Polard, P., Campo, N. and Claverys, J. P. (2013) 'Midcell Recruitment of the DNA Uptake and Virulence Nuclease, EndA, for Pneumococcal Transformation', *PLoS Pathogens*, 9(9). doi: 10.1371/journal.ppat.1003596.

Bergsson, G., Agerberth, B., Jörnvall, H. and Gudmundsson, G. H. (2005) 'Isolation and identification of antimicrobial components from the epidermal mucus of Atlantic cod (*Gadus morhua*)', *FEBS Journal*, 272(19), pp. 4960–4969. doi: 10.1111/j.1742-4658.2005.04906.x.

Bianchi, M., Hakkim, A., Brinkmann, V., Siler, U., Seger, R. A., Zychlinsky, A. and Reichenbach, J. (2009) 'Restoration of NET formation by gene therapy in CGD controls aspergillosis', *Blood*, 114(13), pp. 2619–2622. doi: 10.1182/blood-2009-05-221606.

Birkbeck, T. H., Bordevik, M., Frøystad, M. K. and Baklien, Å. (2007) 'Identification of *Francisella* sp. from Atlantic salmon, *Salmo salar* L., in Chile', *Journal of Fish Diseases*. Blackwell Publishing Ltd, 30(8), pp. 505–507. doi: 10.1111/j.1365-2761.2007.00837.x.

Birkbeck, T. H., Laidler, L. A., Grant, A. N. and Cox, D. I. (2002) '*Pasteurella skyensis* sp.

nov., isolated from Atlantic salmon (*Salmo salar* L.)', *Int. J. Syst. Evol. Microbiol.*, 52(3), pp. 699–704. doi: 10.1099/ijs.0.01884-0.

Blokesch, M. and Schoolnik, G. K. (2008) 'The extracellular nuclease Dns and its role in natural transformation of *Vibrio cholerae*', *Journal of Bacteriology*, 190(21), pp. 7232–7240. doi: 10.1128/JB.00959-08.

Bly, J. E. and Clem, L. W. (1992) 'Temperature and teleost immune functions', *Fish and Shellfish Immunology*, 2(3), pp. 159–171. doi: 10.1016/S1050-4648(05)80056-7.

Boe, D. M., Curtis, B. J., Chen, M. M., Ippolito, J. A. and Kovacs, E. J. (2015) 'Extracellular traps and macrophages: new roles for the versatile phagocyte', *Journal of Leukocyte Biology*, 97(6), pp. 1023–1035. doi: 10.1189/jlb.4R11014-521R.

Boshra, H., Li, J. and Sunyer, J. O. (2006) 'Recent advances on the complement system of teleost fish', *Fish & Shellfish Immunology*, 20(2), pp. 239–262. doi: <https://doi.org/10.1016/j.fsi.2005.04.004>.

Brandes, R. P. and Kreuzer, J. (2005) 'Vascular NADPH oxidases: Molecular mechanisms of activation', *Cardiovascular Research*, 65(1), pp. 16–27. doi: 10.1016/j.cardiores.2004.08.007.

Branzk, N., Lubojemska, A., Hardison, S. E., Wang, Q., Gutierrez, M. G., Brown, G. D. and Papayannopoulos, V. (2014) 'Neutrophils sense microbe size and selectively release neutrophil extracellular traps in response to large pathogens.', *Nature immunology*, 15(11). doi: 10.1038/ni.2987.

Bridges, D. W., Jr, J. J. C., Pedro, D. N., Jr, J. J. C. and Hematological, D. N. P. S. (1976) 'Seasonal Hematological Changes in Winter Flounder, *Pseudopleuronectes americanus*', *Transactions of the American Fisheries Society*, 105(5). doi: 10.1577/1548-8659(1976)105<596.

Brinkmann, V., Goosmann, C., Kühn, L. I. and Zychlinsky, A. (2012) 'Automatic quantification of in vitro NET formation', *Frontiers in Immunology*, 3, p. 413. doi: 10.3389/fimmu.2012.00413.

Brinkmann, V., Reichard, U., Goosmann, C., Fauler, B., Uhlemann, Y., Weiss, D. S., Weinrauch, Y. and Zychlinsky, A. (2004) 'Neutrophil extracellular traps kill bacteria.', *Science (New York, N.Y.)*, 303(5663), pp. 1532–1535. doi: 10.1126/science.1092385.

Brinkmann, V. and Zychlinsky, A. (2007) 'Beneficial suicide: Why neutrophils die to make NETs', *Nature Reviews Microbiology*, 5(8), pp. 577–582. doi: 10.1038/nrmicro1710.

- Brinkmann, V. and Zychlinsky, A. (2012) 'Neutrophil extracellular traps: Is immunity the second function of chromatin?', *Journal of Cell Biology*, pp. 773–783. doi: 10.1083/jcb.201203170.
- Brogden, G. (2013) *Cell-pathogen interactions in common carp (Cyprinus carpio L.): Studies on cell membranes and neutrophil responses (Doctoral dissertation)*. Bibliothek der Tierärztlichen Hochschule Hannover.
- Brogden, G., von Köckritz-Blickwede, M., Adamek, M., Reuner, F., Jung-Schroers, V., Naim, H. Y. and Steinhagen, D. (2012) 'β-Glucan protects neutrophil extracellular traps against degradation by *Aeromonas hydrophila* in carp (*Cyprinus carpio*)', *Fish and Shellfish Immunology*, pp. 1060–1064. doi: 10.1016/j.fsi.2012.08.009.
- Brogden, G., Krimmling, T., Adamek, M., Naim, H. Y., Steinhagen, D. and Von Köckritz-Blickwede, M. (2014) 'The effect of β-glucan on formation and functionality of neutrophil extracellular traps in carp (*Cyprinus carpio* L.)', *Developmental and Comparative Immunology*. Elsevier Ltd, 44(2), pp. 280–285. doi: 10.1016/j.dci.2014.01.003.
- Brookes, P. S., Yoon, Y., Robotham, J. L., Anders, M. W. and Sheu, S.-S. (2004) 'Calcium, ATP, and ROS: a mitochondrial love-hate triangle', *American Journal of Physiology-Cell Physiology*. American Physiological Society, 287(4), pp. C817–C833. doi: 10.1152/ajpcell.00139.2004.
- Brunner, D., Frank, J., Appl, H., Schöffl, H., Pfaller, W. and Gstraunthaler, G. (2010) 'Serum-free cell culture: the serum-free media interactive online database.', *Altex*, 27(1), pp. 53–62. doi: 10.14573/altex.2010.1.53.
- Bruns, S., Kniemeyer, O., Hasenberg, M., Amanianda, V., Nietzsche, S., Thywißen, A., Jeron, A., Latgé, J.-P., Brakhage, A. A. and Gunzer, M. (2010) 'Production of Extracellular Traps against *Aspergillus fumigatus* *In Vitro* and in Infected Lung Tissue Is Dependent on Invading Neutrophils and Influenced by Hydrophobin RodA', *PLoS Pathogens*, 6(4), p. e1000873. doi: 10.1371/journal.ppat.1000873.
- Buchanan, J. T., Simpson, A. J., Aziz, R. K., Liu, G. Y., Kristian, S. A., Kotb, M., Feramisco, J. and Nizet, V. (2006) 'DNase expression allows the pathogen group A *Streptococcus* to escape killing in neutrophil extracellular traps.', *Current biology: CB*, 16(4), pp. 396–400. doi: 10.1016/j.cub.2005.12.039.
- de Buhr, N. and von Köckritz-blickwede, M. (2016) 'How Neutrophil Extracellular Traps Become Visible', *Journal of Immunology Research*, pp. 1–11.
- de Buhr, N., Stehr, M., Neumann, A., Naim, H. Y., Valentin-Weigand, P., von Köckritz-

- Blickwede, M. and Baums, C. G. (2015) 'Identification of a novel DNase of *Streptococcus suis* (EndAsuis) important for neutrophil extracellular trap degradation during exponential growth', *Microbiology (Reading, England)*, 161(4), pp. 838–850. doi: 10.1099/mic.0.000040.
- Buschmann, A. H., Tomova, A., López, A., Maldonado, M. A., Henríquez, L. A., Ivanova, L., Moy, F., Godfrey, H. P. and Cabello, F. C. (2012) 'Salmon aquaculture and antimicrobial resistance in the marine environment', *PLoS ONE*, 7(8), pp. 26–28. doi: 10.1371/journal.pone.0042724.
- Cabello, F. C. (2006) 'Heavy use of prophylactic antibiotics in aquaculture: A growing problem for human and animal health and for the environment', *Environmental Microbiology*, 8(7), pp. 1137–1144. doi: 10.1111/j.1462-2920.2006.01054.x.
- Cao, E., Chen, Y., Cui, Z. and Foster, P. R. (2003) 'Effect of freezing and thawing rates on denaturation of proteins in aqueous solutions', *Biotechnology and Bioengineering*, 82(6), pp. 684–690. doi: 10.1002/bit.10612.
- Carda-Diéguez, M., Ghai, R., Rodríguez-Valera, F. and Amaro, C. (2017) 'Wild eel microbiome reveals that skin mucus of fish could be a natural niche for aquatic mucosal pathogen evolution', *Microbiome*. *Microbiome*, 5(1), p. 162. doi: 10.1186/s40168-017-0376-1.
- Carlson, M., Peterson, C. and Venge, P. (1993) 'The influence of IL-3, IL-5, and GM-CSF on normal human eosinophil and neutrophil C3b-induced degranulation', *Allergy*, 48(6), p. 437–442. Available at: <http://europepmc.org/abstract/MED/8238799>.
- Chalmers, L., Talor, J. F., Roy, W., Preston, A. C., Migaud, H. and Adams, A. (2017) 'A comparison of disease susceptibility and innate immune response between diploid and triploid Atlantic salmon (*Salmo salar*) siblings following experimental infection with *Neoparamoeba perurans*, causative agent of amoebic gill disease', *Parasitology*, 144(9), pp. 1–14. doi: 10.1017/S0031182017000622.
- Cheng, O. Z. and Palaniyar, N. (2013) 'NET balancing: A problem in inflammatory lung diseases', *Frontiers in Immunology*, 4, pp. 1–13. doi: 10.3389/fimmu.2013.00001.
- Chi, H. and Sun, L. (2015) 'Neutrophils of *Scophthalmus maximus* L. produce extracellular traps that capture bacteria and inhibit bacterial infection.', *Developmental and comparative immunology*, 56, pp. 7–12. doi: 10.1016/j.dci.2015.11.005.
- Chow, O. A., Von Köckritz-Blickwede, M., Bright, A. T., Hensler, M. E., Zinkernagel, A. S., Cogen, A. L., Gallo, R. L., Monestier, M., Wang, Y., Glass, C. K. and Nizet, V. (2010) 'Statins enhance formation of phagocyte extracellular traps', *Cell Host and Microbe*, 8(5), pp.

445–454. doi: 10.1016/j.chom.2010.10.005.

Chuammitri, P., Ostojić, J., Andreasen, C. B., Redmond, S. B., Lamont, S. J. and Palić, D. (2009) 'Chicken heterophil extracellular traps (HETs): Novel defense mechanism of chicken heterophils', *Veterinary Immunology and Immunopathology*, 129(1–2), pp. 126–131. doi: 10.1016/j.vetimm.2008.12.013.

Clark, S. R., Ma, A. C., Tavener, S. A., McDonald, B., Goodarzi, Z., Kelly, M. M., Patel, K. D., Chakrabarti, S., McAvoy, E., Sinclair, G. D., Keys, E. M., Allen-Vercoe, E., DeVinney, R., Doig, C. J., Green, F. H. Y. and Kubes, P. (2007) 'Platelet TLR4 activates neutrophil extracellular traps to ensnare bacteria in septic blood', *Nature Medicine*, 13(4), pp. 463–469. doi: 10.1038/nm1565.

Clauss, T. M., Dove, A. D. M. and Arnold, J. E. (2008) 'Hematologic Disorders of Fish', *Veterinary Clinics: Exotic Animal Practice*, 11, pp. 445–462. doi: 10.1016/j.cvex.2008.03.007.

Collet, B. (2014) 'Innate immune responses of salmonid fish to viral infections', *Developmental and Comparative Immunology*. Elsevier Ltd, 43(2), pp. 160–173. doi: 10.1016/j.dci.2013.08.017.

Croxatto, A., Lauritz, J., Chen, C. and Milton, D. L. (2007) '*Vibrio anguillarum* colonization of rainbow trout integument requires a DNA locus involved in exopolysaccharide transport and biosynthesis', *Environmental Microbiology*, 9(2), pp. 370–382. doi: 10.1111/j.1462-2920.2006.01147.x.

Cuatrecasas, P., Fuchs, S. and Anfinsen, C. B. (1967) 'The binding of nucleotides and calcium to the extracellular nuclease of *Staphylococcus aureus*. Studies by gel filtration.', *Journal of Biological Chemistry*, 242(13), pp. 3063–3067.

Dang, G., Cao, J., Cui, Y., Song, N., Chen, L., Pang, H. and Liu, S. (2016) 'Characterization of Rv0888, a Novel Extracellular Nuclease from *Mycobacterium tuberculosis*', *Scientific reports*. Nature Publishing Group, 6, p. 19033. doi: 10.1038/srep19033.

Dekker, L. V., Leitges, M., Altschuler, G., Mistry, N., McDermott, A., Roes, J. and Segal, A. W. (2000) 'Protein kinase C-beta contributes to NADPH oxidase activation in neutrophils', *The Biochemical Journal*, pp. 285–289.

Delves, P. J., Martin, S. J., Burton, D. R. and Roitt, I. M. (2017) *Essential immunology*. John Wiley & Sons.

Denton, J. and Yousef, M. (1975) 'Seasonal changes in hematology of rainbow trout, *Salmo gairdneri*', *Comparative Biochemistry and Physiology Part A*, 51(1), pp. 151–153.



- Derré-Bobillot, A., Cortes-Perez, N. G., Yamamoto, Y., Kharrat, P., Couvé, E., Da Cunha, V., Decker, P., Boissier, M. C., Escartin, F., Cesselin, B., Langella, P., Bermúdez-Humarán, L. G. and Gaudu, P. (2013) 'Nuclease A (Gbs0661), an extracellular nuclease of *Streptococcus agalactiae*, attacks the neutrophil extracellular traps and is needed for full virulence', *Molecular Microbiology*, 89(3), pp. 518–531. doi: 10.1111/mmi.12295.
- Desai, N. a and Shankar, V. (2003) 'Single-strand-specific nucleases', *FEMS Microbiology Reviews*, 26, pp. 457–491.
- Deschesnes, R. G., Huot, J., Valerie, K. and Landry, J. (2001) 'Involvement of p38 in apoptosis-associated membrane blebbing and nuclear condensation.', *Molecular biology of the cell*, 12(6), pp. 1569–82. doi: 10.1091/mbc.12.6.1569.
- Douda, D. N., Jackson, R., Grasemann, H. and Palaniyar, N. (2011) 'Innate Immune Collectin Surfactant Protein D Simultaneously Binds Both Neutrophil Extracellular Traps and Carbohydrate Ligands and Promotes Bacterial Trapping', *The Journal of Immunology*, 187(4), pp. 1856–1865. doi: 10.4049/jimmunol.1004201.
- Douda, D. N., Khan, M. A., Grasemann, H. and Palaniyar, N. (2015) 'SK3 channel and mitochondrial ROS mediate NADPH oxidase-independent NETosis induced by calcium influx', *Proceedings of the National Academy of Sciences*, 112(9), pp. 2817–2822. doi: 10.1073/pnas.1414055112.
- Doulatov, S., Notta, F., Laurenti, E. and Dick, J. E. (2012) 'Hematopoiesis: A human perspective', *Cell Stem Cell*. Elsevier Inc., 10(2), pp. 120–136. doi: 10.1016/j.stem.2012.01.006.
- Doussiere, J. and Vignais, P. V. (1992) 'Diphenylene iodonium as an inhibitor of the NADPH oxidase complex of bovine neutrophils: Factors controlling the inhibitory potency of diphenylene iodonium in a cell-free system of oxidase activation', *European Journal of Biochemistry*, 208(1), pp. 61–71. doi: 10.1111/j.1432-1033.1992.tb17159.x.
- Dutta, T. K., Jana, M., Pahari, P. R. and Bhattacharya, T. (2006) 'The effect of temperature, pH, and salt on amylase in *Heliodyptomus viduus* (Gurney) (Crustacea: Copepoda: Calanoida)', *Turkish Journal of Zoology*, 30(2), pp. 187–195.
- Elson, G., Dunn-Siegrist, I., Daubeuf, B. and Pugin, J. (2007) 'Contribution of Toll-like receptors to the Innate Immune Response to Gram-Negative and Gram-Positive bacteria', *October*, 2(4), pp. 1574–1584. doi: 10.1182/blood-2006-06-032961.
- Epand, R. M. and Epand, R. F. (2009) 'Lipid domains in bacterial membranes and the action of antimicrobial agents', *Biochimica et Biophysica Acta - Biomembranes*. Elsevier B.V.,

1788(1), pp. 289–294. doi: 10.1016/j.bbamem.2008.08.023.

Fadini, G. P., Menegazzo, L., Rigato, M., Scattolini, V., Poncina, N., Bruttocao, A., Ciciliot, S., Mammano, F., Ciubotaru, C. D., Brocco, E., Marescotti, M. C., Cappellari, R., Arrigoni, G., Millionsi, R., De Kreutzenberg, S. V., Albiero, M. and Avogaro, A. (2016) 'NETosis delays diabetic wound healing in mice and humans', *Diabetes*, 65(4), pp. 1061–1071. doi: 10.2337/db15-0863.

Falco, A., Frost, P., Miest, J., Pionnier, N., Irnazarow, I. and Hoole, D. (2012) 'Reduced inflammatory response to *Aeromonas salmonicida* infection in common carp (*Cyprinus carpio* L.) fed with  $\beta$ -glucan supplements', *Fish and Shellfish Immunology*. Elsevier Ltd, 32(6), pp. 1051–1057. doi: 10.1016/j.fsi.2012.02.028.

Fänge, R. and Nilsson, S. (1985) 'The fish spleen: structure and function', *Experientia*, 41(2), pp. 152–158. doi: 10.1007/BF02002607.

FAO, D. of F. and A. (2017) 'FAO yearbook of fishery and aquaculture statistics summary tables', 0, pp. 26–28. doi: 10.5860/CHOICE.50-5350.

Farrera, C. and Fadeel, B. (2013) 'Macrophage Clearance of Neutrophil Extracellular Traps Is a Silent Process', *The Journal of Immunology*, 191(5), pp. 2647–2656. doi: 10.4049/jimmunol.1300436.

Fast, M. D., Sims, D. E., Burka, J. F., Mustafa, A. and Ross, N. W. (2002) 'Skin morphology and humoral non-specific defence parameters of mucus and plasma in rainbow trout, coho and Atlantic salmon', *Comparative Biochemistry and Physiology - A Molecular and Integrative Physiology*, 132(3), pp. 645–657. doi: 10.1016/S1095-6433(02)00109-5.

Ferguson, W. J., Braunschweiger, K. I., Braunschweiger, W. R., Smith, J. R., McCormick, J. J., Wasmann, C. C., Jarvis, N. P., Bell, D. H. and Good, N. E. (1980) 'Hydrogen ion buffers for biological research', *Analytical Biochemistry*, 104(2), pp. 300–310. doi: 10.1016/0003-2697(80)90079-2.

Fernández, J. M., Kemp, G. D., Molle, M. G. and Smith, V. J. (2002) 'Anti-microbial properties of histone H2A from skin secretions of rainbow trout, *Oncorhynchus mykiss*', *Biochem J*, 368(Pt 2), pp. 611–620. doi: 10.1042/BJ20020980 [pii].

Ferrieri, P., Gray, E. D. and Wannamaker, L. W. (1980) 'Biochemical and immunological characterization of the extracellular nucleases of group B streptococci.', *The Journal of experimental medicine*, 151(1), pp. 56–68. Available at: <http://www.pubmedcentral.nih.gov/articlerender.fcgi?artid=2185748&tool=pmcentrez&render type=abstract>.

- Firth, K. J., Johnson, S. C. and Ross, N. W. (2000) 'Characterization of proteases in the skin mucus of Atlantic salmon (*Salmo salar*) infected with the salmon louse (*Lepeophtheirus salmonis*) and in whole-body louse homogenate.', *The Journal of parasitology*, 86(6), pp. 1199–205. doi: 10.1645/0022-3395(2000)086[1199:COPITS]2.0.CO;2.
- Flerova, E. a. and Balabanova, L. V. (2013) 'Ultrastructure of granulocytes of teleost fish (Salmoniformes, Cypriniformes, Perciformes)', *Journal of Evolutionary Biochemistry and Physiology*, 49(2), pp. 223–233. doi: 10.1134/S0022093013020126.
- Floyd, M., Winn, M., Cullen, C., Sil, P., Chassaing, B., Yoo, D. G., Gewirtz, A. T., Goldberg, J. B., McCarter, L. L. and Rada, B. (2016) 'Swimming Motility Mediates the Formation of Neutrophil Extracellular Traps Induced by Flagellated *Pseudomonas aeruginosa*', *PLoS Pathogens*, 12(11), pp. 1–32. doi: 10.1371/journal.ppat.1005987.
- Focareta, T. (1989) 'The Extracellular DNase(s) Of *Vibrio Cholerae*', *PhD Thesis*.
- Forti, R. (2017) *Agriculture, forestry and fishery statistics*. Edited by R. Forti. Luxembourg: Artemis Information Management. doi: 10.2785/45595.
- Frank, J. J., Hawk, I. A. and Levy, C. C. (1975) 'Polyamine activation of staphylococcal nuclease', *Biochimica et Biophysica Acta (BBA): Nucleic Acids And Protein Synthesis*. Elsevier, 390(1), pp. 117–124. doi: 10.1016/0005-2787(75)90014-3.
- Frans, I., Busschaert, P., Dierckens, K., Michiels, C. W., Willems, K. A., Lievens, B., Bossier, P. and Rediers, H. (2013) 'Are type IV pili involved in *Vibrio anguillarum* virulence towards sea bass (*Dicentrarchus labrax* L.) larvae?', *Agricultural Sciences*, 4(6), pp. 30–38. doi: 10.4236/as.2013.46A005.
- Frans, I., Michiels, C. W., Bossier, P., Willems, K. A., Lievens, B. and Rediers, H. (2011) 'Vibrio anguillarum as a fish pathogen: Virulence factors, diagnosis and prevention', *Journal of Fish Diseases*, 34(9), pp. 643–661. doi: 10.1111/j.1365-2761.2011.01279.x.
- Frei, M. (2011) 'Biofiles: Centrifugation', *Biofiles Sigma-Aldrich*, 6(5), pp. 1–32. Available at: <https://www.sigmaaldrich.com/technical-documents/articles/biofiles/centrifugation-separations.html#isopycnic>.
- Fuchs, T. A., Abed, U., Goosmann, C., Hurwitz, R., Schulze, I., Wahn, V., Weinrauch, Y., Brinkmann, V. and Zychlinsky, A. (2007) 'Novel cell death program leads to neutrophil extracellular traps', *Journal of Cell Biology*, 176(2), pp. 231–241. doi: 10.1083/jcb.200606027.
- Fuchs, T. A., Brill, A., Duerschmied, D., Schatzberg, D., Monestier, M., Myers, D. D., Wroblewski, S. K., Wakefield, T. W., Hartwig, J. H. and Wagner, D. D. (2010) 'Extracellular

DNA traps promote thrombosis', *Proceedings of the National Academy of Sciences*, 107(36), pp. 15880–15885. doi: 10.1073/pnas.1005743107.

Funchal, G. A., Jaeger, N., Czepielewski, R. S., Machado, M. S., Muraro, S. P., Stein, R. T., Bonorino, C. B. C. and Porto, B. N. (2015) 'Respiratory syncytial virus fusion protein promotes TLR-4-dependent neutrophil extracellular trap formation by human neutrophils', *PLoS ONE*, 10(4), pp. 1–14. doi: 10.1371/journal.pone.0124082.

Gavillet, M., Martinod, K., Renella, R., Harris, C., Shapiro, N. I., Wagner, D. D. and Williams, D. A. (2015) 'Flow cytometric assay for direct quantification of neutrophil extracellular traps in blood samples', *American Journal of Hematology*, 90(12), pp. 1155–1158. doi: 10.1002/ajh.24185.

Glasauer, S. M. K. and Neuhauss, S. C. F. (2014) 'Whole-genome duplication in teleost fishes and its evolutionary consequences', *Molecular Genetics and Genomics*, 289(6), pp. 1045–1060. doi: 10.1007/s00438-014-0889-2.

Görlach, A., Bertram, K., Hudecova, S. and Krizanova, O. (2015) 'Calcium and ROS: A mutual interplay', *Redox Biology*, 6, pp. 260–271. doi: 10.1016/j.redox.2015.08.010.

Gray, R. D., Lucas, C. D., MacKellar, A., Li, F., Hiersemenzel, K., Haslett, C., Davidson, D. J. and Rossi, A. G. (2013) 'Activation of conventional protein kinase C (PKC) is critical in the generation of human neutrophil extracellular traps', *Journal of Inflammation*, 10(1), p. 12. doi: 10.1186/1476-9255-10-12.

Griffith, J. W., Sokol, C. L. and Luster, A. D. (2014) 'Chemokines and Chemokine Receptors: Positioning Cells for Host Defense and Immunity', *Annual Review of Immunology*, 32(1), pp. 659–702. doi: 10.1146/annurev-immunol-032713-120145.

Guimaraes-Costa, A. B., Nascimento, M. T. C., Froment, G. S., Soares, R. P. P., Morgado, F. N., Conceicao-Silva, F. and Saraiva, E. M. (2009) '*Leishmania amazonensis* promastigotes induce and are killed by neutrophil extracellular traps', *Proceedings of the National Academy of Sciences*, 106(16), pp. 6748–6753. doi: 10.1073/pnas.0900226106.

Gullberg, U., Andersson, E., Garwicz, D., Lindmark, A. and Olsson, I. (1997) 'Biosynthesis, processing and sorting of neutrophil proteins: insight into neutrophil granule development.', *European journal of haematology*, 58(3), pp. 137–53. doi: 10.1111/j.1600-0609.1997.tb00940.x.

Gupta, A. K., Joshi, M. B., Philippova, M., Erne, P., Hasler, P., Hahn, S. and Resink, T. J. (2010) 'Activated endothelial cells induce neutrophil extracellular traps and are susceptible to NETosis-mediated cell death', *FEBS Letters*. Federation of European Biochemical

Societies, 584(14), pp. 3193–3197. doi: 10.1016/j.febslet.2010.06.006.

Guyot, J., Jeminet, G., Prudhomme, M., Sancelme, M. and Meiniel, R. (1993) 'Interaction of the calcium ionophore A.23187 (Calcimycin) with *Bacillus cereus* and *Escherichia coli*', *Letters in Applied Microbiology*. Blackwell Publishing Ltd, 16(4), pp. 192–195. doi: 10.1111/j.1472-765X.1993.tb01394.x.

Hahn, I., Klaus, A., Janze, A. K., Steinwede, K., Ding, N., Bohling, J., Brumshagen, C., Serrano, H., Gauthier, F., Paton, J. C., Welte, T. and Maus, U. A. (2011) 'Cathepsin G and neutrophil elastase play critical and nonredundant roles in lung-protective immunity against *Streptococcus pneumoniae* in mice', *Infection and Immunity*. Edited by J. N. Weiser. 1752 N St., N.W., Washington, DC: American Society for Microbiology, 79(12), pp. 4893–4901. doi: 10.1128/IAI.05593-11.

Hakkim, A., Fuchs, T. a, Martinez, N. E., Hess, S., Prinz, H., Zychlinsky, A. and Waldmann, H. (2011) 'Activation of the Raf-MEK-ERK pathway is required for neutrophil extracellular trap formation.', *Nature*. Nature Publishing Group, 7(2), pp. 75–77. doi: 10.1038/nchembio.496.

Hakkim, A., Furnrohr, B. G., Amann, K., Laube, B., Abed, U. A., Brinkmann, V., Herrmann, M., Voll, R. E. and Zychlinsky, A. (2010) 'Impairment of neutrophil extracellular trap degradation is associated with lupus nephritis', *Proceedings of the National Academy of Sciences*, 107(21), pp. 9813–9818. doi: 10.1073/pnas.0909927107.

Halverson, T. W. R., Wilton, M., Poon, K. K. H., Petri, B. and Lewenza, S. (2015) 'DNA is an antimicrobial component of neutrophil extracellular traps', *PLoS pathogens*, 11, p. e1004593. doi: 10.1371/journal.ppat.1004593.

Hamdani, S. H., McMillan, D. N., Pettersen, E. F., Wergeland, H., Endresen, C., Ellis, A. E. and Secombes, C. J. (1998) 'Isolation of rainbow trout neutrophils with an anti-granulocyte monoclonal antibody', *Veterinary Immunology and Immunopathology*, 63(4), pp. 369–380. doi: 10.1016/S0165-2427(98)00115-9.

Hardie, L. J., Fletcher, T. C. and Secombes, C. J. (1994) 'Effect of Temperature on Macrophage Activation and the Production of Macrophage Activating Factor by Rainbow-Trout (*Oncorhynchus-Mykiss*) Leukocytes', *Developmental and Comparative Immunology*, 18(1), pp. 57–66.

Harris, J. and Bird, D. J. (2000) 'Modulation of the fish immune system by hormones', *Vet. Immunol. Immunopathol.*, 77, pp. 163–176.

Havixbeck, J. and Barreda, D. (2015) 'Neutrophil Development, Migration, and Function in

Teleost Fish', *Biology*, 4(4), pp. 715–734. doi: 10.3390/biology4040715.

Hayashi, F., Smith, K. D., Ozinsky, A., Hawn, T. R., Yi, E. C., Goodlett, D. R., Eng, J. K., Akira, S., Underhill, D. M. and Aderem, A. (2001) 'The innate immune response to bacterial flagellin is mediated by Toll- like receptor 5', *Nature*, 410(6832), p. 1099–103. doi: 10.1038/35074106.

Henke, M. O. and Ratjen, F. (2007) 'Mucolytics in cystic fibrosis', *Paediatric Respiratory Reviews*, 8(1), pp. 24–29. doi: 10.1016/j.prrv.2007.02.009.

Herrera, J. E. and Chaires, J. B. (1994) 'Characterization of Preferred Deoxyribonuclease I Cleavage Sites', *Journal of Molecular Biology*, 236(2), pp. 405–411. doi: <https://doi.org/10.1006/jmbi.1994.1152>.

Hickey, M. E. and Lee, J. L. (2017) 'A comprehensive review of *Vibrio (Listonella) anguillarum*: Ecology, pathology and prevention', *Reviews in Aquaculture*, 1893, pp. 1–26. doi: 10.1111/raq.12188.

Hoare, R., Ngo, T. P. H., Bartie, K. L. and Adams, A. (2017) 'Efficacy of a polyvalent immersion vaccine against *Flavobacterium psychrophilum* and evaluation of immune response to vaccination in rainbow trout fry (*Onchorynchus mykiss L.*)', *Veterinary Research*, 48(1), pp. 1–13. doi: 10.1186/s13567-017-0448-z.

Hoover, G. J., El-Mowafi, A., Simko, E., Kocal, T. E., Ferguson, H. W. and Hayes, M. A. (1998) 'Plasma proteins of rainbow trout (*Oncorhynchus mykiss*) isolated by binding to lipopolysaccharide from *Aeromonas salmonicida*', *Comparative Biochemistry and Physiology - B Biochemistry and Molecular Biology*, 120(3), pp. 559–569. doi: 10.1016/S0305-0491(98)10042-1.

Hoppenbrouwers, T., Autar, A. S. A., Sultan, A. R., Abraham, T. E., Van Cappellen, W. A., Houtsmuller, A. B., Van Wamel, W. J. B., Van Beusekom, H. M. M., Van Neck, J. W. and De Maat, M. P. M. (2017) 'In vitro induction of NETosis: Comprehensive live imaging comparison and systematic review', *PLoS ONE*, 12(5), pp. 1–29. doi: 10.1371/journal.pone.0176472.

Hsia, K. C., Li, C. L. and Yuan, H. S. (2005) 'Structural and functional insight into sugar-nonspecific nucleases in host defense', *Current Opinion in Structural Biology*, 15(1), pp. 126–134. doi: 10.1016/j.sbi.2005.01.015.

Iscove, N. N. and Melchers, F. (1978) 'Complete replacement of serum by albumin, transferrin, and soybean lipid in cultures of lipopolysaccharide-reactive B lymphocytes.', *The Journal of experimental medicine*, 147(3), pp. 923–33. doi: 10.1084/jem.147.3.923.

Jeffery, U., Gray, R. D. and LeVine, D. N. (2016) 'A Simple Fluorescence Assay for Quantification of Canine Neutrophil Extracellular Trap Release', *Journal of Visualized Experiments*, (117), pp. 1–4. doi: 10.3791/54726.

Jeffery, U., Kimura, K., Gray, R., Lueth, P., Bellaire, B. and LeVine, D. (2015) 'Dogs cast NETs too: Canine neutrophil extracellular traps in health and immune-mediated hemolytic anemia', *Veterinary Immunology and Immunopathology*, 168(3–4), pp. 262–268. doi: 10.1016/j.vetimm.2015.10.014.

Ji, Y., Li, J., Qin, Z., Li, A., Gu, Z., Liu, X., Lin, L. and Zhou, Y. (2015) 'Contribution of nuclease to the pathogenesis of *Aeromonas hydrophila*', *Virulence*, 6(5), pp. 515–522. doi: 10.1080/21505594.2015.1049806.

Johansson, L. H., Timmerhaus, G., Afanasyev, S., Jørgensen, S. M. and Krasnov, A. (2016) 'Smoltification and seawater transfer of Atlantic salmon (*Salmo salar* L.) is associated with systemic repression of the immune transcriptome', *Fish and Shellfish Immunology*. Elsevier Ltd, 58, pp. 33–41. doi: 10.1016/j.fsi.2016.09.026.

Jorch, S. K. and Kubes, P. (2017) 'An emerging role for neutrophil extracellular traps in noninfectious disease', *Nature Medicine*, 23(3), pp. 279–287. doi: 10.1038/nm.4294.

Juneau, R. A., Pang, B., Weimer, K. E. D., Armbruster, C. E. and Swords, W. E. (2011) 'Nontypeable *Haemophilus influenzae* initiates formation of neutrophil extracellular traps', *Infection and immunity*, 79(1), pp. 431–438. doi: 10.1128/IAI.00660-10.

Juneau, R. a., Stevens, J. S., Apicella, M. a. and Criss, A. K. (2015) 'A thermonuclease of *Neisseria gonorrhoeae* enhances bacterial escape from killing by neutrophil extracellular traps', *Journal of Infectious Diseases*, 212(2), pp. 316–324. doi: 10.1093/infdis/jiv031.

Jyonouchi, H., Zhang, L. E. I. and Tomita, Y. (1993) 'Studies of Immunomodulating Actions of RNA / Nucleotides . RNA / Nucleotides Enhance In Vitro Immunoglobulin Production by Human Peripheral Blood Mononuclear Cells in Response to T-Dependent Stimuli', *Paediatric Research*, 33(5), pp. 458–465.

Kaattari, S. L. (1992) 'Fish B lymphocytes: Defining their form and function', *Annual Review of Fish Diseases*, 2, pp. 161–180. doi: 10.1016/0959-8030(92)90062-3.

Kahlenberg, J. M. and Kaplan, M. J. (2013) 'Little Peptide, Big Effects: The Role of LL-37 in Inflammation and Autoimmune Disease', *The Journal of Immunology*, 191(10), pp. 4895–4901. doi: 10.4049/jimmunol.1302005.

Kamoshida, G., Kikuchi-Ueda, T., Nishida, S., Tansho-Nagakawa, S., Kikuchi, H., Ubagai, T. and Ono, Y. (2017) 'Spontaneous formation of neutrophil extracellular traps in serum-free

culture conditions', *FEBS Open Bio*, 7(6), pp. 877–886. doi: 10.1002/2211-5463.12222.

Kaplan, M. J. and Radic, M. (2012) 'Neutrophil Extracellular Traps: Double-Edged Swords of Innate Immunity', *The Journal of Immunology*, 189(6), pp. 2689–2695. doi: 10.4049/jimmunol.1201719.

Karl, D. M. and Bailiff, M. D. (1989) 'The Measurement and Distribution of Dissolved Nucleic Acids in Aquatic Environments', *Limnology and Oceanography*, 34(3), pp. 543–558.

Kato, M., Kephart, G. M., Talley, N. J., Wagner, J. M., Sarr, M. G., Bonno, M., MCGovern, T. W. and Gleich, G. J. (1998) 'Eosinophil Infiltration and Degranulation in Normal Human Tissue', *The Anatomical Record*, 252(3), pp. 418–425.

Katzenback, B. A. and Belosevic, M. (2009) 'Isolation and functional characterization of neutrophil-like cells, from goldfish (*Carassius auratus L.*) kidney', *Developmental and Comparative Immunology*, 33(4), pp. 601–611. doi: 10.1016/j.dci.2008.10.011.

Katzenback, B. A., Katakura, F. and Belosevic, M. (2012) 'Regulation of Teleost Macrophage and Neutrophil Cell Development by Growth Factors and Transcription Factors', *Intech*. Edited by H. B. T.-N. A. and C. to F. B. Türker. Rijeka: InTech, pp. 97–150. doi: 10.5772/53589.

Kauzmann, W. (1959) 'Some factors in the separation of protein denaturation', in *Advances in Protein Chemistry*, pp. 1–63. doi: 10.1016/S0065-3233(08)60608-7.

Keijsers, R. R. M. C., Hendriks, A. G. M., Van Erp, P. E. J., Van Cranenbroek, B., Van De Kerkhof, P. C. M., Koenen, H. J. P. M. and Joosten, I. (2014) 'In vivo induction of cutaneous inflammation results in the accumulation of extracellular trap-forming neutrophils expressing ROR $\gamma$ t and IL-17', *Journal of Investigative Dermatology*, 134(5), pp. 1276–1284. doi: 10.1038/jid.2013.526.

Kemenade, B., Groeneveld, A., Rens, B. and Rombout, J. (1994) 'Characterization of Macrophages and Neutrophilic Granulocytes From the Pronephros of Carp (*Cyprinus Carpio*)', *The Journal of experimental biology*, 187(1), pp. 143–58. Available at: <http://www.ncbi.nlm.nih.gov/pubmed/9317515>.

Kendall, R. L. (1988) 'Taxonomic changes in North American trout names', *Trans.Am.Fish.Soc.*, 117(4), p. 321. doi: 10.1577/1548-8659-117.4.321.

Keshari, R. S., Jyoti, A., Dubey, M., Kothari, N., Kohli, M., Bogra, J., Barthwal, M. K. and Dikshit, M. (2012) 'Cytokines Induced Neutrophil Extracellular Traps Formation: Implication for the Inflammatory Disease Condition', *PLoS ONE*, 7(10), p. e48111. doi: 10.1371/journal.pone.0048111.



Kiedrowski, M. R., Crosby, H. A., Hernandez, F. J., Malone, C. L., McNamara, J. O. and Horswill, A. R. (2014) 'Staphylococcus aureus Nuc2 is a functional, surface-attached extracellular nuclease', *PLoS ONE*, 9(4). doi: 10.1371/journal.pone.0095574.

Kim, J., Seo, M., Kim, S. K. and Bae, Y. S. (2016) 'Flagellin-induced NADPH oxidase 4 activation is involved in atherosclerosis', *Scientific Reports*, 6, pp. 1–16. doi: 10.1038/srep25437.

Kim, S. H. and Lee, G. M. (2007) 'Differences in optimal pH and temperature for cell growth and antibody production between two Chinese hamster ovary clones derived from the same parental clone', *Journal of Microbiology and Biotechnology*, 17(5), pp. 712–720.

Kim, S. R., Nonaka, L. and Suzuki, S. (2004) 'Occurrence of tetracycline resistance genes tet(M) and tet(S) in bacteria from marine aquaculture sites', *FEMS Microbiology Letters*, 237(1), pp. 147–156. doi: 10.1016/j.femsle.2004.06.026.

Kobayashi, I., Sekiya, M., Moritomo, T., Ototake, M. and Nakanishi, T. (2006) 'Demonstration of hematopoietic stem cells in ginbuna carp (*Carassius auratus langsdorffii*) kidney', *Developmental and Comparative Immunology*, 30(11), pp. 1034–1046. doi: 10.1016/j.dci.2006.01.005.

von Köckritz-Blickwede, M., Chow, O. A. and Nizet, V. (2009) 'Fetal calf serum contains heat-stable nucleases that degrade neutrophil extracellular traps', *Blood*. Washington, DC: American Society of Hematology, 114(25), pp. 5245–5246. doi: 10.1182/blood-2009-08-240713.

von Köckritz-Blickwede, M., Chow, O., Ghochani, M. and Nizet, V. (2010) *Visualization and functional evaluation of phagocyte extracellular traps*. Third Edit, *Methods in Microbiology*. Third Edit. Elsevier Ltd. doi: 10.1016/S0580-9517(10)37007-3.

Von Köckritz-Blickwede, M., Goldmann, O., Thulin, P., Heinemann, K., Norrby-Teglund, A., Rohde, M. and Medina, E. (2008) 'Phagocytosis-independent antimicrobial activity of mast cells by means of extracellular trap formation', *Blood*, 111(6), pp. 3070–3080. doi: 10.1182/blood-2007-07-104018.

Koiwai, K., Alenton, R. R. R., Kondo, H. and Hirono, I. (2016) 'Extracellular trap formation in kuruma shrimp (*Marsupenaeus japonicus*) hemocytes is coupled with c-type lysozyme.', *Fish & shellfish immunology*, 52, pp. 206–209. doi: 10.1016/j.fsi.2016.03.039.

Krautgartner, W. D. and Vitkov, L. (2008) 'Visualization of neutrophil extracellular traps in TEM', *Micron*, 39(4), pp. 367–372. doi: 10.1016/j.micron.2007.03.007.

Kunitz, M. (1950) 'Crystalline Desoxyribonuclease', *The Journal of General Physiology*, 209

33(4), pp. 363–377. doi: 10.1085/jgp.33.4.349.

Lafferty, K. D., Harvell, C. D., Conrad, J. M., Friedman, C. S., Kent, M. L., Kuris, A. M., Powell, E. N., Rondeau, D. and Saksida, S. M. (2015) 'Infectious Diseases Affect Marine Fisheries and Aquaculture Economics', *Annual Review of Marine Science*. Annual Reviews, 7(1), pp. 471–496. doi: 10.1146/annurev-marine-010814-015646.

Lamas, J., Bruno, D. W., Santos, Y., Anadón, R. and Ellis, A. E. (1991) 'Eosinophilic granular cell response to intraperitoneal injection with *Vibrio anguillarum* and its extracellular products in rainbow trout, *Oncorhynchus mykiss*', *Fish and Shellfish Immunology*, 1(3), pp. 187–194. doi: 10.1016/S1050-4648(10)80004-X.

Lange, M. K., Penagos-Tabares, F., Muñoz-Caro, T., Gärtner, U., Mejer, H., Schaper, R., Hermosilla, C. and Taubert, A. (2017) 'Gastropod-derived haemocyte extracellular traps entrap metastrongyloid larval stages of *Angiostrongylus vasorum*, *Aelurostrongylus abstrusus* and *Troglostrongylus brevior*', *Parasites & Vectors*. Parasites & Vectors, 10(1), p. 50. doi: 10.1186/s13071-016-1961-z.

Lappann, M., Danhof, S., Guenther, F., Olivares-Florez, S., Mordhorst, I. L. and Vogel, U. (2013) 'In vitro resistance mechanisms of *Neisseria meningitidis* against neutrophil extracellular traps', *Molecular Microbiology*, 89(3), pp. 433–449. doi: 10.1111/mmi.12288.

Lee, P. T., Bird, S., Zou, J. and Martin, S. A. M. (2017) 'Phylogeny and expression analysis of C-reactive protein (CRP) and serum amyloid-P (SAP) like genes reveal two distinct groups in fish', *Fish & Shellfish Immunology*. Academic Press, 65, pp. 42–51. doi: 10.1016/j.fsi.2017.03.037.

Lenhart, J. S., Schroeder, J. W., Walsh, B. W. and Simmons, L. A. (2012) 'DNA Repair and Genome Maintenance in *Bacillus subtilis*', *Microbiology and Molecular Biology Reviews*, 76(3), pp. 530–564. doi: 10.1128/MMBR.05020-11.

Li, C., Ho, L., Chang, Z., Tsai, L. and Yang, W. (2003) 'DNA binding and cleavage by the periplasmic endonuclease Vvn from *Vibrio vulnificus*: A novel structure with an old active site', *Microbiology*, 22(15), pp. 1–40.

Li, P., Li, M., Lindberg, M. R., Kennett, M. J., Xiong, N. and Wang, Y. (2010) 'PAD4 is essential for antibacterial innate immunity mediated by neutrophil extracellular traps', *The Journal of Experimental Medicine*, 207(9), pp. 1853–1862. doi: 10.1084/jem.20100239.

Lie, O., Lied, E. and Lambertsen, G. (1990) 'Haematological values in cod (*Gadus morhua*)', *Fiskeridir. Skr., Ser. Ernaering.*, 3(1), pp. 11–17.

Liechti, G. W. and Goldberg, J. B. (2013) 'Helicobacter pylori salvages purines from

extracellular host cell DNA utilizing the Outer Membrane-Associated nuclease NucT', *Journal of Bacteriology*, 195(19), pp. 4387–4398. doi: 10.1128/JB.00388-13.

Lieschke, G. J., Oates, A. C., Crowhurst, M. O., Ward, A. C. and Layton, J. E. (2001) 'Morphologic and functional characterization of granulocytes and macrophages in embryonic and adult zebrafish', *Blood*, 98(10), pp. 3087–3096. doi: 10.1182/blood.V98.10.3087.

Van Der Linden, M., Westerlaken, G. H. A., Van Der Vlist, M., Van Montfrans, J. and Meyaard, L. (2017) 'Differential Signalling and Kinetics of Neutrophil Extracellular Trap Release Revealed by Quantitative Live Imaging', *Scientific Reports*, 7(1), pp. 1–11. doi: 10.1038/s41598-017-06901-w.

Lippolis, J. D., Reinhardt, T. A., Goff, J. P. and Horst, R. L. (2006) 'Neutrophil extracellular trap formation by bovine neutrophils is not inhibited by milk', *Veterinary Immunology and Immunopathology*, 113(1–2), pp. 248–255. doi: 10.1016/j.vetimm.2006.05.004.

Liu, C., Tangsombatvisit, S., Rosenberg, J. M., Mandelbaum, G., Gillespie, E. C., Gozani, O. P., Alizadeh, A. A. and Utz, P. J. (2012) 'Specific post-translational histone modifications of neutrophil extracellular traps as immunogens and potential targets of lupus autoantibodies', *Arthritis Research & Therapy*. BioMed Central Ltd, 14(1), p. R25. doi: 10.1186/ar3707.

Liu, P., Wu, X., Liao, C., Liu, X., Du, J., Shi, H., Wang, X., Bai, X., Peng, P., Yu, L., Wang, F., Zhao, Y. and Liu, M. (2014) 'Escherichia coli and Candida albicans induced macrophage extracellular trap-like structures with limited microbicidal activity', *PLoS ONE*, 9(2). doi: 10.1371/journal.pone.0090042.

Lodish, H., Berk, A., Zipursky, S. L., Matsudaira, P., Baltimore, D. and Darnell, J. (2000) 'Molecular Cell Biology 4th Edition', in *National Center for Biotechnology Information*. Available at: <https://www.ncbi.nlm.nih.gov/books/NBK21733/>.

Lumsden, J. S., Ferguson, H. W., Ostland, V. E. and Byrne, P. J. (1994) 'The mucous coat on gill lamellae of rainbow trout (*Oncorhynchus mykiss*)', *Cell and Tissue Research*, 275(1), pp. 187–193. doi: 10.1007/BF00305386.

Lumsden, J. S., Russell, S., Huber, P., Wybourne, B. A., Ostland, V. E., Minamikawa, M. and Ferguson, H. W. (2008) 'An immune-complex glomerulonephritis of Chinook salmon, *Oncorhynchus tshawytscha* (Walbaum)', *Journal of Fish Diseases*, 31(12), pp. 889–898. doi: 10.1111/j.1365-2761.2008.00952.x.

Macanovic, M. and Lachmann, P. J. (1997) 'Measurement of deoxyribonuclease I (DNase) in the serum and urine of systemic lupus erythematosus (SLE)-prone NZB/NZW mice by a new radial enzyme diffusion assay.', *Clinical and Experimental Immunology*, 108(2), pp.

220–6. doi: 10.1046/j.1365-2249.1997.3571249.x.

Maeda, M. and Taga, N. (1976) 'Extracellular nuclease produced by a marine bacterium. II. Purification and properties of extracellular nuclease from a marine *Vibrio* sp.', *Canadian Journal of Microbiology*. NRC Research Press, 22(10), pp. 1443–1452. doi: 10.1139/m76-214.

Maini, A. A., George, M. J., Motwani, M. P., Day, R. M., Gilroy, D. W., O'Brien, A. J., Demaret, J., Gossez, M., Venet, F., Monneret, G., Dayam, R. M., Botelho, R. J., Almyroudis, N. G., Grimm, M. J., Davidson, B. A., Röhm, M., Urban, C. F., Segal, B. H., Hoffmann, J. H. O., Schaekel, K., Gaiser, M. R., Enk, A. H., Hadaschik, E. N., De Buhr, N., Von Köckritz-Blickwede, M., Wang, X., He, Z., Liu, H., Yousefi, S., Simon, H.-U., Kuijpers, T. W., Tool, A. T. J., Van.der.Schoot, L. A., Ginsel, L. A., Onderwater, J. J. M., Roos, D., Verhoeven, A. J., Mosca, T., Forte, W. C. N., Quinn, M. T., DeLeo, F. R. and Bokoch, G. M. (2016) 'Inter-individual variation of NETosis in healthy donors: Introduction and application of a refined method for extracellular trap quantification', *The Journal of Immunology*, 11(10), pp. 315–327. doi: 10.1007/978-1-4939-6581-6.

Manzenreiter, R., Kienberger, F., Marcos, V., Schilcher, K., Krautgartner, W. D., Obermayer, A., Huml, M., Stoiber, W., Hector, A., Griese, M., Hannig, M., Studnicka, M., Vitkov, L. and Hartl, D. (2012) 'Ultrastructural characterization of cystic fibrosis sputum using atomic force and scanning electron microscopy', *Journal of Cystic Fibrosis*. European Cystic Fibrosis Society, 11(2), pp. 84–92. doi: 10.1016/j.jcf.2011.09.008.

Martin, F. and Kasahara, M. (2010) 'Origin and evolution of the adaptive immune system: genetic events and selective pressures', *Nat Rev Genet*, 11(1), pp. 47–59. doi: 10.1038/nrg2703.Origin.

Martinelle, K., Mattsson, A., Rippner-Blomqvist, B. and Lindner, E. (2010) 'Effect of Different Cell Culture Medium Surfactants on Cell Growth and Viability', in Noll, T. (ed.) *Cells and Culture: Proceedings of the 20th ESACT Meeting*. Dordrecht: Springer Netherlands, pp. 819–822. doi: 10.1007/978-90-481-3419-9\_143.

Masterman, K.-A. (2016) *Immune defence mechanisms of barramundi (Lates calcarifer) peripheral blood against Streptococci*. University of Queensland.

Mcdonough, E., Kamp, H. and Camilli, A. (2016) '*Vibrio cholerae* phosphatases required for the utilization of nucleotides and extracellular DNA as phosphate sources', *Molecular Microbiology*. Hoboken: John Wiley and Sons Inc., 99(3), pp. 453–469. doi: 10.1111/mmi.13128.

McIvor, R. S. and Kenny, G. E. (1978) 'Differences in incorporation of nucleic acid bases

and nucleosides by various *Mycoplasma* and *Acholeplasma* species', *Journal of Bacteriology*, 135(2), pp. 483–489.

McMillan, S., Verner-Jeffreys, D., Weeks, J., Austin, B. and Desbois, A. P. (2015) 'Larva of the greater wax moth, *Galleria mellonella*, is a suitable alternative host for studying virulence of fish pathogenic *Vibrio anguillarum*.', *BMC microbiology*. BMC Microbiology, 15(1), p. 127. doi: 10.1186/s12866-015-0466-9.

Menees, T. S., Lin, C. P., Kojic, D. D., Burgess, J. O. and Lawson, N. C. (2015) 'Depth of cure of bulk fill composites with mono wave and polywave curing lights', *American Journal of Dentistry*, 28(6), pp. 357–361. doi: 10.1002/dev.21214.Developmental.

Menegazzi, R., Decleva, E. and Dri, P. (2012) 'Killing by neutrophil extracellular traps: Fact or folklore?', *Blood*, 119(5), pp. 1214–1216. doi: 10.1182/blood-2011-07-364604.

Metselaar, M., Thompson, K. D., Gratacap, R. M. L., Kik, M. J. L., LaPatra, S. E., Lloyd, S. J., Call, D. R., Smith, P. D. and Adams, A. (2010) 'Association of red-mark syndrome with a Rickettsia-like organism and its connection with strawberry disease in the USA', *Journal of Fish Diseases*, 33(10), pp. 849–858. doi: 10.1111/j.1365-2761.2010.01187.x.

Metzler, K. D., Fuchs, T. A., Nauseef, W. M., Reumaux, D., Roesler, J., Schulze, I., Wahn, V., Papayannopoulos, V. and Zychlinsky, A. (2011) 'Myeloperoxidase is required for neutrophil extracellular trap formation: Implications for innate immunity', *Blood*, 117(3), pp. 953–959. doi: 10.1182/blood-2010-06-290171.

Milton, D. L., O'Toole, R., Hörstedt, P. and Wolf-Watz, H. (1996) 'Flagellin A is essential for the virulence of *Vibrio anguillarum*', *Journal of Bacteriology*, 178(5), pp. 1310–1319. doi: 10.1128/jb.178.5.1310-1319.1996.

Minion, F. C. and Goguen, J. D. (1986) 'Identification and preliminary characterization of external membrane-bound nuclease activities in *Mycoplasma pulmonis*', *Infection and Immunity*, 51(1), pp. 352–354.

Minniti, G., Hagen, L. H., Porcellato, D., Jørgensen, S. M., Pope, P. B. and Vaaje-Kolstad, G. (2017) 'The skin-mucus microbial community of farmed Atlantic salmon (*Salmo salar*)', *Frontiers in Microbiology*, 8(OCT), pp. 1–11. doi: 10.3389/fmicb.2017.02043.

Mitchell, A. and Finch, L. R. (1977) 'Pathways of nucleotide biosynthesis in *Mycoplasma mycoides* subsp. *mycoides*', *Journal of Bacteriology*, 130(3), pp. 1047–1054.

Modrá, H., Svobodová, Z. and Kolářová, J. (1998) 'Comparison of differential leukocyte counts in fish of economic and indicator importance', *Acta Veterinaria Brno*, 67(4), pp. 215–226. doi: 10.2754/avb199867040215.

- Mojsoska, B. and Jenssen, H. (2015) *Peptides and peptidomimetics for antimicrobial drug design, Pharmaceuticals*. doi: 10.3390/ph8030366.
- Moore, G. E., Gerner, R. E. and Franklin, A. (1967) 'Culture of normal human leukocytes', *JAMA*, 199(8), pp. 519–524. doi: 10.1001/jama.1967.03120080053007.
- Moore, S. (1981) 'Pancreatic DNase', *The Enzymes*, 14, pp. 281–296. doi: 10.1016/S1874-6047(08)60341-8.
- Morgan, A. L., Thompson, K. D., Auchinachie, N. A. and Migaud, H. (2008) 'The effect of seasonality on normal haematological and innate immune parameters of rainbow trout *Oncorhynchus mykiss* L.', *Fish and Shellfish Immunology*, 25(6), pp. 791–799. doi: 10.1016/j.fsi.2008.05.011.
- Morshed, M., Hlushchuk, R., Simon, D., Walls, A. F., Obata-Ninomiya, K., Karasuyama, H., Djonov, V., Eggel, A., Kaufmann, T., Simon, H.-U. and Yousefi, S. (2014) 'NADPH Oxidase-Independent Formation of Extracellular DNA Traps by Basophils', *The Journal of Immunology*, 192(11), pp. 5314–5323. doi: 10.4049/jimmunol.1303418.
- Le Morvan, C., Troutaud, D. and Deschaux, P. (1998) 'Differential effects of temperature on specific and nonspecific immune defences in fish', *The Journal of experimental biology*, 201, pp. 165–168.
- Munoz-Caro, T., Mena Huertas, S. J., Aquilino, Conejeros, I., Alarcon, P., Hidalgo, M. A., Burgos, R. A., Hermosilla, C. and Taubert, A. (2015) '*Eimeria bovis*-triggered neutrophil extracellular trap formation is CD11b-, ERK 1/2-, p38 MAP kinase- and SOCE-dependent', *Veterinary research*, 46, p. 23. doi: 10.1186/s13567-015-0155-6.
- Muñoz Caro, T., Hermosilla, C., Silva, L. M. R., Cortes, H. and Taubert, A. (2014) 'Neutrophil extracellular traps as innate immune reaction against the emerging apicomplexan parasite *Besnoitia besnoiti*', *PLoS ONE*. Public Library of Science, 9(3), p. e91415. doi: 10.1371/journal.pone.0091415.
- Muroga, K. (1985) 'An extracellular protease produced by *Vibrio anguillarum*', *Bull. Jap. Soc. Sci. Fish.*, 51(12), pp. 1915–1920. doi: 10.2331/suisan.51.1915.
- Murray, H. M., Gallant, J. W. and Douglas, S. E. (2003) 'Cellular localization of pleurocidin gene expression and synthesis in winter flounder gill using immunohistochemistry and in situ hybridization.', *Cell and Tissue Research*, 312, pp. 197–202. doi: 10.1007/s00441-003-0723-3.
- Mutoloki, S., Brudeseth, B., Reite, O. B. and Evensen, Ø. (2006) 'The contribution of *Aeromonas salmonicida* extracellular products to the induction of inflammation in Atlantic

salmon (*Salmo salar* L.) following vaccination with oil-based vaccines', *Fish and Shellfish Immunology*, 20(1), pp. 1–11. doi: 10.1016/j.fsi.2005.01.005.

Naccache, P. H. and Fernandes, M. J. G. (2016) 'Challenges in the characterization of neutrophil extracellular traps: The truth is in the details', *European Journal of Immunology*, 46(1), pp. 52–55. doi: 10.1002/eji.201546022.

Naffah de Souza, C., Breda, L. C. D., Khan, M. A., Almeida, S. R. de, Câmara, N. O. S., Swezey, N. and Palaniyar, N. (2018) 'Alkaline pH Promotes NADPH Oxidase-Independent Neutrophil Extracellular Trap Formation: A Matter of Mitochondrial Reactive Oxygen Species Generation and Citrullination and Cleavage of Histone', *Frontiers in Immunology*, 8, pp. 1–15. doi: 10.3389/fimmu.2017.01849.

Naka, H., Dias, G. M., Thompson, C. C., Dubay, C., Thompson, F. L. and Crosa, J. H. (2011) 'Complete genome sequence of the marine fish pathogen *Vibrio anguillarum* harboring the pJM1 virulence plasmid and genomic comparison with other virulent strains of *V. anguillarum* and *V. ordalii*', *Infection and Immunity*, 79(7), pp. 2889–2900. doi: 10.1128/IAI.05138-11.

Nakazawa, D., Tomaru, U., Suzuki, A., Masuda, S., Hasegawa, R., Kobayashi, T., Nishio, S., Kasahara, M. and Ishizu, A. (2012) 'Abnormal conformation and impaired degradation of propylthiouracil-induced neutrophil extracellular traps: Implications of disordered neutrophil extracellular traps in a rat model of myeloperoxidase antineutrophil cytoplasmic antibody-associated vasculiti', *Arthritis and Rheumatism*, 64(11), pp. 3779–3787. doi: 10.1002/art.34619.

Nani, S., Fumagalli, L., Sinha, U., Kamen, L., Scapini, P. and Berton, G. (2015) 'Src family kinases and Syk are required for neutrophil extracellular trap formation in response to B-glucan particles', *Journal of Innate Immunity*, 7(1), pp. 59–73. doi: 10.1159/000365249.

Napirei, M., Ludwig, S., Mezrhah, J., Klöckl, T. and Mannherz, H. G. (2009) 'Murine serum nucleases - Contrasting effects of plasmin and heparin on the activities of DNase1 and DNase1-like 3 (DNase1l3)', *FEBS Journal*, 276(4), pp. 1059–1073. doi: 10.1111/j.1742-4658.2008.06849.x.

Neeli, I., Dwivedi, N., Khan, S. and Radic, M. (2009) 'Regulation of extracellular chromatin release from neutrophils', *Journal of Innate Immunity*. Karger Publishers, 1(3), pp. 194–201. doi: 10.1159/000206974.

Neumann, A., Völlger, L., Berends, E. T. M., Molhoek, E. M., Stapels, D. a C., Midon, M., Friães, A., Pingoud, A., Rooijackers, S. H. M., Gallo, R. L., Mörgelin, M., Nizet, V., Naim, H. Y. and von Köckritz-Blickwede, M. (2014) 'Novel Role of the Antimicrobial Peptide LL-37 in

the Protection of Neutrophil Extracellular Traps against Degradation by Bacterial Nucleases', *Journal of Innate Immunity*, 6(6), pp. 860–8. doi: 10.1159/000363699.

Ng, T. H., Chang, S. H., Wu, M. H. and Wang, H. C. (2013) 'Shrimp hemocytes release extracellular traps that kill bacteria', *Developmental and Comparative Immunology*. Elsevier Ltd, 41(4), pp. 644–651. doi: 10.1016/j.dci.2013.06.014.

Ng, T. H., Wu, M. H., Chang, S. H., Aoki, T. and Wang, H. C. (2015) 'The DNA fibers of shrimp hemocyte extracellular traps are essential for the clearance of *Escherichia coli*', *Developmental and Comparative Immunology*. Elsevier Ltd, 48(1), pp. 229–233. doi: 10.1016/j.dci.2014.10.011.

Nie, L., Cai, S.-Y., Shao, J.-Z. and Chen, J. (2018) 'Toll-Like Receptors, Associated Biological Roles, and Signaling Networks in Non-Mammals', *Frontiers in Immunology*, 9, pp. 1–19. doi: 10.3389/fimmu.2018.01523.

Nishino, T. and Morikawa, K. (2002) 'Structure and function of nucleases in DNA repair: Shape, grip and blade of the DNA scissors', *Oncogene*, 21(58), pp. 9022–9032. doi: 10.1038/sj.onc.1206135.

Norqvist, A. (1989) 'Protection of rainbow trout vibriosis and furunculosis by the use of attenuated strains of *Vibrio anguillarum*', *Applied and Environmental Microbiology*, 55(6), pp. 1400–1405.

Norqvist, A., Norrman, B. and Wolf-Watz, H. (1990) 'Identification and characterization of a zinc metalloprotease associated with invasion by the fish pathogen *Vibrio anguillarum*', *Infection and Immunity*, 58(11), pp. 3731–3736.

Noursadeghi, M., Bickerstaff, M. C. M., Gallimore, J. R., Herbert, J., Cohen, J. and Pepys, M. B. (2000) 'Role of serum amyloid P component in bacterial infection: Protection of the host or protection of the pathogen', *Proceedings of the National Academy of Sciences*, 97(26), pp. 14584–14589. doi: 10.1073/pnas.97.26.14584.

Novriadi, R. (2016) 'Vibriosis in aquaculture', *Omni-Akuatika*, 12(1), pp. 1–12. doi: 10.20884/1.oa.2016.12.1.24.

Oh, H., Siano, B. and Diamond, S. (2008) 'Neutrophil Isolation Protocol', *Journal of Visualized Experiments*, (17), pp. 1–2. doi: 10.3791/745.

Okada, Y. (2017) 'Chapter 8 - Proteinases and Matrix Degradation', in Budd, R. C., Gabriel, S. E., McInnes, I. B., and O'Dell, J. R. B. T.-K. and F. T. of R. (Tenth E. (eds) *Kelley and Firestein's Textbook of Rheumatology (Tenth Edition)*, pp. 106–125. doi: <https://doi.org/10.1016/B978-0-323-31696-5.00008-5>.



- Olmsted, S. S., Khanna, K. V, Ng, E. M., Whitten, S. T., Johnson, O. N., Markham, R. B., Cone, R. A. and Moench, T. R. (2005) 'Low pH immobilizes and kills human leukocytes and prevents transmission of cell-associated HIV in a mouse model', *BMC Infectious Diseases*, 5(1), p. 79. doi: 10.1186/1471-2334-5-79.
- Olsen, A. B., Hjortaa, M., Tengs, T., Hellberg, H. and Johansen, R. (2015) 'First description of a new disease in rainbow trout (*Oncorhynchus mykiss*) similar to heart and skeletal muscle inflammation (HSMI) and detection of a gene sequence related to piscine orthoreovirus (PRV)', *PLoS ONE*, 10(7), pp. 1–14. doi: 10.1371/journal.pone.0131638.
- Ostafin, M., Pruchniak, M. P., Ciepiela, O., Reznick, A. Z. and Demkow, U. (2016) 'Different procedures of DPI addition affects neutrophil extracellular traps (NETs) formation', *Analytical Biochemistry*, 509, pp. 60–66. doi: 10.1016/j.ab.2016.05.003.
- Otonello, L., Gnerre, P., Bertolotto, M., Mancini, M., Dapino, P., Russo, R., Garibotto, G., Barreca, T. and Dallegri, F. (2004) 'Leptin as a uremic toxin interferes with neutrophil chemotaxis', *Journal of the American Society of Nephrology*, 15(9), pp. 2366–2372. doi: 10.1097/01.ASN.0000139321.98029.40.
- Øverland, H. S., Pettersen, E. F., Rønneseth, A. and Wergeland, H. I. (2010) 'Phagocytosis by B-cells and neutrophils in Atlantic salmon (*Salmo salar* L.) and Atlantic cod (*Gadus morhua* L.)', *Fish and Shellfish Immunology*, 28(1), pp. 193–204. doi: 10.1016/j.fsi.2009.10.021.
- Palić, D., Andreasen, C. B., Ostojić, J., Tell, R. M. and Roth, J. A. (2007) 'Zebrafish (*Danio rerio*) whole kidney assays to measure neutrophil extracellular trap release and degranulation of primary granules', *Journal of Immunological Methods*, 319(1–2), pp. 87–97. doi: 10.1016/j.jim.2006.11.003.
- Palić, D., Beck, L. S., Palić, J. and Andreasen, C. B. (2011) 'Use of rapid cytochemical staining to characterize fish blood granulocytes in species of special concern and determine potential for function testing', *Fish and Shellfish Immunology*, 30(2), pp. 646–652. doi: 10.1016/j.fsi.2010.12.024.
- Palić, D., Ostojić, J., Andreasen, C. B. and Roth, J. a. (2007) 'Fish cast NETs: Neutrophil extracellular traps are released from fish neutrophils', *Developmental and Comparative Immunology*, 31(8), pp. 805–816. doi: 10.1016/j.dci.2006.11.010.
- Palmer, L. J., Cooper, P. R., Ling, M. R., Wright, H. J., Huissoon, A. and Chapple, I. L. C. (2012) 'Hypochlorous acid regulates neutrophil extracellular trap release in humans', *Clinical and Experimental Immunology*, 167(2), pp. 261–268. doi: 10.1111/j.1365-2249.2011.04518.x.

Papayannopoulos, V. (2017) 'Neutrophil extracellular traps in immunity and disease', *Nature Reviews Immunology*, 18(2), pp. 1–14. doi: 10.1038/nri.2017.105.

Papayannopoulos, V., Metzler, K. D., Hakkim, A. and Zychlinsky, A. (2010) 'Neutrophil elastase and myeloperoxidase regulate the formation of neutrophil extracellular traps', *Journal of Cell Biology*, 191(3), pp. 677–691. doi: 10.1083/jcb.201006052.

Parker, H., Albrett, A. M., Kettle, A. J. and Winterbourn, C. C. (2012) 'Myeloperoxidase associated with neutrophil extracellular traps is active and mediates bacterial killing in the presence of hydrogen peroxide', *Journal of Leukocyte Biology*, 91(3), pp. 369–376. doi: 10.1189/jlb.0711387.

Parker, H., Dragunow, M., Hampton, M. B., Kettle, A. J. and Winterbourn, C. C. (2012) 'Requirements for NADPH oxidase and myeloperoxidase in neutrophil extracellular trap formation differ depending on the stimulus', *Journal of Leukocyte Biology*, 92(4), pp. 841–849. doi: 10.1189/jlb.1211601.

Parra, D., Reyes-Lopez, F. E. and Tort, L. (2015) 'Mucosal immunity and B cells in teleosts: Effect of vaccination and stress', *Frontiers in Immunology*, 6(JUN), pp. 1–12. doi: 10.3389/fimmu.2015.00354.

Patat, S. A., Carnegie, R. B., Kingsbury, C., Gross, P. S., Chapman, R. and Schey, K. L. (2004) 'Antimicrobial activity of histones from hemocytes of the Pacific white shrimp', *European Journal of Biochemistry*, 271(23–24), pp. 4825–4833. doi: 10.1111/j.1432-1033.2004.04448.x.

Paul, J. H. and Carlson, D. J. (1984) 'Genetic material in the marine environment: implications for bacterial DNA.', *Limnology Oceanography*, 29(5), pp. 1091–1095.

Payne, C. M., Glasser, L., Tischler, M. E., Wyckoff, D., Cromey, D., Fiederlein, R. and Bohnert, O. (1994) 'Programmed cell death of the normal human neutrophil: An *in vitro* model of senescence', *Microscopy Research and Technique*, 28(4), pp. 327–344. doi: 10.1002/jemt.1070280408.

Perera, N. C., Schilling, O., Kittel, H., Back, W., Kremmer, E. and Jenne, D. E. (2012) 'NSP4, an elastase-related protease in human neutrophils with arginine specificity', *Proceedings of the National Academy of Sciences*, 109(12), pp. 6229–6234. doi: 10.1073/pnas.1200470109.

Pettersen, E. F., Bjerknes, R. and Wergeland, H. I. (2000) 'Studies of Atlantic salmon (*Salmo salar* L.) blood, spleen and head kidney leucocytes using specific monoclonal antibodies, immunohistochemistry and flow cytometry', *Fish & Shellfish Immunology*, 10(8),

pp. 695–710. doi: 10.1006/fsim.2000.0284.

Phillipson, M. and Kubes, P. (2011) 'The neutrophil in vascular inflammation', *Nature medicine*, 17(11), pp. 1381–90. doi: 10.1038/nm.2514.

Pietretti, D. and Wiegertjes, G. F. (2014) 'Ligand specificities of Toll-like receptors in fish: indications from infection studies', *Developmental and Comparative Immunology*, 43(2), pp. 205–22. doi: 10.1016/j.dci.2013.08.010.

Pijanowski, L., Golbach, L., Kolaczowska, E., Scheer, M., Verburg-van Kemenade, B. M. L. and Chadzinska, M. (2013) 'Carp neutrophilic granulocytes form extracellular traps via ROS-dependent and independent pathways.', *Fish & shellfish immunology*, 34(5), pp. 1244–52. doi: 10.1016/j.fsi.2013.02.010.

Pijanowski, L., Scheer, M., Verburg-van Kemenade, B. M. L. and Chadzinska, M. (2015) 'Production of inflammatory mediators and extracellular traps by carp macrophages and neutrophils in response to lipopolysaccharide and/or interferon- $\gamma$ ', *Fish and Shellfish Immunology*, 42(2), pp. 473–482. doi: 10.1016/j.fsi.2014.11.019.

Pilsczek, F. H., Salina, D., Poon, K. K. H., Fahey, C., Yipp, B. G., Sibley, C. D., Robbins, S. M., Green, F. H. Y., Surette, M. G., Sugai, M., Bowden, M. G., Hussain, M., Zhang, K. and Kubes, P. (2010) 'A Novel Mechanism of Rapid Nuclear Neutrophil Extracellular Trap Formation in Response to *Staphylococcus aureus*', *The Journal of Immunology*, 185(12), pp. 7413–7425. doi: 10.4049/jimmunol.1000675.

Pinchuk, G. E., Ammons, C., Culley, D. E., Li, S. M. W., McLean, J. S., Romine, M. F., Neilson, K. H., Fredrickson, J. K. and Beliaev, A. S. (2008) 'Utilization of DNA as a sole source of phosphorus, carbon, and energy by *Shewanella spp.*: Ecological and physiological implications for dissimilatory metal reduction', *Applied and Environmental Microbiology*, 74(4), pp. 1198–1208. doi: 10.1128/AEM.02026-07.

Pohl, F. M., Thomae, R. and Karst, A. (1982) 'Temperature Dependence of the Activity of DNA-Modifying Enzymes: Endonucleases and DNA Ligase', *European Journal of Biochemistry*, 123(1), pp. 141–152. doi: 10.1111/j.1432-1033.1982.tb06510.x.

Poirier, A. C., Schmitt, P., Rosa, R. D., Vanhove, A. S., Kieffer-Jaquinod, S., Rubio, T. P., Charrière, G. M. and Destoumieux-Garzón, D. (2014) 'Antimicrobial histones and DNA traps in invertebrate immunity: evidences in *Crassostrea gigas*', *The Journal of Biological Chemistry*, 289(36), pp. 24821–31. doi: 10.1074/jbc.M114.576546.

Press, C. M. L. and Evensen, O. (1999) 'The morphology of the immune system in teleost fishes', *Fish and Shellfish Immunology*, 9(4), pp. 309–318. doi: 10.1006/fsim.1998.0181.

Puyet, A., Greenberg, B. and Lacks, S. A. (1990) 'Genetic and structural characterization of endA. A membrane-bound nuclease required for transformation of *Streptococcus pneumoniae*', *Journal of Molecular Biology*, 213(4), pp. 727–738. doi: 10.1016/S0022-2836(05)80259-1.

Quinn, M. T. (2013) *The Neutrophils: New Outlook for Old Cells*. 3rd edn, Imperial College Press. 3rd edn. Imperial College Press. doi: 10.1017/CBO9781107415324.004.

Rakers, S., Niklasson, L., Steinhagen, D., Kruse, C., Schaubert, J., Sundell, K. and Paus, R. (2013) 'Antimicrobial peptides (AMPs) from fish epidermis: Perspectives for investigative dermatology', *Journal of Investigative Dermatology*, 133(5), pp. 1140–1149. doi: 10.1038/jid.2012.503.

Randelli, E., Buonocore, F. and Scapigliati, G. (2008) 'Cell Markers and Determinants in Fish Immunology', *Fish and Shellfish Immunology*, 25(4), pp. 326–340. doi: 10.1016/j.fsi.2008.03.019.

Reichel, M., Muñoz-Caro, T., Sanchez Contreras, G., Rubio García, A., Magdowski, G., Gärtner, U., Taubert, A. and Hermosilla, C. (2015) 'Harbour seal (*Phoca vitulina*) PMN and monocytes release extracellular traps to capture the apicomplexan parasite *Toxoplasma gondii*', *Developmental and Comparative Immunology*, 50(2), pp. 106–115. doi: 10.1016/j.dci.2015.02.002.

Reite, O. B. and Evensen, Ø. (2006) 'Inflammatory cells of teleostean fish: A review focusing on mast cells/eosinophilic granule cells and rodlet cells', *Fish and Shellfish Immunology*, 20(2), pp. 192–208. doi: 10.1016/j.fsi.2005.01.012.

Rezania, S., Amirmozaffari, N., Tabarraei, B. and Jeddi-tehrani, M. (2011) 'Extraction, Purification and Characterization of Lipopolysaccharide from *Escherichia coli* and *Salmonella typhi*', *Avicenna Journal of Medical Biotechnology*, 3(1), pp. 3–9.

Richards, R. C., O'Neil, D. B., Thibault, P. and Ewart, K. V (2001) 'Histone H1: an antimicrobial protein of Atlantic salmon (*Salmo salar*).', *Biochemical and Biophysical Research Communications*, 284, pp. 549–555. doi: 10.1006/bbrc.2001.5020.

Riganti, C., Gazzano, E., Polimeni, M., Costamagna, C., Bosia, A. and Ghigo, D. (2004) 'Diphenyleneiodonium inhibits the cell redox metabolism and induces oxidative stress', *Journal of Biological Chemistry*, 279(46), pp. 47726–47731. doi: 10.1074/jbc.M406314200.

Riyapa, D., Buddhisa, S., Korbsrisate, S., Cuccui, J., Wren, B. W., Stevens, M. P., Ato, M. and Lertmemongkolchai, G. (2012) 'Neutrophil extracellular traps exhibit antibacterial activity against *Burkholderia pseudomallei* and are influenced by bacterial and host factors',

*Infection and Immunity*, 80(11), pp. 3921–3929. doi: 10.1128/IAI.00806-12.

Robb, C. T., Dyrinda, E. a, Gray, R. D., Rossi, A. G. and Smith, V. J. (2014) 'Invertebrate extracellular phagocyte traps show that chromatin is an ancient defence weapon', *Nature communications*. Nature Publishing Group, 5(4627), pp. 1–11. doi: 10.1038/ncomms5627.

Rombout, J. H. W. M., Huttenhuis, H. B. T., Picchiatti, S. and Scapigliati, G. (2005) 'Phylogeny and ontogeny of fish leucocytes', *Fish and Shellfish Immunology*, 19(5), pp. 441–455. doi: 10.1016/j.fsi.2005.03.007.

Ruchin, A. B. (2006) 'Effect of light on white blood cell count in carp *Cyprinus carpio L*', *Izvestiia Akademii nauk. Serii biologicheskaja / Rossijskaja akademiia nauk*, 33(5), pp. 634–7. doi: 10.1134/S1062359006050153.

Saffarzadeh, M., Juenemann, C., Queisser, M. A., Lochnit, G., Barreto, G., Galuska, S. P., Lohmeyer, J. and Preissner, K. T. (2012) 'Neutrophil extracellular traps directly induce epithelial and endothelial cell death: A predominant role of histones', *PLoS ONE*, 7(2). doi: 10.1371/journal.pone.0032366.

Saitoh, T., Komano, J., Saitoh, Y., Misawa, T., Takahama, M., Kozaki, T., Uehata, T., Iwasaki, H., Omori, H., Yamaoka, S., Yamamoto, N. and Akira, S. (2012) 'Neutrophil Extracellular Traps Mediate a Host Defense Response to Human Immunodeficiency Virus-1', *Cell Host & Microbe*, 12(1), pp. 109–116. doi: 10.1016/j.chom.2012.05.015.

Sami, S., Fischer-Scherl, T., Hoffmann, R. W. and Pfeil-Putzien, C. (1992) 'Immune complex-mediated glomerulonephritis associated with bacterial kidney disease in the rainbow trout (*Oncorhynchus mykiss*)', *Vet Pathol*, 29, pp. 169–174. Available at: <http://www.ncbi.nlm.nih.gov/pubmed/1385916>.

Sasaki, Y., Maita, M. and Okamoto, N. (2002) 'Rainbow trout neutrophils are responsible for non-specific cytotoxicity', *Fish & Shellfish Immunology*, 12(3), pp. 243–252. doi: <http://dx.doi.org/10.1006/fsim.2001.0368>.

Schorn, C., Janko, C., Latzko, M., Chaurio, R., Schett, G. and Herrmann, M. (2012) 'Monosodium urate crystals induce extracellular DNA traps in neutrophils, eosinophils, and basophils but not in mononuclear cells', *Frontiers in Immunology*, 3, pp. 1–8. doi: 10.3389/fimmu.2012.00277.

Scocchi, M., Pallavicini, A., Salgaro, R., Bociek, K. and Gennaro, R. (2009) 'The salmonid cathelicidins: A gene family with highly varied C-terminal antimicrobial domains', *Comparative Biochemistry and Physiology - B Biochemistry and Molecular Biology*, 152(4), pp. 376–381. doi: 10.1016/j.cbpb.2009.01.003.

Secombes, C. J., Wang, T. and Bird, S. (2011) 'The interleukins of fish', *Developmental and Comparative Immunology*, 35(12), pp. 1336–1345. doi: 10.1016/j.dci.2011.05.001.

Secundino, I., Lizcano, A., Roupé, K. M., Wang, X., Cole, J. N., Olson, J., Ali, S. R., Dahesh, S., Amayreh, L. K., Henningham, A., Varki, A. and Nizet, V. (2016) 'Host and pathogen hyaluronan signal through human siglec-9 to suppress neutrophil activation', *Journal of Molecular Medicine*, 94(2), pp. 219–233. doi: 10.1007/s00109-015-1341-8.

Seitz, P. and Blokesch, M. (2013) 'DNA-uptake machinery of naturally competent *Vibrio cholerae*', *Proceedings of the National Academy of Sciences*, 110(44), pp. 17987–17992. doi: 10.1073/pnas.1315647110.

Seper, A., Fengler, V. H. I., Roier, S., Wolinski, H., Kohlwein, S. D., Bishop, A. L., Camilli, A., Reidl, J. and Schild, S. (2011) 'Extracellular nucleases and extracellular DNA play important roles in *Vibrio cholerae* biofilm formation', *Molecular Microbiology*, 82(4), pp. 1015–1037. doi: 10.1111/j.1365-2958.2011.07867.x.

Seper, A., Hosseinzadeh, A., Gorkiewicz, G., Lichtenegger, S., Roier, S., Leitner, D. R., Röhm, M., Grutsch, A., Reidl, J., Urban, C. F. and Schild, S. (2013) '*Vibrio cholerae* Evades Neutrophil Extracellular Traps by the Activity of Two Extracellular Nucleases', *PLoS Pathogens*, 9(9). doi: 10.1371/journal.ppat.1003614.

Sepulcre, M. P., Alcaraz-Pérez, F., López-Muñoz, A., Roca, F. J., Meseguer, J., Cayuela, M. L. and Mulero, V. (2009) 'Evolution of lipopolysaccharide (LPS) recognition and signaling: fish TLR4 does not recognize LPS and negatively regulates NF-kappaB activation', *Journal of Immunology*. American Association of Immunologists, 182(4), pp. 1836–45. doi: 10.4049/jimmunol.0801755.

Shah, P. L., Scott, S. F., Knight, R. A., Marriott, C., Ranasinha, C. and Hodson, M. E. (1996) 'In vivo effects of recombinant human DNase I on sputum in patients with cystic fibrosis', *Thorax*, 51(2), pp. 119–125.

Shak, S., Capon, D. J., Hellmiss, R., Marsters, S. A. and Baker, C. L. (1990) 'Recombinant human DNase I reduces the viscosity of cystic fibrosis sputum.', *Proceedings of the National Academy of Sciences of the United States of America*, 87(23), pp. 9188–92. doi: 10.1073/pnas.87.23.9188.

de Silva, S. S. and Soto, D. (2009) 'Climate change and aquaculture: potential impacts, adaptation and mitigation', *Food and Agricultural Organization of the United Nations (FAO) Fisheries and Aquaculture*, (530), pp. 151–213. doi: 10.1371.

Singer, J. T., Choe, W., Schmidt, K. A. and Makula, R. A. (1992) 'Virulence plasmid pJM1

prevents the conjugal entry of plasmid DNA into the marine fish pathogen *Vibrio anguillarum* 775', *Journal of General Microbiology*, 138(12), pp. 2485–2490.

Skirvin, R. M., Chu, M. C., Mann, M. L., Young, H., Sullivan, J. and Fermanian, T. (1986) 'Stability of tissue culture medium pH as a function of autoclaving, time, and cultured plant material', *Plant Cell Reports*, 5(4), pp. 292–294. doi: 10.1007/BF00269825.

Smith, P. (2008) 'Antimicrobial resistance in aquaculture', *Revue Scientifique Et Technique*, 27(1), pp. 243–264. doi: 10.1787/5jxvl3dwwk3f0-en.

Smith, V. J., Desbois, A. P. and Dyrinda, E. A. (2010) 'Conventional and unconventional antimicrobials from fish, marine invertebrates and micro-algae', *Marine Drugs*, 8(4), pp. 1213–1262. doi: 10.3390/md8041213.

Smith, V. J. and Dyrinda, E. A. (2015) 'Antimicrobial proteins: From old proteins, new tricks', *Molecular immunology*, 68(2), pp. 383–398. doi: 10.1016/j.molimm.2015.08.009.

Sollberger, G., Amulic, B. and Zychlinsky, A. (2016) 'Neutrophil Extracellular Trap Formation Is Independent of De Novo Gene Expression', *PLoS ONE*, 11(6), p. e0157454. doi: 10.1371/journal.pone.0157454.

Sommerset, I., Krossøy, B., Biering, E. and Frost, P. (2005) 'Vaccines for fish in aquaculture', *Expert Review of Vaccines*. Taylor & Francis, 4(1), pp. 89–101. doi: 10.1586/14760584.4.1.89.

Sorensen, K. K., Sveinbjornsson, B., Dalmo, R. A., Smedsroed, B. and Bertheussen, K. (1997) 'Isolation, cultivation and characterization of head kidney macrophages from Atlantic cod, *Gadus morhua* L.', *Journal of Fish Diseases*, 20(2), pp. 93–107. doi: 10.1046/j.1365-2761.1997.d01-112.x.

Standish, A. J. and Weiser, J. N. (2009) 'Human Neutrophils Kill *Streptococcus pneumoniae* via Serine Proteases', *The Journal of Immunology*, 183(4), pp. 2602–2609. doi: 10.4049/jimmunol.0900688.

Stapels, D. A. C., Geisbrecht, B. V. and Rooijackers, S. H. M. (2015) 'Neutrophil serine proteases in antibacterial defense', *Current Opinion in Microbiology*. Elsevier Ltd, 23, pp. 42–28. doi: 10.1016/j.mib.2014.11.002.

Stentiford, G. D., Sritunyalucksana, K., Flegel, T. W., Williams, B. A. P., Withyachumnarnkul, B., Itsathitphaisarn, O. and Bass, D. (2017) 'New Paradigms to Help Solve the Global Aquaculture Disease Crisis', *PLoS Pathogens*, 13(2), pp. 1–6. doi: 10.1371/journal.ppat.1006160.

Stephan, A. and Fabri, M. (2015) 'The NET, the trap and the pathogen: Neutrophil extracellular traps in cutaneous immunity', *Experimental Dermatology*, 24(3), pp. 161–166. doi: 10.1111/exd.12599.

Stoeckle, M. Y., Soboleva, L. and Charlop-Powers, Z. (2017) 'Aquatic environmental DNA detects seasonal fish abundance and habitat preference in an urban estuary', *PLoS ONE*, 12(4), pp. 1–15. doi: 10.1371/journal.pone.0175186.

Storisteanu, D. M., Pocock, J. M., Cowburn, A. S., Juss, J. K., Nadesalingam, A., Nizet, V. and Chilvers, E. R. (2017) 'Evasion of Neutrophil Extracellular Traps by Respiratory Pathogens', *American Journal of Respiratory Cell and Molecular Biology*, 56(4), pp. 423–431. doi: 10.2135/crosci2013.11.0764.

Strober, W. (2015) 'Trypan Blue Exclusion Test of Cell Viability', *Current Protocols in Immunology*, 111, pp. 1–3. doi: 10.1002/0471142735.ima03bs111.

Sumby, P., Barbian, K. D., Gardner, D. J., Whitney, A. R., Welty, D. M., Long, R. D., Bailey, J. R., Parnell, M. J., Hoe, N. P., Adams, G. G., Deleo, F. R. and Musser, J. M. (2005) 'Extracellular deoxyribonuclease made by group A *Streptococcus* assists pathogenesis by enhancing evasion of the innate immune response.', *Proceedings of the National Academy of Sciences of the United States of America*, 102(5), pp. 1679–84. doi: 10.1073/pnas.0406641102.

Sur Chowdhury, C., Giaglis, S., Walker, U. A., Buser, A., Hahn, S. and Hasler, P. (2014) 'Enhanced neutrophil extracellular trap generation in rheumatoid arthritis: analysis of underlying signal transduction pathways and potential diagnostic utility', *Arthritis Research & Therapy*, 16(3), p. R122. doi: 10.1186/ar4579.

Tan, S. C. and Yiap, B. C. (2009) 'DNA, RNA, and protein extraction: The past and the present', *Journal of Biomedicine and Biotechnology*, 2009. doi: 10.1155/2009/574398.

Tavares-Dias, M., de Castro Monteiro, A. M., Affonso, E. G. and Amaral, K. D. S. (2011) 'Weight-length relationship, condition factor and blood parameters of farmed *Cichla temensis* Humboldt, 1821 (Cichlidae) in central Amazon', *Neotropical Ichthyology*, 9(1), pp. 113–119. doi: 10.1590/S1679-62252011005000010.

Thammavongsa, V., Missiakas, D. M. and Schneewind, O. (2013) '*Staphylococcus aureus* Degrades Neutrophil Extracellular Traps to Promote Immune Cell Death', 342(November), pp. 155–158. doi: 10.1126/science.1242255.

The World Bank (2014) 'Reducing Disease Risk In Aquaculture', *The World Bank. Agriculture and Environmental Services*, (88257), p. 119.



- Theilgaard-Mönch, K., Porse, B. T. and Borregaard, N. (2006) 'Systems biology of neutrophil differentiation and immune response', *Current Opinion in Immunology*, 18(1), pp. 54–60. doi: 10.1016/j.coi.2005.11.010.
- Thermo Fisher Scientific (2010) 'Chapter 8 - Nucleic Acid Detection and Analysis', *Molecular Probes™ Handbook*.
- Thompson, K. D. (2017) *Immunology: Improvement of innate and adaptive immunity, Fish Diseases: Prevention and Control Strategies*. Elsevier. doi: 10.1016/B978-0-12-804564-0.00001-6.
- Thomsen, P. F., Møller, P. R., Sigsgaard, E. E., Knudsen, S. W., Jørgensen, O. A. and Willerslev, E. (2016) 'Environmental DNA from seawater samples correlate with trawl catches of subarctic, deepwater fishes', *PLoS ONE*, 11(11), pp. 1–22. doi: 10.1371/journal.pone.0165252.
- Tinsley, J. W., Lyndon, A. R. and Austin, B. (2011) 'Antigenic and cross-protection studies of biotype 1 and biotype 2 isolates of *Yersinia ruckeri* rainbow trout, *Oncorhynchus mykiss* (Walbaum)', *Journal of Applied Microbiology*, 111(1), pp. 8–16. doi: 10.1111/j.1365-2672.2011.05020.x.
- Tkachenko, A., Da Silva, L., Hearne, J., Parveen, S. and Waguespack, Y. (2013) 'An assay to screen bacterial adhesion to mucus biomolecules', *Letters in Applied Microbiology*, 56(1), pp. 79–82. doi: 10.1111/lam.12003.
- Tort, L., Balasch, J. C. and Mackenzie, S. (2003) 'Fish immune system. A crossroads between innate and adaptive responses', *Immunologia*, 22, pp. 277–286.
- Tran, T. M., MacIntyre, A., Hawes, M. and Allen, C. (2016) 'Escaping Underground Nets: Extracellular DNases Degrade Plant Extracellular Traps and Contribute to Virulence of the Plant Pathogenic Bacterium *Ralstonia solanacearum*', *PLoS Pathogens*, 12(6), pp. 1–26. doi: 10.1371/journal.ppat.1005686.
- Tripathi, S., Verma, A., Kim, E. J., White, M. R. and Hartshorn, K. L. (2014) 'LL-37 modulates human neutrophil responses to influenza A virus', *Journal of Leukocyte Biology*, 96(5), pp. 931–938. doi: 10.1189/jlb.4A1113-604RR.
- Uchiyama, S., Döhrmann, S., Timmer, A. M., Dixit, N., Ghochani, M., Bhandari, T., Timmer, J. C., Sprague, K., Bubeck-Wardenburg, J., Simon, S. I. and Nizet, V. (2015) 'Streptolysin O rapidly impairs neutrophil oxidative burst and antibacterial responses to Group A Streptococcus', *Frontiers in Immunology*, 6(NOV), pp. 1–10. doi: 10.3389/fimmu.2015.00581.

Ueki, S., Konno, Y., Takeda, M., Hirokawa, M., Matsuwaki, Y., Ohta, N., Yamamoto, S., Wada, A. and Weller, P. F. (2016) 'Eosinophil ETosis-derived DNA traps: their presence in secretions and their functional attributes', *Journal of Allergy and Clinical Immunology*, 137(1), pp. 258–267. doi: 10.1016/j.jaci.2015.04.041.

Urban, C. F., Ermert, D., Schmid, M., Abu-Abed, U., Goosmann, C., Nacken, W., Brinkmann, V., Jungblut, P. R. and Zychlinsky, A. (2009) 'Neutrophil extracellular traps contain calprotectin, a cytosolic protein complex involved in host defense against *Candida albicans*', *PLoS Pathogens*, 5(10), p. e1000639. doi: 10.1371/journal.ppat.1000639.

Urban, C. F., Reichard, U., Brinkmann, V. and Zychlinsky, A. (2006) 'Neutrophil extracellular traps capture and kill *Candida albicans* yeast and hyphal forms.', *Cellular microbiology*, 8(4), pp. 668–76. doi: 10.1111/j.1462-5822.2005.00659.x.

Uribe, C., Folch, H., Enriquez, R. and Moran, G. (2011) 'Innate and adaptive immunity in teleost fish: a review.', *Veterinárni Medicina*, 56(10), pp. 486–503. doi: 10.1016/j.pestbp.2010.09.001.

Walker, M. J., Hollands, A., Sanderson-Smith, M. L., Cole, J. N., Kirk, J. K., Henningham, A., McArthur, J. D., Dinkla, K., Aziz, R. K., Kansal, R. G., Simpson, A. J., Buchanan, J. T., Chhatwal, G. S., Kotb, M. and Nizet, V. (2007) 'DNase Sda1 provides selection pressure for a switch to invasive group A streptococcal infection', *Nature Medicine*, 13(8), pp. 981–985. doi: 10.1038/nm1612.

Wang, H. and Griffiths, M. W. (2009) 'Mg<sup>2+</sup>-free buffer elevates transformation efficiency of *Vibrio parahaemolyticus* by electroporation', *Letters in Applied Microbiology*, 48(3), pp. 349–354. doi: 10.1111/j.1472-765X.2008.02531.x.

Wang, L., Shen, D., Wu, H. and Ma, Y. (2017) 'Resistance of hypervirulent *Klebsiella pneumoniae* to both intracellular and extracellular killing of neutrophils', *PLoS ONE*, 12(3), pp. 1–10. doi: 10.1371/journal.pone.0173638.

Wangkahart, E., Scott, C., Secombes, C. J. and Wang, T. (2016) 'Re-examination of the rainbow trout (*Oncorhynchus mykiss*) immune response to flagellin: *Yersinia ruckeri* flagellin is a potent activator of acute phase proteins, anti-microbial peptides and pro-inflammatory cytokines in vitro', *Developmental and Comparative Immunology*. Elsevier Ltd, 57, pp. 75–87. doi: 10.1016/j.dci.2015.12.017.

Wardini, A. B., Guimaraes-Costa, A. B., Nascimento, M. T. C., Nadaes, N. R., Danelli, M. G. M., Mazur, C., Benjamin, C. F., Saraiva, E. M. and Pinto-da-Silva, L. H. (2010) 'Characterization of neutrophil extracellular traps in cats naturally infected with feline leukemia virus', *Journal of General Virology*, 91(1), pp. 259–264. doi: 10.1099/vir.0.014613-

0.

Warnatsch, A., Ioannou, M., Wang, Q. and Papayannopoulos, V. (2015) 'Neutrophil extracellular traps license macrophages and Th17 cells for cytokine production in atherosclerosis', *Science*, 349(6245), pp. 316–320. doi: 10.1126/science.aaa8064.Neutrophil.

Wartha, F., Beiter, K., Albiger, B., Fernebro, J., Zychlinsky, A., Normark, S. and Henriques-Normark, B. (2007) 'Capsule and D-alanylated lipoteichoic acids protect *Streptococcus pneumoniae* against neutrophil extracellular traps', *Cellular Microbiology*, 9(5), pp. 1162–71. doi: 10.1111/j.1462-5822.2006.00857.x.

Waters, J. C. (2009) 'Accuracy and precision in quantitative fluorescence microscopy', *Journal of Cell Biology*, 185(7), pp. 1135–1148. doi: 10.1083/jcb.200903097.

Watts, J. E. M., Schreier, H. J., Lanska, L. and Hale, M. S. (2017) 'The rising tide of antimicrobial resistance in aquaculture: Sources, sinks and solutions', *Marine Drugs*, 15(6), pp. 1–16. doi: 10.3390/md15060158.

Wei, Z., Batagov, A. O., Carter, D. R. F. and Krichevsky, A. M. (2016) 'Fetal Bovine Serum RNA Interferes with the Cell Culture derived Extracellular RNA', *Scientific Reports*. Nature Publishing Group, 6, pp. 1–6. doi: 10.1038/srep31175.

Wei, Z., Hermosilla, C., Taubert, A., He, X., Wang, X., Gong, P., Li, J., Yang, Z. and Zhang, X. (2016) 'Canine neutrophil extracellular traps release induced by the apicomplexan parasite *Neospora caninum in vitro*', *Frontiers in Immunology*, 7(OCT). doi: 10.3389/fimmu.2016.00436.

Weinrauch, Y., Drujan, D., Shapiro, S. D., Weiss, J. and Zychlinsky, A. (2002) 'Neutrophil elastase targets virulence factors of enterobacteria', *Nature*, 417, p. 91. Available at: <http://dx.doi.org/10.1038/417091a>.

Wernersson, S., Reimer, J. M., Poorafshar, M., Karlson, U., Wermenstam, N., Bengtén, E., Wilson, M., Pilström, L. and Hellman, L. (2006) 'Granzyme-like sequences in bony fish shed light on the emergence of hematopoietic serine proteases during vertebrate evolution', *Developmental and Comparative Immunology*, 30(10), pp. 901–918. doi: 10.1016/j.dci.2005.10.014.

Wiklund, T. and Dalsgaard, I. (1998) 'Occurrence and significance of atypical *Aeromonas salmonicida* in non-salmonid and salmonid fish species: A review', *Diseases of Aquatic Organisms*, 32(1), pp. 49–69. doi: 10.3354/dao032049.

Willett, C. E., Cortes, A., Zuasti, A. and Zapata, A. G. (1999) 'Early hematopoiesis and

developing lymphoid organs in the zebrafish', *Developmental Dynamics*, 214(4), pp. 323–336. doi: 10.1002/(SICI)1097-0177(199904)214:4<323::AID-AJA5>3.0.CO;2-3.

Winkelstein, J. A., Marino, M. C., Johnston, R. B., Boyle, J., Curnutte, J., Gallin, J. I., Malech, H. L., Holland, S. M., Ochs, H., Quie, P., Buckley, R. H., Foster, C. B., Chanock, S. J. and Dickler, H. (2000) 'Chronic Granulomatous Disease: Report on a National Registry of 368 Patients', *Medicine*, 79(3), pp. 155–169.

Wood, C. M. and Pärt, P. (2000) 'Intracellular pH regulation and buffer capacity in CO<sub>2</sub>/HCO<sub>3</sub>-buffered media in cultured epithelial cells from rainbow trout gills', *Journal of Comparative Physiology*, 170(3), pp. 175–184. Available at: <http://www.ncbi.nlm.nih.gov/pubmed/10841257>.

Xing, Z., Gauldie, J., Cox, G., Baumann, H., Jordana, M., Lei, X.-F. and Achong, M. K. (1998) 'IL-6 Is an Antiinflammatory Cytokine Required for Controlling Local or Systemic Acute Inflammatory Responses', *J. Clin. Invest*, 101(2), pp. 311–320. doi: 10.1172/JCI1368.

Xu, J., Zhang, X., Monestier, M., Esmon, N. L. and Esmon, C. T. (2011) 'Extracellular Histones Are Mediators of Death through TLR2 and TLR4 in Mouse Fatal Liver Injury', *The Journal of Immunology*, 187(5), pp. 2626–2631. doi: 10.4049/jimmunol.1003930.

Xu, J., Zhang, X., Pelayo, R., Monestier, M. and Ammollo, C. T. (2010) 'Extracellular histones are major mediators of death in sepsis', *Nature Medicine*, 15(11), pp. 1318–1321. doi: 10.1038/nm.2053.Extracellular.

Yang, H., Biermann, M. H., Brauner, J. M., Liu, Y., Zhao, Y. and Herrmann, M. (2016) 'New insights into neutrophil extracellular traps: Mechanisms of formation and role in inflammation', *Frontiers in Immunology*, 7, pp. 1–8. doi: 10.3389/fimmu.2016.00302.

Yang, W. (2011) 'Nucleases: Diversity of structure, function and mechanism', *Quarterly Reviews of Biophysics*, 44(1), pp. 1–93. doi: 10.1017/S0033583510000181.

Yipp, B. G. and Kubes, P. (2013) 'NETosis: how vital is it?', *Blood*, 122(16), pp. 2784–94. doi: 10.1182/blood-2013-04-457671.

Yipp, B. G., Petri, B., Salina, D., Jenne, C. N., Scott, B. N. V., Zbytnuik, L. D., Pittman, K., Asaduzzaman, M., Wu, K., Meijndert, H. C., Malawista, S. E., de Boisfleury Chevance, A., Zhang, K., Conly, J. and Kubes, P. (2012) 'Infection-induced NETosis is a dynamic process involving neutrophil multitasking *in vivo*', *Nature Medicine*, 18(9), pp. 1386–1393. doi: 10.1038/nm.2847.

Yoo, D., Floyd, M., Winn, M., Moskowitz, S. M. and Rada, B. (2014) 'NET formation induced by *Pseudomonas aeruginosa* cystic fibrosis isolates measured as release of

myeloperoxidase–DNA and neutrophil elastase–DNA complexes', *Immunology Letters*. Elsevier, 160(2), pp. 186–194.

Young, R. L., Malcolm, K. C., Kret, J. E., Caceres, S. M., Poch, K. R., Nichols, D. P., Taylor-Cousar, J. L., Saavedra, M. T., Randell, S. H., Vasil, M. L., Burns, J. L., Moskowitz, S. M. and Nick, J. A. (2011) 'Neutrophil extracellular trap (NET)-mediated killing of *Pseudomonas aeruginosa*: Evidence of acquired resistance within the CF airway, independent of CFTR', *PLoS ONE*, 6(9). doi: 10.1371/journal.pone.0023637.

Yousefi, S., Gold, J. A., Andina, N., Lee, J. J., Kelly, A. M., Kozlowski, E., Schmid, I., Straumann, A., Reichenbach, J., Gleich, G. J. and Simon, H. U. (2008) 'Catapult-like release of mitochondrial DNA by eosinophils contributes to antibacterial defense', *Nature Medicine*, 14(9), pp. 949–953. doi: 10.1038/nm.1855.

Yousefi, S., Morshed, M., Amini, P., Stojkov, D., Simon, D., Von Gunten, S., Kaufmann, T. and Simon, H. U. (2015) 'Basophils exhibit antibacterial activity through extracellular trap formation', *Allergy: European Journal of Allergy and Clinical Immunology*, 70(9), pp. 1184–1188. doi: 10.1111/all.12662.

Zapata, A., Diez, B., Cejalvo, T., Gutiérrez-De Frías, C. and Cortés, A. (2006) 'Ontogeny of the immune system of fish', *Fish and Shellfish Immunology*, 20(2), pp. 126–136. doi: 10.1016/j.fsi.2004.09.005.

Zawrotniak, M. and Rapala-Kozik, M. (2013) 'Neutrophil extracellular traps (NETs) - Formation and implications', *Acta Biochimica Polonica*, pp. 277–284. doi: 2013\_486 [pii].

Zhang, X., Zhuchenko, O., Kuspa, A. and Soldati, T. (2016) 'Social amoebae trap and kill bacteria by casting DNA NETs', *Nature Communications*, 7, p. 10938. doi: 10.1038/ncomms10938.

Zhao, M. L., Chi, H. and Sun, L. (2017) 'Neutrophil extracellular traps of *Cynoglossus semilaevis*: Production characteristics and antibacterial effect', *Frontiers in Immunology*, 8, pp. 1–9. doi: 10.3389/fimmu.2017.00290.

Zhao, W., Fogg, D. K. and Kaplan, M. J. (2015) 'A novel image-based quantitative method for the characterization of NETosis', *Journal of Immunological Methods*, 423, pp. 104–110. doi: 10.1016/j.jim.2015.04.027.

Zhu, L. yun, Nie, L., Zhu, G., Xiang, L. xing and Shao, J. zhong (2012) 'Advances in research of fish immune-relevant genes: A comparative overview of innate and adaptive immunity in teleosts', *Developmental and Comparative Immunology*. Elsevier Ltd, 39(1–2), pp. 39–62. doi: 10.1016/j.dci.2012.04.001.

Zhu, Y., Cao, X., Tao, G., Xie, W., Hu, Z. and Xu, D. (2013) 'The lymph index: A potential hematological parameter for viral infection', *International Journal of Infectious Diseases*, 17(7), pp. 490–493. doi: 10.1016/j.ijid.2012.12.002.

Zinkernagel, A. S., Timmer, A. M., Pence, M. A., Locke, J. B., John, T., Turner, C. E., Mishalian, I., Sriskandan, S., Hanski, E. and Nizet, V. (2009) 'The IL-8 Protease SpyCEP/ScpC of Group A Streptococcus Promotes Resistance to Neutrophil Killing', *Cell Host and Microbe*, 4(2), pp. 170–178. doi: 10.1016/j.chom.2008.07.002.The.

Zou, J., Mercier, C., Koussounadis, A. and Secombes, C. (2007) 'Discovery of multiple beta-defensin like homologues in teleost fish', *Molecular Immunology*, 44(4), pp. 638–647. doi: 10.1016/j.molimm.2006.01.012.

Zou, J. and Secombes, C. (2016) 'The Function of Fish Cytokines', *Biology*, 5(2), p. 23. doi: 10.3390/biology5020023.

